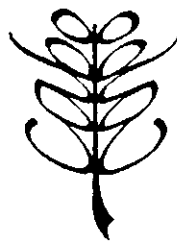


**AGRISCATT**  
**Quality analysis, data description and**  
**statistical analysis of the DUTSCAT 1988 data**

B.A.M. Bouman  
M.A.M. Vissers  
D. Uenk

**CABO report no. 136**  
**1990**



*750 792223*

**Centre for Agrobiological Research**  
**P.O. Box 14, 6700 AA Wageningen, The Netherlands**

## THE HISTORY OF THE

1787

1787

THE HISTORY OF THE  
1787

THE HISTORY OF THE  
1787

1787

THE HISTORY OF THE  
1787

THE HISTORY OF THE  
1787

1787

## Abstract

The radar backscatter behaviour of agricultural crops was investigated in different frequency bands (1.2-17.3 GHz), and preliminary conclusions were drawn on the use of multi-frequency radar observations for classification and growth monitoring of sugar beet, potato and winter wheat. The radar data were collected during the Agriscatt 1988 campaign over the Dutch test site flevopolder, with the Delft University of Technology SCATterometer (DUTSCAT). Data interpretation was preceded by a quality analysis of the radar data.

### Quality analysis

Field-average radar data (radar backscatter expressed in  $\gamma$ ) with standard deviation  $> 3$  dB, and with a large deviation from 'surrounding' data (other frequencies, incidence angles, polarization) were rejected for analysis. Except for the X-band, the remaining data set appeared internally fairly consistent.

The DUTSCAT radar data were compared with 'historical' ground-based and airborne (SLAR) X-band radar data (collected by the ROVE team), and with airborne C- and X-band radar data collected with the ERASME scatterometer during Agriscatt 1988. The general trends (crop type differences, temporal and angular dependency) in ~~X-band~~  $\gamma$  measured with DUTSCAT agreed well with those observed in the other data sets. On an absolute scale, the ~~X-band~~ DUTSCAT data were consistently some 3-5 dB higher than the other data sets. The X-band in the DUTSCAT data was labelled 'suspicious'.

Only for wheat, differences were found between the temporal  $\gamma$  in the ground-based data set, and the temporal  $\gamma$  in the airborne (SLAR, DUTSCAT) data set.

### Frequency behaviour

The relative positions of the frequency bands were in general accordance with radar backscatter theory:  $\gamma$  L-band  $< \gamma$  S-band  $< \gamma$  C-band  $< \gamma$  X-band  $< \gamma$  Ku1-band  $\sim \gamma$  Ku2-band.

The data description and the statistical analyses indicated that the backscatter behaviour of beet, potato and wheat was very much the same in the high frequencies, the X-, Ku1- and Ku2-band. The backscatter behaviour in the C-band resembled strongly that in the other high frequency bands, but the dynamic range and the content of variation was lower. In general lines, the backscatter behaviour in the low frequencies, L- and S-band, also resembled that in the high frequencies. However, some differences in angular behaviour of crops and soil, the low correlations between the low and the high frequencies, and specific examples like ridge orientation in potato and lodging in wheat (namely the L-band), indicated that low frequency microwaves interacted differently with crop canopies than high frequency microwaves.

### Preliminary prospects for application possibilities

With bare soil, the highest relative content of variation (spatial) was found in the low frequencies, and with full crop covers in the high frequencies (mutually comparable). Bare soil types ('beet-soil', 'potato-soil', 'wheat-soil' (40-50% cover)) were best discriminated in the low frequencies (namely the L-band), and crop types in the high frequencies (either X-, Ku1- or Ku2-band).

the first of these is the fact that the  
 the second is the fact that the

the third is the fact that the

the fourth is the fact that the

the fifth is the fact that the

the sixth is the fact that the

the seventh is the fact that the

the eighth is the fact that the

the ninth is the fact that the

the tenth is the fact that the

the eleventh is the fact that the

the twelfth is the fact that the

the thirteenth is the fact that the

the fourteenth is the fact that the

the fifteenth is the fact that the

## List of tables and figures

### Tables:

Table 1 Clusters of 'suspicious' field-average radar data that were removed from the data set

Table 2a unavailable track data (HH polarization)

Table 2b unavailable track data (VV polarization)

Table 3 Some statistics on the final DUTSCAT 1988 data set

Table 4 Maximum effect of lodging on the radar backscatter in the different frequency bands

Table 5 Difference in dB between DUTSCAT and ERASME

Table 6 Coefficient of correlation ( $r^2$ ) between track data of DUTSCAT and ERASME

Table 7 Coefficient of correlation ( $r^2$ ) between HH and VV polarised radar backscatter, per sortie, frequency and nominal incidence angle; All track data were used and the number of data pairs was  $\sim 28$  per correlation (average for whole table)

Table 8 Coefficient of correlation ( $r^2$ ) between the radar backscatter at  $20^\circ$  incidence angle at the 6 DUTSCAT frequencies, per sortie and per state of polarization; The number of data pairs was  $\sim 25$  per coefficient of correlation (average for whole table)

Table 9 Coefficient of correlation ( $r^2$ ) between the radar backscatter at  $40^\circ$  incidence angle at the 6 DUTSCAT frequencies, per sortie and per state of polarization; The number of data pairs was  $\sim 25$  per coefficient of correlation (average for whole table)

Table 10 Coefficient of correlation ( $r^2$ ) between the radar backscatter at  $60^\circ$  incidence angle at the 6 DUTSCAT frequencies, per sortie and per state of polarization; The number of data pairs was  $\sim 25$  per coefficient of correlation (average for whole table)

Table 11 Coefficient of correlation ( $r^2$ ) between the radar backscatter at five incidence angles, per frequency band and per state of polarization (sortie 2); The number of data pairs was  $\sim 25$  for each coefficient of correlation (average for whole table)

Table 12 Coefficient of correlation ( $r^2$ ) between the radar backscatter at five incidence angles, per frequency band and per state of polarization (sortie 6); The number of data pairs was  $\sim 25$  for each coefficient of correlation (average for whole table)

Table 13 Coefficient of correlation ( $r^2$ ) between radar backscatter at two  $10^\circ$  neighbouring incidence angles; The data of all seven sorties were lumped for all crop types

Table 14 Coefficient of correlation ( $r^2$ ) between the radar backscatter (of all seven sorties) and the crop growth parameters cover, height, fresh canopy biomass, dry canopy biomass and Leaf Area Index (LAI) for potato;  $r^2$  was calculated per frequency band, incidence angle and state of polarization; The number of data pairs was  $\sim 25$  for each coefficient of correlation (average for whole table)

Table 15 Coefficient of correlation ( $r^2$ ) between the radar backscatter (of all seven sorties) and the crop growth parameters cover, height, fresh canopy biomass, dry canopy biomass and Leaf Area Index (LAI) for beet;  $r^2$  was calculated per frequency band, incidence angle and state of polarization; The number of data pairs was  $\sim 25$  for each coefficient of correlation (average for whole table)

Table 16 Coefficient of correlation ( $r^2$ ) between the radar backscatter (of all seven sorties) and the crop growth parameters cover, height, fresh canopy biomass, dry canopy biomass and Leaf Area Index (LAI) for wheat;  $r^2$  was calculated per frequency band, incidence angle and state of polarization; The number of data pairs was  $\sim 25$  for each coefficient of correlation (average for whole table)

Table 17 Coefficient of correlation ( $r^2$ ) between the radar backscatter (of all seven sorties) and volumetric moisture content of 0-5 cm top soil, per crop(-soil) type, state of polarization, incidence angle and frequency band; The number of data pairs was  $\sim 17$  for each coefficient of correlation (average for whole table)

### Figures:

Fig. 1 Location of the Dutch Agriscatt test site in South Flevoland

Fig. 2 The seven test parcels with the DUTSCAT flight line. The division of test parcels into fields is schematically indicated.

Fig. 3 Radar backscatter (sortie 3, HH, 40° i.a.) along the flight track

Fig. 4 Radar backscatter (sortie 3, VV, 40° i.a.) along the flight track

Fig. 5 Radar backscatter (sortie 6, HH, 40° i.a.) along the flight track

Fig. 6 Radar backscatter (sortie 6, VV, 40° i.a.) along the flight track

Fig. 7 Average radar backscatter (sortie 3, VV) as a function of frequency

Fig. 8 Average radar backscatter (sortie 6, HH) as a function of frequency

Fig. 9 Standard deviation (sortie 2, Ku2-band, VV, 40° i.a.) versus radar backscatter

Fig. 10 Standard deviation (sortie 5, Ku2-band, VV, 40° i.a.) versus radar backscatter

Fig. 11 Frequency distribution of the standard deviation of the radar backscatter in steps of 0.2 dB (all frequency bands, sortie 1-2)

Fig. 12 Frequency distribution of the standard deviation of the radar backscatter in steps of 0.2 dB (all frequency bands, sortie 3-7)

Fig. 13 Radar backscatter (Ku1-band, HH, sortie 2) versus incidence angle for potato with ridge orientations perpendicular (perp.) and parallel (para.) to the incident microwaves

Fig. 14 Radar backscatter (L-band, HH, sortie 2) versus incidence angle for potato with ridge orientations perpendicular (perp.) and parallel (para.) to the incident microwaves

Fig. 15 Radar backscatter (Ku1-band, VV, sortie 4) versus incidence angle for potato with ridge orientations perpendicular (perp.) and parallel (para.) to the incident microwaves

Fig. 16 Radar backscatter (L-band, VV, sortie 4) versus incidence angle for potato with ridge orientations perpendicular (perp.) and parallel (para.) to the incident microwaves

Fig. 17 Radar backscatter (Ku1-band, HH sortie 1) versus incidence angle for bare 'beet-soil' with a rolled and a unrolled (rough) surface

Fig. 18 Radar backscatter (S-band, HH sortie 1) versus incidence angle for bare 'beet-soil' with a rolled and a unrolled (rough) surface

Fig. 19 Radar backscatter (Ku2-band, VV, sortie 3) versus incidence angle for wheat, 'high' and 'low' refer to the relative height of the crop

Fig. 20 Radar backscatter (X-band, HH, sortie 6) versus incidence angle for lodged and non-lodged (erect) wheat crops

Fig. 21 Radar backscatter (L-band, HH, sortie 6) versus incidence angle for lodged and non-lodged (erect) wheat crops

Fig. 22 Radar backscatter of 'beet-soil', 'potato-soil' and 'wheat-soil' (sortie 2, L-band, HH) as a function of incidence angle

Fig. 23 Radar backscatter of 'beet-soil', 'potato-soil' and 'wheat-soil' (sortie 2, Ku1-band, VV) as a function of incidence angle

Fig. 24 Radar backscatter of beet, potato and wheat (sortie 5, Ku2-band, VV) as a function of incidence angle

Fig. 25 Radar backscatter of beet, potato and wheat (sortie 3, X-band, VV) as a function of incidence angle

Fig. 26 Radar backscatter of beet, potato and wheat (sortie 4, S-band, VV) as a function of incidence angle

Fig. 27 Radar backscatter of beet, potato and wheat (sortie 7, L-band, HH) as a function of incidence angle

Fig. 28 Feature space plot (sortie 2, VV, 15° i.a.) of the S-band versus the L-band for 'potato-soil', 'beet-soil' and 'wheat-soil'

Fig. 29 Feature space plot (sortie 5, VV, 40°&50° i.a.) of the S-band versus the L-band for potato, beet and wheat

Fig. 30 Feature space plot (sortie 2, VV, 15° i.a.) of the Ku1-band versus the L-band for 'potato-soil', 'beet-soil' and 'wheat-soil'

Fig. 31 Feature space plot (sortie 5, VV, 40°&50° i.a.) of the Ku1-band versus the L-band for potato, beet and wheat

Fig. 32 Feature space plot (sortie 2, VV, 15° i.a.) of the Ku1-band versus the S-band for 'potato-soil', 'beet-soil' and 'wheat-soil'

Fig. 33 Feature space plot (sortie 5, VV, 40°&50° i.a.) of the Ku1-band versus the S-band for potato, beet and wheat

Fig. 34 Radar backscatter of beet (C-, X-, Ku2-band, VV, 40° i.a.) in the course of the growing season

Fig. 35 Average crop cover and dry canopy biomass of beet in the course of the growing season

Fig. 36 Radar backscatter of beet (L-, S-, Ku1-band, VV, 40° i.a.) in the course of the growing season

Fig. 37 Leaf Area Index (LAI) of beet in the course of the growing season, the numbers in the legend refer to the fieldnumbers of the crops

Fig. 38 Radar backscatter of potato (C-, X-, Ku2-band, VV, 40° i.a.) in the course of the growing season

Fig. 39 Average crop cover and dry canopy biomass of potato in the course of the growing season

Fig. 40 Radar backscatter of potato (L-, S-, Ku1-band, VV, 40° i.a.) in the course of the growing season

Fig. 41 Leaf Area Index (LAI) of potato in the course of the growing season, the numbers in the legend refer to the fieldnumbers of the crops

Fig. 42 Radar backscatter of wheat (C-, X-, Ku2-band, VV, 40° i.a.) in the course of the growing season

Fig. 43 Average crop cover and dry canopy biomass of wheat in the course of the growing season

Fig. 44 Radar backscatter of wheat (L-, S-, Ku1-band, VV, 40° i.a.) in the course of the growing season

Fig. 45 Leaf Area Index (LAI) of wheat in the course of the growing season, the numbers in the legend refer to the fieldnumbers of the crops

Fig. 46 Average moisture content of the top soil (0-5 cm) of beet, potato and wheat in the course of the growing season

Fig. 47 Radar backscatter of bare 'potato-soil', 'beet-soil' and 'wheat-soil' (sortie 2, VV, 40° i.a.) as a function of frequency

Fig. 48 Radar backscatter of beet, potato and wheat (sortie 4, VV, 40° i.a.) as a function of frequency, the 'mainly bare soil' curve is the frequency curve of figure 47

Fig. 49 Radar backscatter of beet, potato and wheat (sortie 7, VV, 40° i.a.) as a function of frequency, the 'mainly bare soil' curve is the frequency curve of figure 47

Fig. 50 Radar backscatter of the main crop types (sortie 3, L-, S-, Ku1-band, VV, 30° i.a.)

Fig. 51 Radar backscatter of the main crop types (sortie 3, L-, S-, Ku1-band, VV, 60° i.a.)

Fig. 52 Radar backscatter of the main crop types (sortie 6, L-, S-, Ku1-band, VV, 30° i.a.)

Fig. 53 Radar backscatter of the main crop types (sortie 6, L-, S-, Ku1-band, VV, 60° i.a.)

Fig. 54 Radar backscatter of the main crop types (sortie 3, C-, X-, Ku2-band, VV, 30° i.a.)

Fig. 55 Radar backscatter of the main crop types (sortie 3, C-, X-, Ku2-band, VV, 60° i.a.)

Fig. 56 Radar backscatter of the main crop types (sortie 6, C-, X-, Ku2-band, VV, 30° i.a.)

Fig. 57 Radar backscatter of the main crop types (sortie 6, C-, X-, Ku2-band, VV, 60° i.a.)

Fig. 58 SLAR Flevoland (48°-67° i.a.) and ROVE X-band radar backscatter (50° i.a.) for beet in the course of the growing season

Fig. 59 SLAR Brabant (48°-67° i.a.) and ROVE X-band radar backscatter (50° i.a.) for beet in the course of the growing season

Fig. 60 SLAR Flevoland (48°-67° i.a.) and ROVE X-band radar backscatter (50° i.a.) for potato in the course of the growing season

Fig. 61 SLAR Brabant (48°-67° i.a.) and ROVE X-band radar backscatter (50° i.a.) for potato in the course of the growing season



Fig. 62 SLAR Flevoland (48°-67° i.a.) and ROVE X-band radar backscatter (50° i.a.) for wheat in the course of the growing season

Fig. 63 SLAR Brabant (48°-67° i.a.) and ROVE X-band radar backscatter (50° i.a.) for wheat in the course of the growing season

Fig. 64 DUTSCAT (40°, 50° and 60° i.a.) and SLAR (48°-67° i.a.) X-band radar backscatter for beet in the course of the growing season

Fig. 65 DUTSCAT and ROVE X-band radar backscatter (50° i.a.) for beet in the course of the growing season

Fig. 66 DUTSCAT (40°, 50° and 60° i.a.) and SLAR (48°-67° i.a.) X-band radar backscatter for potato in the course of the growing season

Fig. 67 DUTSCAT and ROVE X-band radar backscatter (50° i.a.) for potato in the course of the growing season

Fig. 68 DUTSCAT (40°, 50° and 60° i.a.) Ku1-band and SLAR (48°-67° i.a.) X-band radar backscatter for beet in the course of the growing season

Fig. 69 DUTSCAT Ku1-band and ROVE X-band radar backscatter (50° i.a.) for beet in the course of the growing season

Fig. 70 DUTSCAT (40°, 50° and 60° i.a.) Ku1-band and SLAR (48°-67° i.a.) X-band radar backscatter for potato in the course of the growing season

Fig. 71 DUTSCAT Ku1-band and ROVE X-band radar backscatter (50° i.a.) for potato in the course of the growing season

Fig. 72 DUTSCAT (40°, 50° and 60° i.a.) Ku1-band and SLAR (48°-67° i.a.) X-band radar backscatter for wheat in the course of the growing season

Fig. 73 DUTSCAT Ku1-band and ROVE X-band radar backscatter (50° i.a.) for wheat in the course of the growing season

Fig. 74 DUTSCAT Ku1-band, ROVE X-band and ROVE Q-band radar backscatter (20° i.a.) for beet in the course of the growing season

Fig. 75 DUTSCAT Ku1-band, ROVE X-band and ROVE Q-band radar backscatter (40° i.a.) for beet in the course of the growing season

Fig. 76 DUTSCAT Ku1-band, ROVE X-band and ROVE Q-band radar backscatter (20° i.a.) for potato in the course of the growing season

Fig. 77 DUTSCAT Ku1-band, ROVE X-band and ROVE Q-band radar backscatter (40° i.a.) for potato in the course of the growing season

Fig. 78 DUTSCAT Ku1-band, ROVE X-band and ROVE Q-band radar backscatter (20° i.a.) for wheat in the course of the growing season

Fig. 79 DUTSCAT Ku1-band, ROVE X-band and ROVE Q-band radar backscatter (40° i.a.) for wheat in the course of the growing season

Fig. 80 DUTSCAT and ERASME radar backscatter (sortie 3, C-band, 20° i.a., HH) along the flight track

Fig. 81 DUTSCAT and ERASME radar backscatter (sortie 6, C-band, 40° i.a., HH) along the flight track

Fig. 82 DUTSCAT and ERASME radar backscatter (sortie 4, X-band, 40° i.a., VV) along the flight track

Fig. 83 DUTSCAT and ERASME radar backscatter (sortie 6, X-band, 40° i.a., VV) along the flight track

Fig. 84 ERASME X-band radar backscatter (20° i.a., VV) for the main crops in the course of the growing season

Fig. 85 ERASME X-band radar backscatter (40° i.a., VV) for the main crops in the course of the growing season

Fig. 86 Relative content of variation in the frequency bands, per incidence angle (all track data of sortie 1, VV polarization)

Fig. 87 Relative content of variation in the frequency bands, per incidence angle (all track data of sortie 2, VV polarization)

Fig. 88 Relative content of variation in the frequency bands, per incidence angle (all track data of sortie 3, VV polarization)

Fig. 89 Relative content of variation in the frequency bands, per incidence angle (all track data of sortie 4, VV polarization)

Fig. 90 Relative content of variation in the frequency bands, per incidence angle (all track data of sortie 5, VV polarization)

Fig. 91 Relative content of variation in the frequency bands, per incidence angle (all track data of sortie 6, VV polarization)

Fig. 92 Relative content of variation in the frequency bands, per incidence angle (all track data of sortie 7, VV polarization)

Fig. 93 Relative content of variation in the frequency bands, per incidence angle (all track data of sortie 1, HH polarization)

Fig. 94 Relative content of variation in the frequency bands, per incidence angle (all track data of sortie 6, HH polarization)

Fig. 95 Relative content of variation in the frequency bands, per incidence angle (all track data of sortie 7, HH polarization)

Fig. 96 Relative content of variation in the frequency bands, per incidence angle group (Beet, all sorties, VV polarization)

Fig. 97 Relative content of variation in the frequency bands, per incidence angle group (Beet, all sorties, HH polarization)

Fig. 98 Relative content of variation in the frequency bands, per incidence angle group (Potato, all sorties, VV polarization)

Fig. 99 Relative content of variation in the frequency bands, per incidence angle group (Potato, all sorties, HH polarization)

Fig. 100 Relative content of variation in the frequency bands, per incidence angle group (Wheat, all sorties, VV polarization)

Fig. 101 Relative content of variation in the frequency bands, per incidence angle group (Wheat, all sorties, HH polarization)

**Fig. 102 Relative content of variation in the frequency bands, per incidence angle group (all track data of all sorties, VV polarization)**

**Fig. 103 Relative content of variation in the frequency bands, per incidence angle group (all track data of all sorties, HH polarization)**

## 1 Introduction

This report presents a quality analysis and a data interpretation of the DUTSCAT (Delft University of Technology SCATterometer) data collected over the Flevopolder in 1988 during the Agriscatt campaign. Data interpretation was carried out in relation to crop type and crop growth of sugar beet, potato and winter wheat. The purpose of this study was to compare the backscatter behaviour of agricultural crops in different frequency bands (1.2-17.3 GHz), and to draw preliminary conclusions for crop classification and growth monitoring.

Data quality analysis and the removal of low-quality data are described in chapter 2. After a phenomenological description of the radar data in chapter 3, the DUTSCAT data were compared to historical X-band ROVE data (ground-based and airborne), and with radar data simultaneously collected with the ERASME during Agriscatt 1988 in chapter 4. A comparison with DUTSCAT 1987 data is made throughout the text. In chapter 5, the phenomenological data interpretation is supported by statistical correlation and principal component analysis. Finally, chapter 6 summarizes the previous chapters and presents preliminary conclusions for crop classification and growth monitoring.

Overviews of the Agriscatt campaign and its objectives in general are given by Attema (1989) and by Hoekman (1990).

### 1.1 The Flevopolder test site

The test site was located in Southern Flevoland and comprised seven rectangular shaped agricultural parcels of about 80 ha. These parcels were subdivided into fields by the farmers to grow several crop types and varieties. Figure 1 gives the location of the test site in Southern Flevoland, and figure 2 illustrates the seven test parcels with the flight line of the (side-looking) DUTSCAT. All fields in the seven test parcels were measured by DUTSCAT. During the DUTSCAT overpasses, ground truth was collected on three fields of sugar beet, potato and winter wheat each. The ground truth comprised, amongst others: top soil moisture content (stratified in the layer of 0-15 cm), crop cover, crop height, fresh and dry canopy biomass and LAI. Visual observations were made of phenological development stage and any anomalies like disease infection or weed cover.

More details on the test site, and on the collected ground truth and measurement accuracy are given by Vissers et al. (1989).

### 1.2 DUTSCAT radar data

DUTSCAT was operated in six frequency bands: L- (1.2 GHz), S- (3.2 GHz), C- (5.3 GHz), X- (9.7 GHz), Ku1 (13.7 GHz) and Ku2 (17.3 GHz). The radar backscatter was measured seven times in the growing season at vertical (VV) and horizontal (HH) co-polarization: April 22, May 2, June 14, July 5, July 14, July 26 and August 16 (numbered sortie 1-7 from here on). Unfortunately, between May 2 and June 14, the DUTSCAT antenna was being calibrated in Denmark so that only one sortie (no. 3) was carried out in the most interesting period of the growing season (exponential growth May-June).

The incidence angles were 20°, 30°, 40°, 50° and 60°, extended with 10° and 15° at sorties 1 and 2. At each angle of incidence, state of polarization and frequency, DUTSCAT was externally calibrated on corner reflectors for each sortie by the Technical University of Delft (TUD).

During sortie 1 and 2, DUTSCAT data in 1988 were compressed during recording due to wrong attenuator settings. Decompression of the data was carried out through an especially designed decompression algorithm at the TUD. Technical details on the DUTSCAT, and on data decompression,

processing and calibration are given by Snoeij and Swart (1987) and Snoeij et al. (1989). A technical quality analysis of the DUTSCAT 1988 data was performed at ESA/EARTHNET (James, 1989a). The Physics and Electronics Laboratory TNO computed the average radar backscatter in  $\gamma$  (radar cross section per unit projected area), and the standard deviation, for all agricultural fields in the seven test parcels. Also, radar data of very low quality were already discarded (P. Luik, 1990).



Fig. 1 Location of the Dutch Agriscatt test site in South Flevoland

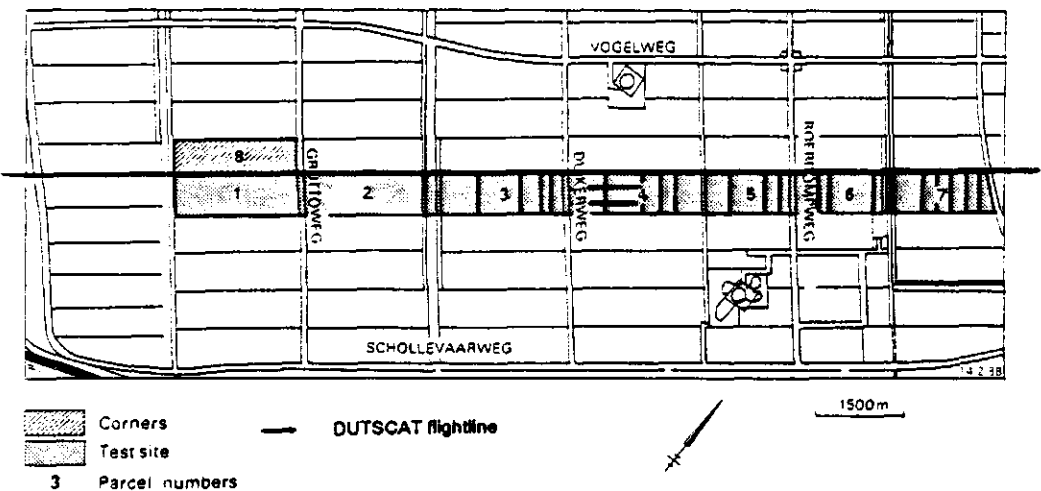


Fig. 2 The seven test parcels with the DUTSCAT flight line. The division of test parcels into fields is schematically indicated.

## 2 General quality analysis

### 2.1 Track plots

The first step was the analyses of 78 so called track plots.

These plots show the radar backscatter of all fields along the flight track in all frequencies at one state of polarization and at one angle of incidence, for one sortie. Some examples of these plots are given in figures 3-6.

From these analyses, the following generalizations are derived:

- General theory predicts that a higher frequency gives a higher radar backscatter. This pattern occurs mainly for the L-, S-, C- and X-band. The relative positions of the Ku1- and Ku2-band are not in accordance with general theory. They mutually alternate with different angles of incidence and states of polarization, figures 7-8, and sometimes even overlap with the X-band. The relative position of the X-band presents some special problems, see pages 41, 45, 65.
- At sortie 1 and 2 the relative position of the S-band is higher than the C-band. This could well be the effect of the decompression.
- In the frequency bands of the last four sorties the relative position of a (field average)  $\gamma$  value corresponds with the crop type on the field.

The track plots of the last four sorties look fairly well: the dynamic range of the various bands looks good but the relative position of the higher frequency bands are not according to general theory. However, there still appear some 'suspicious' data in this set which regard individual fields in specific tracks as well as whole tracks.

CABO

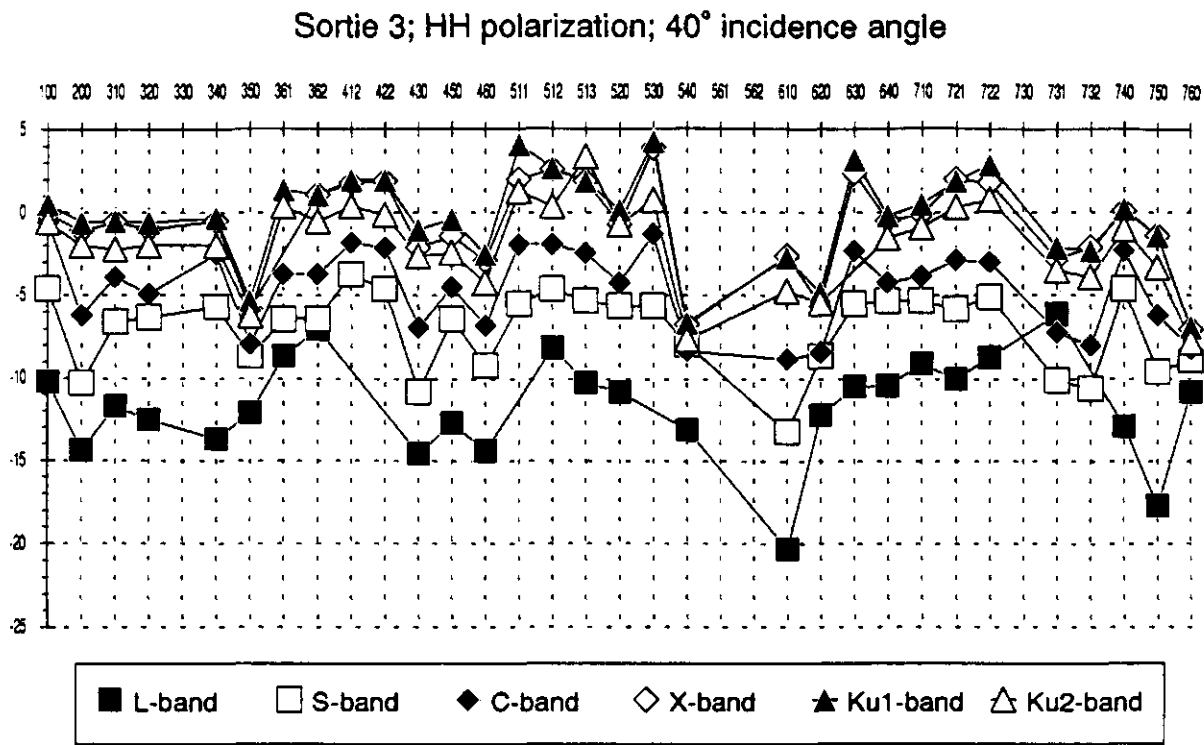


Fig. 3 Radar backscatter (sortie 3, HH, 40° i.a.) along the flight track

CABO

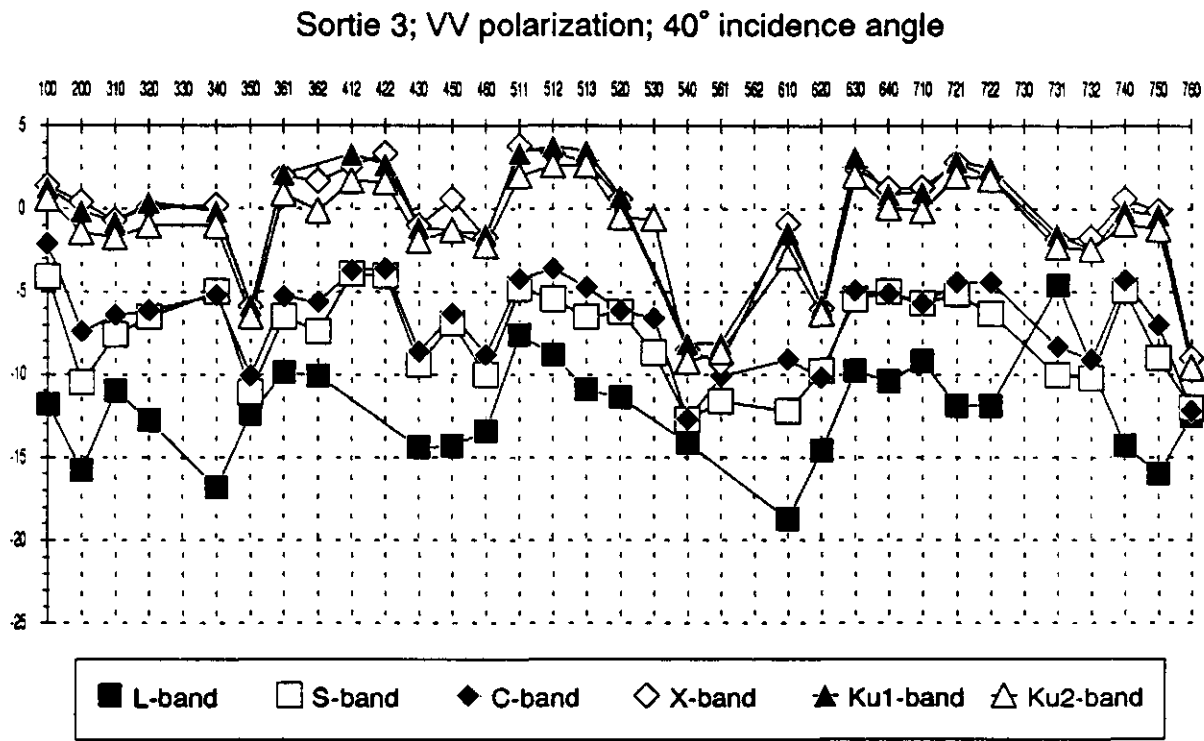


Fig. 4 Radar backscatter (sortie 3, VV, 40° i.a.) along the flight track

CABO

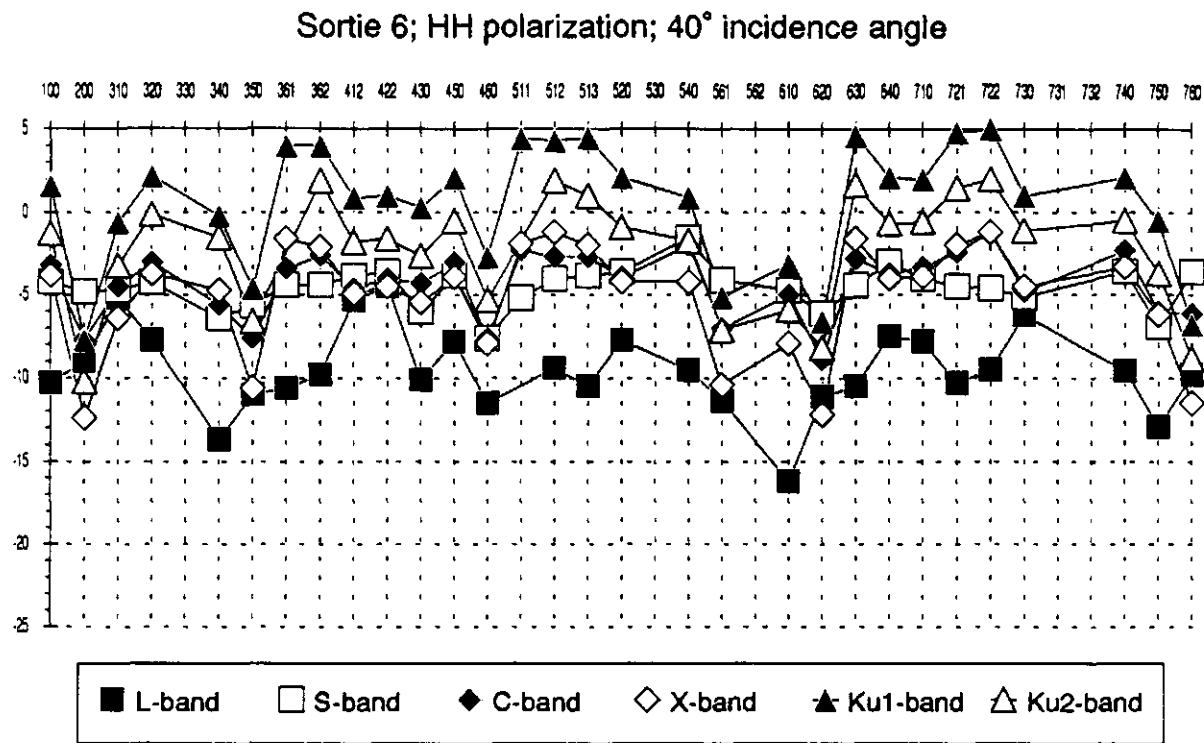


Fig. 5 Radar backscatter (sortie 6, HH, 40° i.a.) along the flight track

CABO

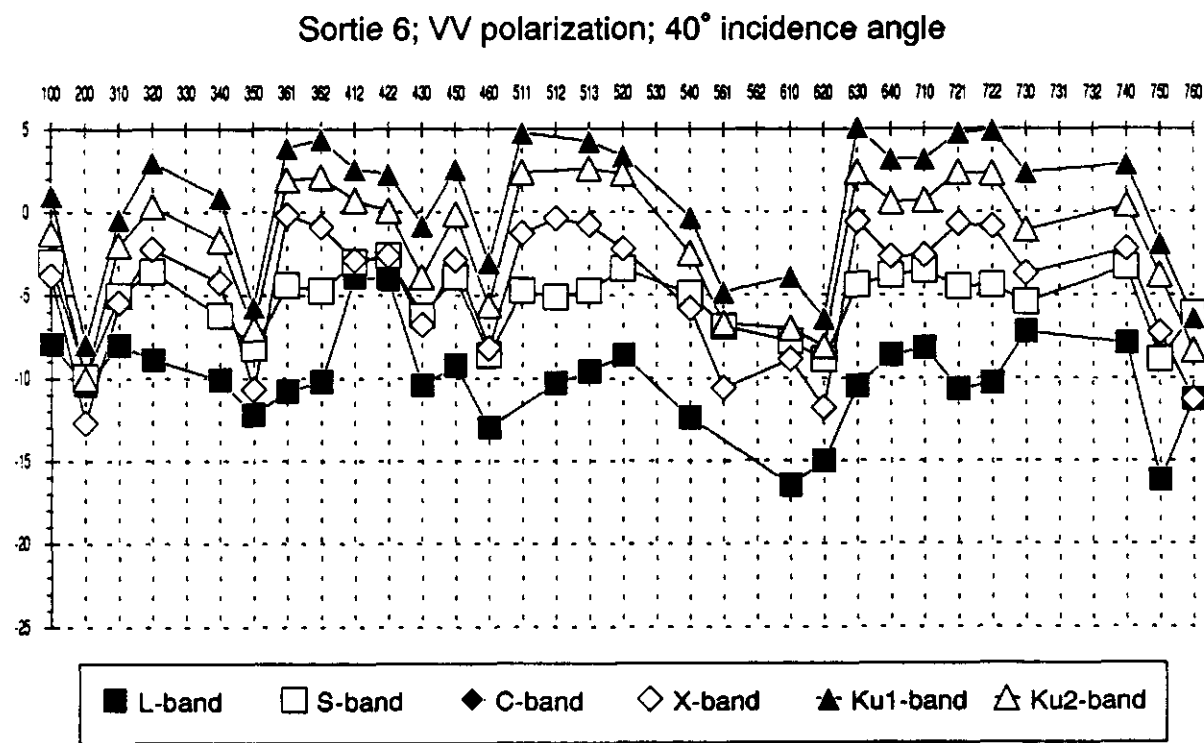


Fig. 6 Radar backscatter (sortie 6, VV, 40° i.a.) along the flight track



CABO

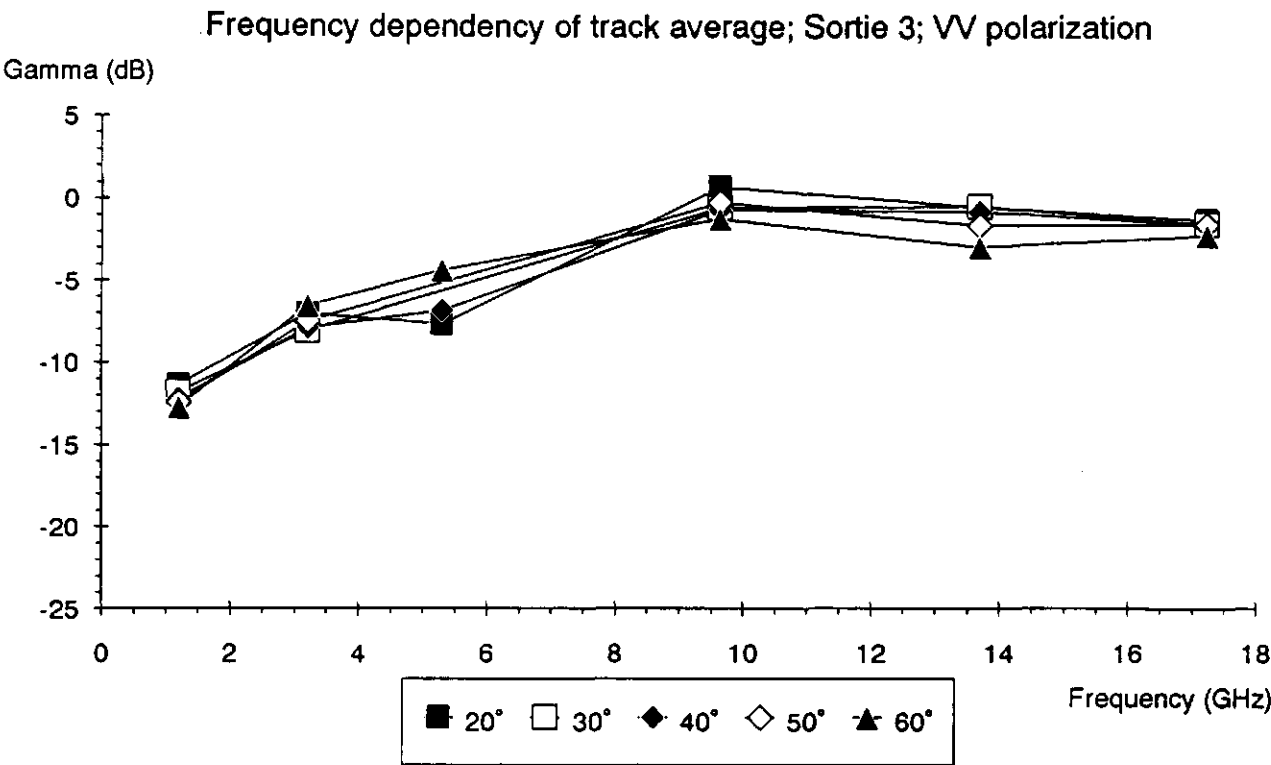


Fig. 7 Average radar backscatter (sortie 3, VV) as a function of frequency

CABO

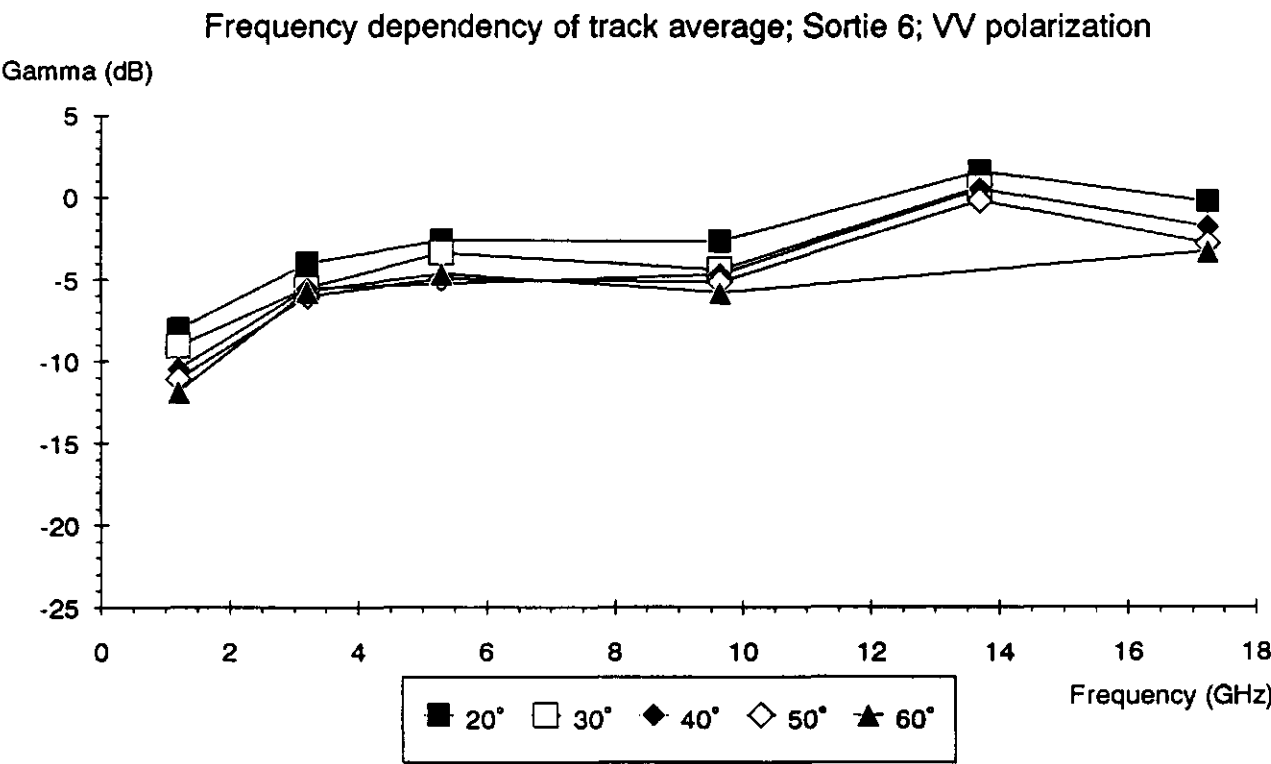


Fig. 8 Average radar backscatter (sortie 6, HH) as a function of frequency

## 2.2 Standard deviation

Because of the non-linearity of the decompression algorithm (applied at the TUD on the data of sortie 1 and 2), not all the data are corrected with the same 'reliability'. In CABO report no. 135 (Bouman et al, 1990), it was shown how 'unreliable' or 'suspicious' data could be recognized through their relation with other data and their standard deviation. In theory, the standard deviation of field-average backscatter values should be centred around 1 dB. If the radar data were saturated during recording, the standard deviation of the field averages increases with the decompression. This is illustrated in figures 9-10 where the standard deviation is plotted against the field average  $\gamma$  for the Ku2-band (compressed at sortie 2 and not compressed at sortie 5). At sortie 5 the standard deviation is indeed nicely centred around 1 dB, regardless of the value of the field-average  $\gamma$ . At sortie 2, however, the standard deviation seems correlated with the level of the radar backscatter  $\gamma$ . All standard deviations are higher than 1 dB, and a whole cluster of fields has standard deviation values between 3 and 5! These fields are mostly potato and 'other crops' where the fields with lower standard deviations are mostly wheat and beet. Therefore, the quality of the decompressed radar data is related to the type of the crop on the field.

To evaluate the performance of a whole frequency band, the frequency distribution of the standard deviation is investigated, figures 11-12. All bands show a distribution close around the theoretical 1 dB at sorties 3-7. The distribution for the L-, S-, C-, X- and Ku1-band at sortie 1 and 2 appears also reasonable centred around 1 dB but with more standard deviation in the classes  $> 2$  dB. But the frequency distribution for the Ku2-band at sorties 1 and 2 deviates largely from the other bands. The standard deviation is quite regularly spread over all the classes with a relatively high occurrence in the class  $> 4$  dB. This distribution is independent of the state of polarization and the angle of incidence.

Compared to the 1987 DUTSCAT data set, this set appears to have a higher reliability. Compression of radar data occurred only at sortie 1 and 2. Of these two sorties, the decompression performance was relatively poor for the Ku2-band, while this year it was much better for the C-band than in 1987.

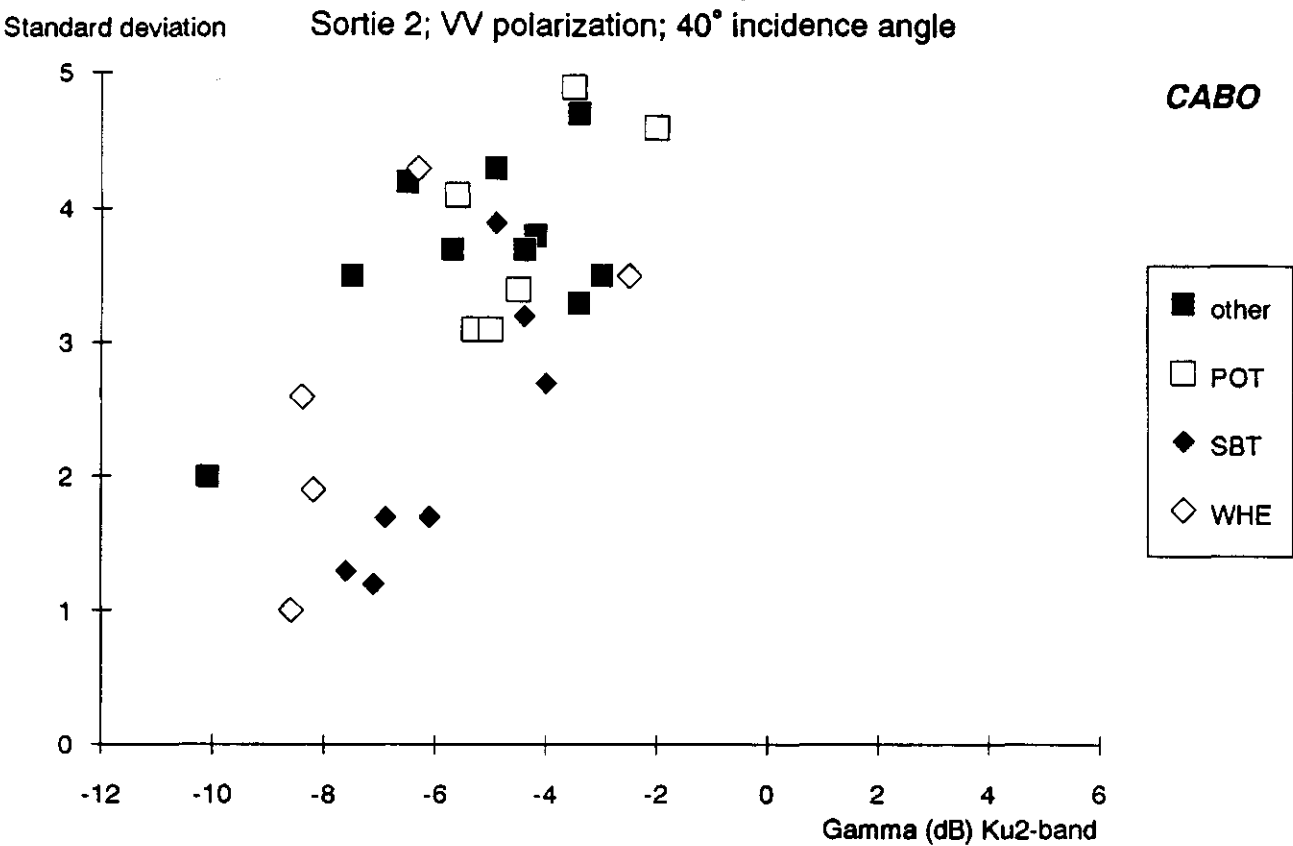


Fig. 9 Standard deviation (sortie 2, Ku2-band, VV, 40° i.a.) versus radar backscatter

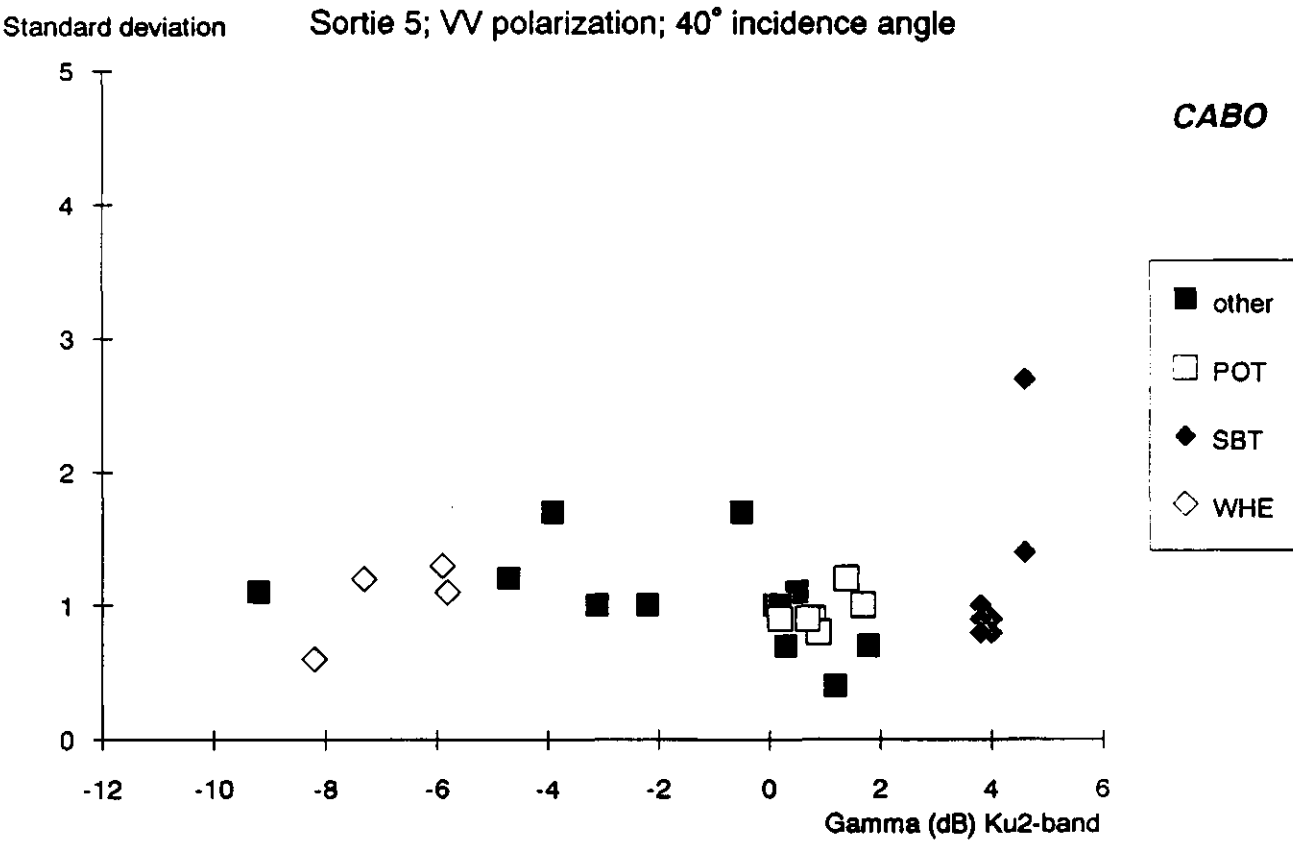


Fig. 10 Standard deviation (sortie 5, Ku2-band, VV, 40° i.a.) versus radar backscatter

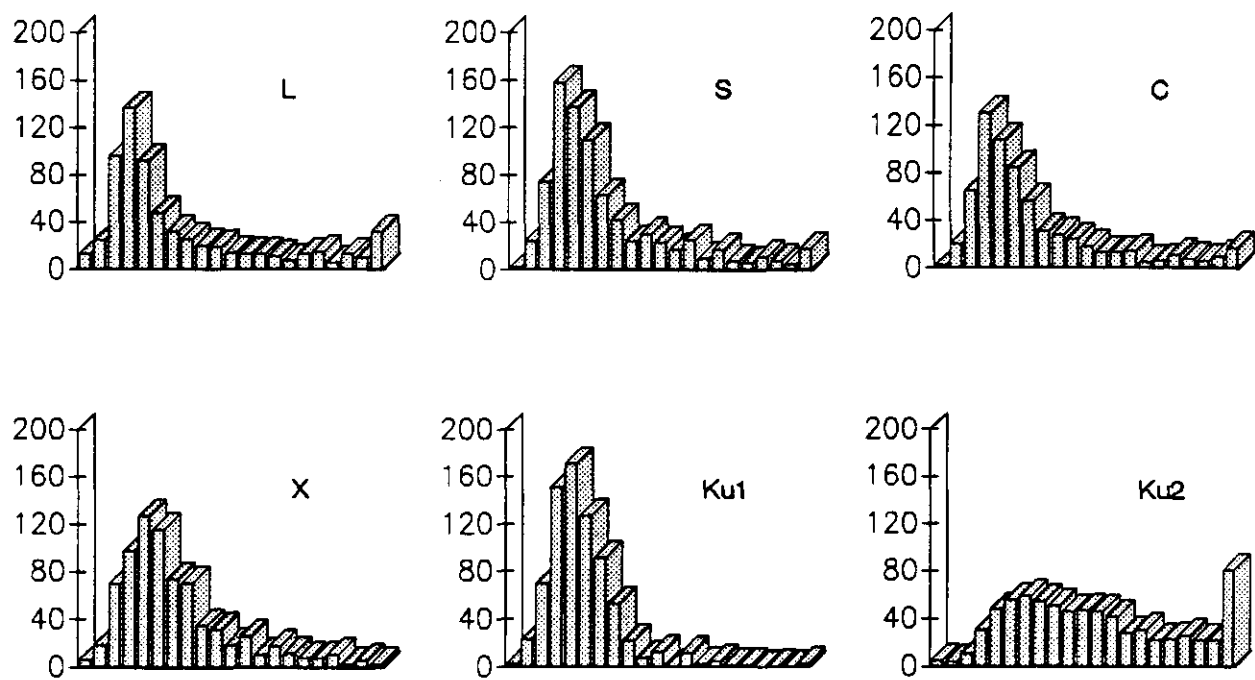


Fig. 11 Frequency distribution of the standard deviation of the radar backscatter in steps of 0.2 dB (all frequency bands, sortie 1-2)

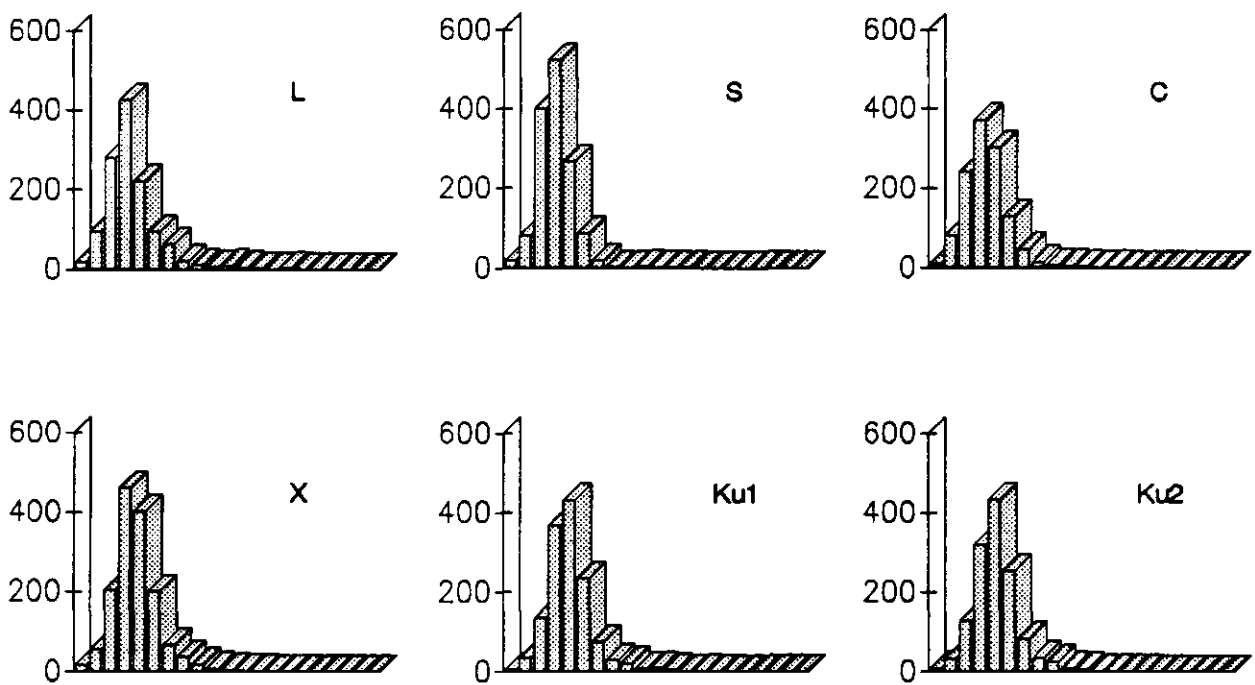


Fig. 12 Frequency distribution of the standard deviation of the radar backscatter in steps of 0.2 dB (all frequency bands, sortie 3-7)

2.3 Final data selection

The combination of the analyses in the previous paragraphs lead to a removal of suspicious data in the delivered data set.

First, in analogy with the 1987 data set, the radar data from individual fields with a standard deviation > 3 dB were removed. In the remaining data there were still a number of data-clusters which deviated from normal expected patterns. Some are known to be the result of an instrument failure. Others might have been the result of the decompression (only for sortie 1 and 2) or could have been the result of a 'wrong' attenuator setting. Table 1 sums up these deviating clusters. For the sake of a reliable data set, these clusters were also removed .

Table 1 Clusters of 'suspicious' field-average radar data that were removed from the data set

Sortie	Band	Polarization	Incidence angle	Remarks
1	X	HH	15°	
1	X	HH	60°	
2	C	HH	40°	Stdev > 1.8 dB
2	Ku1	HH	40°	Large spread
4	C	HH	20°-60°	
6	Ku1	HH	20°	Fields < 610
7	C	HH	20°-60°	Instr. failure
1	X	VV	15°	
3	C	VV	30°	
4	C	VV	60°	
7	C	VV	20°-60°	Instr. failure

To complete the overview of the final data set, table 2 shows for which frequencies whole track data were not present in the original data set delivered by the FEL-TNO (excluded by the FEL-TNO or not recorded by DUTSCAT).

Table 2a unavailable track data (HH polarization)

Sortie	Incidence angle						
	10°	15°	20°	30°	40°	50°	60°
1					C;Ku1		
2				C;Ku2			L;Ku1
3				all			
4			S				
5			S		Ku2		Ku1
6							
7							

Table 2b unavailable track data (VV polarization)

Sortie	Incidence angle						
	10°	15°	20°	30°	40°	50°	60°
1							X
2		C	L		C		
3			all			C	
4				C			
5			S;C			C	
6				Ku2	C		Ku1
7				all	C	C;Ku2	C

## 2.4 Overview final data set

This chapter presents a general overview of the 1988 DUTSCAT final data set (after all the exclusions described in previous chapters). Table 3 gives some statistics of the data: the minimum, maximum, average and number of field-average  $\gamma$  values is given for each frequency band, state of polarization and sortie.

When compared to the final data set of the 1987 data (Bouman et al, 1990) there are some general conclusions:

- The 1988 data set contains about three times the number of field-averaged backscatter values of the 1987 set.
- The mean values per sortie and per frequency band are, on the average, 2 dB higher in 1988 than in 1987.
- The dynamic range per frequency band is higher in 1988 than in 1987: the average dynamic range (over all sorties) for the L-, S- and Ku1-band in 1987 is respectively 11, 10 and 10 dB, where it is 19, 11 and 13 dB in 1988. Especially the higher values in the L-band are remarkable.

These differences are mainly caused by the fact that in 1987 all data were originally compressed during recording, while in 1988, compression only occurred during sortie 1 and 2. Therefore the 1988 data set is considered more reliable than the 1987 data set.

After phenomenological data description (chapter 3), the 1988 data set will also be compared with 'historical' X-band radar data (collected by the ROVE team), and with ERASME data (collected during Agriscatt 1988). This comparison will contribute to the assessment of the DUTSCAT 1988 data quality.

Table 3 Some statistics on the final DUTSCAT 1988 data set

L-band ; HH					L-band ; VV			
SRT	MIN	MEAN	MAX	N	MIN	MEAN	MAX	N
1	-28.3	-14.6	-0.3	151	-22.9	-13.0	-1.3	149
2	-22.8	-13.2	3.5	133	-21.3	-13.1	1.4	134
3	-21.6	-11.5	-6.1	103	-19.5	-11.9	-4.6	130
4	-18.1	-9.4	-1.0	129	-20.4	-10.3	-0.5	130
5	-17.9	-8.5	-1.9	129	-18.5	-9.3	-2.7	131
6	-17.6	-9.1	-2.2	133	-17.9	-9.8	-3.1	135
7	-24.4	-12.0	-5.0	136	-22.0	-12.0	-4.2	107
S-band ; HH					S-band ; VV			
SRT	MIN	MEAN	MAX	N	MIN	MEAN	MAX	N
1	-15.7	-9.0	-0.9	200	-15.6	-9.8	-2.8	192
2	-17.5	-10.6	-2.1	199	-15.7	-10.5	-3.0	166
3	-13.2	-6.8	-3.7	124	-13.2	-7.2	-3.9	159
4	-9.4	-4.4	-1.7	126	-11.6	-4.2	-0.3	158
5	-10.6	-4.9	-1.9	128	-12.3	-5.2	-0.5	126
6	-10.4	-4.6	-0.6	152	-10.9	-5.2	-1.1	152
7	-17.3	-7.3	-3.0	160	-14.0	-7.8	-3.1	124
C-band ; HH					C-band ; VV			
SRT	MIN	MEAN	MAX	N	MIN	MEAN	MAX	N
1	-21.0	-13.2	-2.5	149	-16.4	-10.3	-1.3	166
2	-18.3	-9.8	2.7	147	-15.3	-9.7	-1.4	143
3	-11.1	-5.0	-0.6	114	-13.9	-6.1	-0.5	95
4				0	-11.5	-2.6	3.6	88
5	-11.4	-5.3	-0.9	158	-11.0	-4.9	-1.0	93
6	-9.2	-4.0	1.2	153	-10.2	-3.8	-0.3	119
7				0				0
X-band ; HH					X-band ; VV			
SRT	MIN	MEAN	MAX	N	MIN	MEAN	MAX	N
1	-12.7	-7.9	-0.6	136	-12.4	-7.4	0.8	144
2	-11.8	-6.4	2.0	186	-11.8	-7.1	2.1	177
3	-7.8	-0.7	6.2	122	-10.6	-0.2	5.1	154
4	-7.1	0.3	5.9	156	-8.1	0.6	6.7	155
5	-13.6	-3.1	2.3	157	-12.2	-3.0	2.6	155
6	-12.5	-4.9	0.5	153	-12.7	-4.5	1.5	150
7	-11.1	-5.2	0.9	159	-12.9	-4.0	1.4	124
Ku1-band ; HH					Ku1-band ; VV			
SRT	MIN	MEAN	MAX	N	MIN	MEAN	MAX	N
1	-10.6	-5.2	1.9	179	-10.7	-4.9	2.0	209
2	-7.4	-3.6	1.6	153	-9.4	-5.6	0.7	180
3	-7.5	-0.8	4.3	122	-9.5	-1.1	3.8	150
4	-7.9	-0.6	4.7	152	-8.9	-0.5	5.6	155
5	-8.4	-0.2	4.4	124	-9.7	-0.6	4.9	152
6	-7.8	0.2	5.2	133	-7.9	0.5	5.6	97
7	-13.6	-4.3	1.7	154	-13.5	-3.8	2.1	110
Ku2-band ; HH					Ku2-band ; VV			
SRT	MIN	MEAN	MAX	N	MIN	MEAN	MAX	N
1	-14.8	-6.7	-1.5	154	-11.3	-5.3	-0.2	151
2	-12.7	-6.7	-0.2	138	-11.7	-6.8	-1.8	117
3	-8.2	-2.1	3.4	122	-9.7	-1.5	2.9	153
4	-9.7	-3.1	2.2	146	-11.1	-2.1	3.3	155
5	-7.4	-1.0	4.1	125	-9.2	-0.3	6.3	150
6	-10.7	-2.2	3.0	147	-10.5	-2.0	3.7	117
7	-13.0	-4.7	0.9	146	-13.9	-4.6	1.2	90

### 3 Qualitative description

The description of the final data set is focussed on the VV polarized radar backscatter of the three main crops beet, potato and wheat. The differences between the VV and HH backscatter are only small and for a general description the interpretation of one state of polarization suffices. However, because of the exclusion of suspicious data (previous paragraph), some examples will be illustrated by the HH polarized radar backscatter.

The description will take into account:

- The occurrence of some interesting features in the radar backscatter related to specific phenomena in the field (§ 3.1).
- The angular behaviour of the radar backscatter for the different crop types (§ 3.2).
- The discrimination of the different crop types by the different frequencies (§ 3.3).
- The temporal behaviour of the radar backscatter for the different crop types (§ 3.4).
- The frequency behaviour of the radar backscatter for the different crop types (§ 3.5).
- The specific crop behaviour of the radar backscatter for the different frequencies (§ 3.6).

#### 3.1 Special features

During the examination of the angle plots of the DUTSCAT 1988 data, a number of interesting features were detected which related to specific ground conditions. These features will be described per crop type.

Potato:

For some potato fields the effect of the orientation of the ridges with respect to the incident radar beam was clearly recognized. Two out of the seven measured potato fields (fields 412 and 422) had a ridge direction perpendicular to the incident radar beam. The other five fields had a ridge direction along that of the radar beam.

At sortie 1 and 2, when the soil was bare, the fields with the perpendicular ridge direction had a higher radar backscatter than the other fields. This effect was present in all frequency bands and the magnitude of it depended on the angle of incidence, figures 13-14. Clearly, the microwaves were especially reflected from the sides of the perpendicularly oriented ridges. At low and steep angles of incidence, this effect was relatively smallest. At medium angles of incidence, the effect was largest with a maximum at 30° incidence angle, corresponding with the slope angle of the ridges.

Somewhere between sortie 3 and 4, the canopy of the crop closed and completely covered the underlying soil. In all frequency bands but the L-band, the effect of ridge orientation was no longer detectable on the radar backscatter, figure 15. Apparently the microwaves at these wavelengths could not penetrate the canopy sufficiently to allow for a soil contribution in the backscatter. In the L-band, however, the effect of ridge orientation was still present, figure 16. Thus the microwaves at 25 cm wavelength could penetrate the canopy (two-way) and the soil contributed significantly to the radar backscatter.

The observations for the higher frequency bands completely agree with the findings of Bouman and van Kasteren (1991) in the historical ROVE ground-based X-band data set.



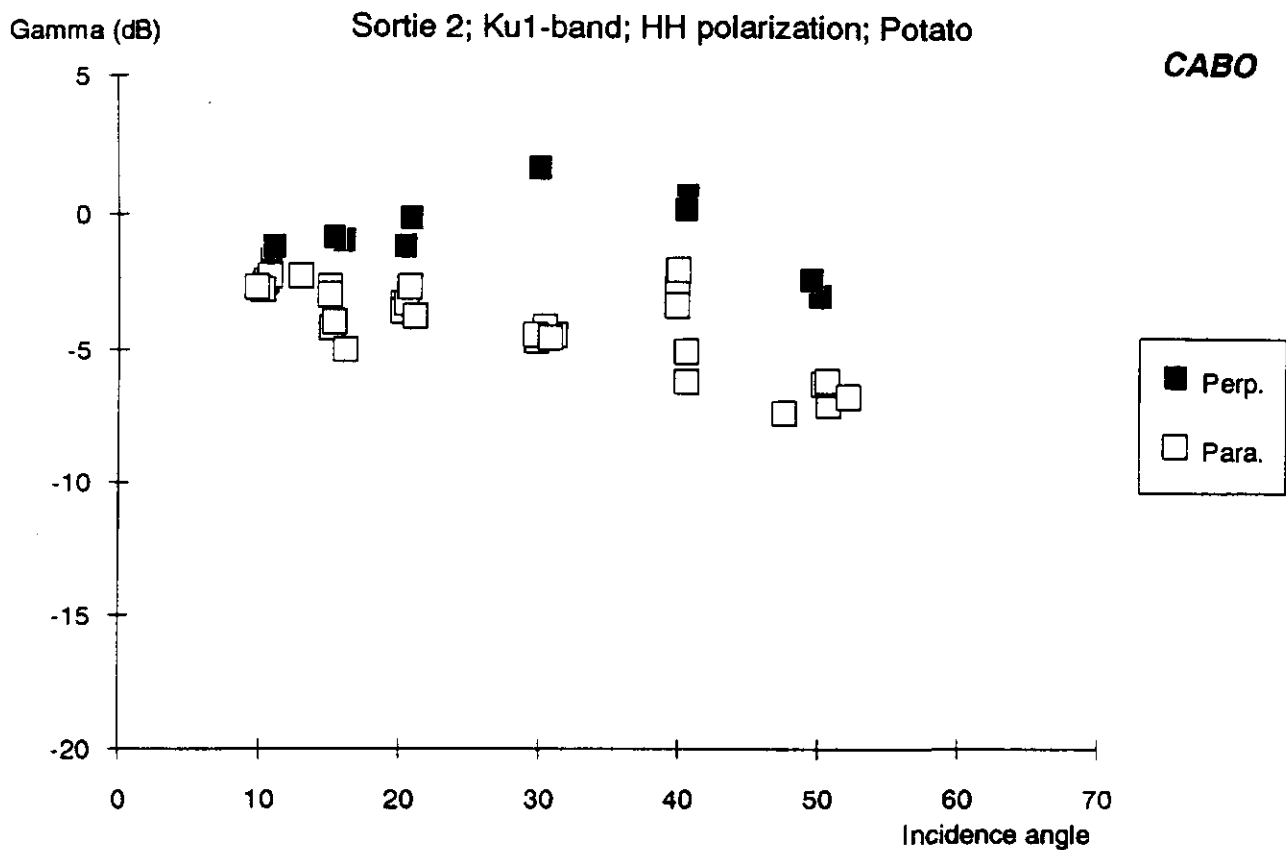


Fig. 13 Radar backscatter (Ku1-band, HH, sortie 2) versus incidence angle for potato with ridge orientations perpendicular (perp.) and parallel (para.) to the incident microwaves

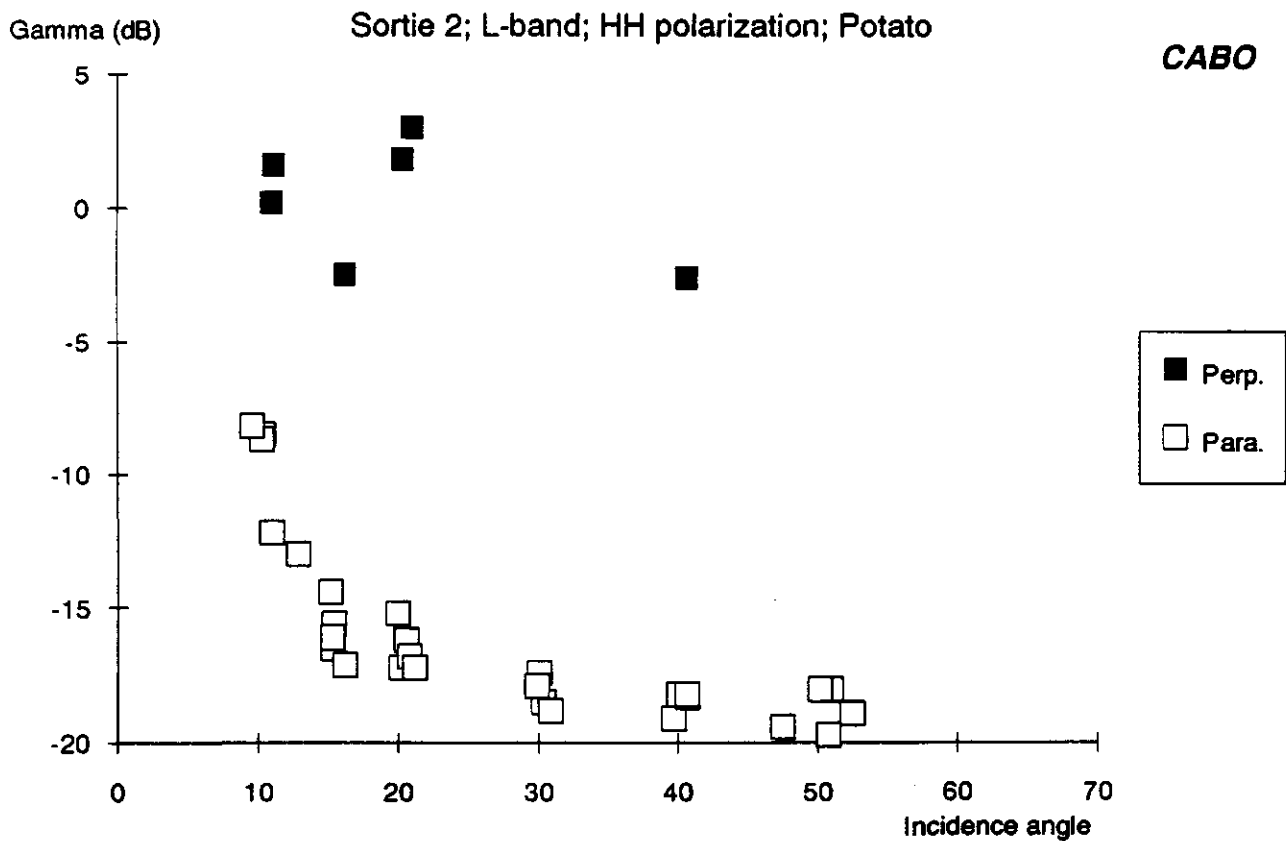


Fig. 14 Radar backscatter (L-band, HH, sortie 2) versus incidence angle for potato with ridge orientations perpendicular (perp.) and parallel (para.) to the incident microwaves

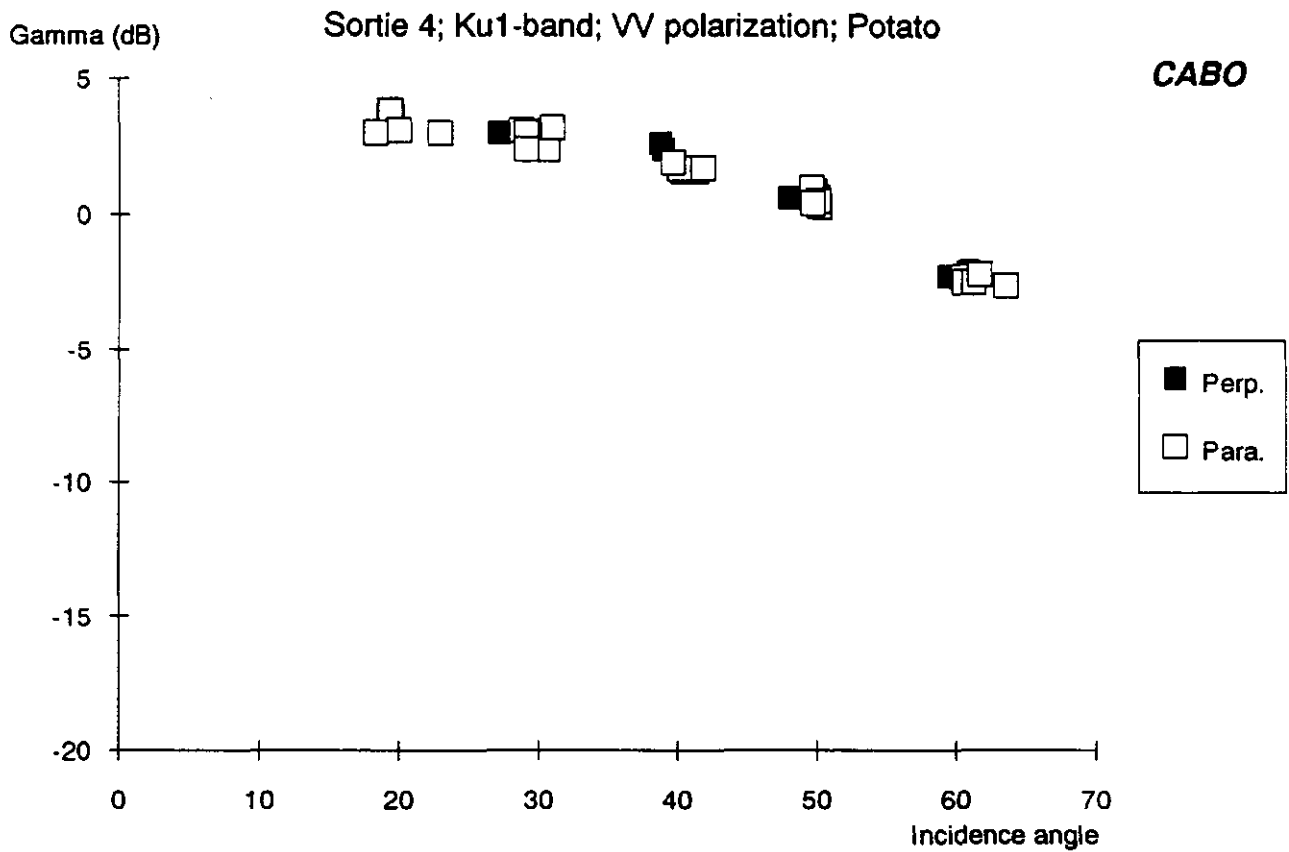


Fig. 15 Radar backscatter (Ku1-band, VV, sortie 4) versus incidence angle for potato with ridge orientations perpendicular (perp.) and parallel (para.) to the incident microwaves

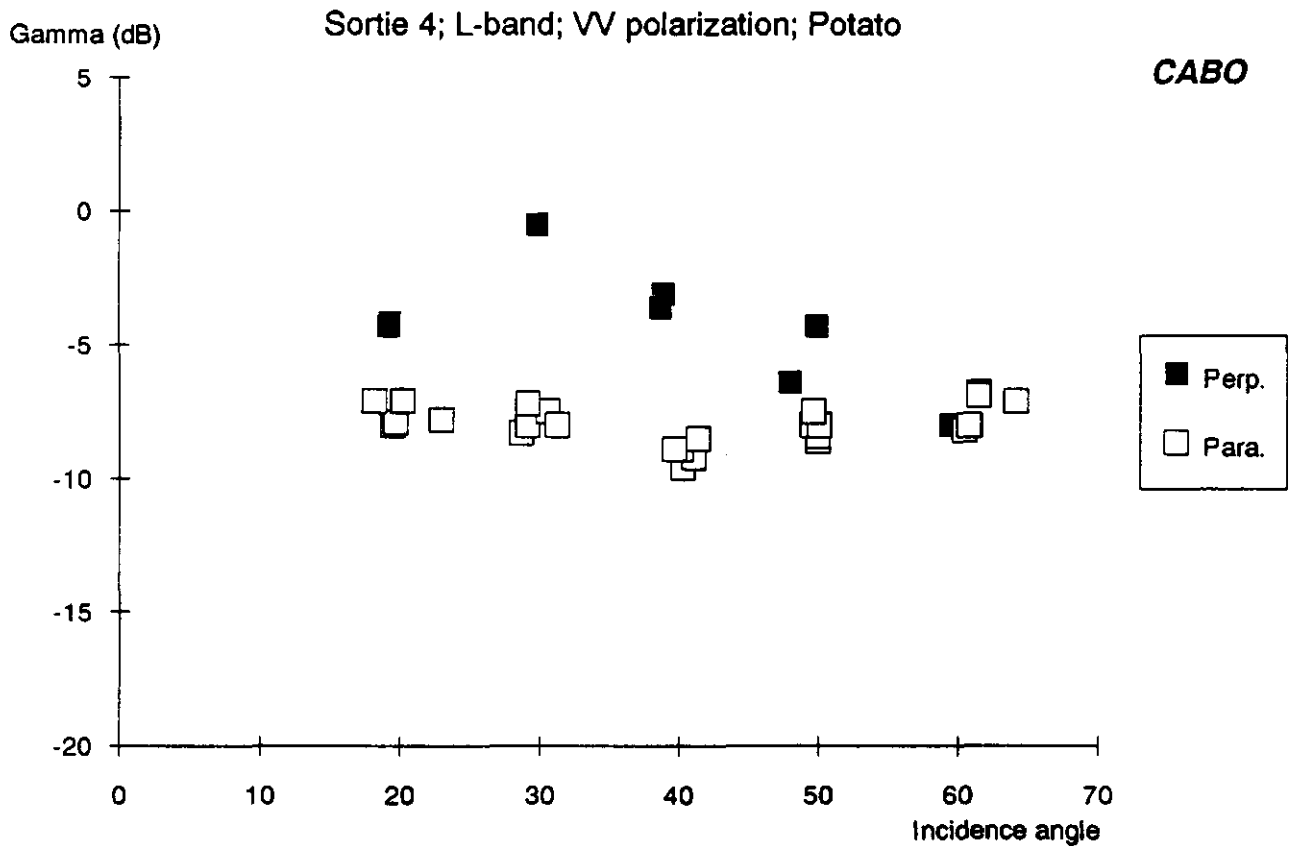


Fig. 16 Radar backscatter (L-band, VV, sortie 4) versus incidence angle for potato with ridge orientations perpendicular (perp.) and parallel (para.) to the incident microwaves

Beet:

At sortie 1 the effect of surface roughness of the soil was detected in the radar backscatter. After sowing of the beet, the fields 511, 512 and 513 were smoothed with a so-called Cambridge roll before sortie 1. The other fields (361, 362, 721 and 722) were rolled after sortie 1 and thus still had a relatively rough surface.

The effect of this difference in surface roughness depended on the frequency band and the angle of incidence. At low frequency bands, the effect was best notable. In the Ku1-band, there was no effect at all where in the S-band the effect could amount to 4 dB difference, figures 17-18. The 'rolled' surfaces had a lower radar backscatter than the 'unrolled', rough surfaces. Apparently, the 'rolled' surface was still rough to wavelengths up to the X-band. Only at the C-, S- and L-band did the 'rolled' surface become specular to the incident microwaves, resulting in lower values of the radar backscatter.

Wheat:

Two interesting features were detected in the radar backscatter of wheat: a possible effect of crop height and the effect of lodging of the crop.

At sortie 3, three fields (540, 561 and 760) had a crop which was some 10 cm higher than the crops on the other fields. The radar backscatter from these crops was lower than that of the other crops in the high frequencies of the Ku1-, Ku2- and the X-band, figure 19. The differences were only small, about 1 dB at HH and 2 dB at VV polarization, but agree well with historical observations in the ROVE ground-based X-band data set (Bouman and van Kasteren, 1989). In the lower frequency bands, there were no differences between the radar backscatter of these fields.

At sortie 6, the canopy of the crop on field 540 was for 50% lodged while the crops on the other fields still stood mostly erect. This effect of lodging had a large effect on the radar backscatter in all frequency bands and angles of incidence, figures 20-21. The backscatter of the lodged field was higher than that of the non-lodged fields. Table 4 summarizes the maximum differences between the lodged crop and the others in all frequency bands. The effect was largest at the X-band, and seemed to decrease both with higher frequencies (only a tendency) and lower frequencies (more clearly recognized).

Table 4 Maximum effect of lodging on the radar backscatter in the different frequency bands

Polarization	Frequency band					
	L	S	C	X	Ku1	Ku2
HH	2	4.5	5	8	7	6
VV	-	4	4.5	6	6	5

Again, the observations agree very well with those made by Bouman and van Kasteren (1989).

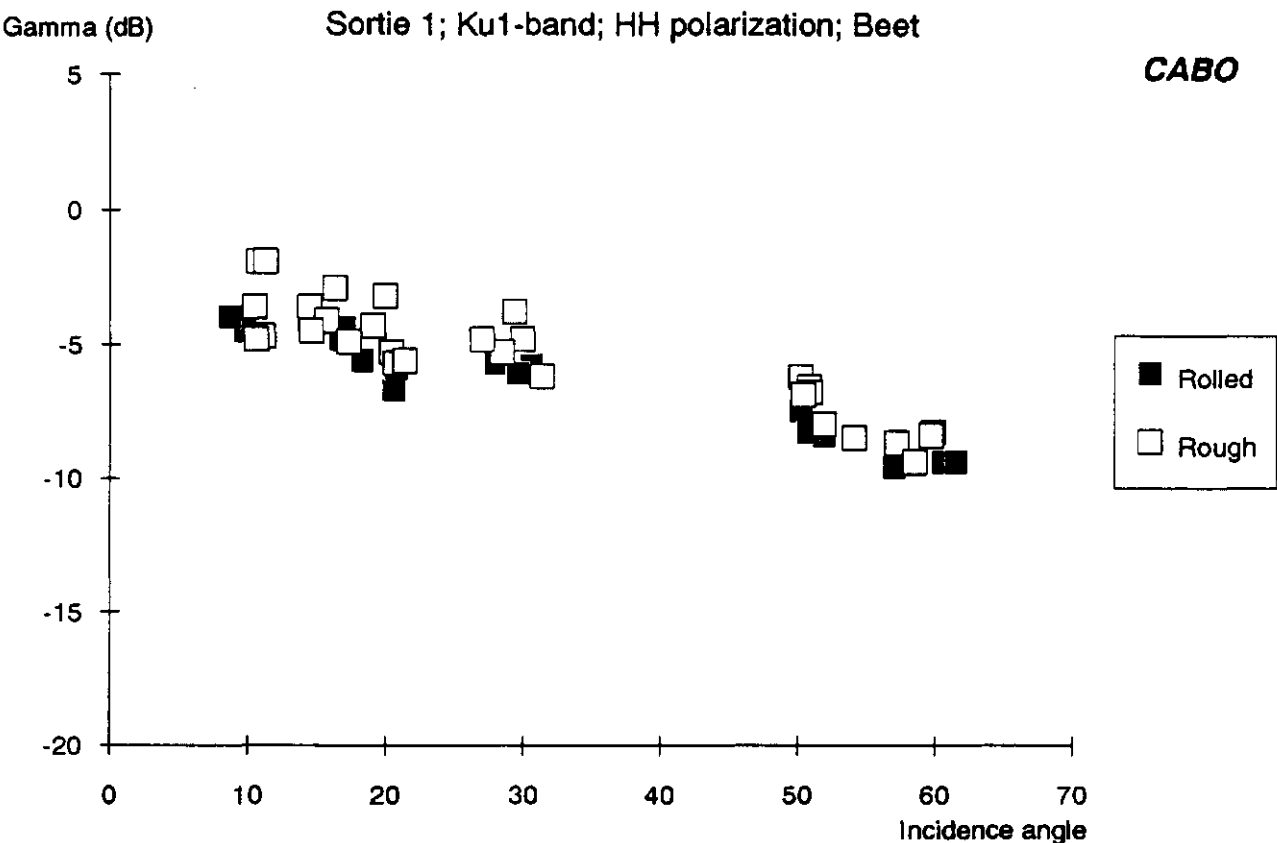


Fig. 17 Radar backscatter (Ku1-band, HH sortie 1) versus incidence angle for bare 'beet-soil' with a rolled and a unrolled (rough) surface

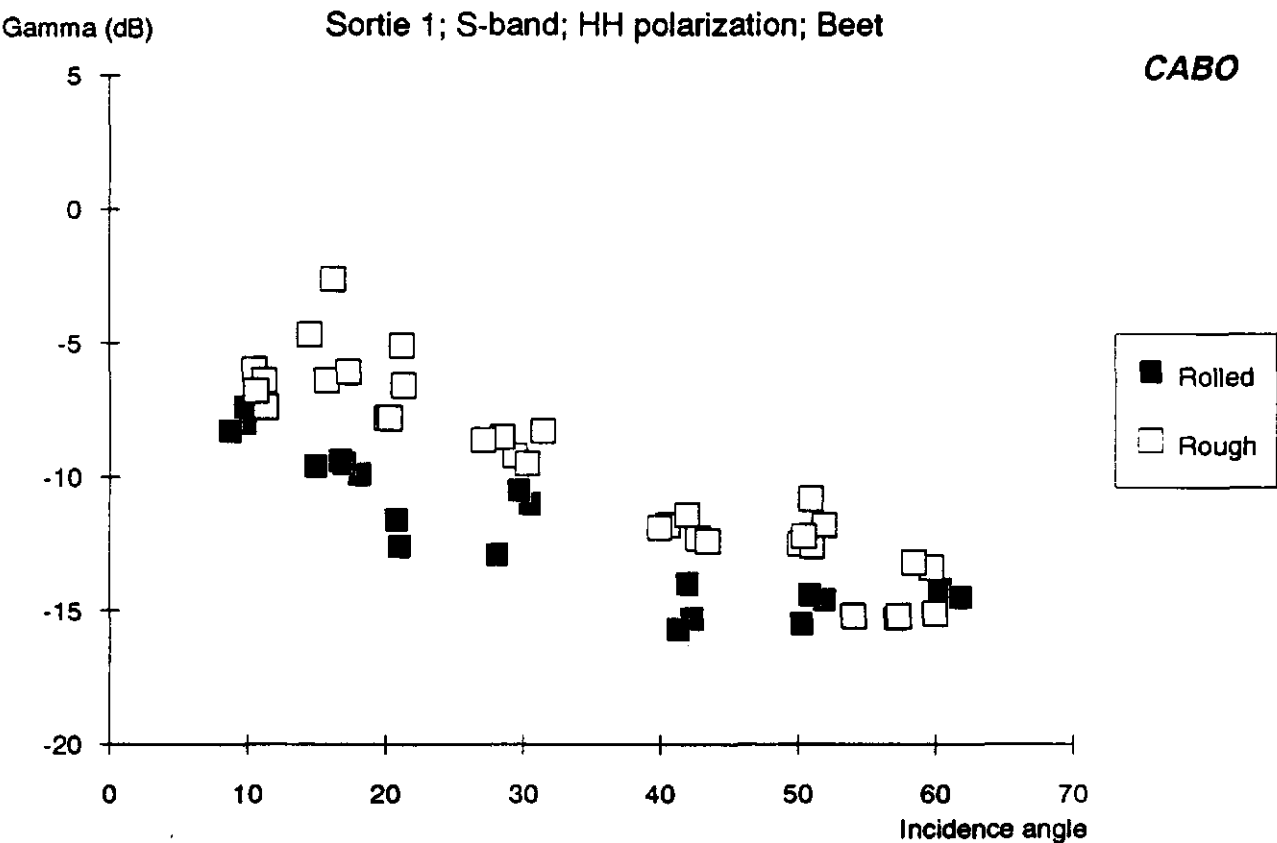


Fig. 18 Radar backscatter (S-band, HH sortie 1) versus incidence angle for bare 'beet-soil' with a rolled and a unrolled (rough) surface

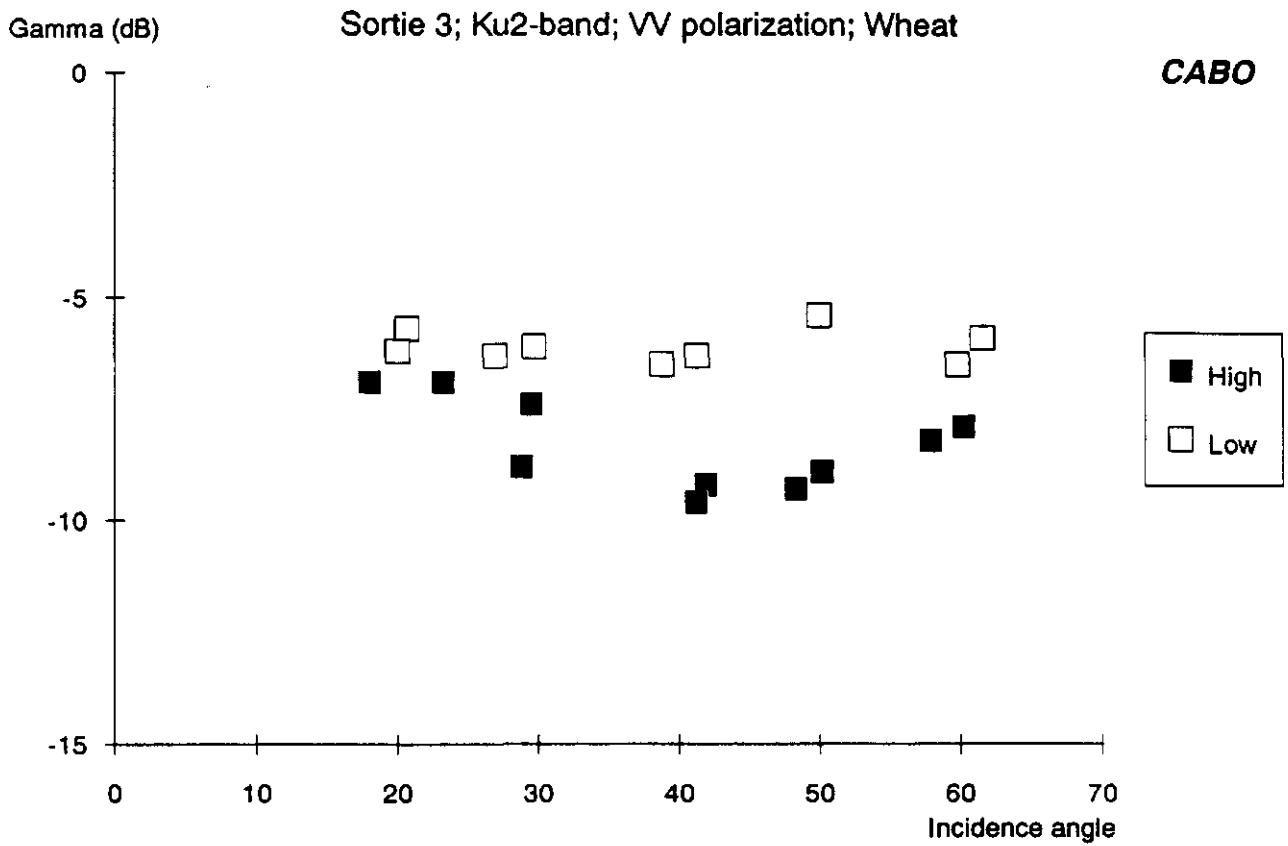


Fig. 19 Radar backscatter (Ku2-band, VV, sortie 3) versus incidence angle for wheat, 'high' and 'low' refer to the relative height of the crop

For the investigation of general trends in the radar data, the fields with the special features described above are excluded from further analysis:

- radar data of fields 412 and 422: all sorties, all frequencies
- radar data of fields 511, 512 and 513: sortie 1, all frequencies
- radar data of field 540: sortie 6, all frequencies

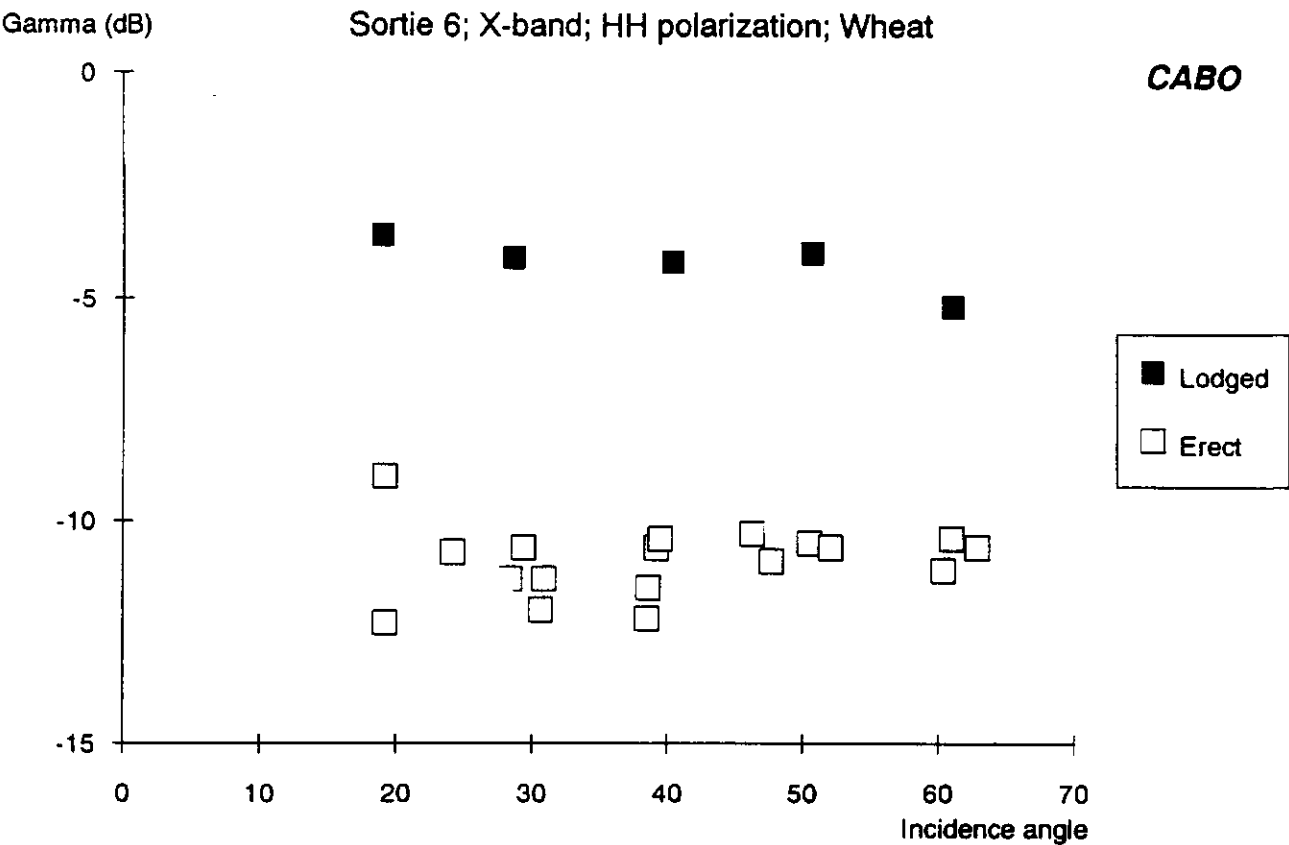


Fig. 20 Radar backscatter (X-band, HH, sortie 6) versus incidence angle for lodged and non-lodged (erect) wheat crops

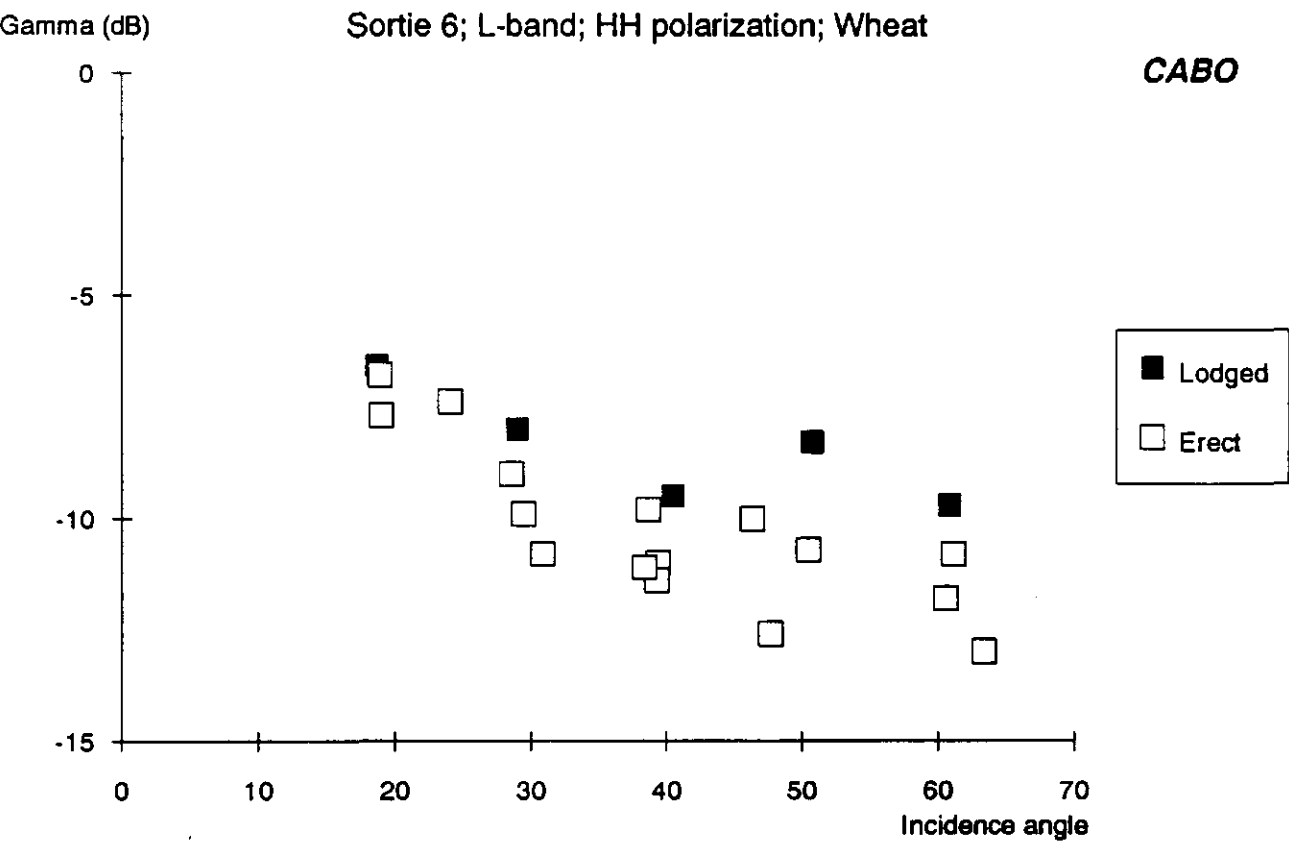


Fig. 21 Radar backscatter (L-band, HH, sortie 6) versus incidence angle for lodged and non-lodged (erect) wheat crops

### 3.2 Angular behaviour

The angular behaviour of the radar backscatter of the three crop types is presented for a selection of sorties and frequencies in figures 22-27.

In general the angular dependency of the radar backscatter for each crop type is smooth (there are no severe fluctuations in the order of several dB). Two general situations will be described: mainly bare soil (sorties 1-2) and closed crop covers (sorties 4-7)

#### Mainly bare soil:

A clear angular dependency is present for the lower frequencies: the radar backscatter steeply decreases from 10° to 20° incidence angle, after which it only decreases a little more with further increasing incidence angle. In the L-band, the 'crop-soil' types are grouped together and a differentiation can be made already between winter wheat (already 40-50% cover at sortie 1 and 2) and the 'crop-soil' of beet and potato (0% cover), figure 22. The angular dependency decreases with increasing frequency band. From the Ku1-band on, the curves are horizontal and all 'crop-soil' types are grouped together in narrow clusters, figure 23. No 'crop-soil' type discrimination can be made here.

These observed trends agree with the trends found in the 1987 data set. In 1987, the clusters of 'crop-soil' types were more separated from each other and 'crop-soil' types could already be differentiated at sortie 1. The differences between the 'crop-soil' types were, however, also not very large.

#### Closed crop canopies:

The angular curves of the closed crop canopies show a gradual change from the high to the low frequency bands. In the Ku2-band, the following patterns are recognized, figure 24:

- the angular curves of beet are horizontal (reflecting the plagiophile leaf angle distribution (de Wit, 1965)),
- the radar backscatter of potato decreases with increasing incidence angle (reflecting a planophile leaf angle distribution (de Wit, 1965)),
- the angular curves of wheat are horizontal.

Furthermore, the backscatter of beet is (except at the low angles of incidence) higher than that of potato, and that of wheat is lower than that of potato.

With decreasing frequency band, the relative position and patterns of (some of) the curves gradually change. In the X-band, figure 25, the curve of potato is less angular dependent and the level of the curve reaches that of beet. The curve of wheat remains relatively unchanged (horizontal). In the S-band, figure 26, the curves of beet and potato are both horizontal and largely overlap. The curve of wheat now also changes, it has become more angular dependent: the radar backscatter increases from medium angles of incidence with increasing angle of incidence. The backscatter at 20° incidence angle is also generally larger than that at 30° incidence angle. Therefore, the curves appear either concave (since no measurements were made at incidence angles lower than 20°, this can not truly be verified) or increasing with incidence angle. In the L-band, figure 27, the changes in the (relative) patterns are largest.

The angular curves of beet and potato are both horizontal now, but the backscatter of potato is higher than that of beet. The curve of wheat has again completely changed from that in the S-band. Now the backscatter decreases with increasing incidence angle from 20° onwards. In general, the radar backscatter of wheat is lower than that of beet.

The differences between the angular curves of the various sorties with a crop cover (sorties 3-7) are small. Naturally, the patterns presented above become more pronounced from 40-50% crop cover of beet and potato (sortie 3) to the middle and end of the growing season with a fully developed and completely closed crop cover (sortie 5, 6 and 7). Especially the relative position of the curves of potato change relatively most (with respect to those of beet) during the growing season. In the L-band, the backscatter of potato is generally on the same level as that of beet at sortie 3. One sortie later, the backscatter of potato becomes higher than that of beet at high angles of incidence while it is still on the same level at low and medium incidence angle. At sortie 5, the backscatter of potato is generally higher than that of beet at all angles of incidence and remains so up to sortie 7.

The general trends in this data set again agree with the findings in the 1987 data set. However, because of the large loss of data in 1987, the observed trends here can only be confirmed partially. On the other hand, the 1987 data do not contradict the findings here.



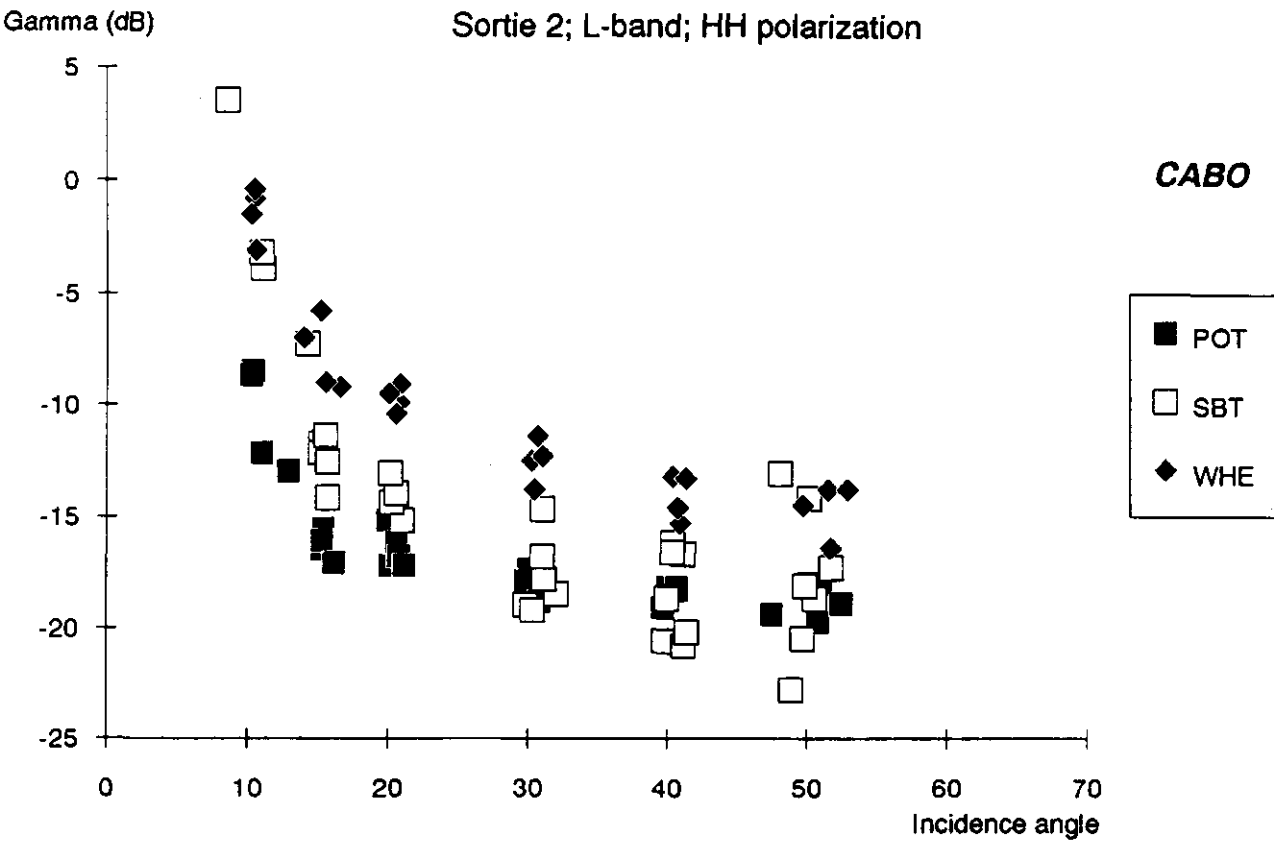


Fig. 22 Radar backscatter of 'beet-soil', 'potato-soil' and 'wheat-soil' (sortie 2, L-band, HH) as a function of incidence angle

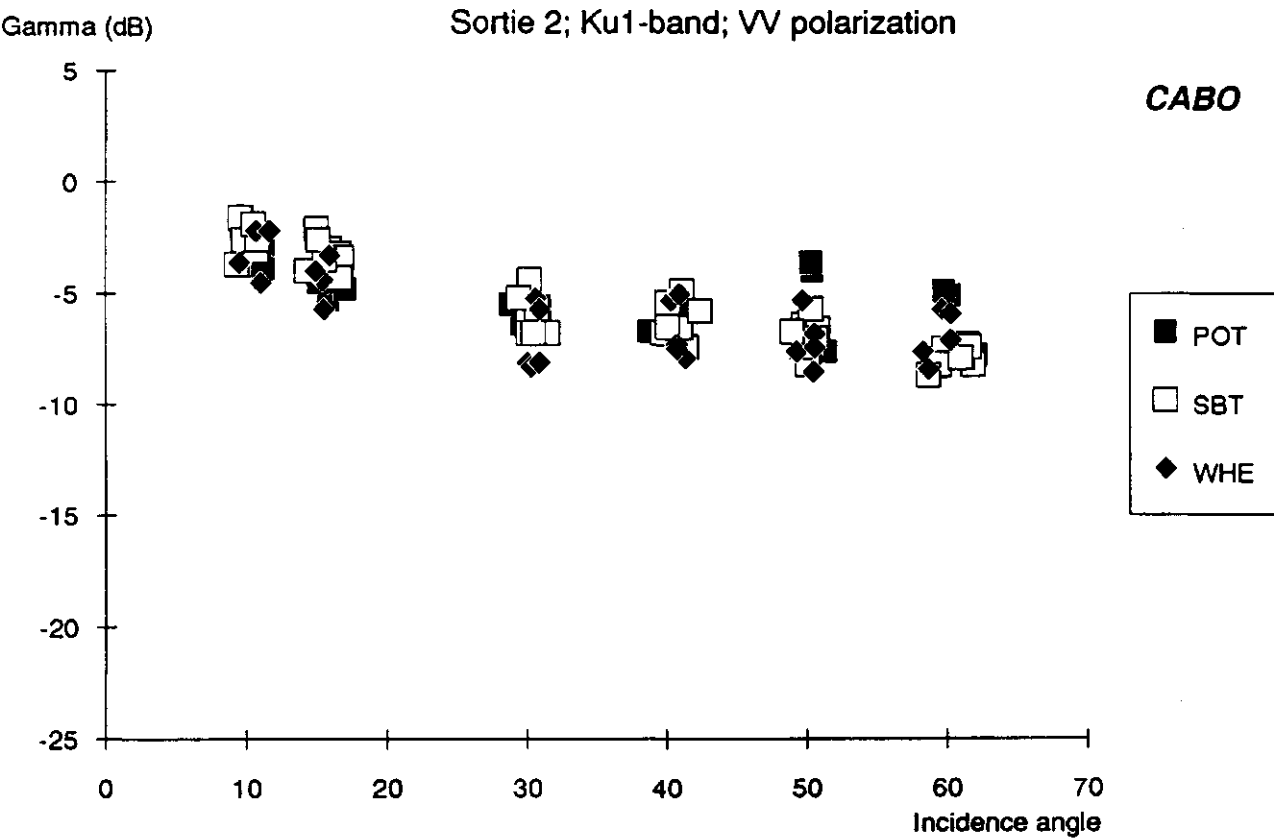


Fig. 23 Radar backscatter of 'beet-soil', 'potato-soil' and 'wheat-soil' (sortie 2, Ku1-band, VV) as a function of incidence angle

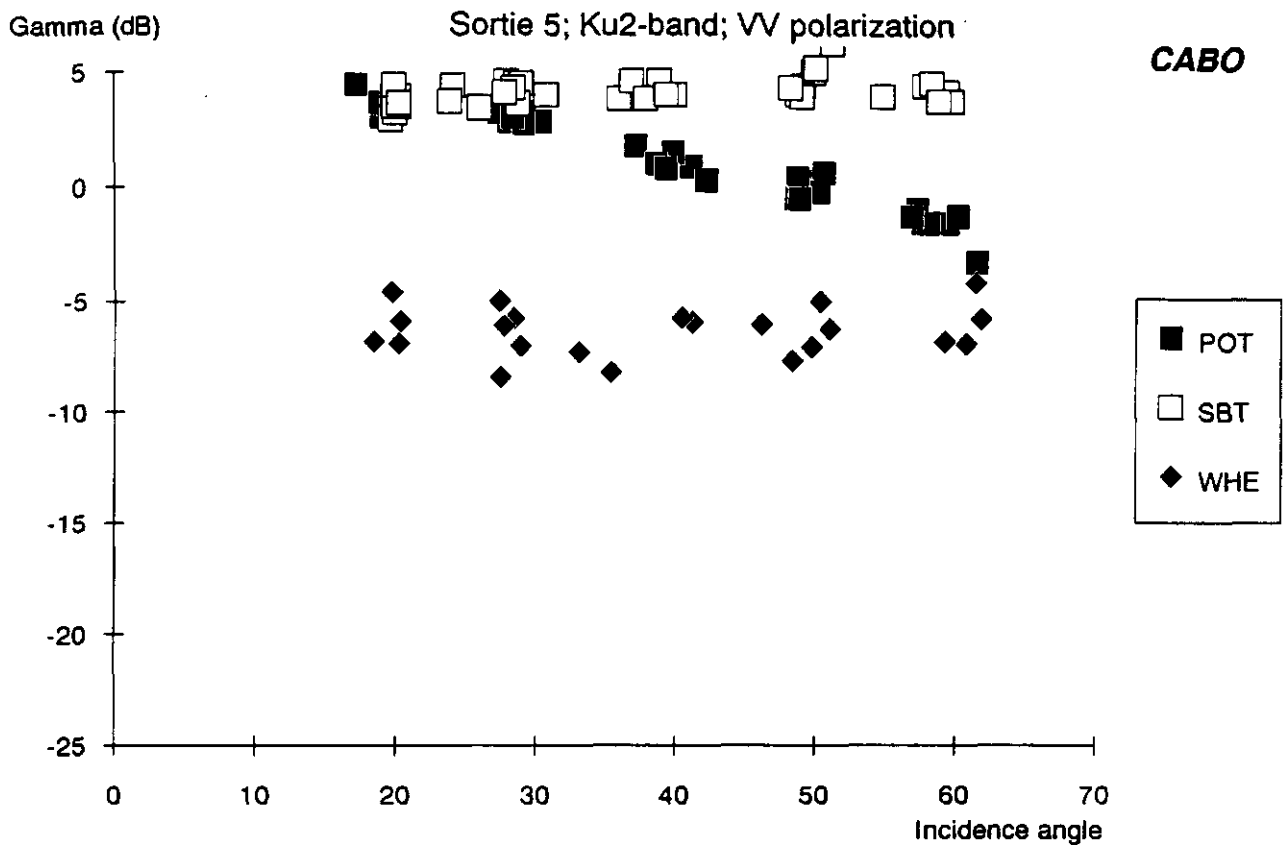


Fig. 24 Radar backscatter of beet, potato and wheat (sortie 5, Ku2-band, VV) as a function of incidence angle

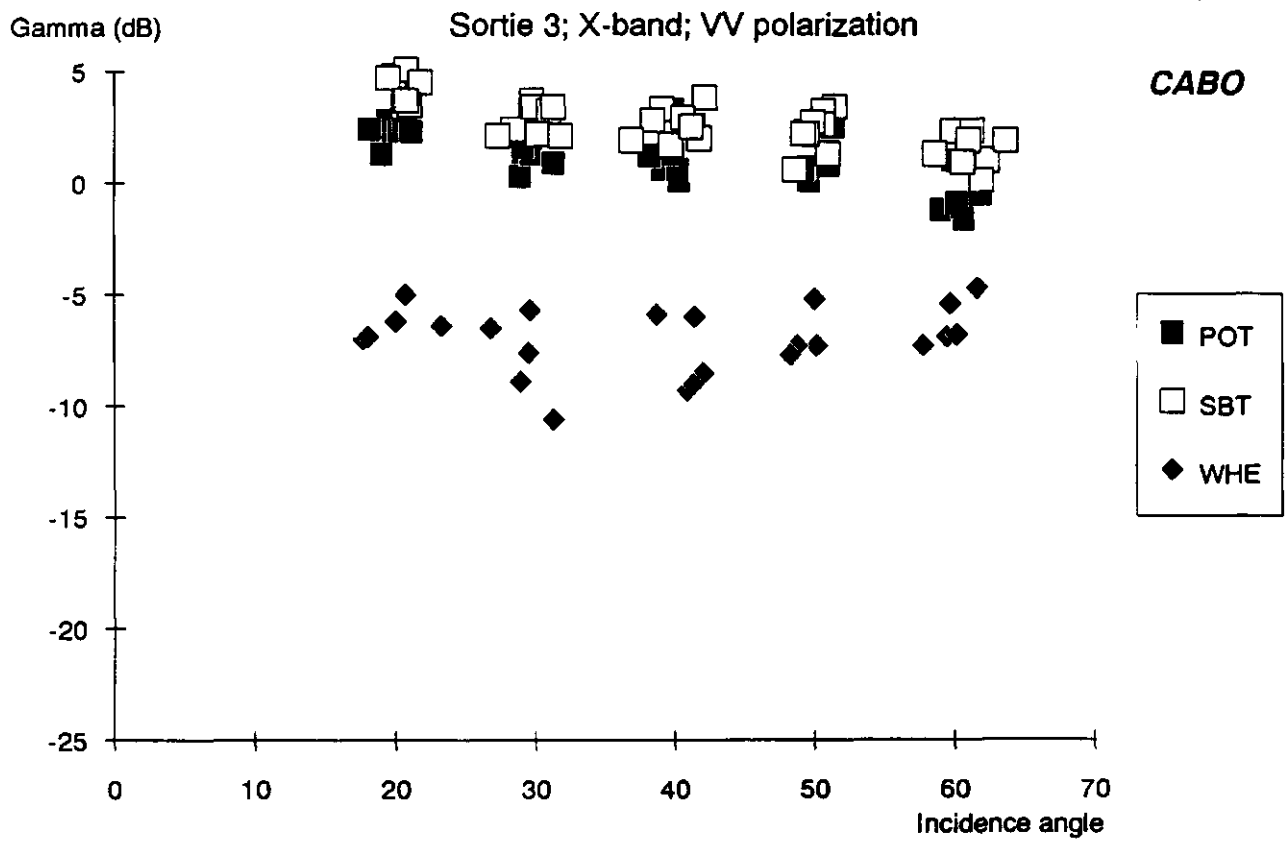


Fig. 25 Radar backscatter of beet, potato and wheat (sortie 3, X-band, VV) as a function of incidence angle

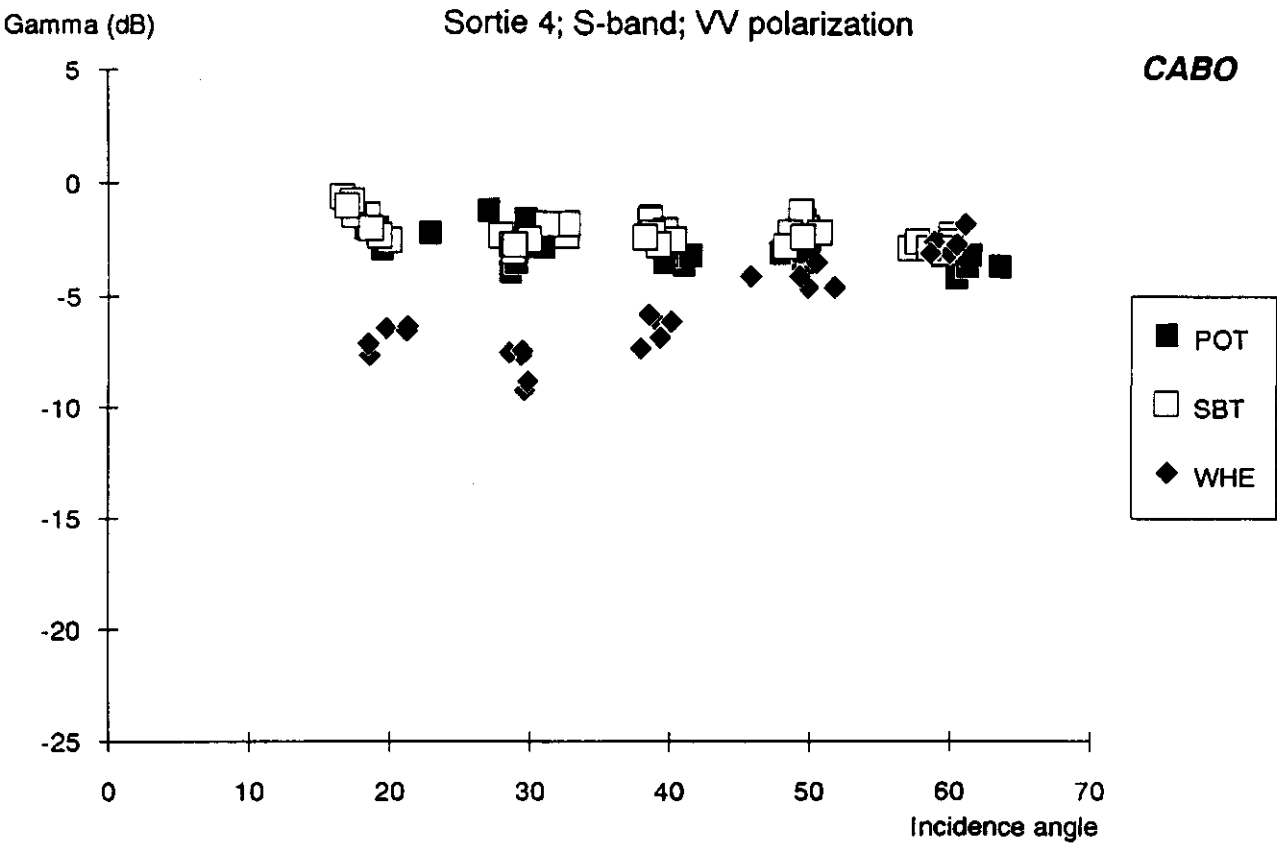


Fig. 26 Radar backscatter of beet, potato and wheat (sortie 4, S-band, VV) as a function of incidence angle

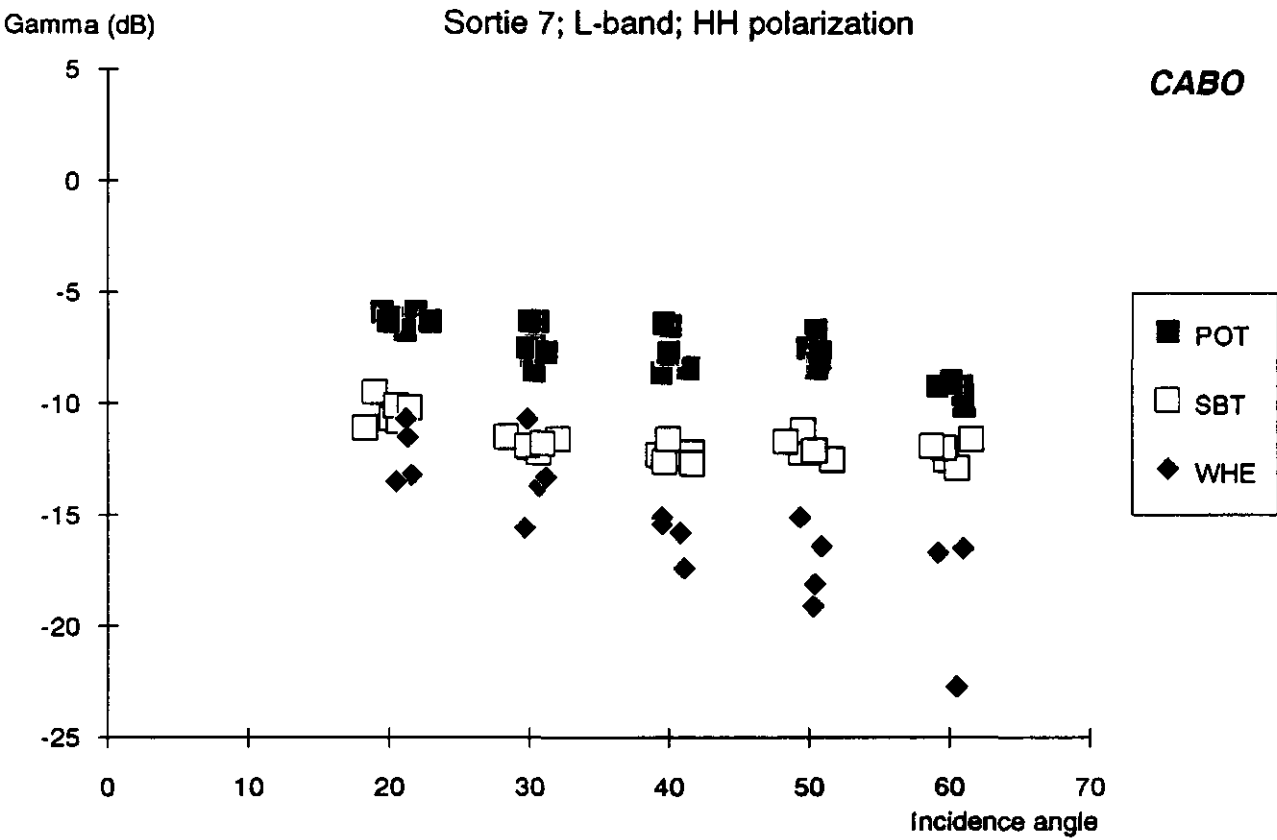


Fig. 27 Radar backscatter of beet, potato and wheat (sortie 7, L-band, HH) as a function of incidence angle

### 3.3 Crop type discrimination

Based on the analysis in the previous paragraph, the frequency bands are divided into two frequency groups. One group containing the L- and S-band, and a second group containing the C-, X-, Ku1- and Ku2-band. From figures 22-27 it is derived that a combination of two frequencies from either groups will give the best possibilities for crop type discrimination. Clusters of crop types in two frequency bands are visualized in feature space plots, figures 28-33. Combinations are made here of the L-S, L-Ku1 and S-Ku1 bands for mainly bare soil (sortie 2) and crops with closed cover (sortie 5), in analogy with the analysis of the 1987 data set.

For mainly bare soil the L-band offers the best possibilities. Especially at steep incidence angles, figures 28, 30 and 32, the L-band clearly separates all three 'crop-soils'. The S-band only separates 'wheat-soil' (with 40-50% cover) from 'potato-soil', while the clusters of beet and potato have some overlap. In the Ku1-band, there is only a very slight distinction between 'beet-' and 'potato-soil' while the 'wheat-soil' (with 40-50% cover) encompasses both the other 'crop-soils'. All three 'crop-soil' types in this band are narrowly clustered between -2 and -5 dB.

For crops, the best frequency for discrimination is one of the high frequency bands X-, Ku1- or Ku2-band, at a medium to high angle of incidence, figure 31. Here, the crops are well separated in the Ku1-band: beet has the highest level of radar backscatter, potato a medium level, and wheat the lowest level. In the L-band, the clusters of beet and wheat have some overlap, and in the S-band, the backscatter of beet is nearly on the same level as that of potato, figures 29 and 33. The combined use of a low and a high frequency may increase the (classification) sensitivity, figure 31, but does not seem imperative.

When compared to the results with the 1987 data, some differences exist in the Ku1-band. First, the discriminating possibilities between the 'bare-soil' types was slightly better in 1987. The opposite is true, however, for the crops with closed cover. In 1987, potato and beet had about the same radar backscatter in this band, while in 1988 the backscatter of beet was clearly higher. The similarity between the backscatter of beet and potato in 1987 could be the result of the compression of the original recordings. Both years, the pattern in the L-band was similar: at the end of the growing season the backscatter of potato increased above that of beet.

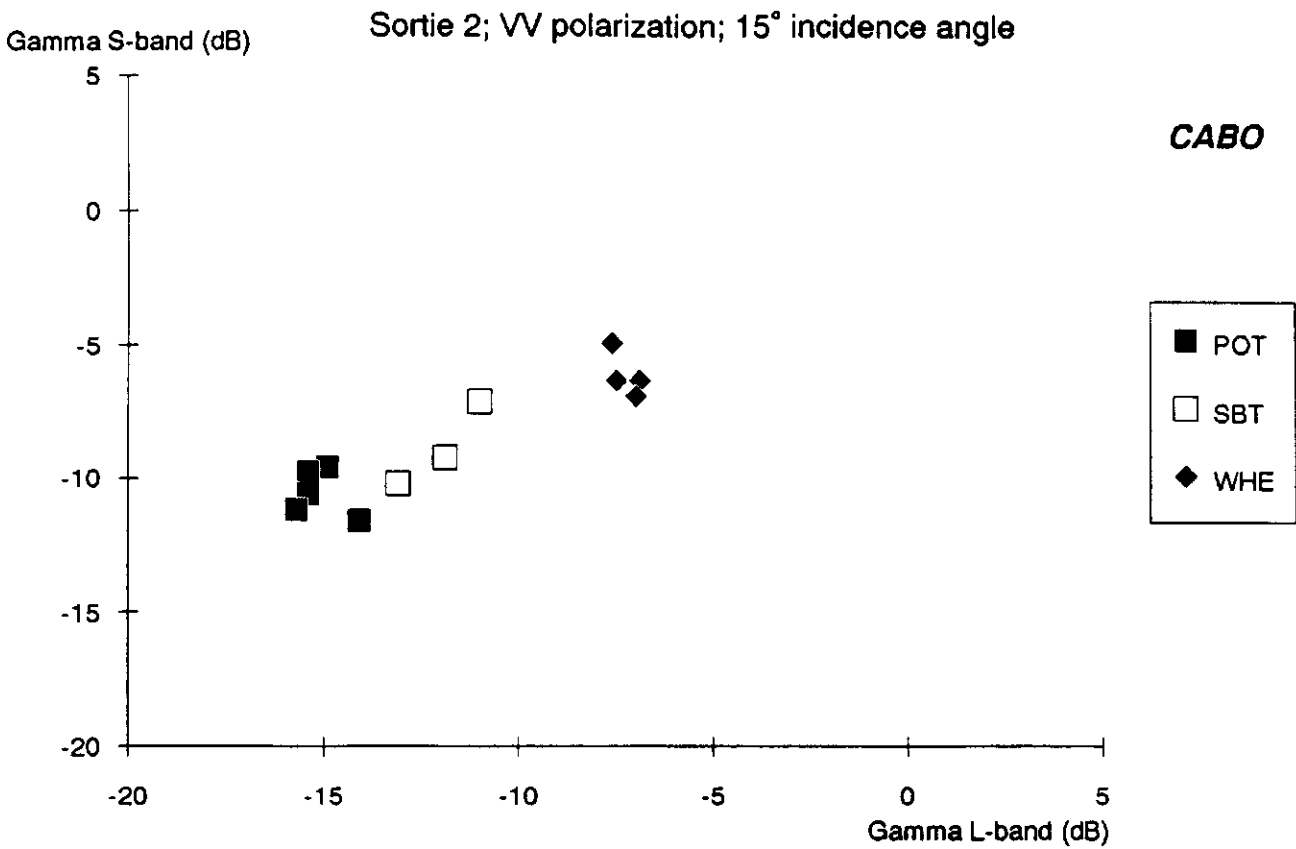


Fig. 28 Feature space plot (sortie 2, VV, 15° i.a.) of the S-band versus the L-band for 'potato-soil', 'beet-soil' and 'wheat-soil'

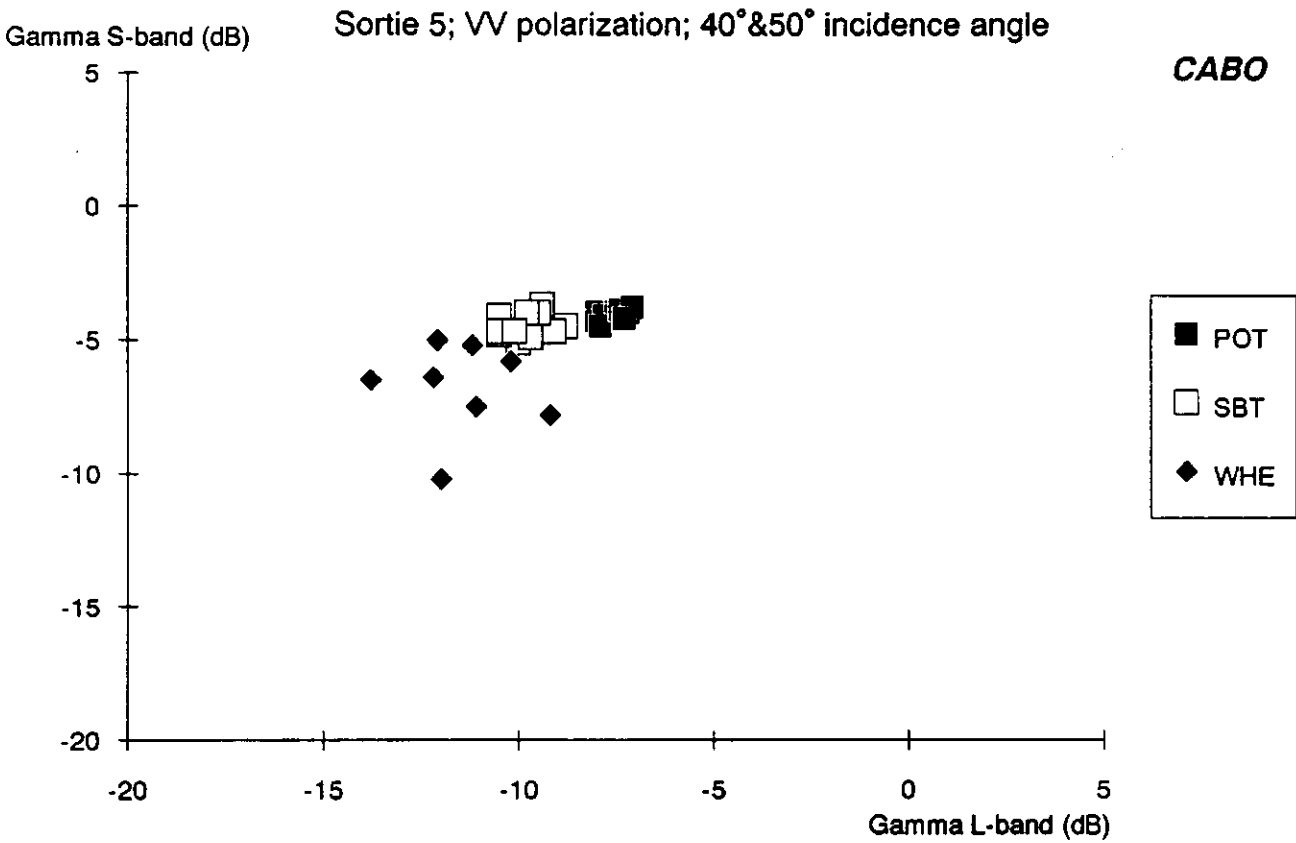
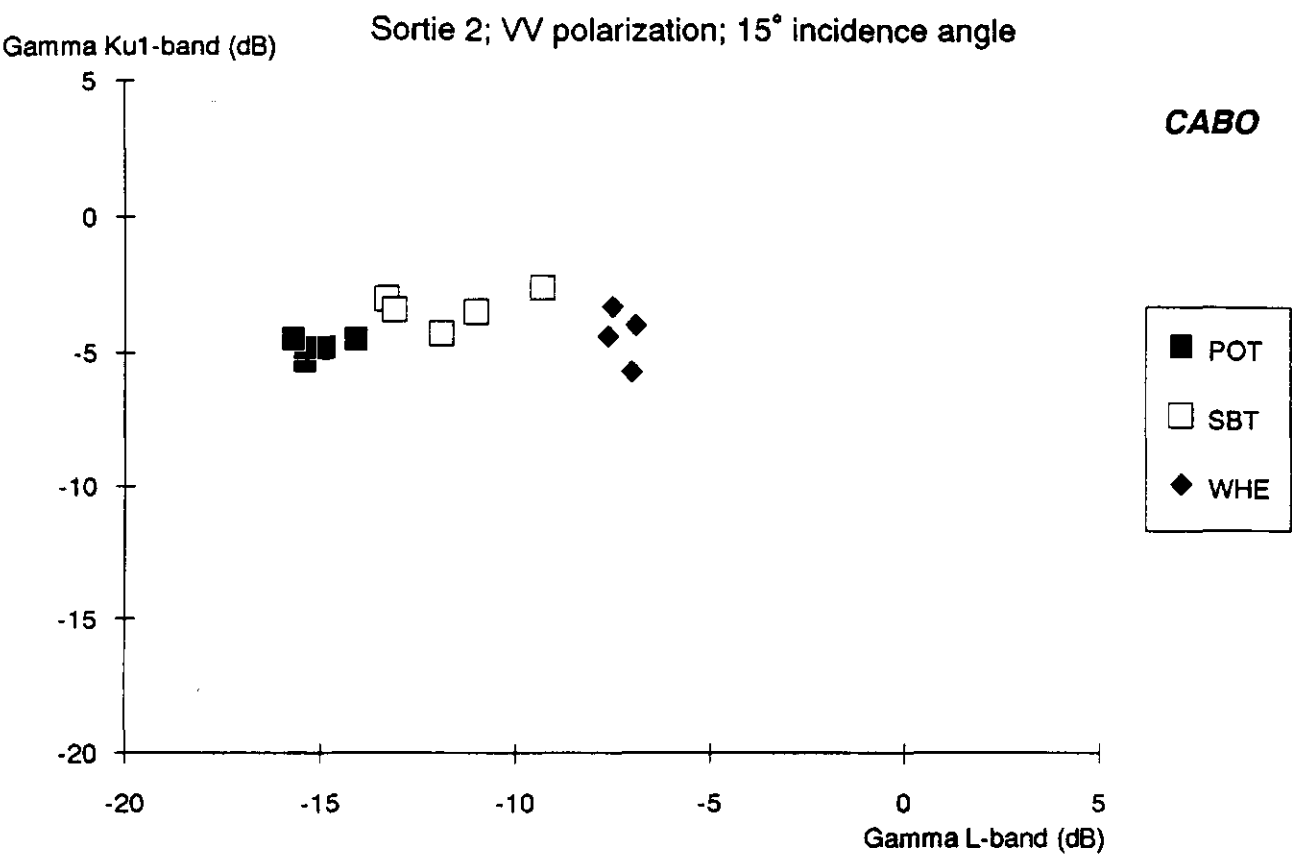


Fig. 29 Feature space plot (sortie 5, VV, 40°&50° i.a.) of the S-band versus the L-band for potato, beet and wheat



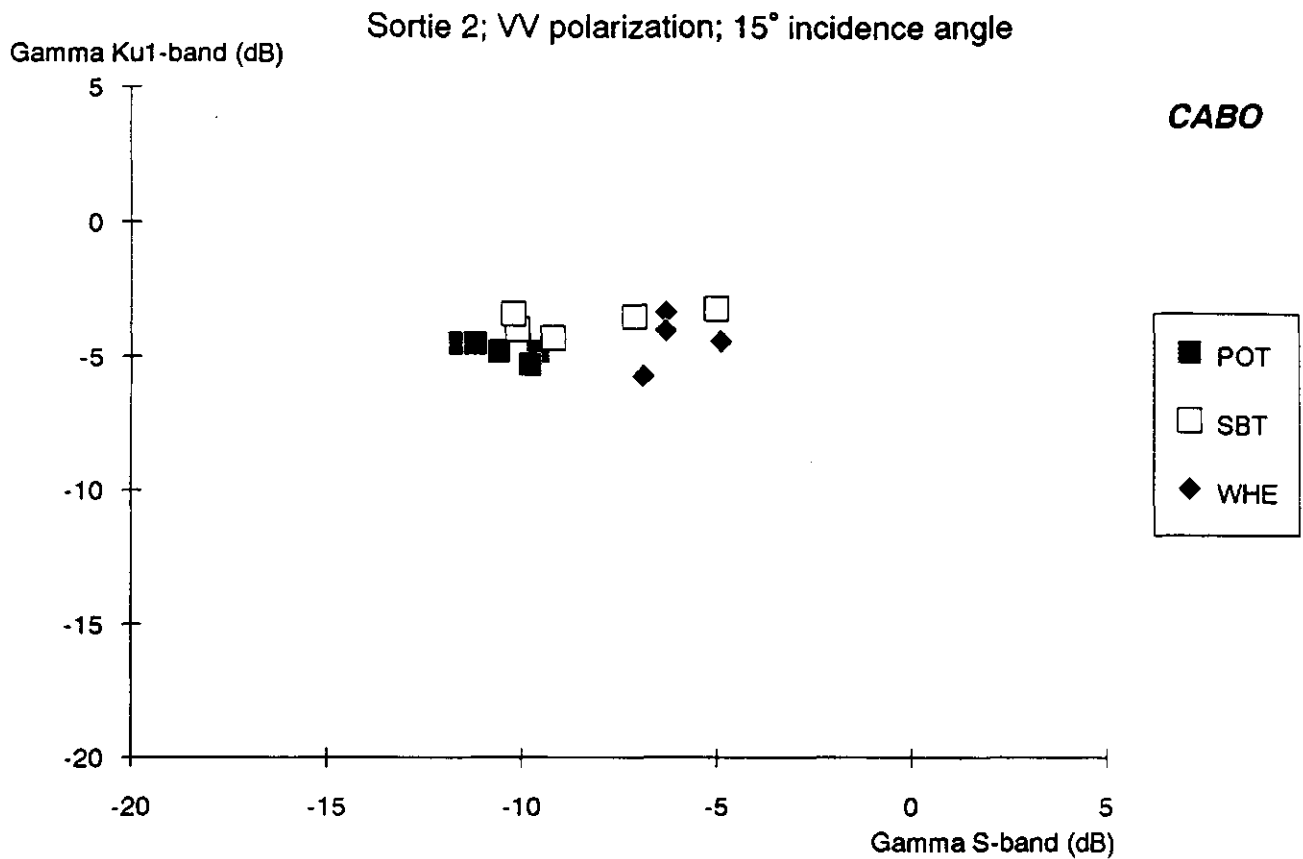


Fig. 32 Feature space plot (sortie 2, VV, 15° i.a.) of the Ku1-band versus the S-band for 'potato-soil', 'beet-soil' and 'wheat-soil'

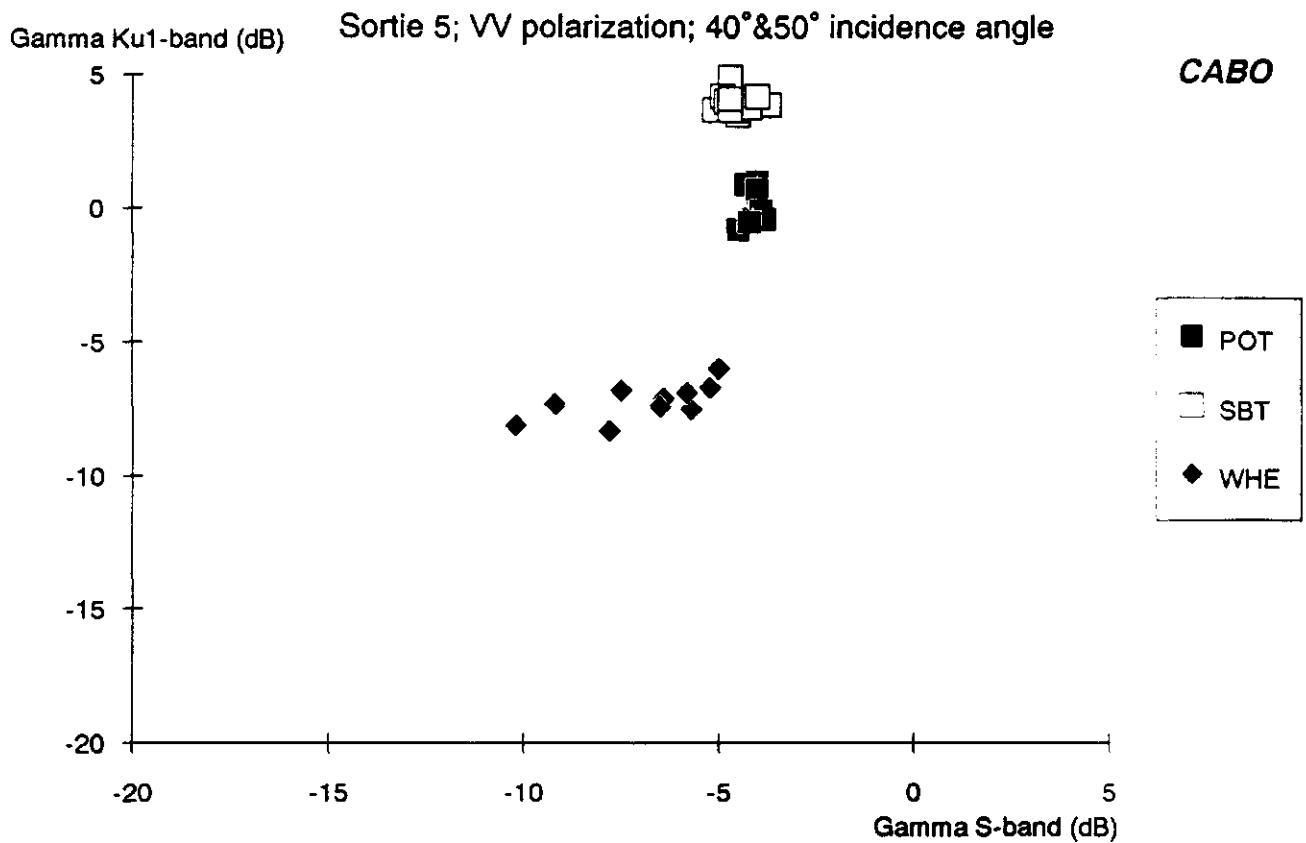


Fig. 33 Feature space plot (sortie 5, VV, 40°&50° i.a.) of the Ku1-band versus the S-band for potato, beet and wheat

### 3.4 Temporal behaviour

For the three main crop types, the change in the radar backscatter in time (VV polarization; 40° incidence angle) is plotted together with the growth of the crops expressed by crop cover (expressed in fraction), dry canopy biomass and Leaf Area Index (LAI), figures 34-45. The average moisture content of the top soil (0-5 cm) at the different sorties is plotted in figure 46. A description is made of the radar backscatter per crop type, with cross references to phenomena that occur at other crop types too.

Beet (figures 34-37):

At all sorties, the individual fields are nicely clustered in all frequency bands. The radar backscatter generally increases with crop growth between sortie 2 and sortie 4. After this, the backscatter stays at a plateau with a decreasing trend towards the end of the growing season (sortie 7). Compared to the growth of the crop, the dynamics of the radar backscatter in the different frequency bands are as follows:

- in L-band  $\gamma$  increases 8 dB until sortie 4 (cover: 0.78, biomass: 2250 kg/ha, LAI: 3)
- in S-band  $\gamma$  increases 10.5 dB until sortie 4 (cover: 0.78, biomass: 2250 kg/ha, LAI: 3)
- in C-band  $\gamma$  increases 12 dB until sortie 4 (cover: 0.78, biomass: 2250 kg/ha, LAI: 3)
- in X-band  $\gamma$  increases 16 dB until sortie 4 (cover: 0.78, biomass: 2250 kg/ha, LAI: 3)
- in Ku1-band  $\gamma$  increases 11 dB until sortie 4 (cover: 0.78, biomass: 2250 kg/ha, LAI: 3)
- in Ku2-band  $\gamma$  increases 10 dB until sortie 5 (cover: 0.82, biomass: 3500 kg/ha, LAI: 3.5)

The backscatter thus saturates at the mid-stage of growth, cover: 0.78-0.82, biomass: 2250-3500 kg/ha, LAI: 3-3.5. The growth of beet increases further, cover: 0.97, biomass: 6000 kg/ha, LAI: 5, but this is not registered by (increases in) the radar backscatter in any of the frequency bands. The largest dynamics are found in the X-band and the smallest in the L-band.

There are two remarkable features in these temporal curves which also occur for the other crop types:

- 1) There is a small dip in the radar backscatter in all frequency bands except the X- and the C-band at sortie 2 (day 123). This dip is not present at all incidence angles. A similar feature was found in the 1987 data set. There, the dip correlated somewhat with the moisture content in the top soil but this was not sufficient for a full explanation. Here too, the moisture content in the top soil also decreased from sortie 1 to sortie 2, figure 46. Again, this difference of about 1-2% is not considered sufficiently to explain for the dip in the radar backscatter.
- 2) There is a deviating behaviour in the X-band which is reproduced in the other incidence angles and for the other crops. The backscatter increases very steeply from sortie 2 to sortie 3 and 4 (relatively more than in all other frequencies) and then drops some 5 dB between sortie 4 and sortie 5. Between sortie 6 and sortie 7, the backscatter remains stable for beet, but increases for both potato and wheat (figures 40 and 44). This pattern is not consistent with that in the neighbouring frequency bands and can not be explained by field observations. Although some other bands also show the dip from sortie 4 to sortie 5 (namely the C- and the S-band), the rest of the pattern is not reproduced. Unfortunately, there were no C-band measurements after sortie 5. Based on this analysis, the whole X-band must also be labelled as 'suspicious' data (for the time being).



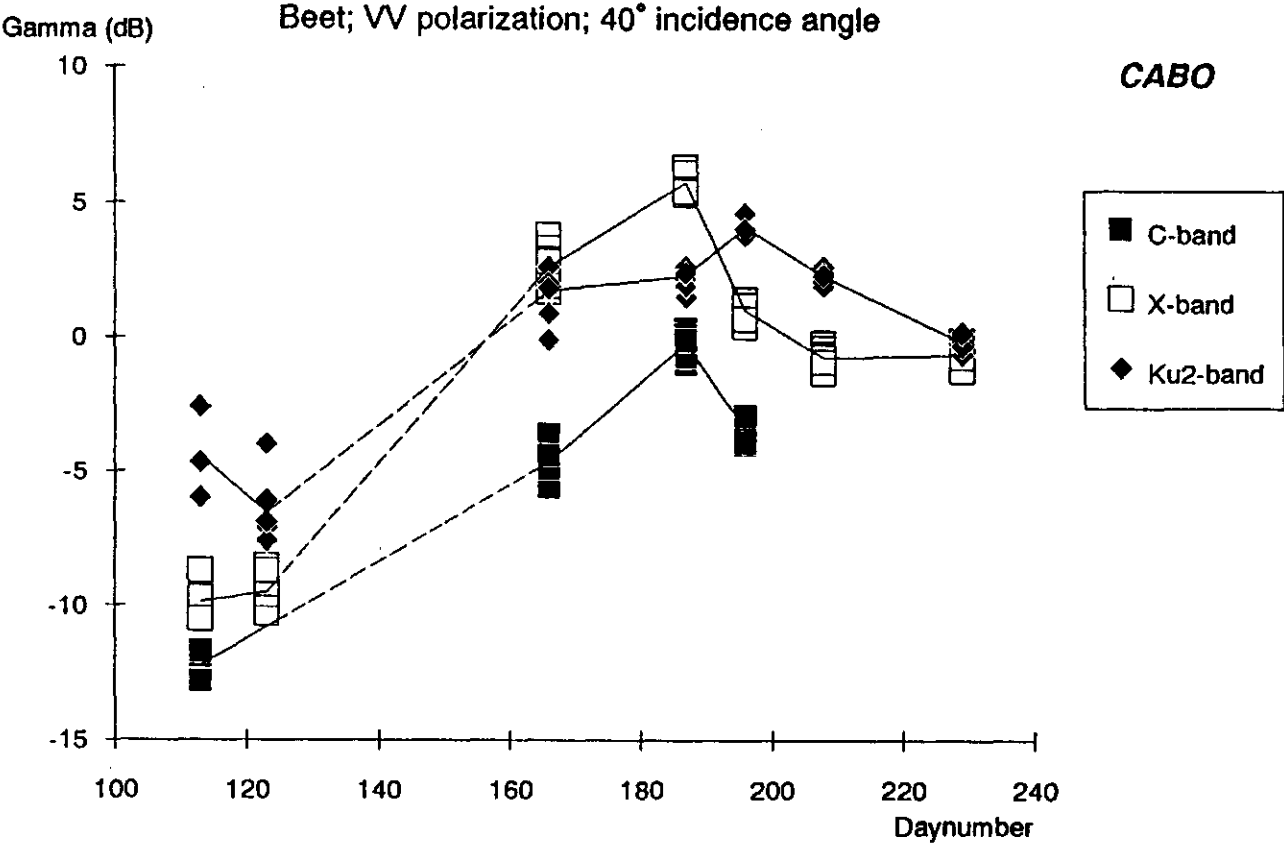


Fig. 34 Radar backscatter of beet (C-, X-, Ku2-band, VV, 40° i.a.) in the course of the growing season

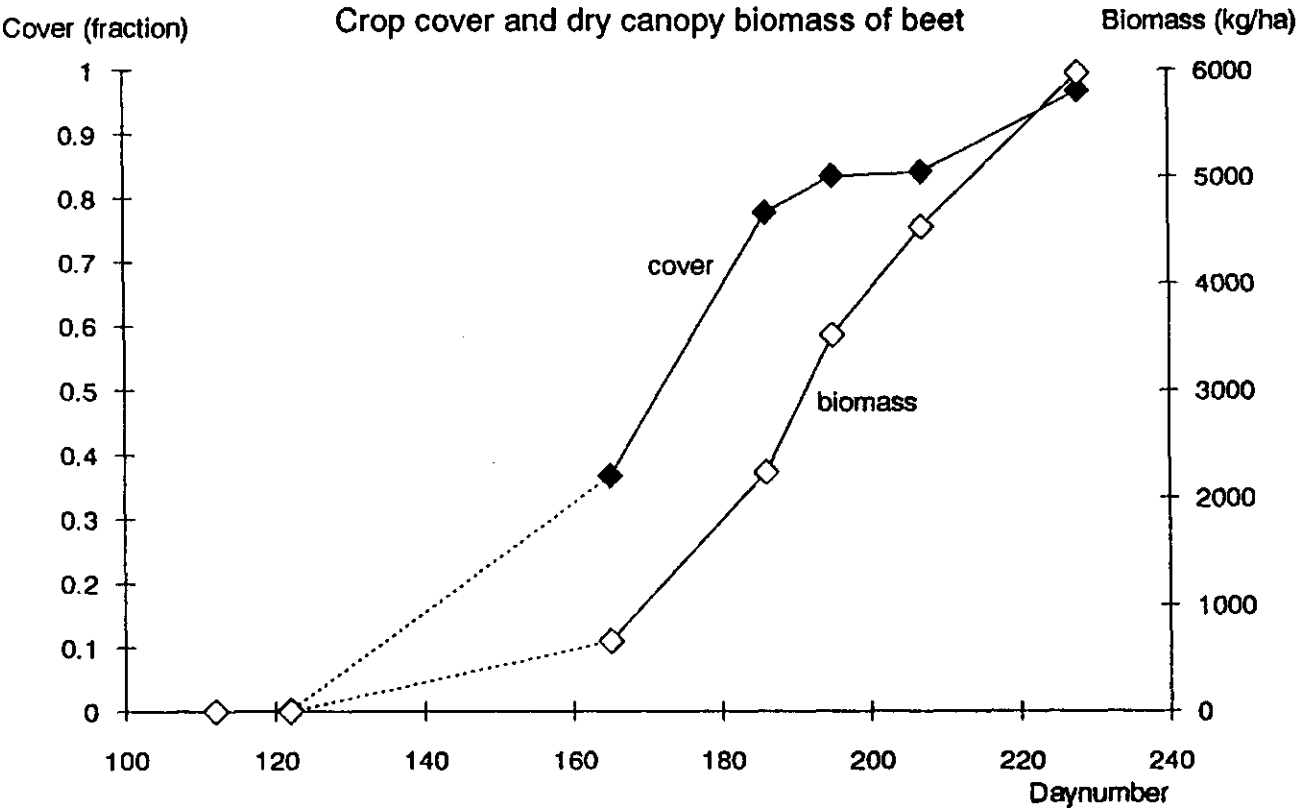


Fig. 35 Average crop cover and dry canopy biomass of beet in the course of the growing season

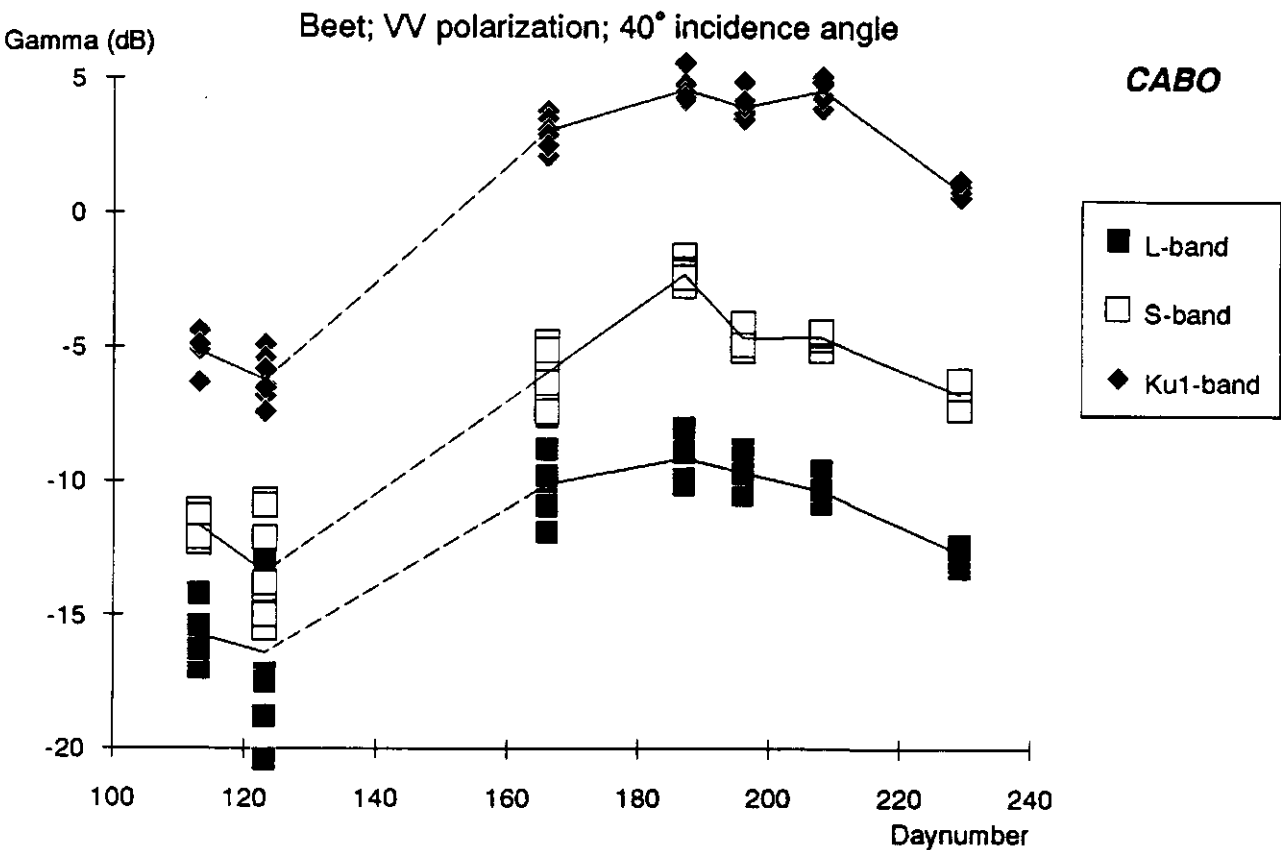


Fig. 36 Radar backscatter of beet (L-, S-, Ku1-band, VV, 40° i.a.) in the course of the growing season

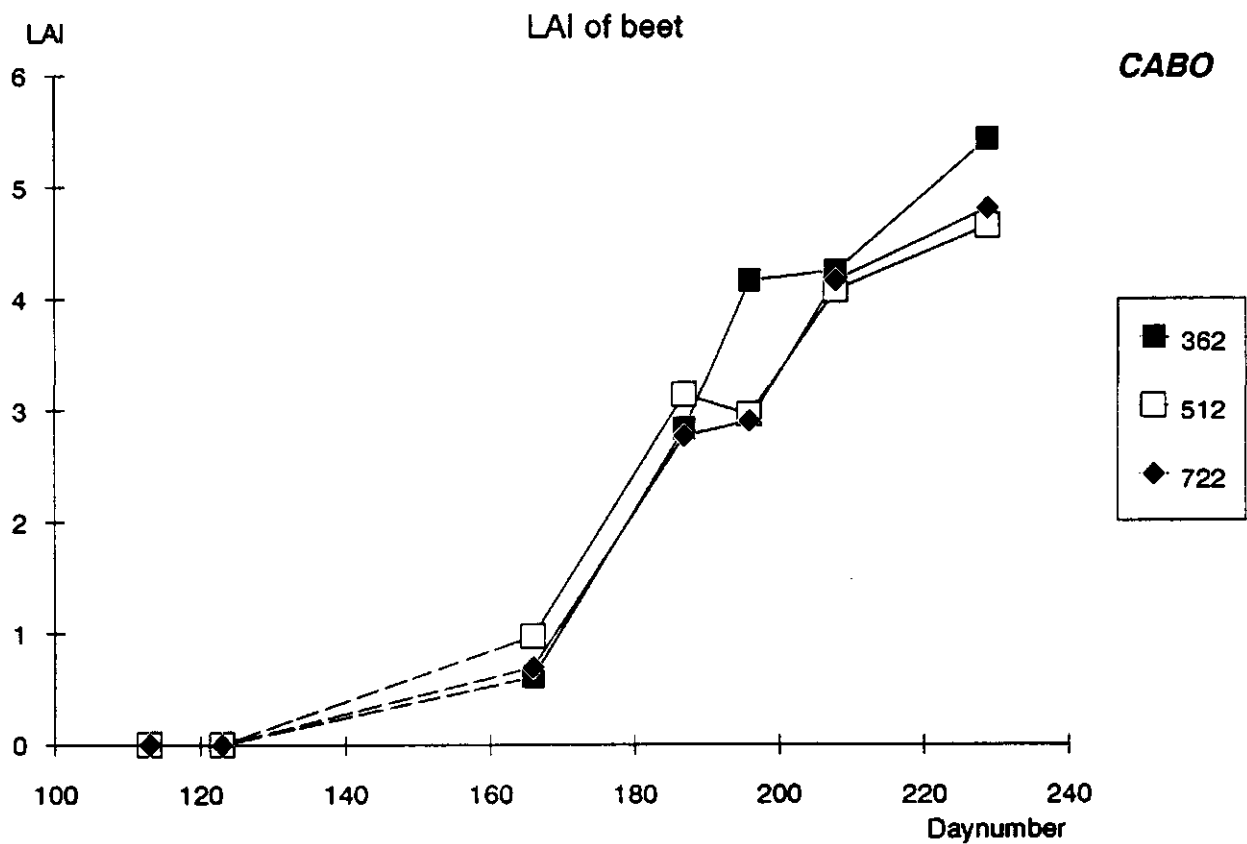


Fig. 37 Leaf Area Index (LAI) of beet in the course of the growing season, the numbers in the legend refer to the fieldnumbers of the crops

When the temporal radar backscatter of beet is compared with the changes in the soil moisture content, figure 46, only some relationship appears at sortie 7. The large difference in soil moisture content of 15% between sortie 6 and 7 coincides with the dip in radar backscatter of beet. However, it is not very likely that this decrease in soil moisture content is responsible for that in the radar backscatter at high frequencies. It is also not in accordance to what was found in the 1987 data set (Bouman et al, 1990).

The general trends observed here are in some agreement with the trends observed in the 1987 data set. This agreement concerns mostly the increase in radar backscatter with crop growth until saturation of the backscatter in the midst of the growing season. However, there are two differences:

1) The dynamic range in backscatter is much lower in 1987 than in 1988. Two explanations are possible. First, high levels of radar backscatter in 1987 could have been reduced by the compression in the original recordings. The decompression algorithm could then have failed to restore such backscatter values. This explanation is somewhat supported by the fact that the backscatter levels in the midst of the growing season (day 170-220) are some 2-3 dB higher (in the L-, S- and Ku1-band) in 1988 than in 1987. Secondly, the higher dynamic range in the 1988 data could be an artefact due to the compression of the original recordings of sortie 1 and sortie 2 (mainly bare soil). The data of the sorties 3-7 (50-100% crop cover) were not compressed. The relatively large range in backscatter between sorties 1-2 and 3-7 might then have been caused by this difference.

The backscatter of bare soil in 1987 is similar in the L-band, but some 3-5 dB lower in the S- and the Ku1-band in 1988 than in 1987. This difference also contributes to the larger dynamics in 1988. Since the soil moisture contents were high in both years, 30-35%, this is not the cause for these differences (at sortie 2, the moisture contents were even the same (30%) in both years).

2) In 1988 the backscatter slowly decreases from the midst of the growing season (sortie 4) to the end (sortie 7). In 1987, however, the backscatter remained more or less on a stable level during this period. Again, this difference could have been caused by the compression of the original data in 1987.

Compared to 1987, it is unfortunate that in the long range between sortie 2 and sortie 3 no radar data were acquired. Only one sortie (no. 3) was carried out in 1988 in the most interesting period of the growing season, i.e. the phase of exponential crop growth (circa May-June).

Potato (figures 38-41):

Like for beet, the individual fields are nicely clustered. Also, the curves of L-, S- and Ku1-band are characterised by a small dip of 2-3 dB at sortie 2. After sortie 2 the radar backscatter increases in all frequency bands with the growth of the crop:

- in L-band  $\gamma$  increases 10 dB until sortie 5 (cover: 0.93, biomass: 2250 kg/ha, LAI: 3)
- in S-band  $\gamma$  increases 9 dB until sortie 4 (cover: 0.89, biomass: 1500 kg/ha, LAI: 2.5)
- in C-band  $\gamma$  increases 10 dB until sortie 4 (cover: 0.89, biomass: 1500 kg/ha, LAI: 2.5)
- in X-band  $\gamma$  increases 12.5 dB until sortie 4 (cover: 0.89, biomass: 1500 kg/ha, LAI: 2.5)
- in Ku1-band  $\gamma$  increases 9.5 dB until sortie 6 (cover: 0.90, biomass: 2750 kg/ha, LAI: 3.5)
- in Ku2-band  $\gamma$  increases 5 dB until sortie 6 (cover: 0.90, biomass: 2750 kg/ha, LAI: 3.5)

The backscatter again saturates at the mid-stage of growth, cover: 0.89-0.93, biomass: 1500-2750 kg/ha, LAI: 2.5-3.5. The growth of potato increases further, cover: 0.96, biomass: 3300 kg/ha, LAI: 5, but this is not registered by (increases in) the radar backscatter in any of the frequency bands. The general shapes of the temporal curves resemble those of beet. Only where the radar backscatter of beet slowly decreases in the midst of the growing season (from sortie 4 to sortie 7), the backscatter of potato remains on a stable level. The 'radar-growth' range of potato is in general comparable to that of beet with average of about 10 dB. Again, the largest dynamics are found in the X-band, with the annotation that the X-band curves are 'suspicious' (too high backscatter levels at sortie 3 and 4). The smallest dynamics are found in the Ku2-band, e.g. 5 dB only.

For potato, the similarities between the 1987 and the 1988 data are generally larger than for beet. In the L- and the Ku1-band, nearly the exact temporal curves are reproduced. The backscatter in the midst of the season is on the same level in 1987 and in 1988. In the L-band, the backscatter of bare soil is even on the same level (resulting in comparable dynamic ranges) while in the Ku1-band it is some 2-5 dB lower in 1988 than in 1987. This latter can be explained by the differences in soil moisture content between these years. In 1988 the moisture content was some 8% and 6% lower in sortie 1 and 2 respectively than in 1987. The lack of a difference in the L-band could (hypothetically) be the result of the deeper penetration of L-band microwaves in the soil, thereby smoothening the differences in moisture content in the 0-5 cm top soil.

Only in the S-band, the differences between 1987 and 1988 are quite large. The differences are comparable to those described for beet: a lower backscatter from the bare soil in 1988 and a higher backscatter from the closed crop cover. Possibly the original data in the S-band in 1987 were more compressed than those in the other two bands.

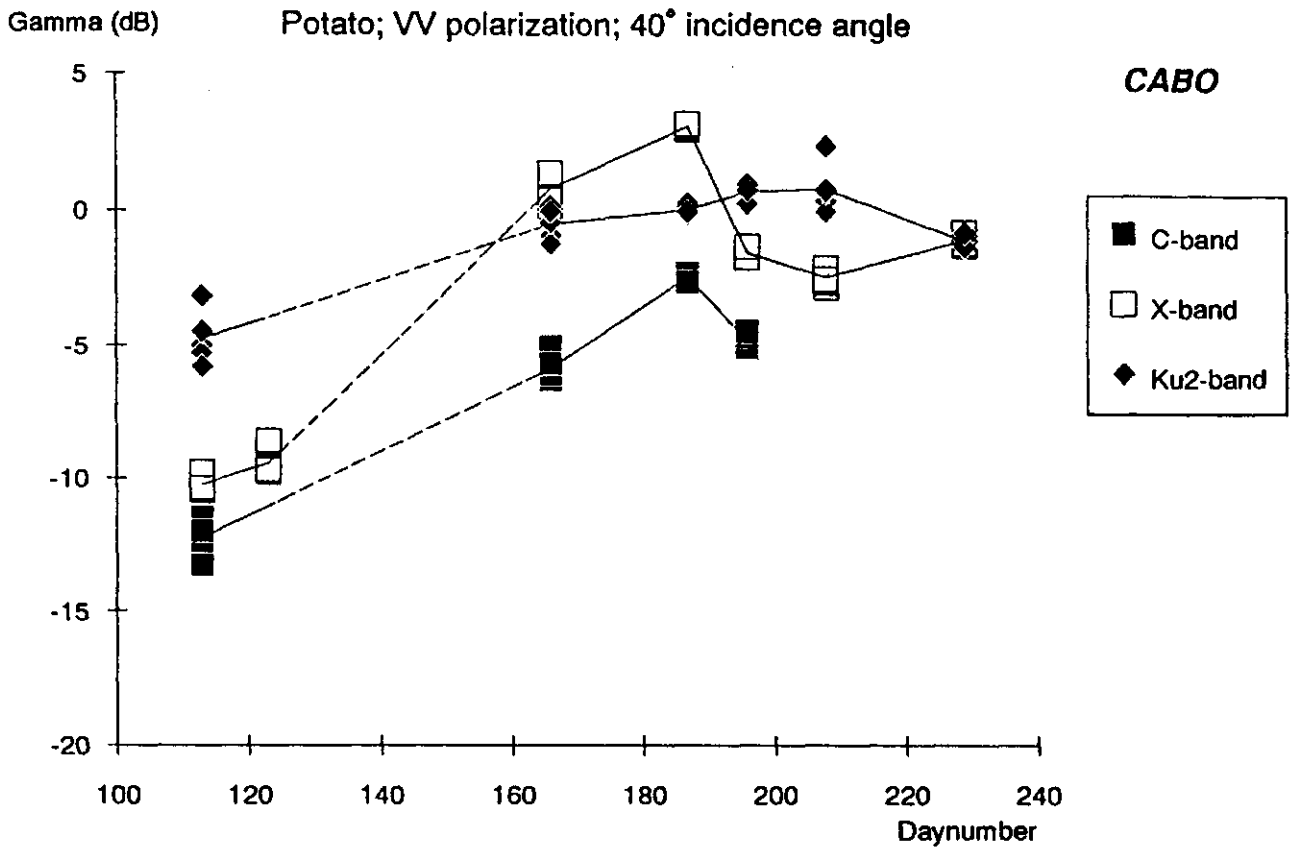


Fig. 38 Radar backscatter of potato (C-, X-, Ku2-band, VV, 40° i.a.) in the course of the growing season

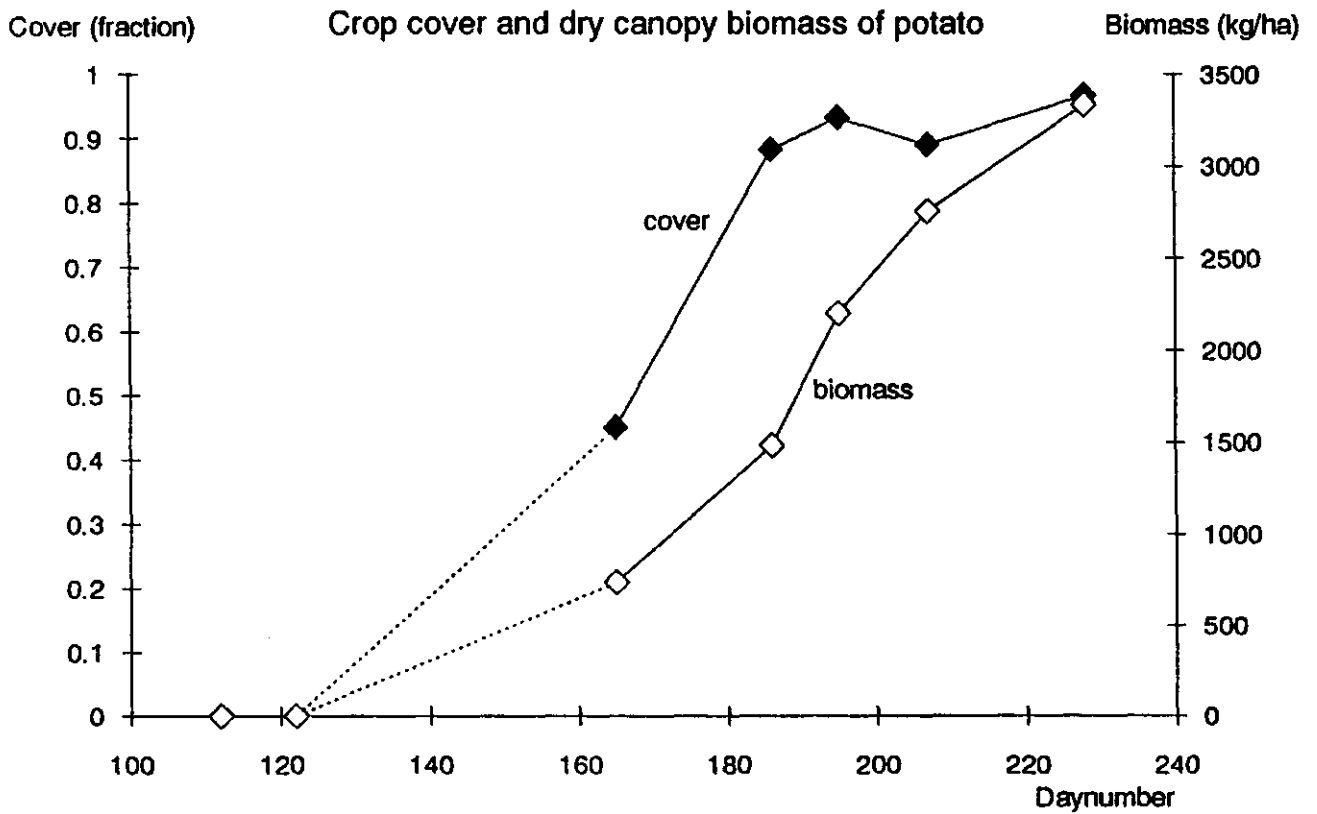


Fig. 39 Average crop cover and dry canopy biomass of potato in the course of the growing season

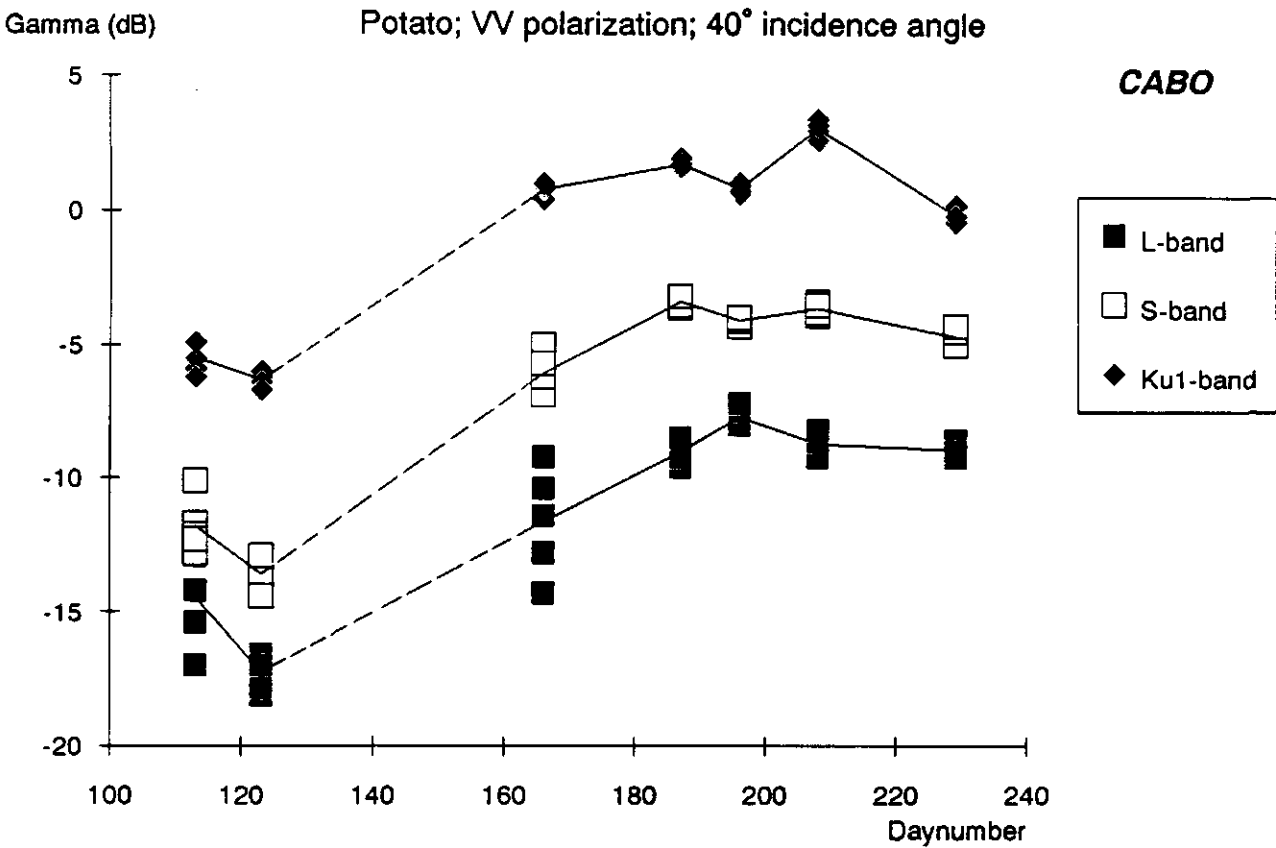


Fig. 40 Radar backscatter of potato (L-, S-, Ku1-band, VV, 40° i.a.) in the course of the growing season

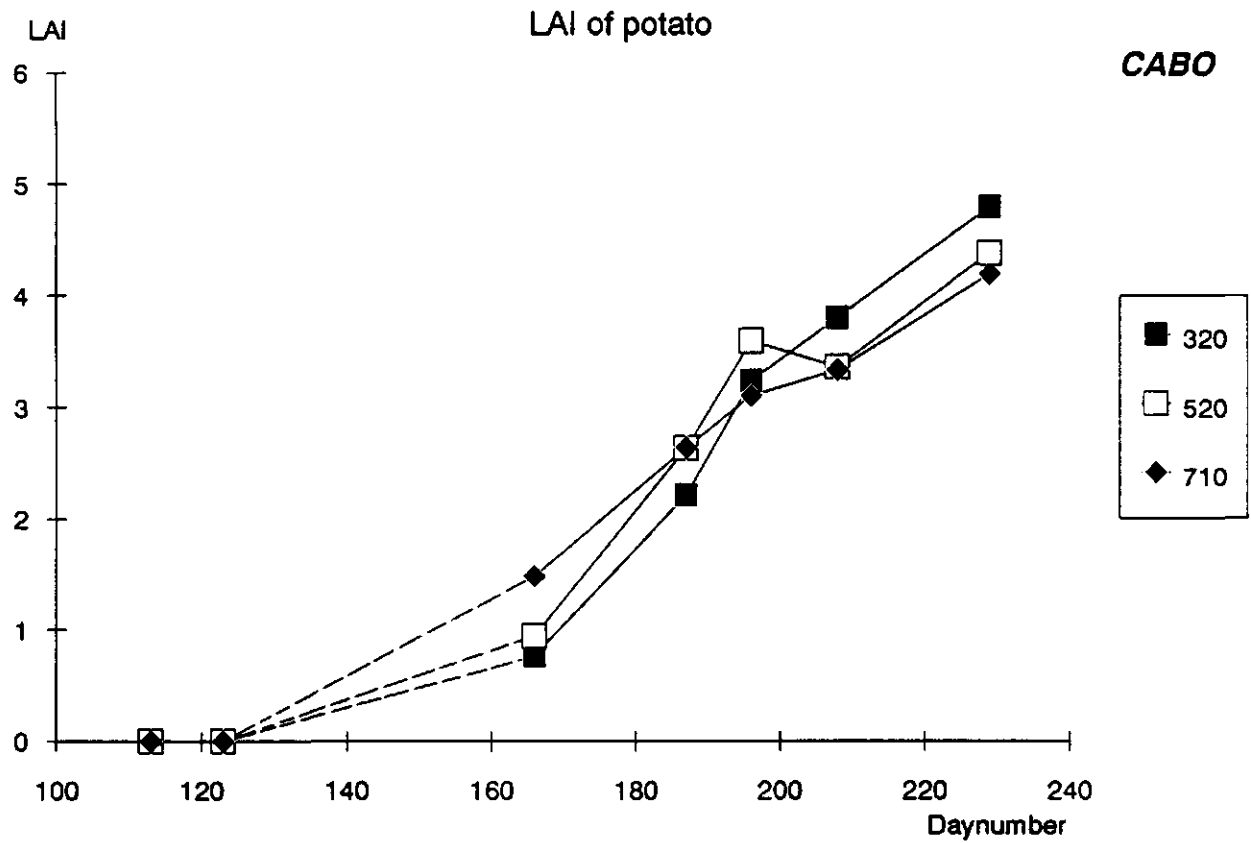


Fig. 41 Leaf Area Index (LAI) of potato in the course of the growing season, the numbers in the legend refer to the fieldnumbers of the crops

### Wheat (figures 42-45):

The curves of wheat differ largely from those of beet and potato. In fact, no 'radar-growth' curves can be recognized at all in the temporal curves. Between sortie 1 and sortie 3, there is neither a general increase nor a decrease in radar backscatter with the growth of the crops. Overall, the shape of the temporal curves better matches that of the soil moisture content, figure 46. Like the radar backscatter, the soil moisture content remains on the same level between sortie 1 and sortie 3. There is a plateau of high moisture contents during the sorties 4-6, and then the moisture content drops again to the level of sorties 1-3. This pattern is fairly well reproduced in the S-band while some of the features are recognized in the other bands (namely the decrease in backscatter between sortie 6 and sortie 7). A better insight in the behaviour of the backscatter of wheat might be obtained by an analysis of the curves of individual fields.

The overall 'radar-growth' range is small, some 2-4 dB only. Only the S-band shows an increase of 6 dB between sortie 3 and sortie 4. In all frequency bands the spread between the backscatter of the individual fields is larger than that of beet and potato.

The observations here compare well with those made for the 1987 data. Neither in 1987 nor in 1988 is a 'radar-growth' curve recognizable in the temporal backscatter curves. The curves in 1987 do not resemble those in 1988. The observations in both years support the hypothesis that, in most frequency bands, the backscatter of wheat is more determined by the underlying soil background than by the crop itself (the shapes of the curves of the moisture content of the top soil also differ between 1987 and 1988). This hypothesis will have to be tested with statistical correlation analyses (§ 5.3.2) and theoretical model approaches. In the higher frequency bands, X- to Ku2-band, this contradicts historical observations made for the X- and Q-band ground-based ROVE data set.

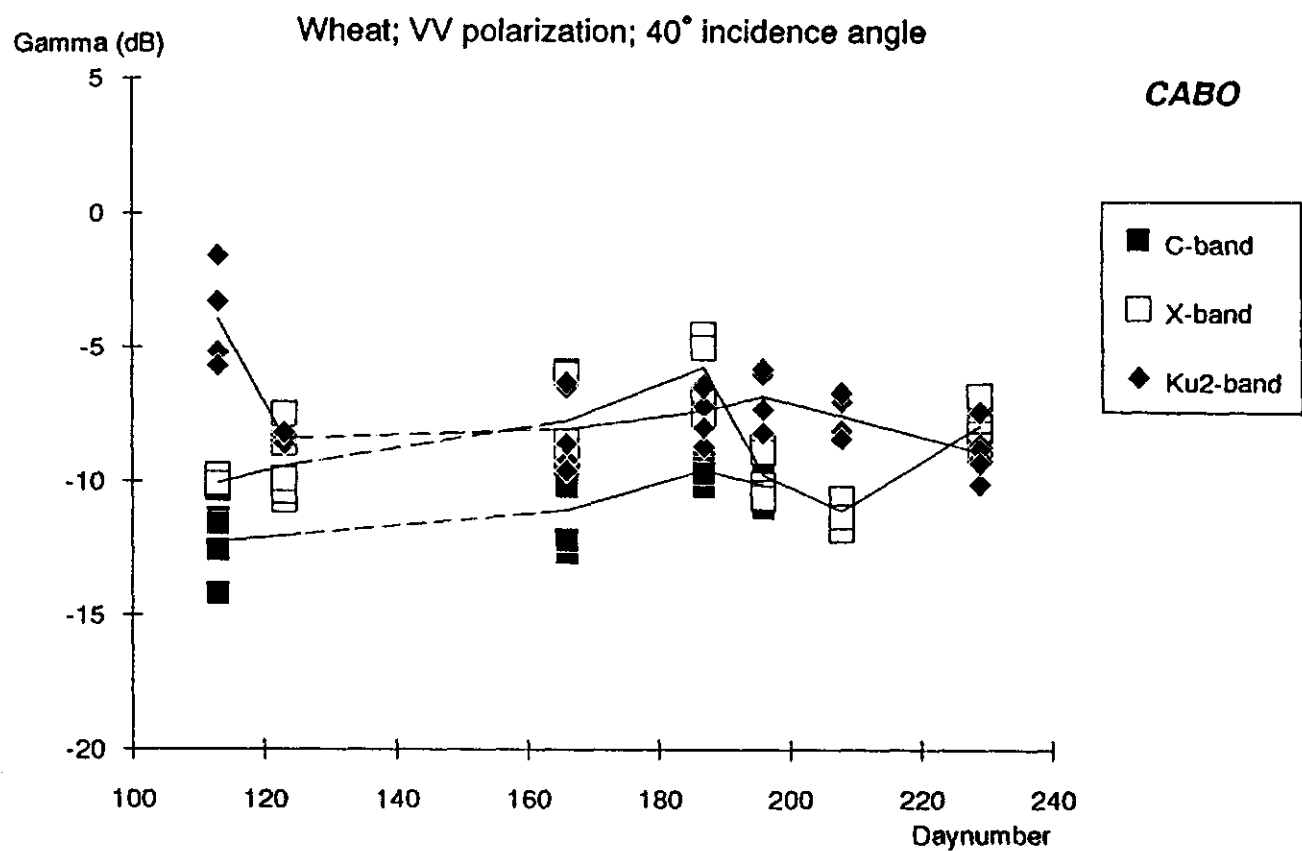


Fig. 42 Radar backscatter of wheat (C-, X-, Ku2-band, VV, 40° i.a.) in the course of the growing season

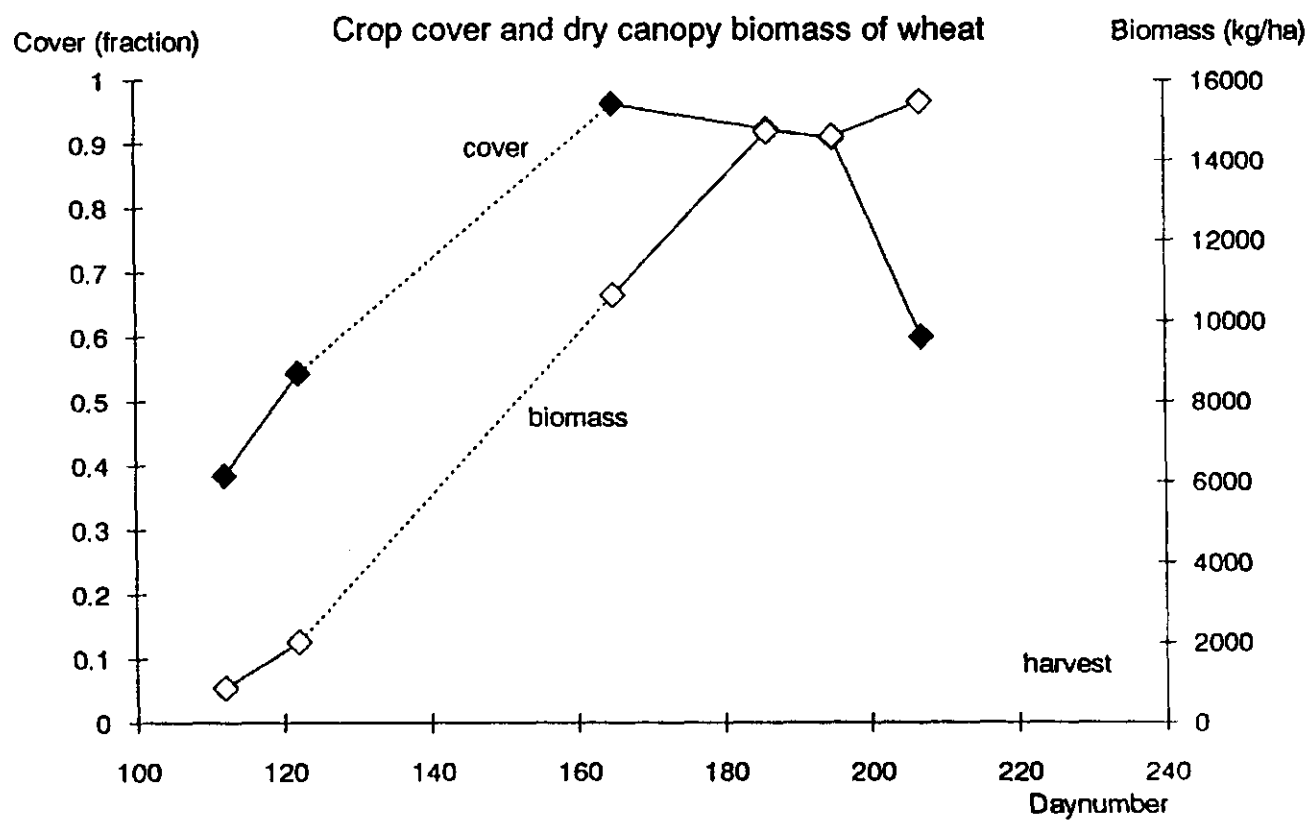


Fig. 43 Average crop cover and dry canopy biomass of wheat in the course of the growing season



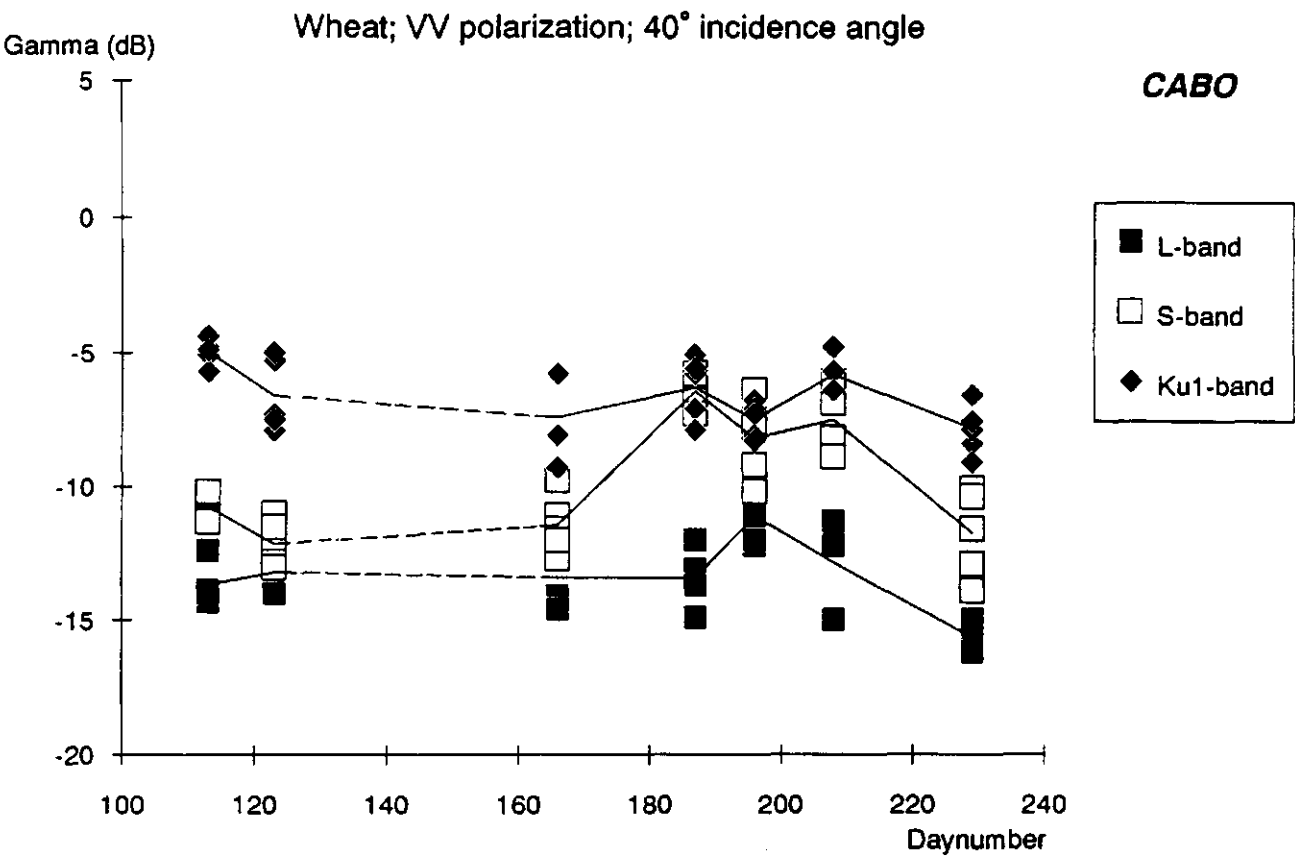


Fig. 44 Radar backscatter of wheat (L-, S-, Ku1-band, VV, 40° i.a.) in the course of the growing season

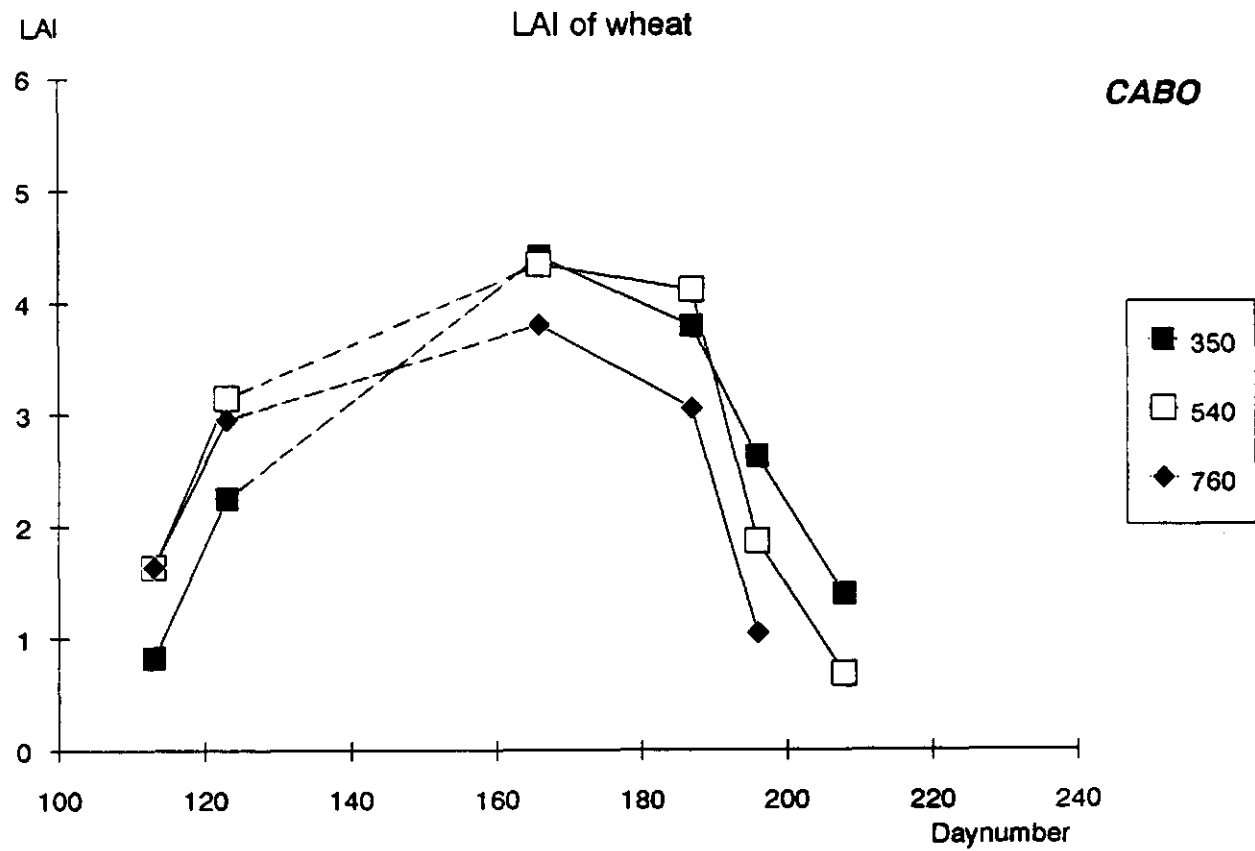


Fig. 45 Leaf Area Index (LAI) of wheat in the course of the growing season, the numbers in the legend refer to the fieldnumbers of the crops

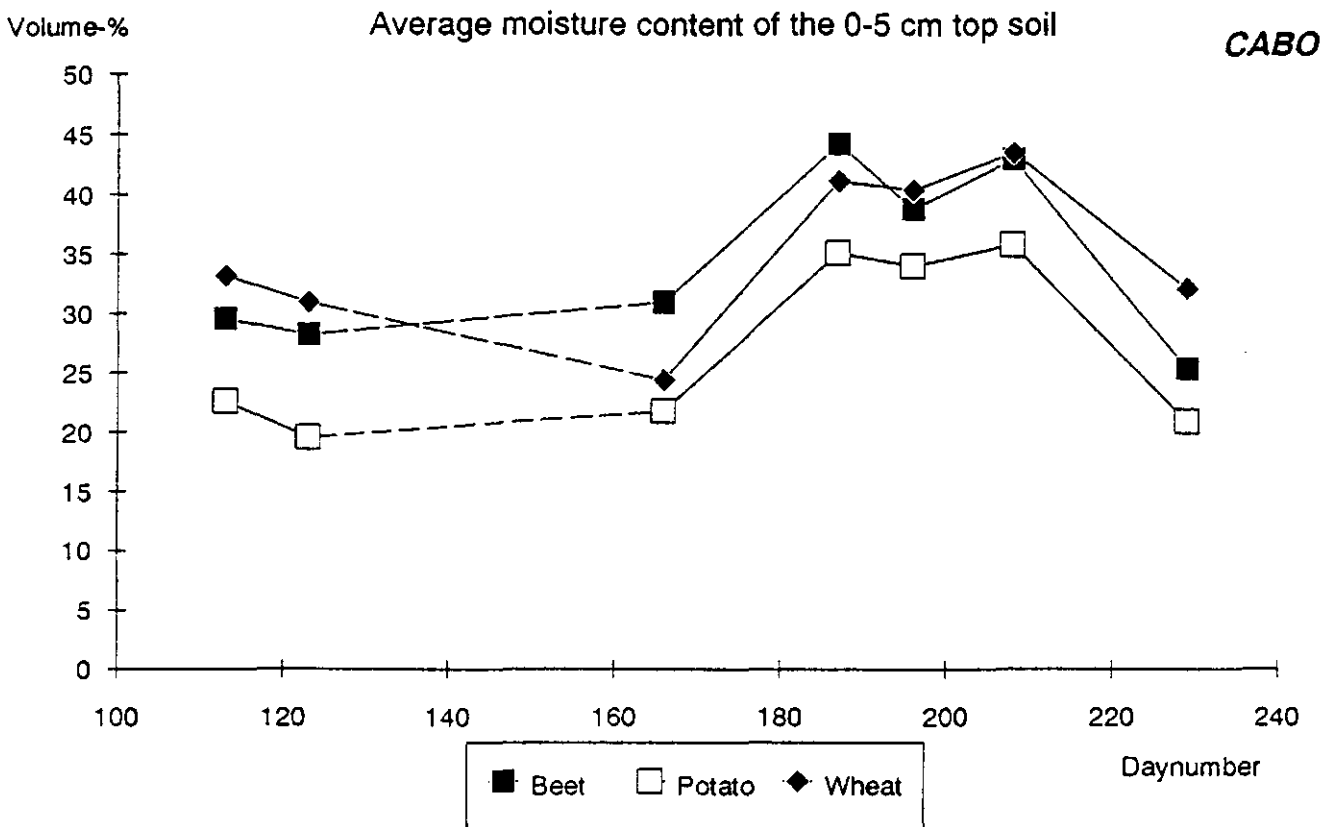


Fig. 46 Average moisture content of the top soil (0-5 cm) of beet, potato and wheat in the course of the growing season

### 3.5 Frequency behaviour

Figures 47-49 give the frequency behaviour of the radar backscatter of the three main crop types for mainly bare soil (sortie 2), a closed crop cover in the midst of the growing season (sortie 4) and a closed crop cover at the end of the growing season (sortie 7) respectively. The average curve of the mainly bare soil, figure 47, is repeated in figures 48 and 49 as a reference curve for mainly bare soil. It should be noted, that a reference to bare soil is always related to the moisture content and surface roughness of that soil (which are subject to changes in time).

For mainly bare soil, the radar backscatter increases with increasing frequency from the L-band to the Ku1-band, irrespective of the type of soil. The backscatter in the Ku2-band is on the same level or a bit lower than that in the Ku1-band.

With a closed crop cover in the midst of the growing season, the curves differ for the different crop types. The curves for beet and potato are of comparable shape and lie some 8-12 dB above the soil curve. For these crops, the backscatter now increases with increasing frequency only until the X-band, and then slightly decreases again in the Ku-bands (note: the high backscatter in the X-band at sortie 4 might be an artefact, § 3.4). The curve of wheat deviates from those of beet and potato. It only lies some 3 dB above that of the mainly bare soil in the frequency bands between the L- and the X-band, with a very remarkable peak of 8 dB in the S-band. This peak is no artefact since it appears at all angles of incidence for wheat while it is absent in the same tracks for the other crops. In both the Ku-bands, the backscatter of wheat is still the same as that of mainly bare soil. The peak in the S-band was also recognized in the temporal

backscatter curves of wheat in figure 44. Here the relation with the soil moisture content in this band was quite clear. Therefore, this peak in figure 48 is probably caused by the soil moisture underneath the crop. It still remains a question, however, why the effect of soil moisture is not so remarkable in the other frequency bands.

At the end of the growing season the curves of beet and potato are still some 8 dB above that of the mainly bare soil, figure 49. Now, for both crops the backscatter increases again up to the Ku1-band after which it very slightly decreases (like the backscatter of the mainly bare soil). Especially notable is the crossing of the two curves at the position of where the C-band data should have been. As remarked before, the backscatter of potato at the end of the season is higher than that of beet in the L- and the S-band. The curve of wheat is very comparable to that of the mainly bare soil. The peak in the S-band has vanished (lower soil moisture content again, figure 46) and there seems to be no influence of the crop on the radar backscatter.

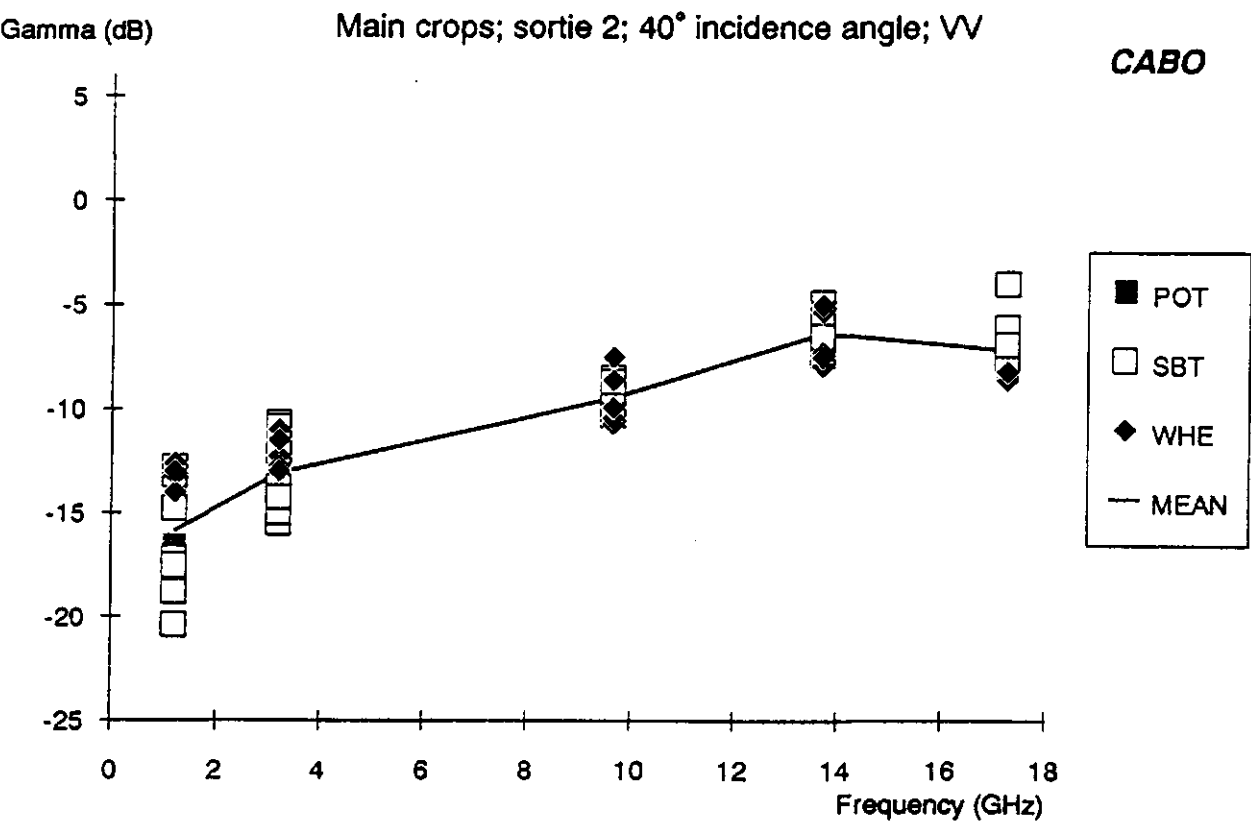


Fig. 47 Radar backscatter of bare 'potato-soil', 'beet-soil' and 'wheat-soil' (sortie 2, VV, 40° i.a.) as a function of frequency

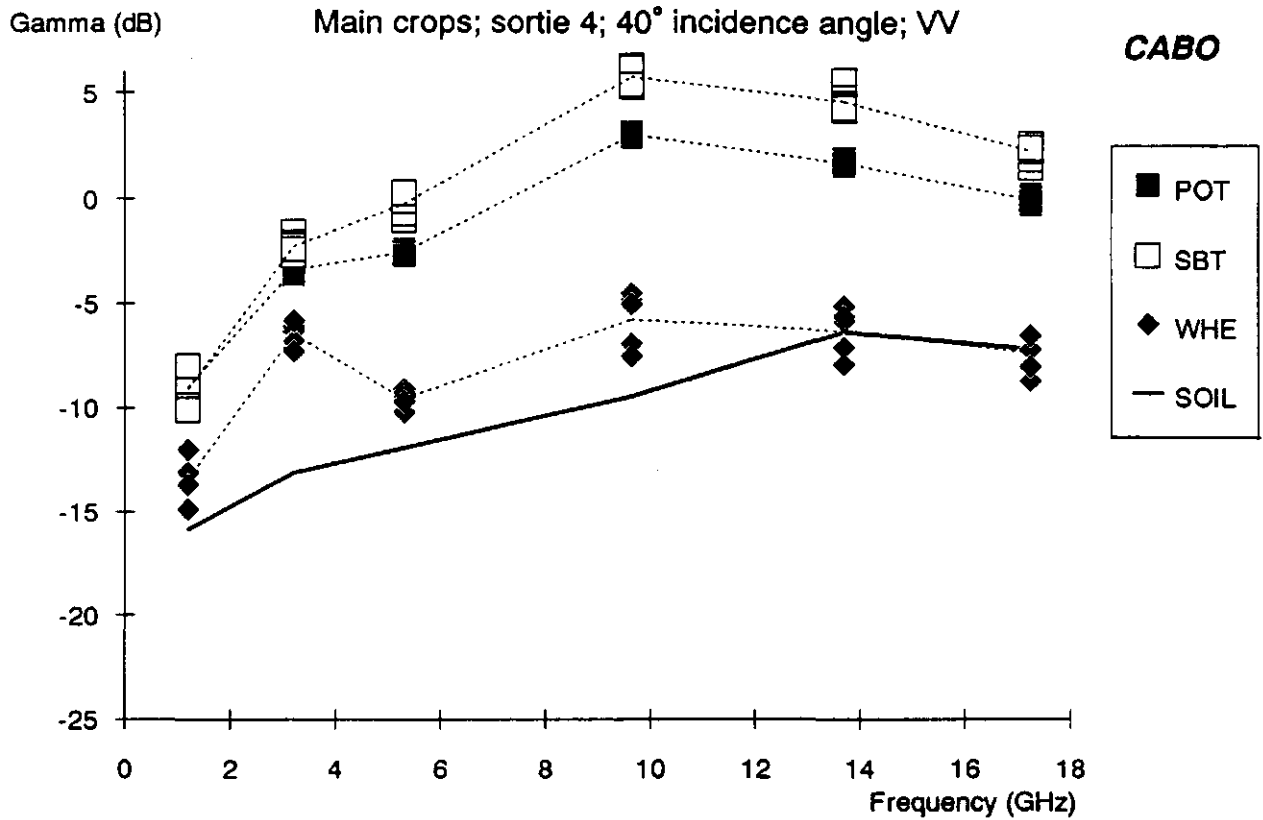


Fig. 48 Radar backscatter of beet, potato and wheat (sortie 4, VV, 40° i.a.) as a function of frequency, the 'mainly bare soil' curve is the frequency curve of figure 47

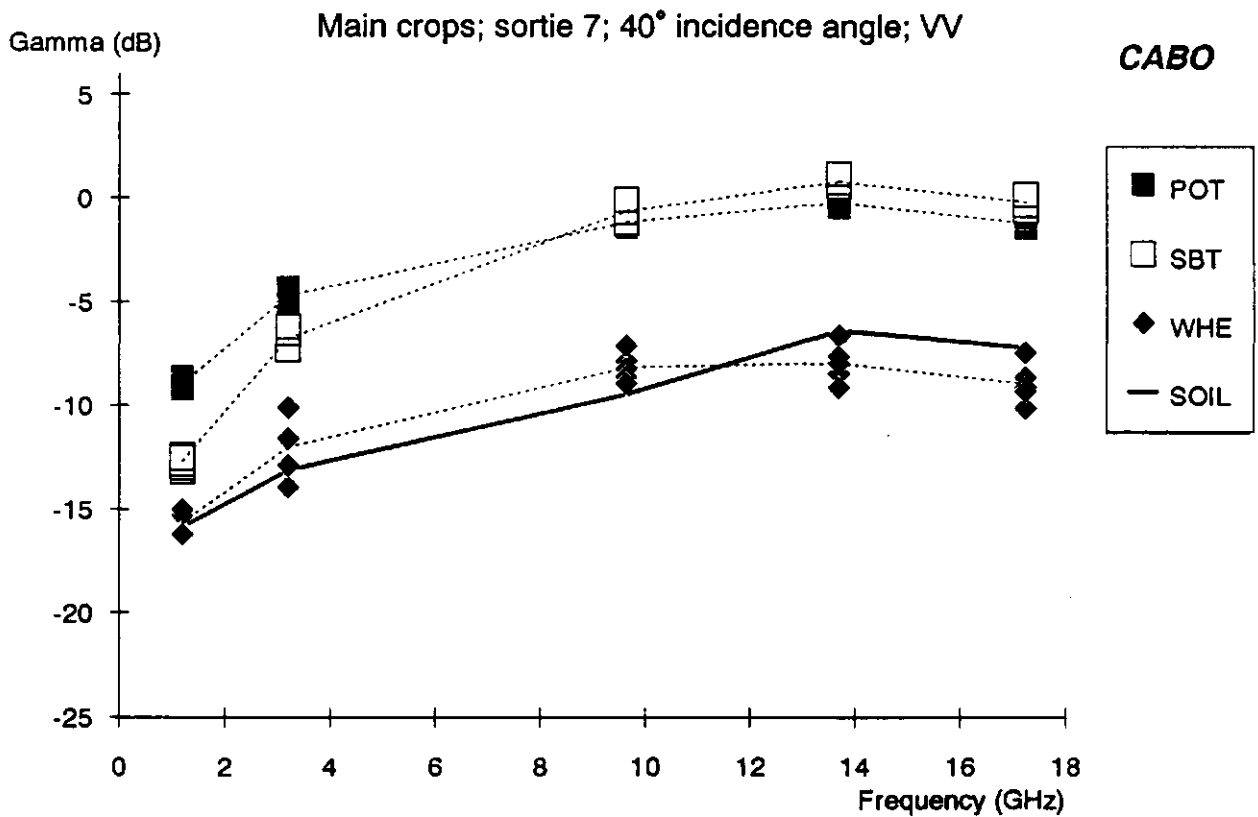


Fig. 49 Radar backscatter of beet, potato and wheat (sortie 7, VV, 40° i.a.) as a function of frequency, the 'mainly bare soil' curve is the frequency curve of figure 47

### 3.6 General crop comparison

A general comparison of the crop types in the different frequency bands at 30° and 60° incidence angle for two sorties is given in figures 50-57. These figures show some small differences between the two angles of incidence for beet and potato in the L-, S- and Ku1-bands. Again the backscatter of potato is lower than or equal to that of beet except for the L- and S-band at sortie 6. There, the backscatter of potato is higher than that of beet.

As remarked before, the backscatter of wheat gives the highest variation in all frequency bands.

For the C-, X- and Ku1-bands, the backscatter of potato at 60° incidence angle is lower than that of beet (especially at sortie 6). This angular behaviour was mentioned before in paragraph 3.2.

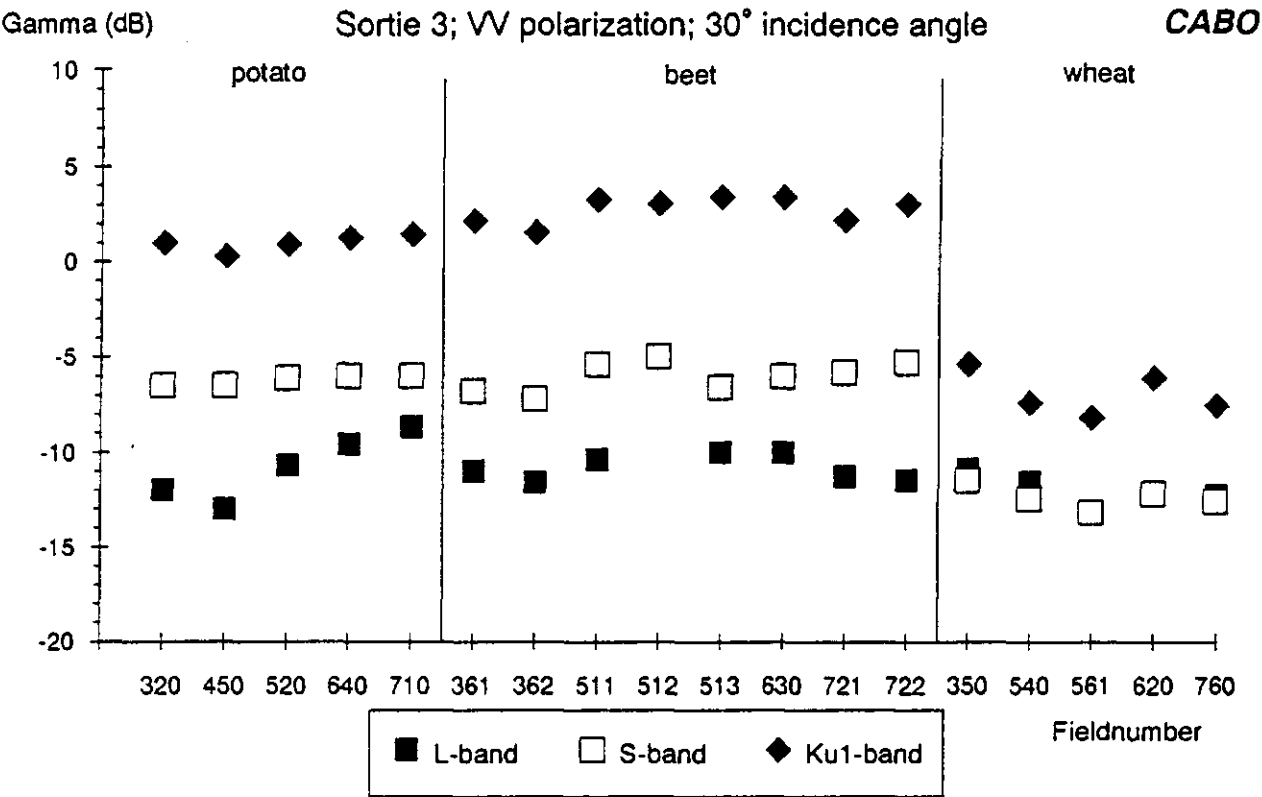


Fig. 50 Radar backscatter of the main crop types (sortie 3, L-, S-, Ku1-band, VV, 30° i.a.)

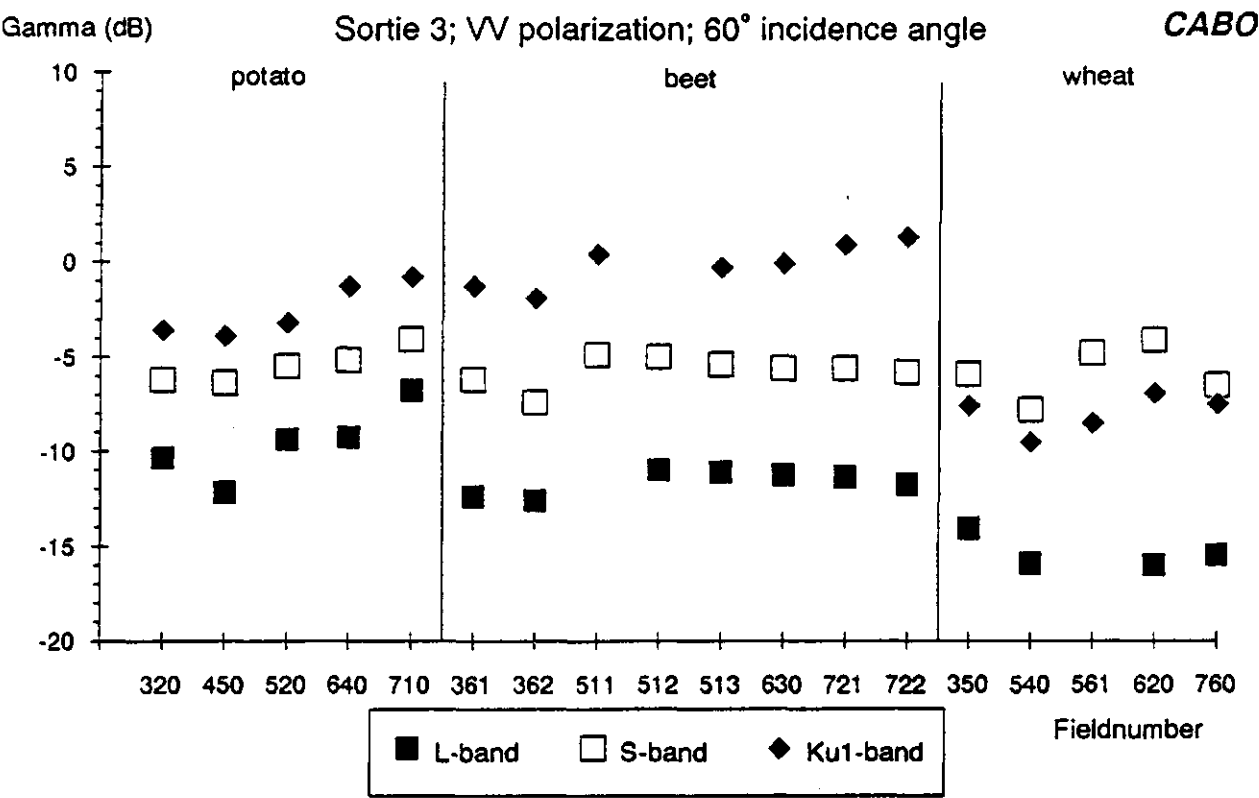


Fig. 51 Radar backscatter of the main crop types (sortie 3, L-, S-, Ku1-band, VV, 60° i.a.)

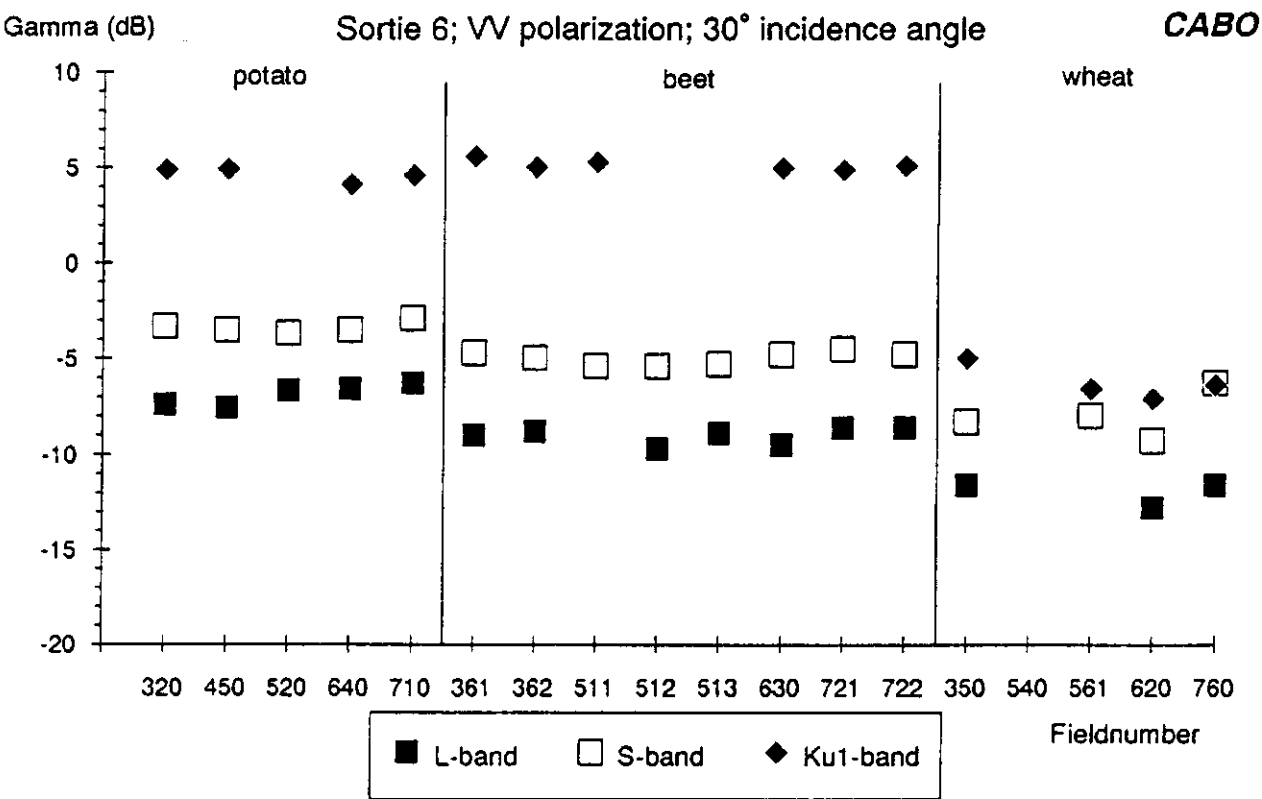


Fig. 52 Radar backscatter of the main crop types (sortie 6, L-, S-, Ku1-band, VV, 30° i.a.)

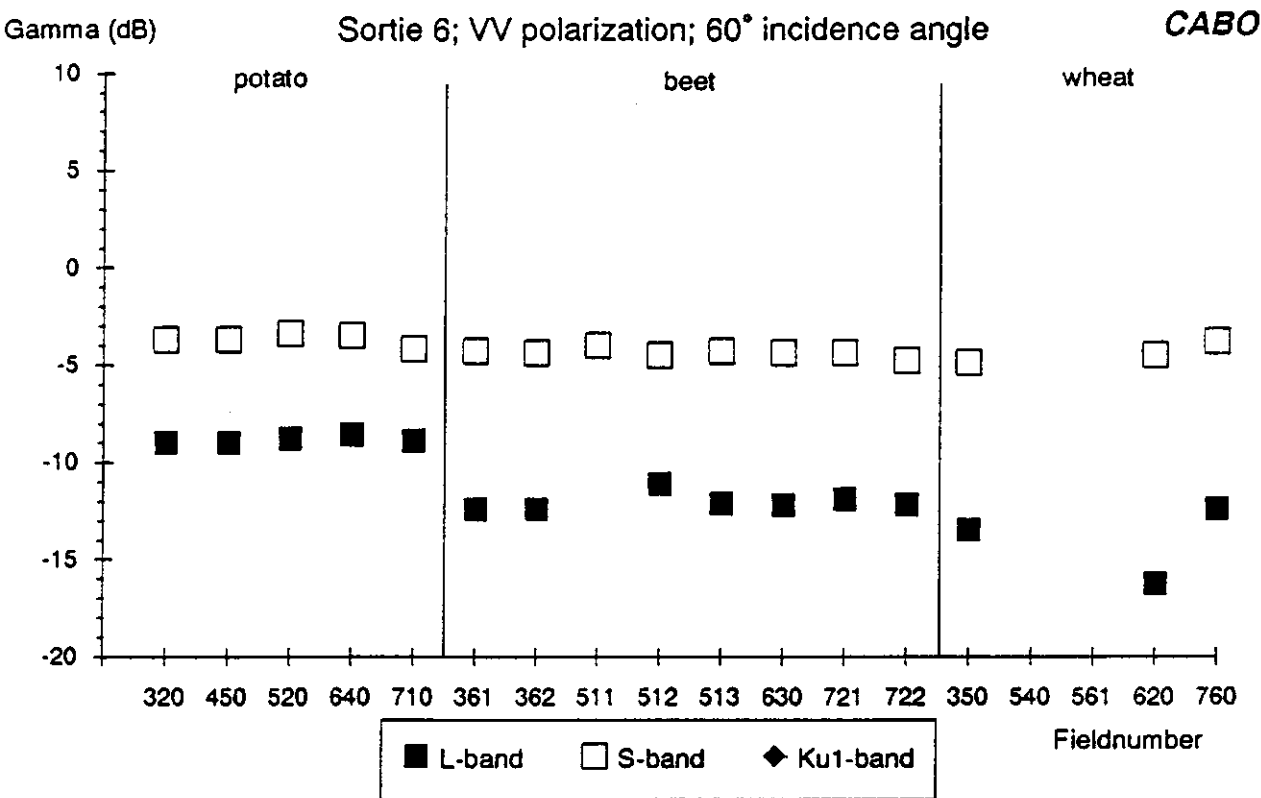


Fig. 53 Radar backscatter of the main crop types (sortie 6, L-, S-, Ku1-band, VV, 60° i.a.)

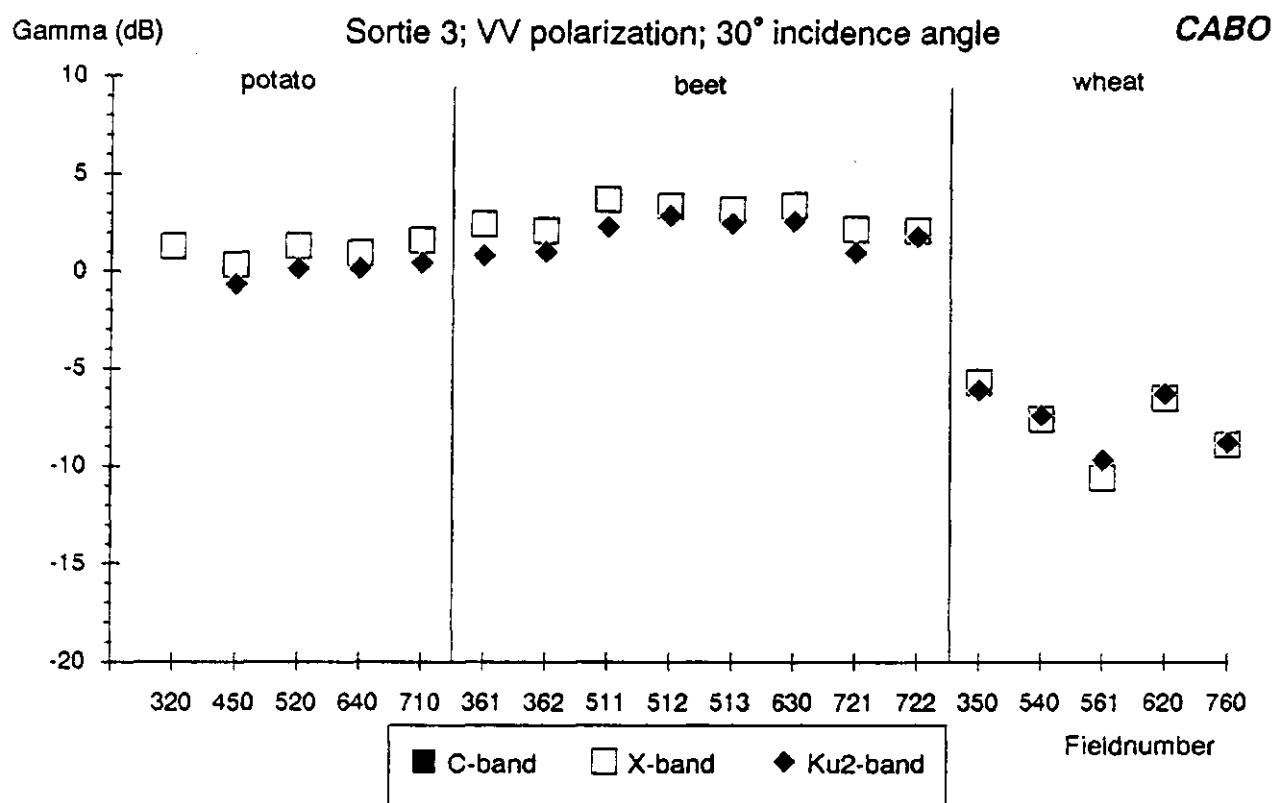


Fig. 54 Radar backscatter of the main crop types (sortie 3, C-, X-, Ku2-band, VV, 30° i.a.)

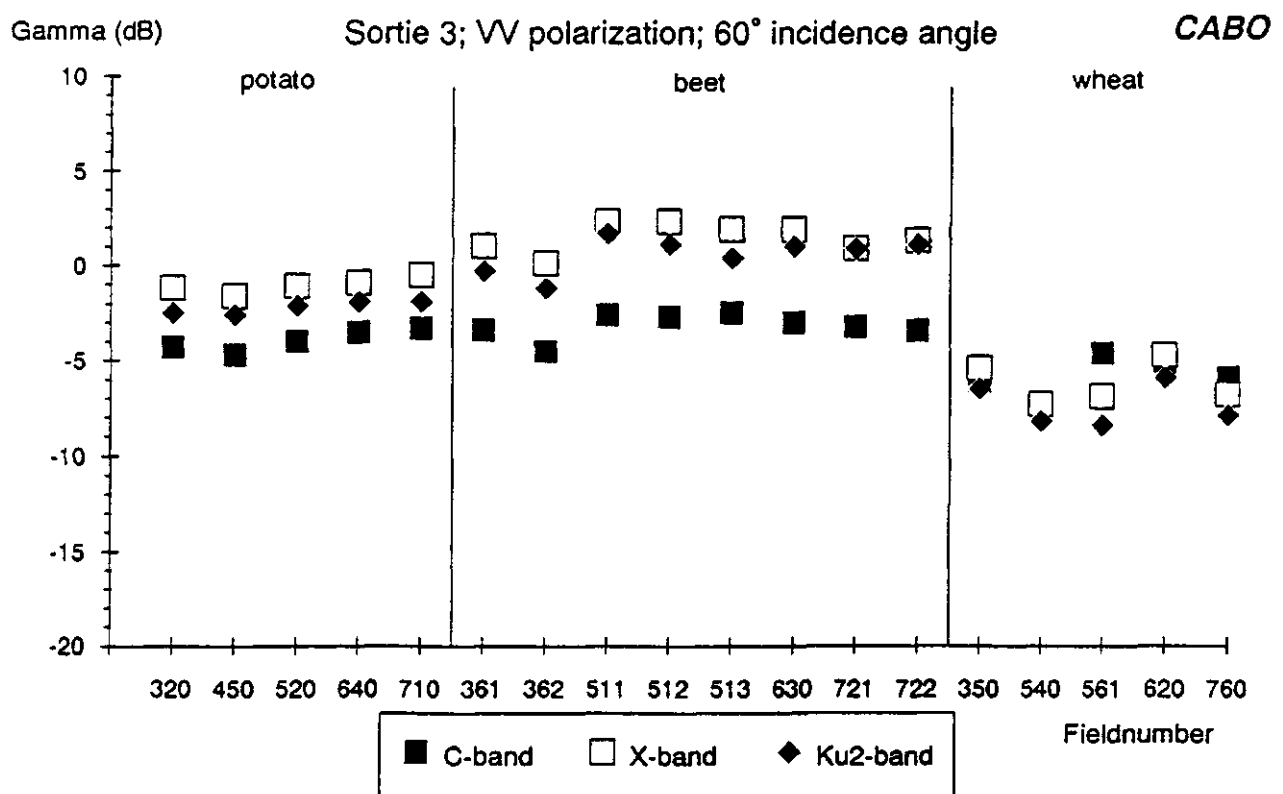


Fig. 55 Radar backscatter of the main crop types (sortie 3, C-, X-, Ku2-band, VV, 60° i.a.)



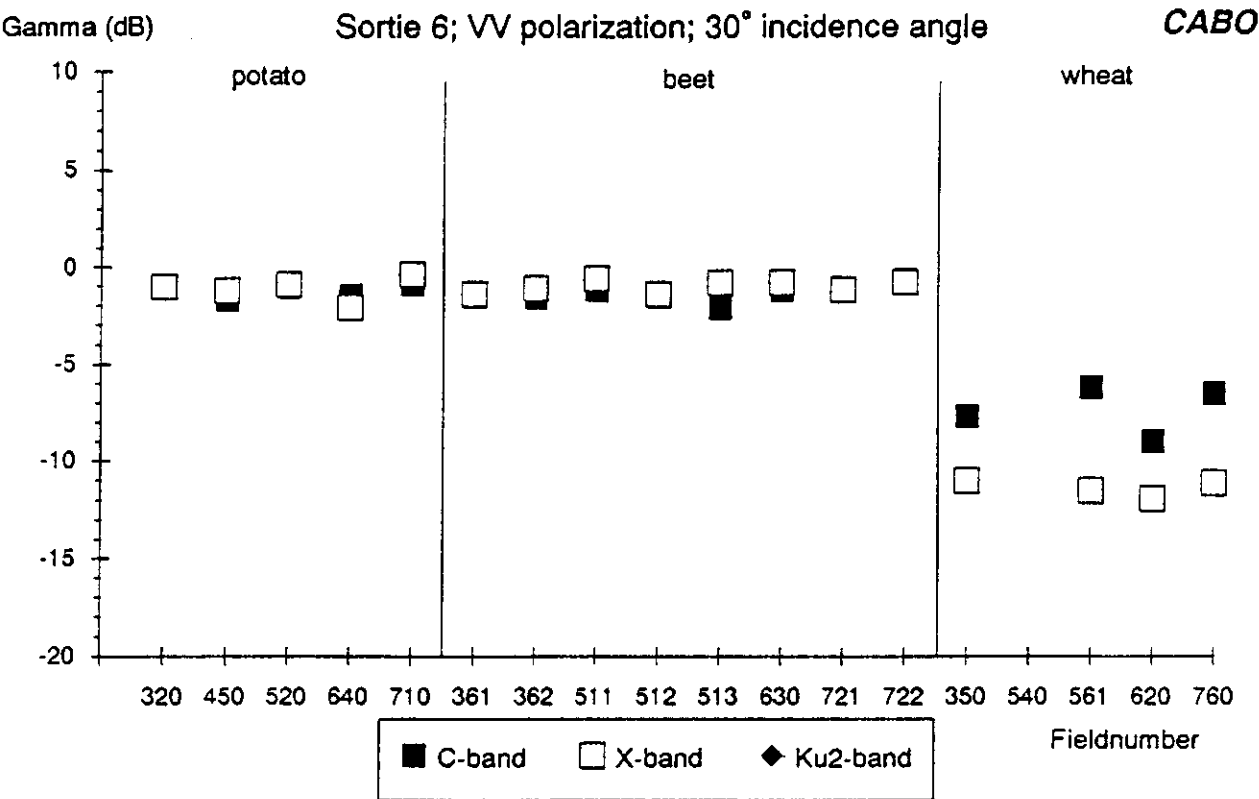


Fig. 56 Radar backscatter of the main crop types (sortie 6, C-, X-, Ku2-band, VV, 30° i.a.)

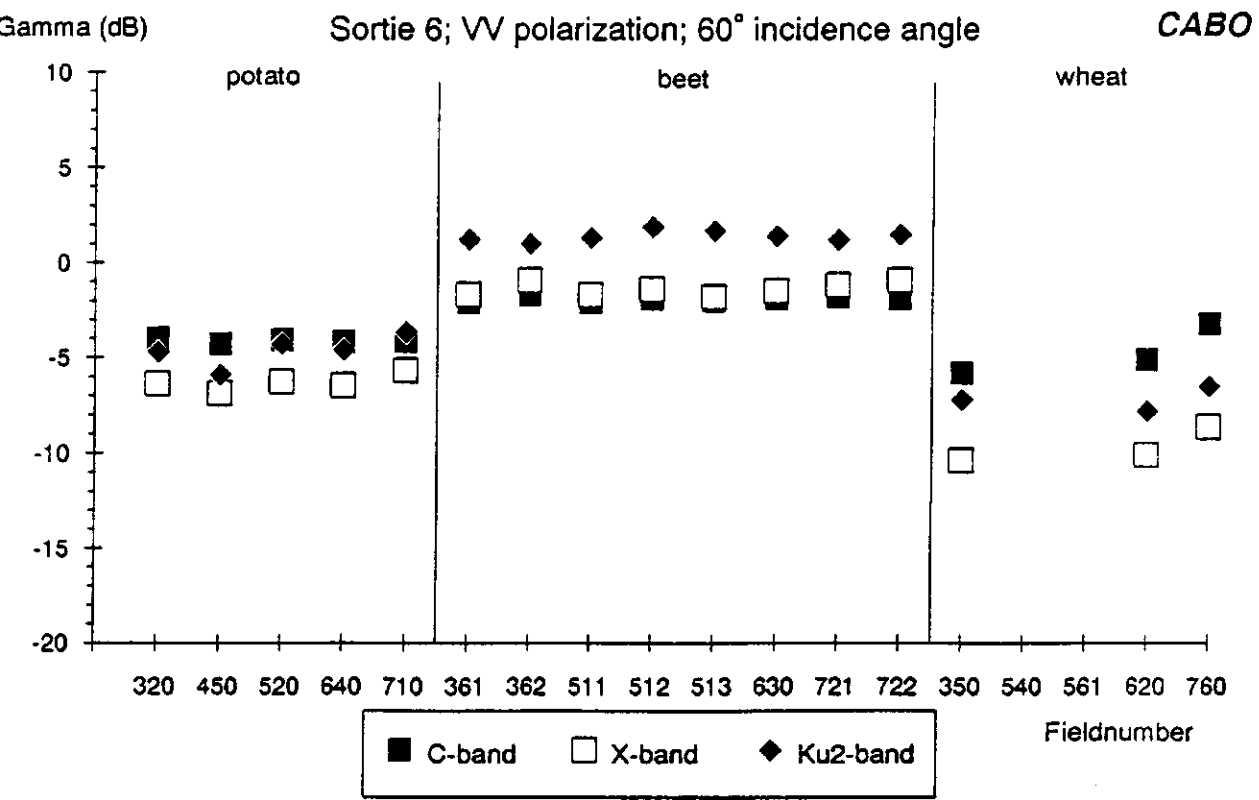


Fig. 57 Radar backscatter of the main crop types (sortie 6, C-, X-, Ku2-band, VV, 60° i.a.)

## 4 Comparison with other systems

The DUTSCAT data were compared with historical data acquired by the ROVE team in their ground-based X- and Q-band measurement programme with the Dutch digital SLAR data from the 1984 campaign and with data from the French scatterometer ERASME from the Agriscatt 1988 campaign. First, the ground-based X-band data will be compared with the SLAR data to get an insight in the consistency between these data types.

### 4.1 X-band ground-based measurements and SLAR data

In 1984, radar data were obtained with the Dutch digital SLAR in May (day 130), June (day 177) and July (day 200) over three agricultural test area's (Flevoland, Groningen and Brabant). All recordings were externally calibrated with corner reflectors. The data were acquired in high angles of incidence ( $76^{\circ}$ - $84^{\circ}$ ) and in medium angles of incidence ( $48^{\circ}$ - $67^{\circ}$ ), of which the latter are used for comparison here. In the images, the field-average radar backscatter was calculated for fields of beet, potato and wheat. Because these fields were chosen all over the image, the whole range of incidence angles between  $48^{\circ}$  and  $67^{\circ}$  is present in the data. Van der Burg and Uenk (1989) presented the average radar backscatter per crop type (with standard deviation) for all three test sites.

The ground-based radar data were collected during 1975-1981 on small agricultural test fields at different locations (Bouman and van Kasteren, 1989). Whereas the spatial sampling in these data was low, the temporal sampling was high. The data were also externally calibrated using corner reflectors.

Figures 58-63 present the radar backscatter of three years of ground based radar data with the SLAR 1984 data for beet, potato and wheat respectively. The ground-based data are plotted for the  $50^{\circ}$  incidence angle and taken from experiments near Wageningen and in Flevoland. The SLAR data are given from the Flevoland and the Brabant test areas (crop-average backscatter values plus and minus the standard deviation). The SLAR data of the Groningen site behaved very similar to those of the Brabant site. For all three 'crops', the SLAR data of the mainly bare soil on day 130 of both the Flevoland and Brabant site were lower than the ground-based data. This could be due to differences in soil background. For the crops, the radar backscatter of beet was perfectly on the same level in the ground-based measurements as in the airborne measurements. The SLAR data of potato were also on the same level for the Brabant site, but about 2.5 dB lower for the Flevoland site. The same average level was also obtained for wheat but here the spread in the ground-based curves was much larger than for the other two crops. For both beet and potato, the same general trend of increasing radar backscatter with crop growth is observed in both data sets. For wheat, the generally 'hollow' temporal curves of the ground-based observations are not recognized in the SLAR data. There may be two reasons for this difference. First, three observations in the growing season might not suffice for the reconstruction of a hollow curve. If the radar backscatter of the soil in the SLAR data was higher, a more hollow curve would have been the result. Secondly, the ground-based measurement programme has shown that the backscatter of wheat is highly variable throughout the years (Bouman and van Kasteren, 1989).

CABO

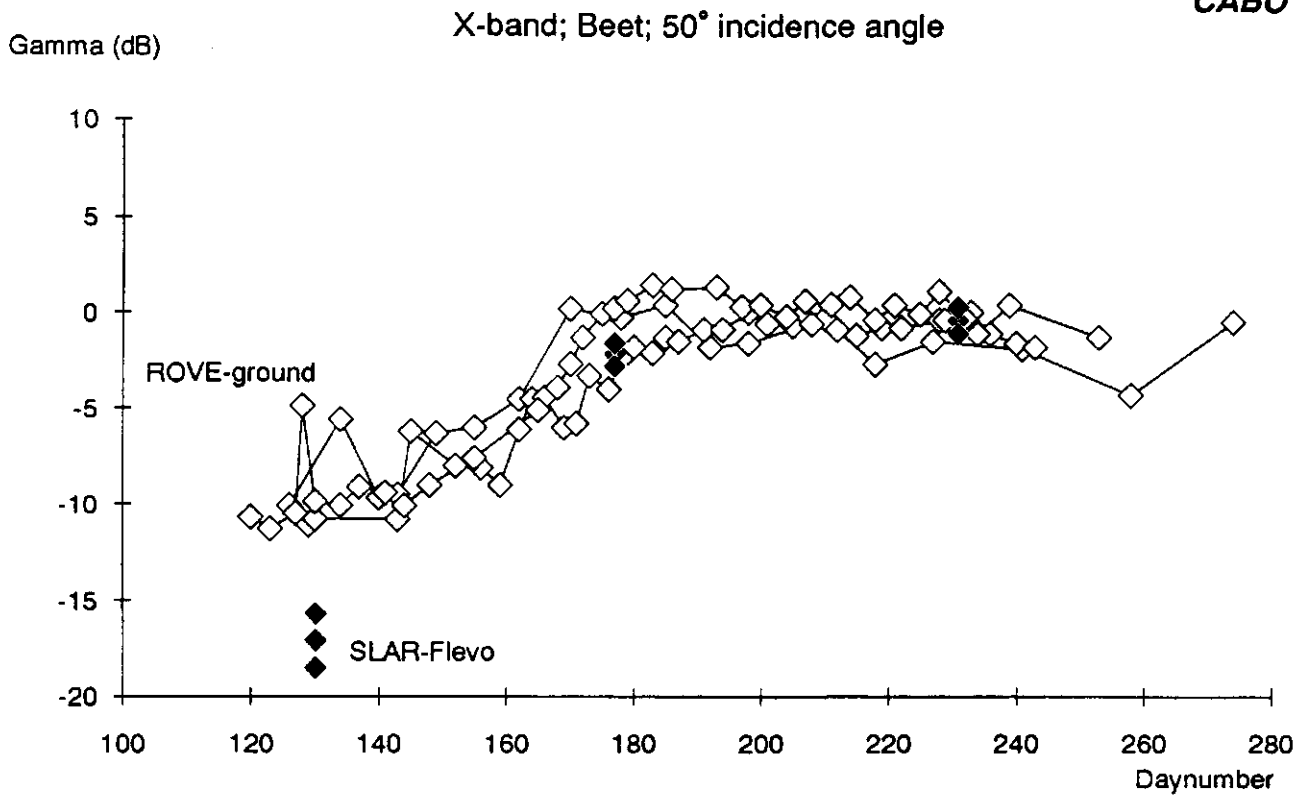


Fig. 58 SLAR Flevoland (48°-67° i.a.) and ROVE X-band radar backscatter (50° i.a.) for beet in the course of the growing season

CABO

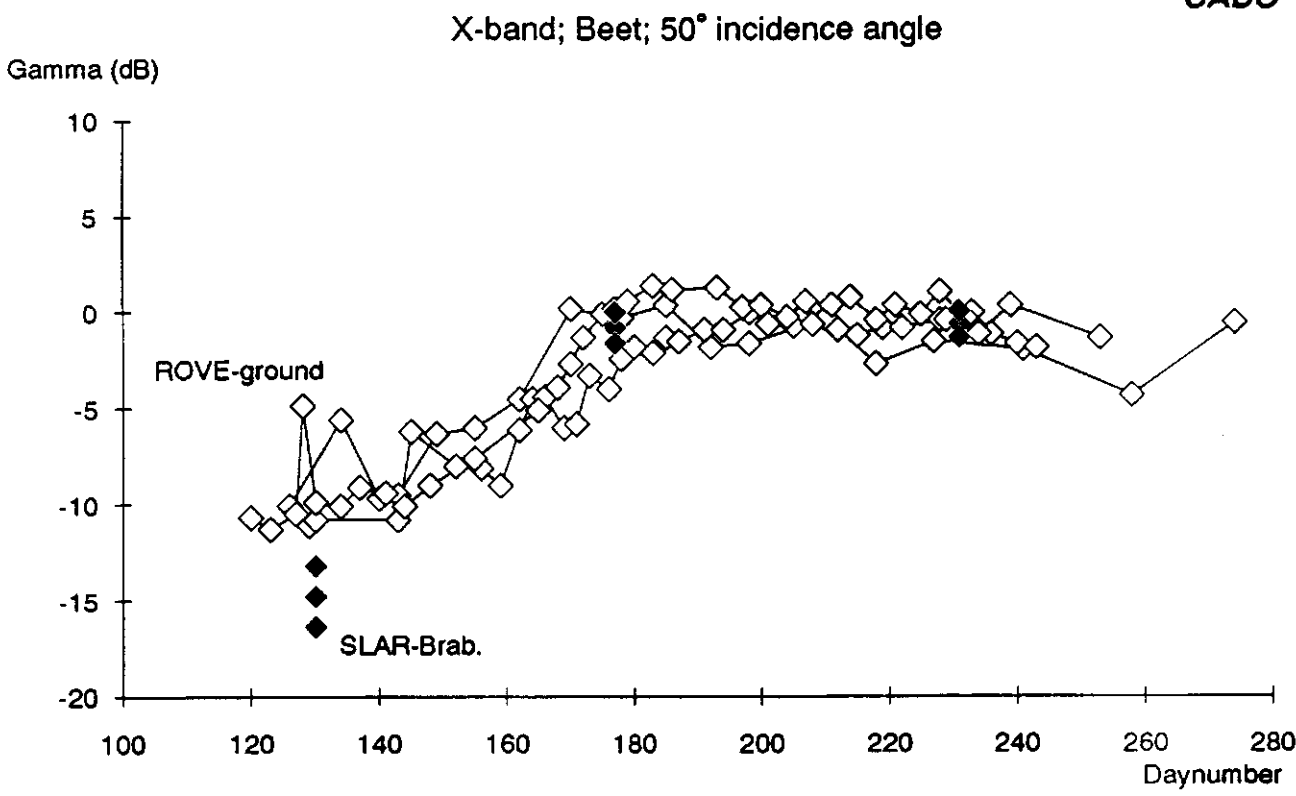


Fig. 59 SLAR Brabant (48°-67° i.a.) and ROVE X-band radar backscatter (50° i.a.) for beet in the course of the growing season

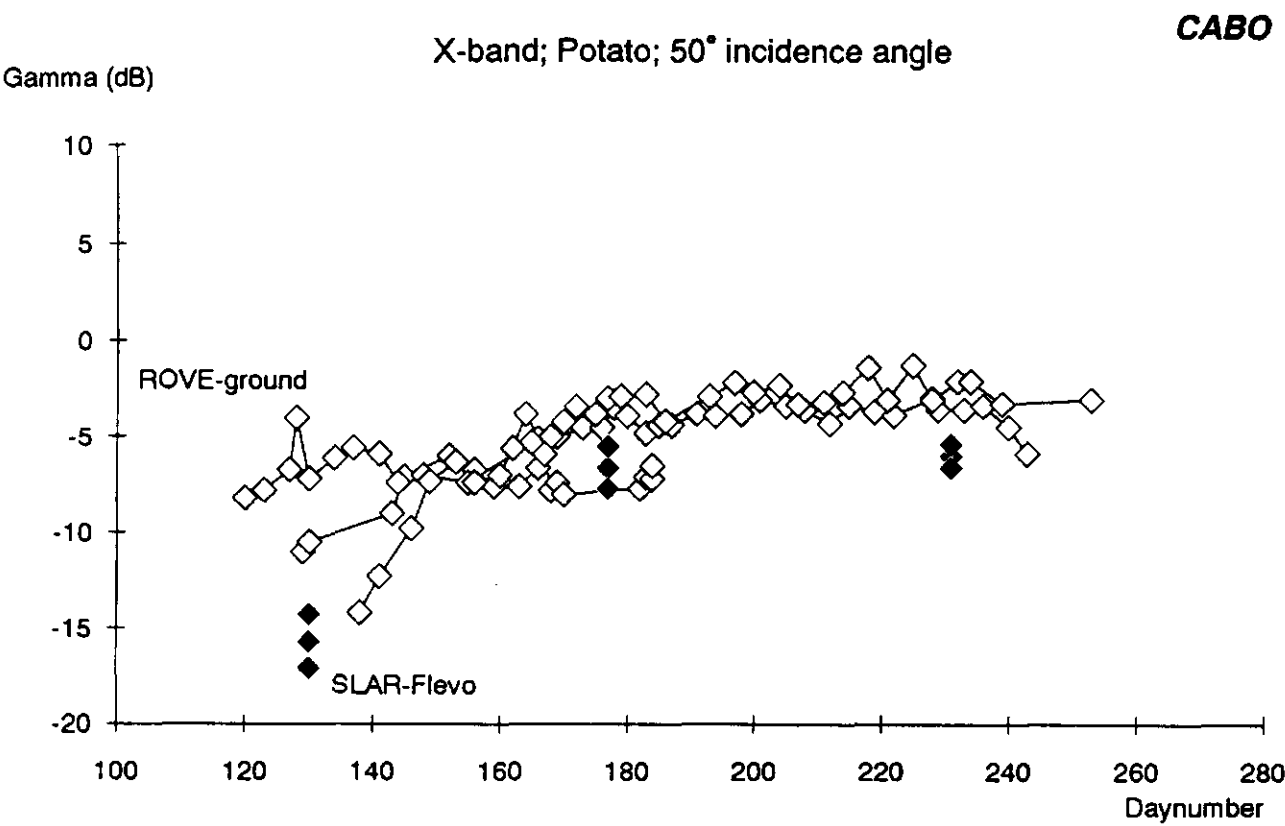


Fig. 60 SLAR Flevoland (48°-67° i.a.) and ROVE X-band radar backscatter (50° i.a.) for potato in the course of the growing season

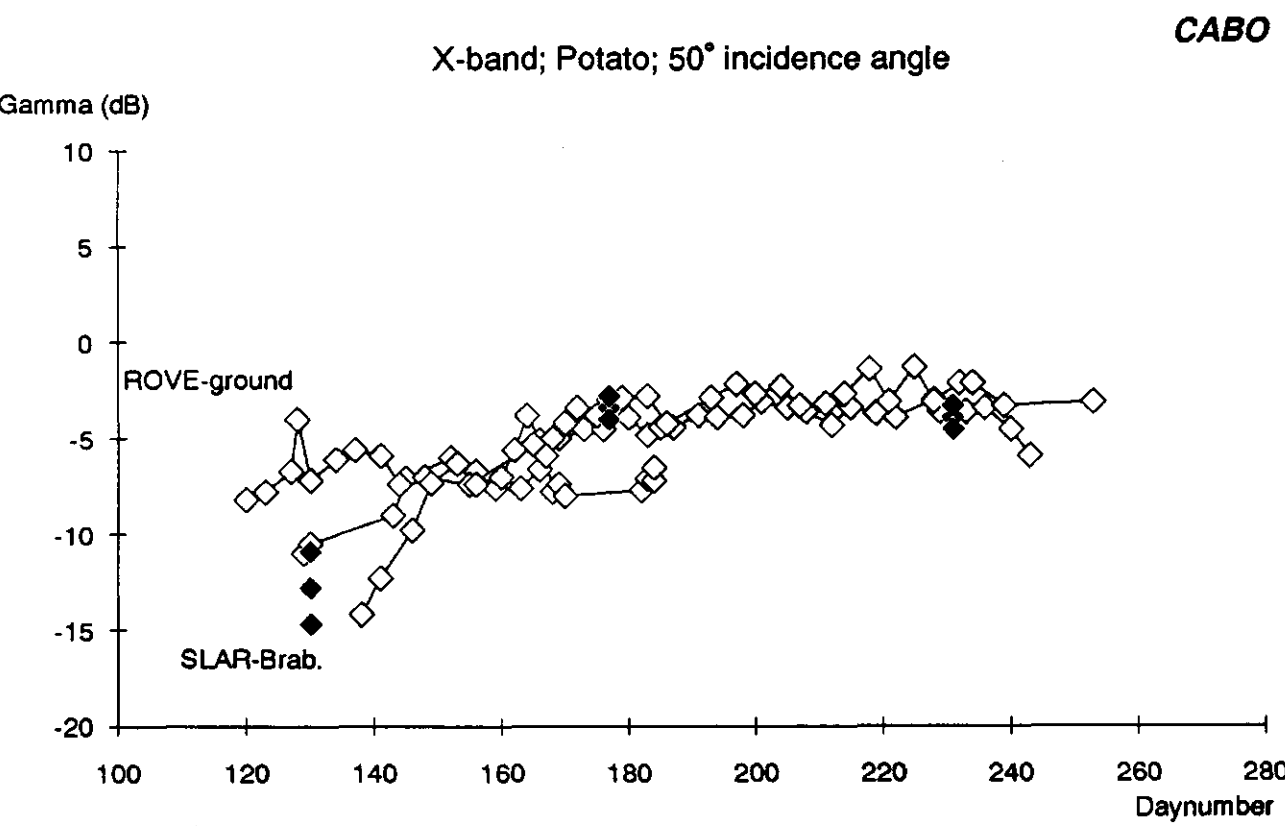


Fig. 61 SLAR Brabant (48°-67° i.a.) and ROVE X-band radar backscatter (50° i.a.) for potato in the course of the growing season

CABO

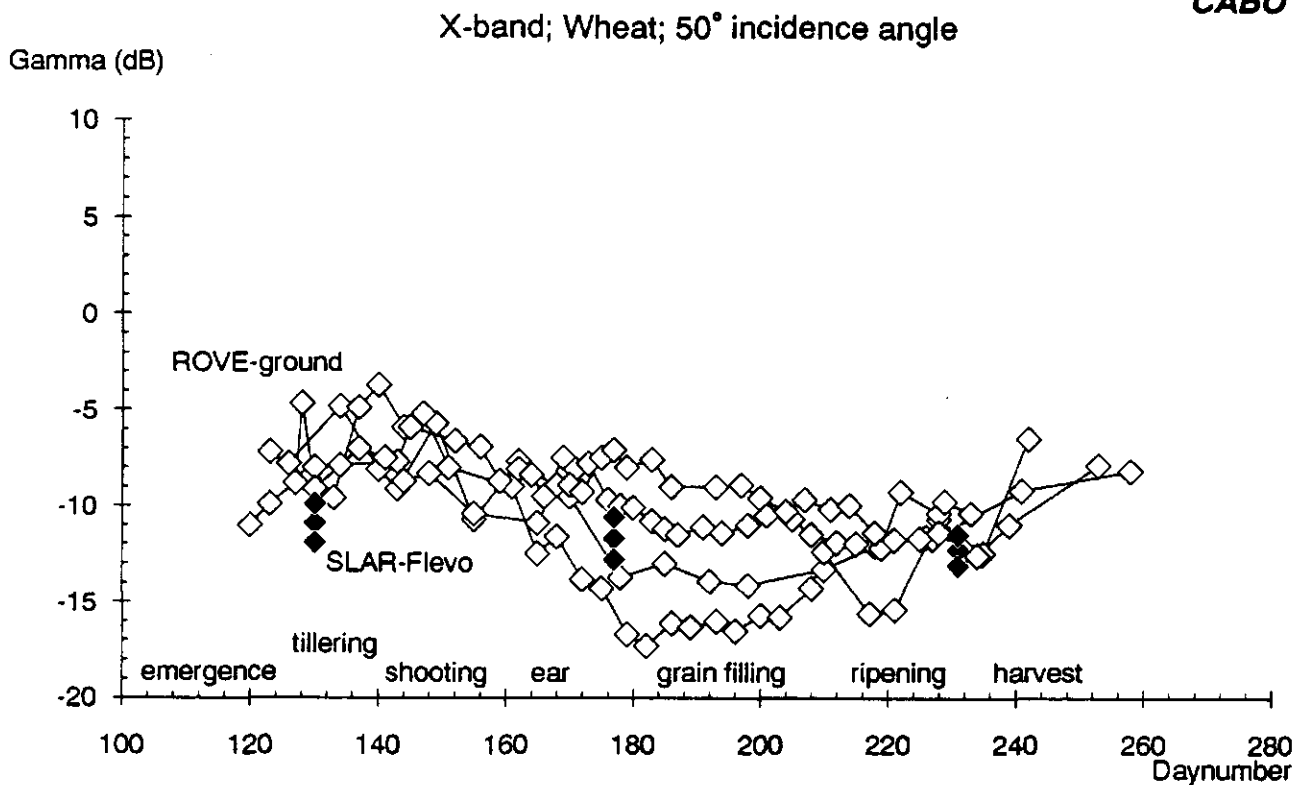


Fig. 62 SLAR Flevoland (48°-67° i.a.) and ROVE X-band radar backscatter (50° i.a.) for wheat in the course of the growing season

CABO

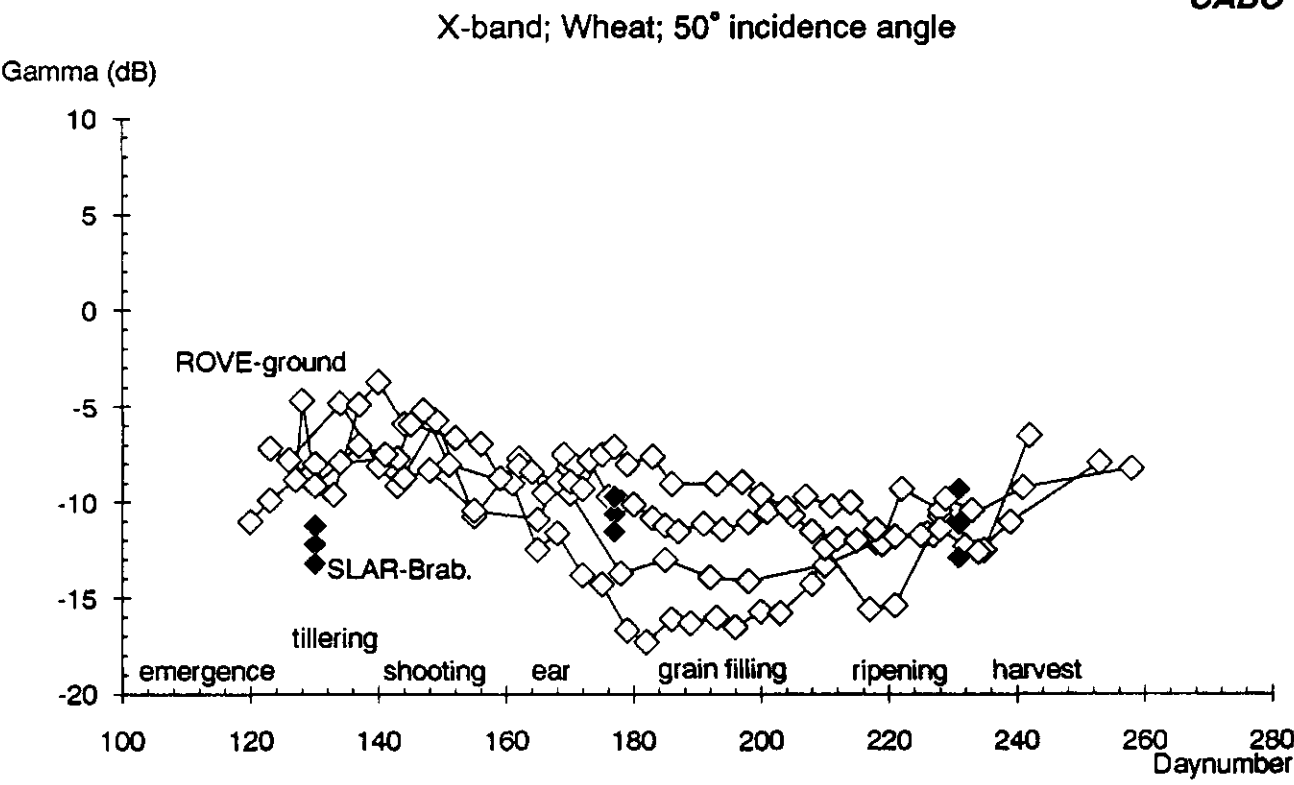


Fig. 63 SLAR Brabant (48°-67° i.a.) and ROVE X-band radar backscatter (50° i.a.) for wheat in the course of the growing season

In 1975 and 1977 the temporal curves of wheat were very pronounced (hollow). In 1979 they were less so and in 1980 the 'hollowness' was completely absent. In the latter year, this was explained by a poor growth and development of the crop (low cover, height and biomass).

Overall, these figures show a fair consistency between the X-band ground-based and airborne SLAR data with respect to absolute level (all crops) and general trend (beet and potato). Only the example of wheat indicates possible differences between ground-based and airborne measurements.

## 4.2 Comparison with DUTSCAT

In figures 64-67 the X-band radar data of the DUTSCAT are plotted with the SLAR 1984 and the ground-based X-band data for beet and potato respectively. For the comparison with the SLAR data, the recordings in the 40°, 50° and 60° incidence angles are lumped, and for the comparison with the ground-based data the 50° incidence angle is selected. Again, the X-band DUTSCAT data appear suspicious (see also § 3.4). Both crops show a decrease in radar backscatter after sortie 4 that is neither present in the SLAR data nor in the ground-based data. The temporal curve compares well with the trends in the other data sets between sortie 1 and sortie 4, but the backscatter level of the crops is some 5 dB too high.

In the DUTSCAT data, the backscatter clusters of potato are broader than that of beet. This is caused by the lumping of the incidence angles. For beet the radar backscatter is on the same level at all incidence angles where for potato there is a clear angular dependency (§ 3.2).

Because of the suspicious data in the X-band, the Ku1-band is also compared with the two historical data sets. The frequency difference between the X- and the Ku1-band is only small, 9.7 GHz versus 13.7 GHz, and therefore no large differences in radar backscatter are expected. In figures 68-73, the DUTSCAT data in the Ku1-band are plotted with the ground-based and SLAR X-band data for beet, potato and wheat respectively. For both beet and potato the trends in the temporal radar backscatter are now comparable in all three data sets. The only difference is the relatively low level of radar backscatter in the Ku1-band at sortie 7. This low level agrees fine with the general backscatter levels in the other two data sets for both crops, but it does not agree with the trend of a stable level from about day 180 to the end of the season. In general, the DUTSCAT data in the Ku1-band are some 3-5 dB higher than the ground-based X-band data, and some 5 dB higher than the X-band SLAR data. The difference in backscatter between the Ku1-band and the SLAR data is even larger for mainly bare soil, i.e. 8-10 dB.

For wheat (figures 72-73), the trend in the temporal radar backscatter in the Ku1-band agrees more with the SLAR data than with the ground-based data. In the first case, a slightly decreasing radar backscatter is observed in the course of the growing season for both data sets. In the Ku1-band, this trend is enhanced by the relatively low radar backscatter at sortie 7, which was also observed for beet and potato. Because this occurs for all three crops, this relatively low level could perhaps be a measurement error and not a truly occurring field phenomenon. In the comparison with the ground-based data, the hollow temporal curve is not recognized in the radar backscatter in the Ku1-band. The absolute backscatter level in the Ku1-band is some 3-7 dB higher than the average ground-based X-band backscatter, and some 5 dB higher than the X-band SLAR data.

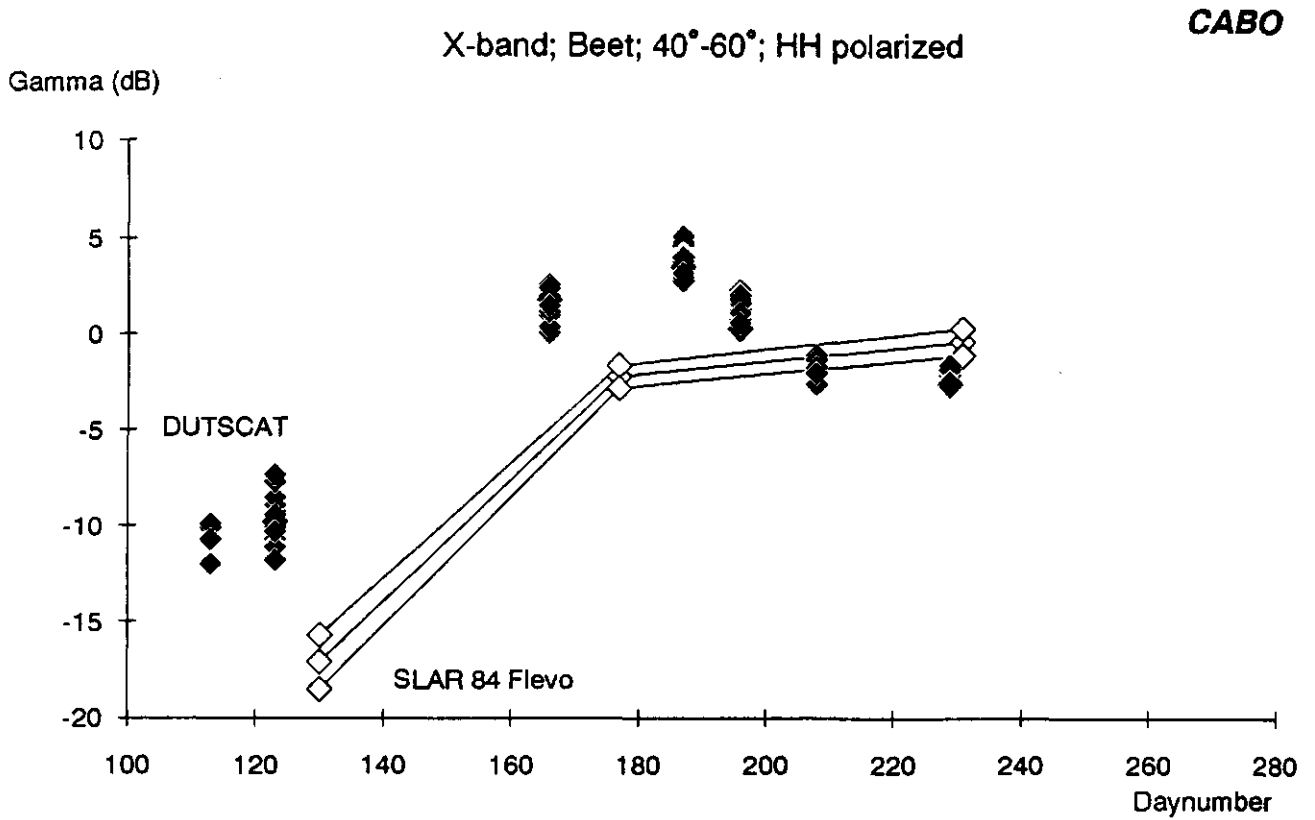


Fig. 64 DUTSCAT (40°, 50° and 60° i.a.) and SLAR (48°-67° i.a.) X-band radar backscatter for beet in the course of the growing season

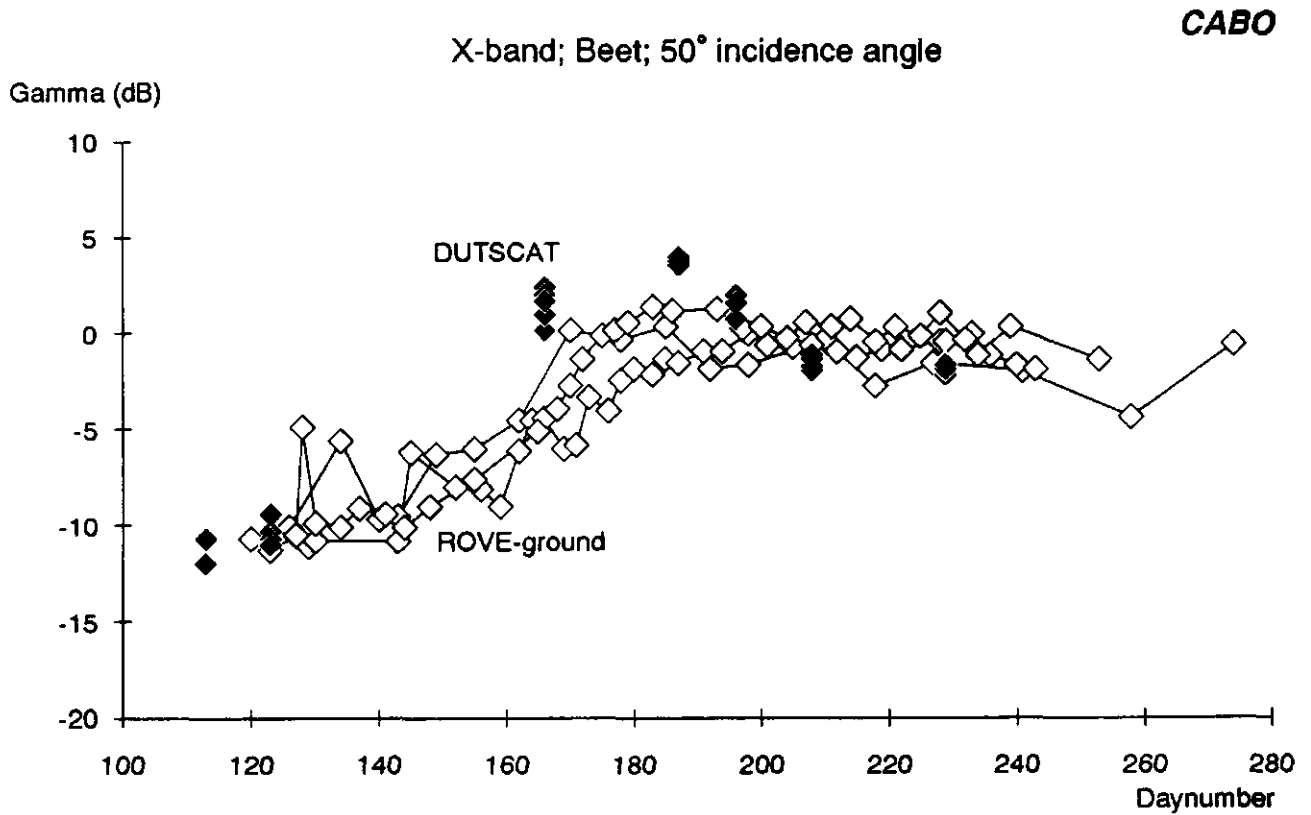


Fig. 65 DUTSCAT and ROVE X-band radar backscatter (50° i.a.) for beet in the course of the growing season

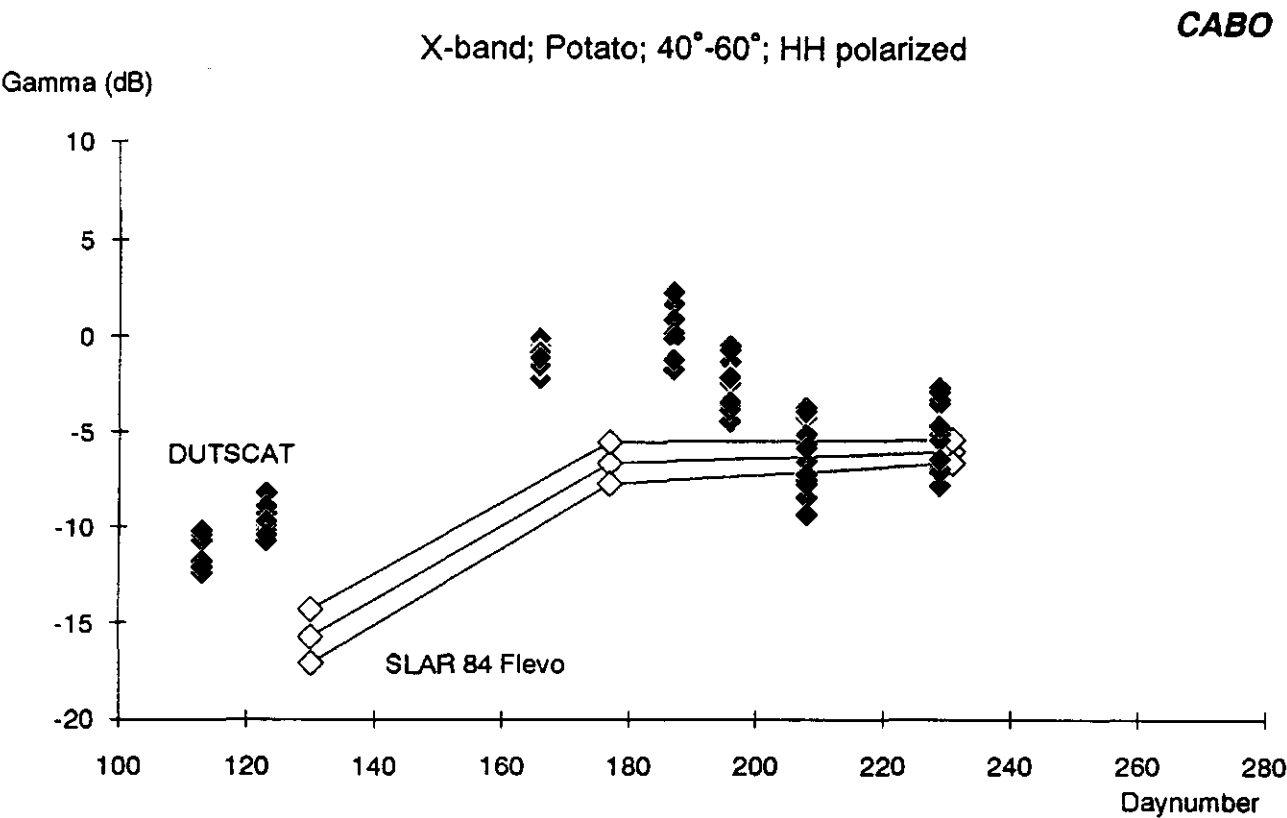


Fig. 66 DUTSCAT (40°, 50° and 60° i.a.) and SLAR (48°-67° i.a.) X-band radar backscatter for potato in the course of the growing season

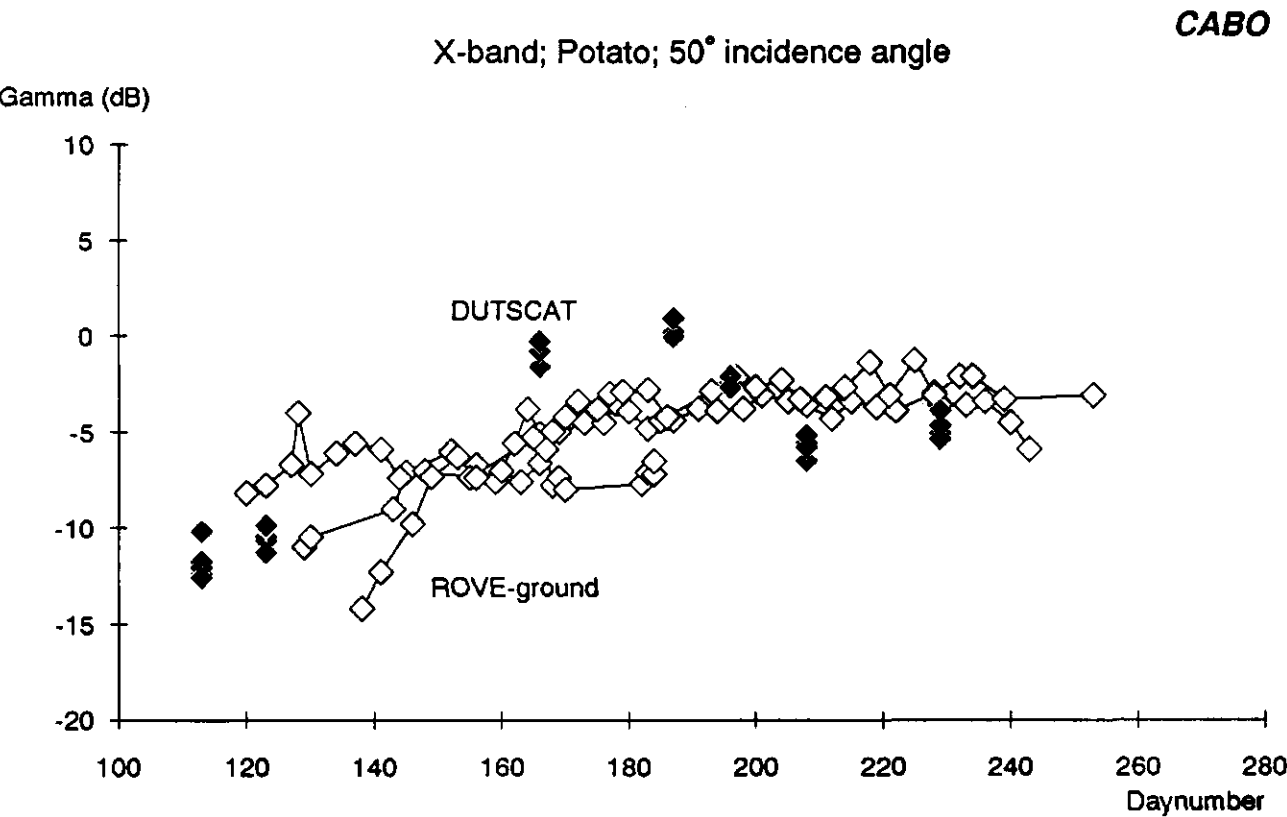


Fig. 67 DUTSCAT and ROVE X-band radar backscatter (50° i.a.) for potato in the course of the growing season



CABO

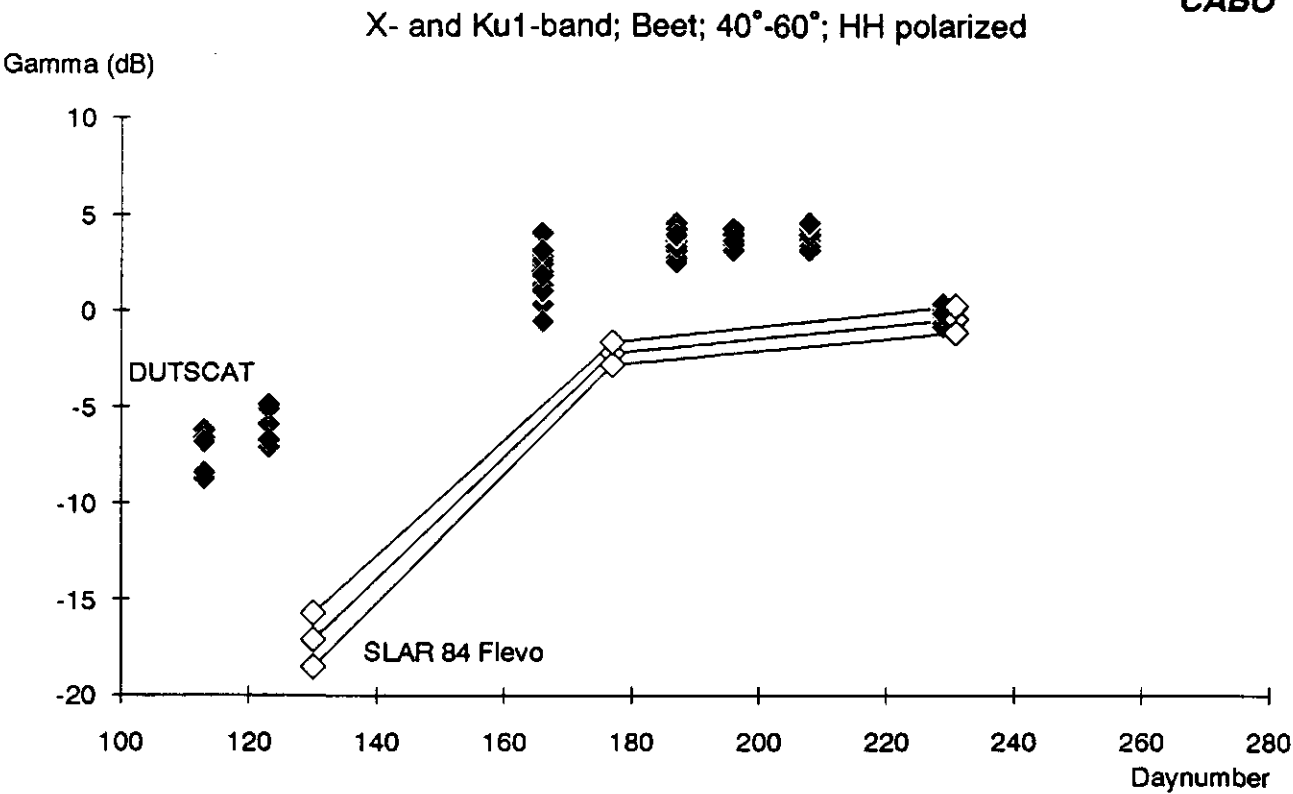


Fig. 68 DUTSCAT (40°, 50° and 60° i.a.) Ku1-band and SLAR (48°-67° i.a.) X-band radar backscatter for beet in the course of the growing season

CABO

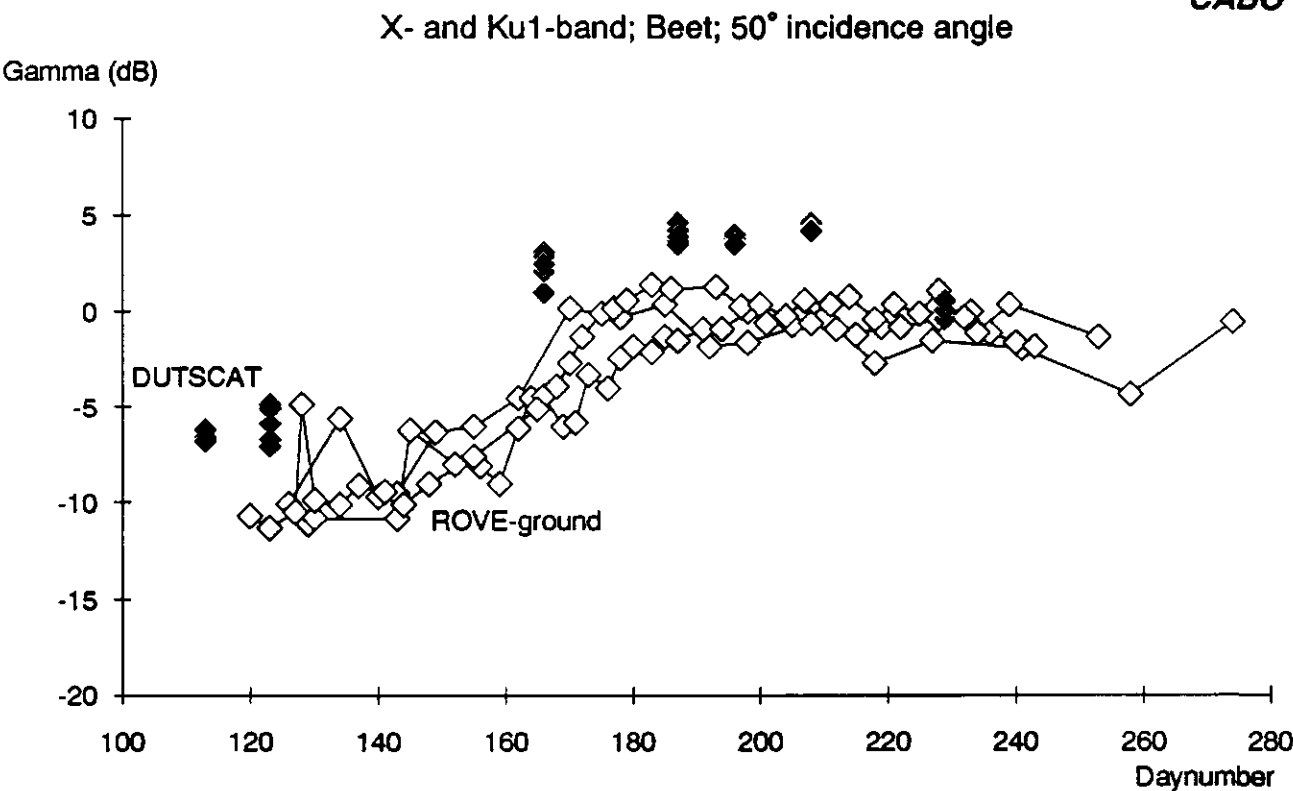


Fig. 69 DUTSCAT Ku1-band and ROVE X-band radar backscatter (50° i.a.) for beet in the course of the growing season

CABO

X- and Ku1-band; Potato; 40°-60°; HH polarized

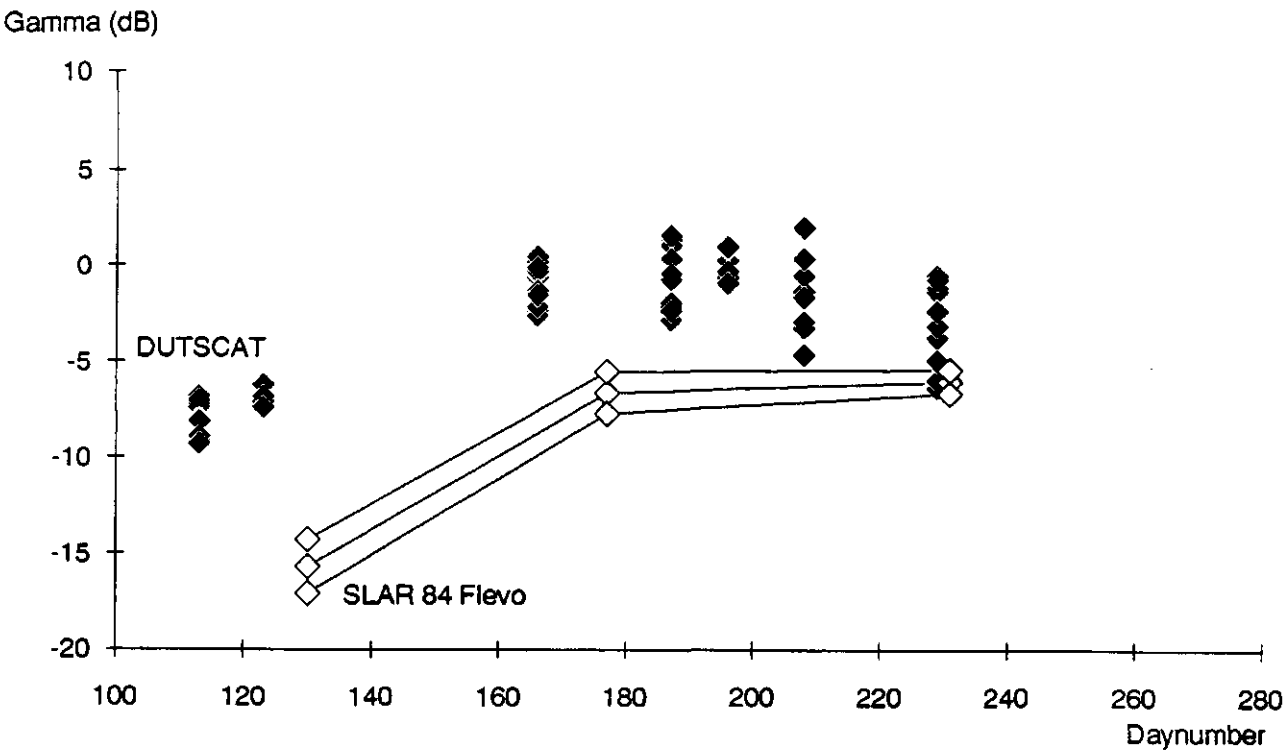


Fig. 70 DUTSCAT (40°, 50° and 60° i.a.) Ku1-band and SLAR (48°-67° i.a.) X-band radar backscatter for potato in the course of the growing season

CABO

X- and Ku1-band; Potato; 50° incidence angle

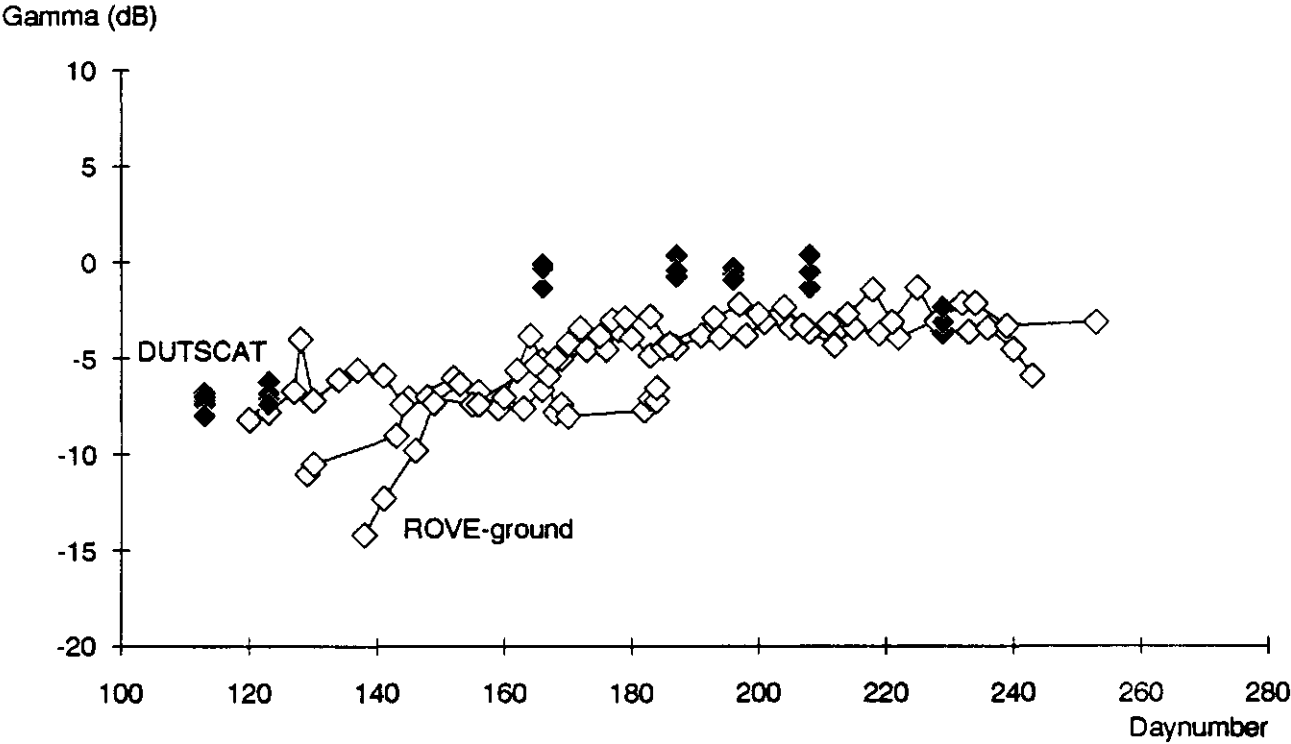


Fig. 71 DUTSCAT Ku1-band and ROVE X-band radar backscatter (50° i.a.) for potato in the course of the growing season

CABO

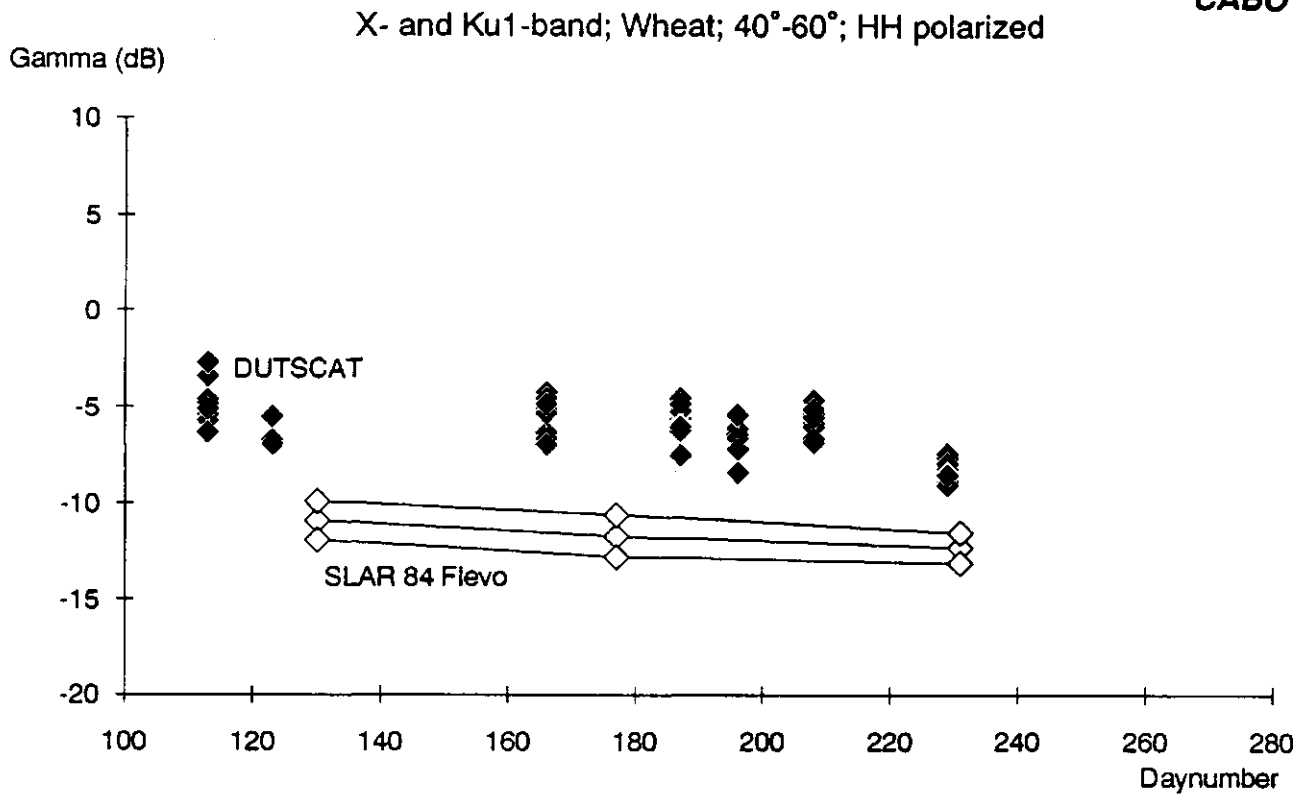


Fig. 72 DUTSCAT (40°, 50° and 60° i.a.) Ku1-band and SLAR (48°-67° i.a.) X-band radar backscatter for wheat in the course of the growing season

CABO

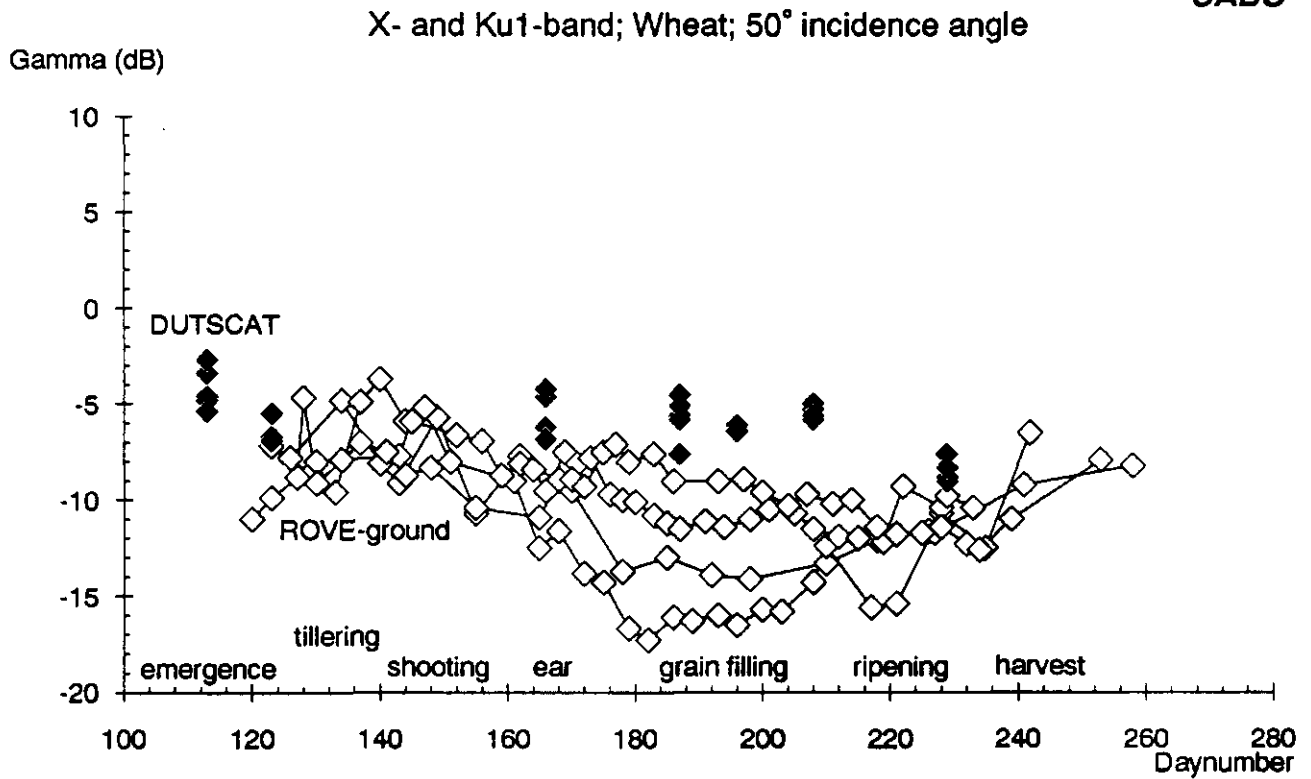


Fig. 73 DUTSCAT Ku1-band and ROVE X-band radar backscatter (50° i.a.) for wheat in the course of the growing season

Both the comparison of the DUTSCAT and the SLAR measurements with the ground-based data for wheat indicate a possible difference between ground-based and airborne observations. Hollow temporal curves that occur in the ground-based observations are not recognized in the airborne observations. Both the 1987 and the 1988 DUTSCAT data indicate that the backscatter of wheat (in all frequency bands) reacts more on the changes in soil moisture content than on the growth of the crop. This suggests a relatively high transparency of wheat for microwaves.

For this comparison, it should be remembered that the ground-based measurements of wheat display a large variability between the years (Bouman and van Kasteren, 1989). In 1977, very pronounced, hollow 'radar-growth' curves were observed. With a close row spacing, there was no influence of variation in the soil moisture content notable on the radar backscatter in the midst of the growing season. With larger row spacing, increases in the moisture content were clearly recognized, even at medium angles of incidence. In 1979, the hollowness of the 'radar-growth' curves was less pronounced. With the relatively coarse temporal sampling with airborne observations, the subtlety of such curves will probably not be recognized. Than in 1980, the 'radar-growth' curve was not hollow at all and its shape was completely explained by the variations in soil moisture content. This observation completely agrees with the airborne DUTSCAT measurements of wheat. However, in 1980, the absence of the typical hollow 'radar-growth' curve was explained by the very poor growth and development of the crop. This was not true for the wheat crops in the DUTSCAT data set.

Overall, it is clear that the radar backscatter of wheat is still relatively poorly understood. Observed features can only partly be explained and the variability in radar backscatter is very high.

### 4.3 Ground-based Q-band measurements

In 1980, the radar backscatter of crops was both measured in the X-band and in the Q-band (35 GHz). This provides the opportunity of comparing the frequency dependency in the ground-based observations with those in the DUTSCAT data. In figures 74-79, the ground-based radar backscatter in both bands is plotted for beet, potato and wheat respectively, and at 20° and 40° incidence angle. For all three crops the Q-band radar backscatter is higher than the X-band radar backscatter. For beet and potato the difference is a very constant 3-4 dB at all angles of incidence. For wheat, the difference depends on the angle of incidence and is variable during the growing season. It averages some 4 dB at 20° incidence angle to some 6 dB at 60° incidence (unpublished data). Again, the poor growth and development of this wheat crop is recalled here. For bare soil, the variability is even higher and appears related to the surface roughness and to the variation in soil moisture content (unpublished data). With a high soil moisture content the difference in radar backscatter between the bands is lower than with a low moisture content (note also the 'soil moisture peak' on day 130 in figures 74-79). The difference is higher for a relatively smooth surface than for a rough surface, and like for wheat, it is also higher at high incidence angles than at low incidence angles. Overall, the Q-band radar backscatter is on the average 0.7 dB and 4 dB higher than the X-band radar backscatter for respectively a rough and a smooth soil at 20° incidence angle, and 3 dB and 5 dB respectively at 40° incidence angle.

The DUTSCAT data show a different frequency behaviour in the range of the X-band to the Ku2-band (§ 3.5). After the X-band, the backscatter either increases a little in the Ku1-band (bare soil, beet and potato at the end of the season), remains on the same level in the Ku1-band, or decreases a bit in the Ku1-band (all crops in the middle of the growing season). Since the high levels of X-band radar backscatter at sortie 3 and 4 are suspicious, the last trend (decreasing backscatter in Ku1-band) seems not very likely. After the Ku1-band the radar backscatter generally decreases a little (1-2 dB) in the Ku2-band. Overall, the DUTSCAT data do not indicate an increase (or only a slight one) in radar backscatter with increasing frequency after the X-band. However, the whole range from 17.3 GHz (Ku2-band) to 35 GHz (Q-band) is not covered by these data.

In figures 74-79, the Ku1-band radar backscatter of the DUTSCAT data is also plotted. For both beet and potato, the trends in the Ku1-band and the X- and Q-band are similar, but the Ku1-backscatter level compares much better with the Q-band than with the X-band. This is surprising since one would expect the opposite because the frequency of the Ku1-band is closer to that of the X-band than to that of the Q-band. For wheat, the trend in the Ku1-band radar backscatter hardly resembles that in either the ground-based X- or Q-band. The Ku1-band backscatter decreases from the level of the Q-band at sortie 1 and 2 to that between both bands at 40° incidence angle, and to that of the X-band at 20° incidence angle.

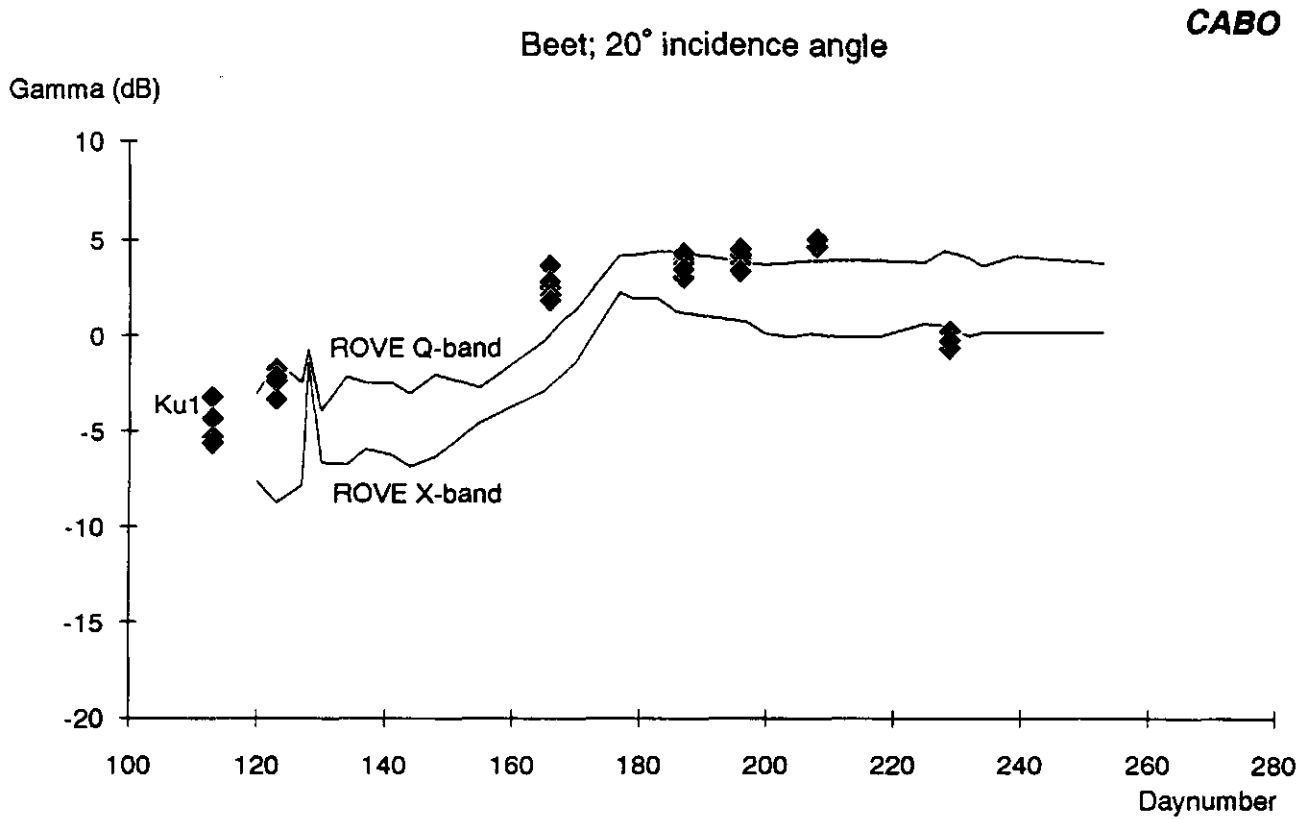


Fig. 74 DUTSCAT Ku1-band, ROVE X-band and ROVE Q-band radar backscatter (20° i.a.) for beet in the course of the growing season

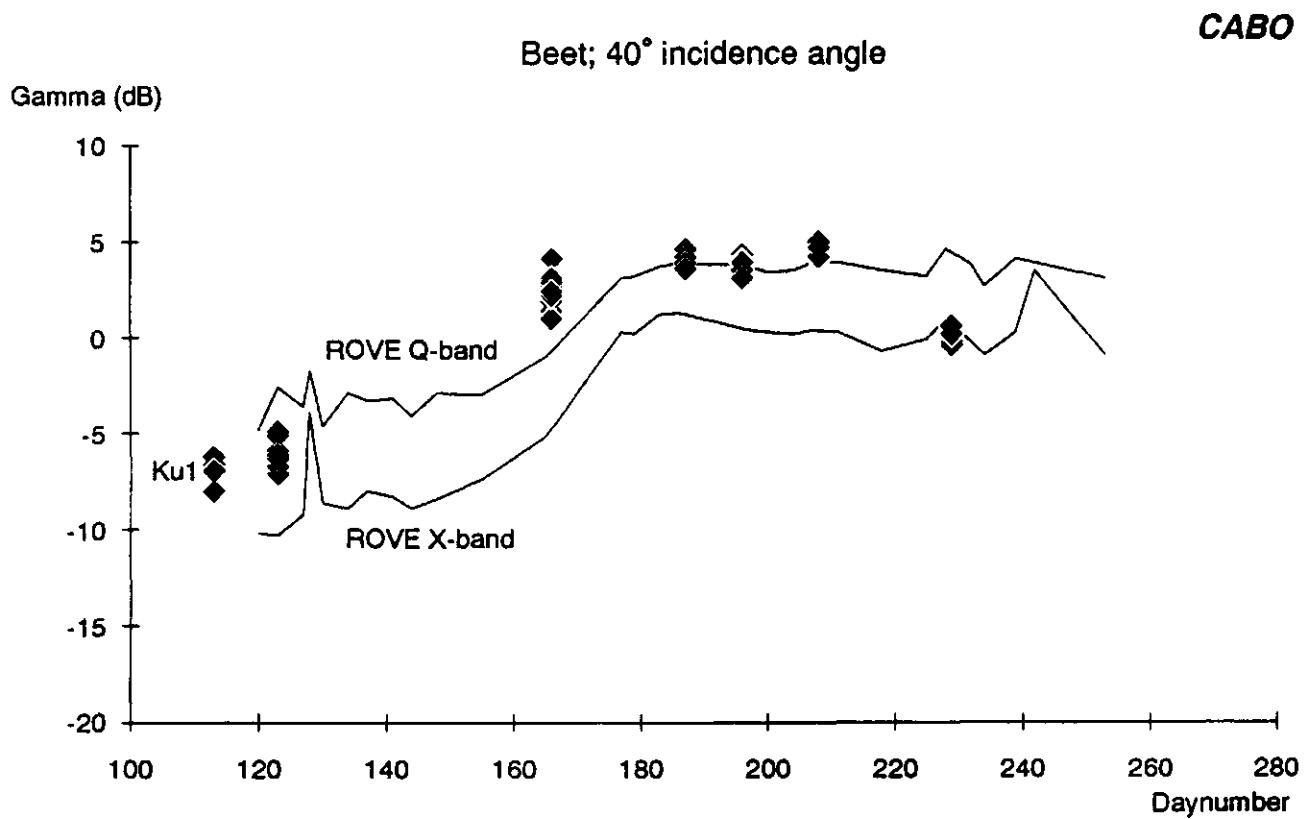


Fig. 75 DUTSCAT Ku1-band, ROVE X-band and ROVE Q-band radar backscatter (40° i.a.) for beet in the course of the growing season

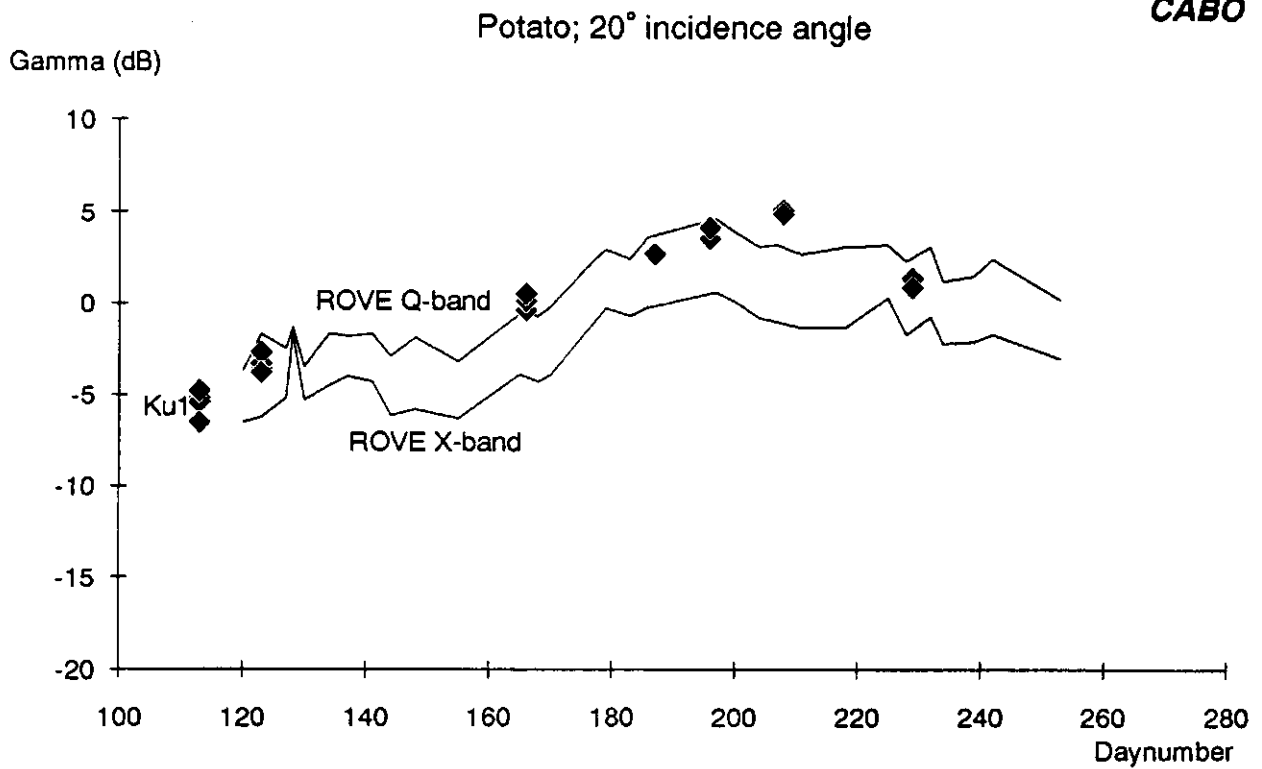
**CABO**

Fig. 76 DUTSCAT Ku1-band, ROVE X-band and ROVE Q-band radar backscatter (20° i.a.) for potato in the course of the growing season

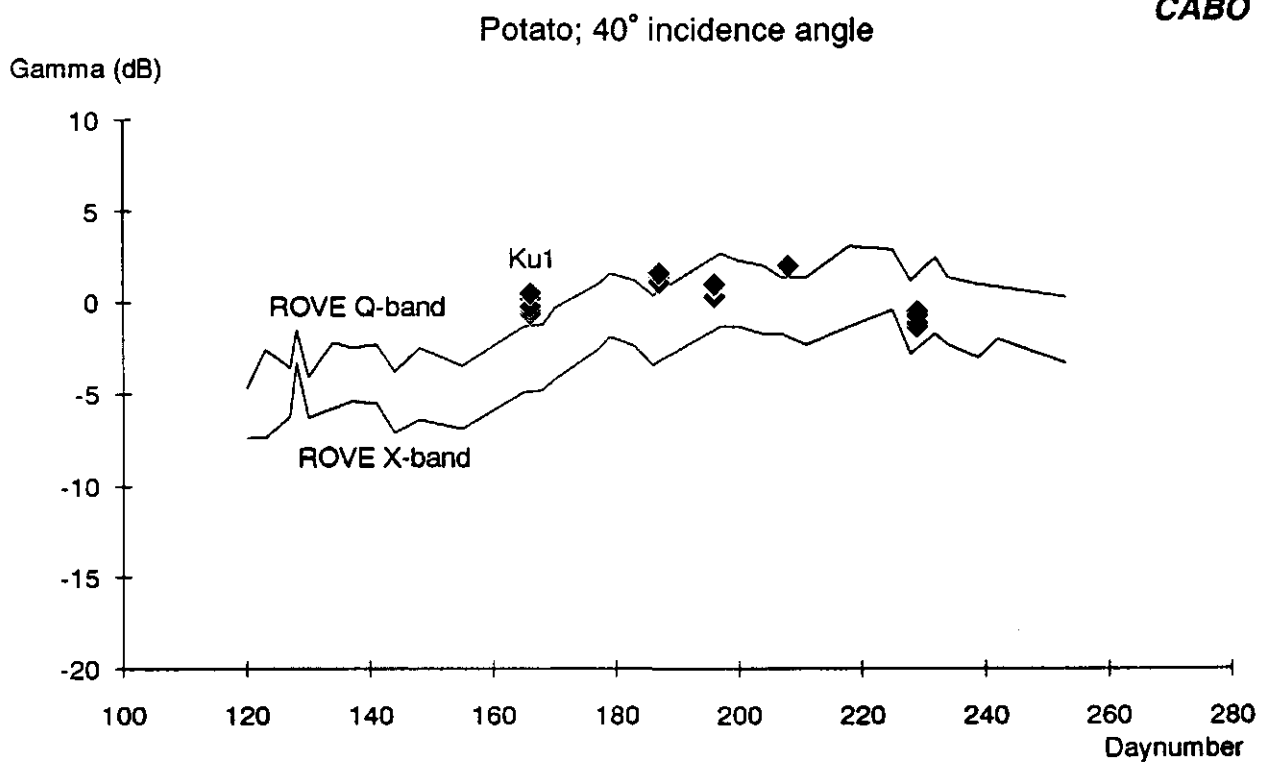
**CABO**

Fig. 77 DUTSCAT Ku1-band, ROVE X-band and ROVE Q-band radar backscatter (40° i.a.) for potato in the course of the growing season

CABO

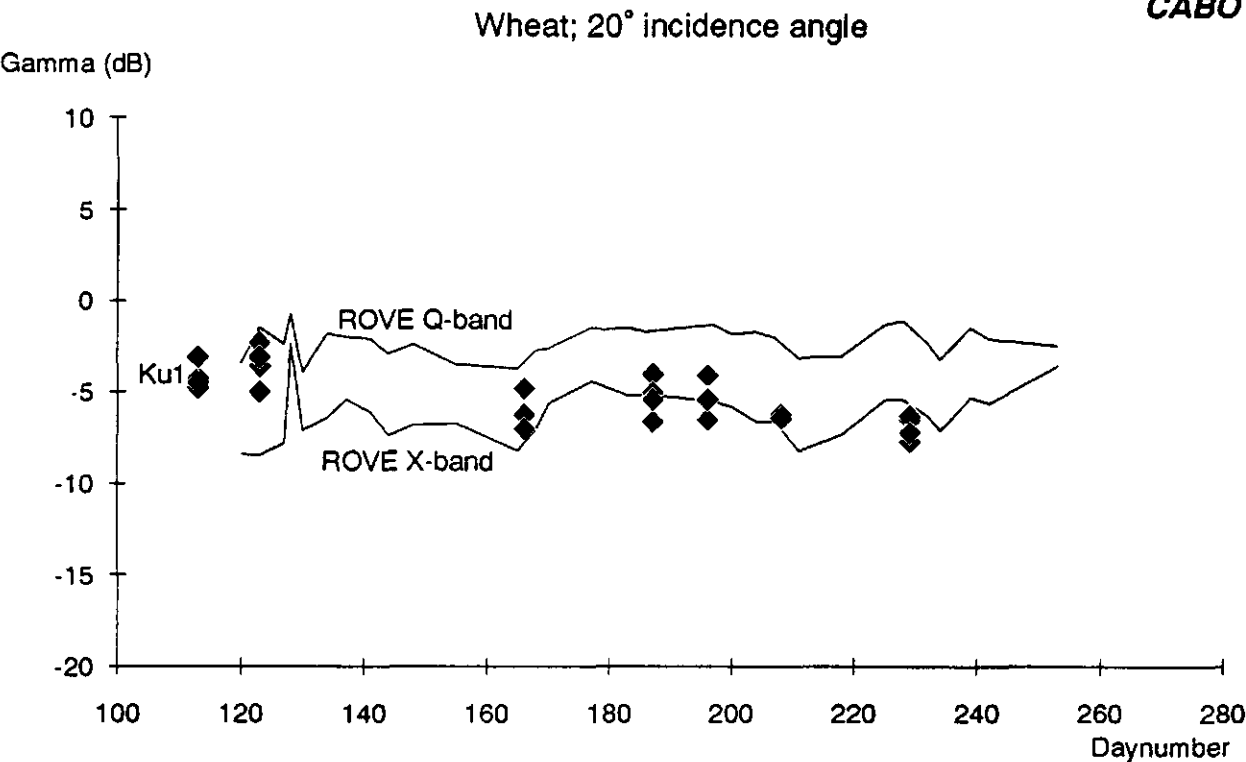


Fig. 78 DUTSCAT Ku1-band, ROVE X-band and ROVE Q-band radar backscatter (20° i.a.) for wheat in the course of the growing season

CABO

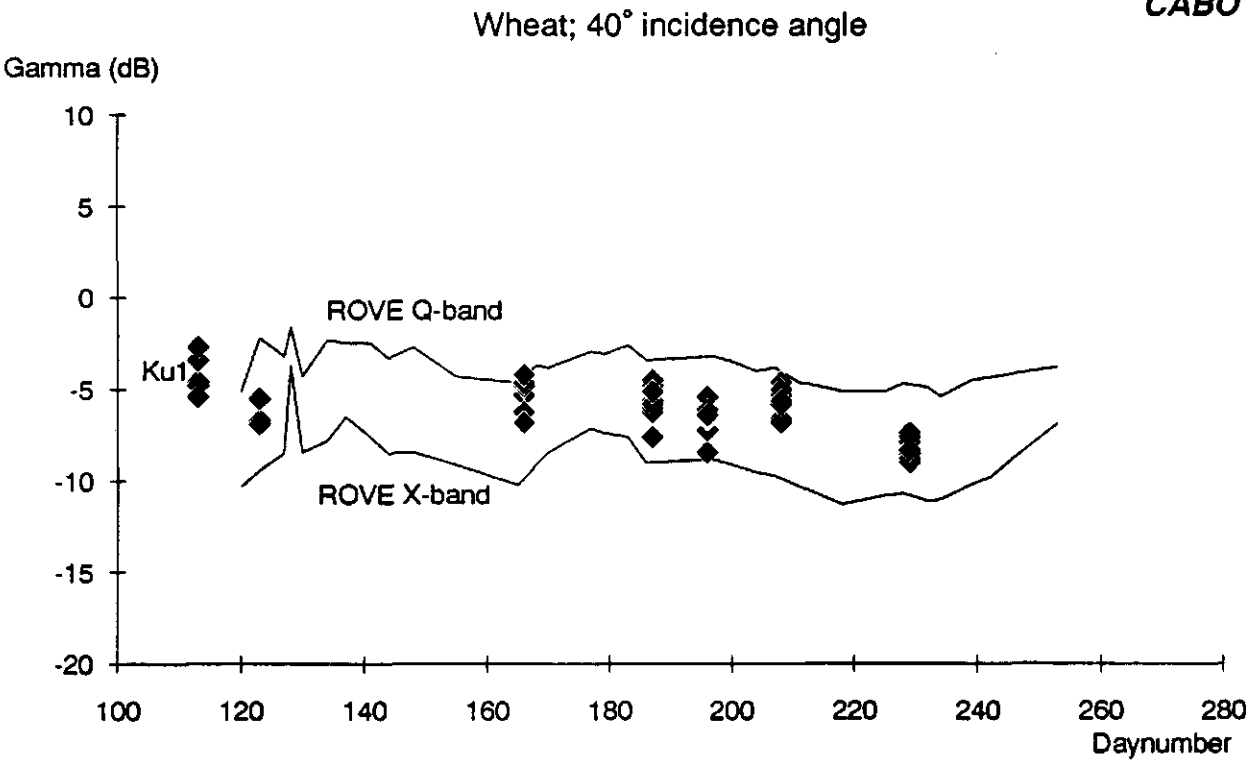


Fig. 79 DUTSCAT Ku1-band, ROVE X-band and ROVE Q-band radar backscatter (40° i.a.) for wheat in the course of the growing season



#### 4.4 Comparison DUTSCAT with ERASME

During the Agriscatt 1988 campaign the French forward-looking scatterometer ERASME (Bernard et al., 1986) measured the Flevoland test site during sortie 3, 4, 5 and 6 simultaneously with DUTSCAT (Hoekman, 1990). Measurements were taken in the X-band VV and HH polarization and in the C-band HH polarization (C-band VV polarization measurements were not carried out due to a technical failure). The forward-looking scatterometer measured at two different antenna tilts, 23° and 38°. A quality assessment of the ERASME data was performed at ESA/EARTHNET (James, 1989b). For comparison with DUTSCAT the data at 20°, 30° and 40° incidence angle were selected. For ERASME two sets of  $\gamma$  values at 30° incidence angle were obtained, one from the 23° and one from the 38° antenna pointing angle (in the latter named as 30°a and 30°b respectively). Theoretically, these two sets should be the same, but in practice there is a difference of several dB (0-3 dB).

In figures 80-83 the track plots of DUTSCAT and ERASME are compared. All the figures show that the DUTSCAT data are higher than the ERASME data. A total overview of the offset (DUTSCAT-ERASME) is given in table 5.

Table 5 Difference in dB between DUTSCAT and ERASME; track averaged values

SORTIE	BAND	POL	20°	30°a	30°b	40°
3	C	HH	5.25	*	*	5.57
4	C	HH	4.68	3.27	3.22	8.43
5	C	HH	4.57	7.70	4.87	6.32
6	C	HH	6.52	7.69	9.38	8.06
3	X	HH	8.44	*	*	6.36
4	X	HH	8.17	7.38	8.30	8.83
5	X	HH	2.79	4.66	4.76	7.24
6	X	HH	3.75	3.28	3.69	3.53
3	X	VV	6.70	5.62	6.06	4.33
4	X	VV	8.40	8.31	7.71	9.35
5	X	VV	2.34	6.22	5.51	4.92
6	X	VV	3.33	2.65	2.47	2.79

Table 5 shows that the offset between the two systems is not consistent and varies from 2.34 dB to 9.38 dB. At sortie 3 the C- and X-band HH polarization measurements at 30° incidence angle were not available for DUTSCAT.

CABO

Sortie 3; C-band; 20° incidence angle; HH

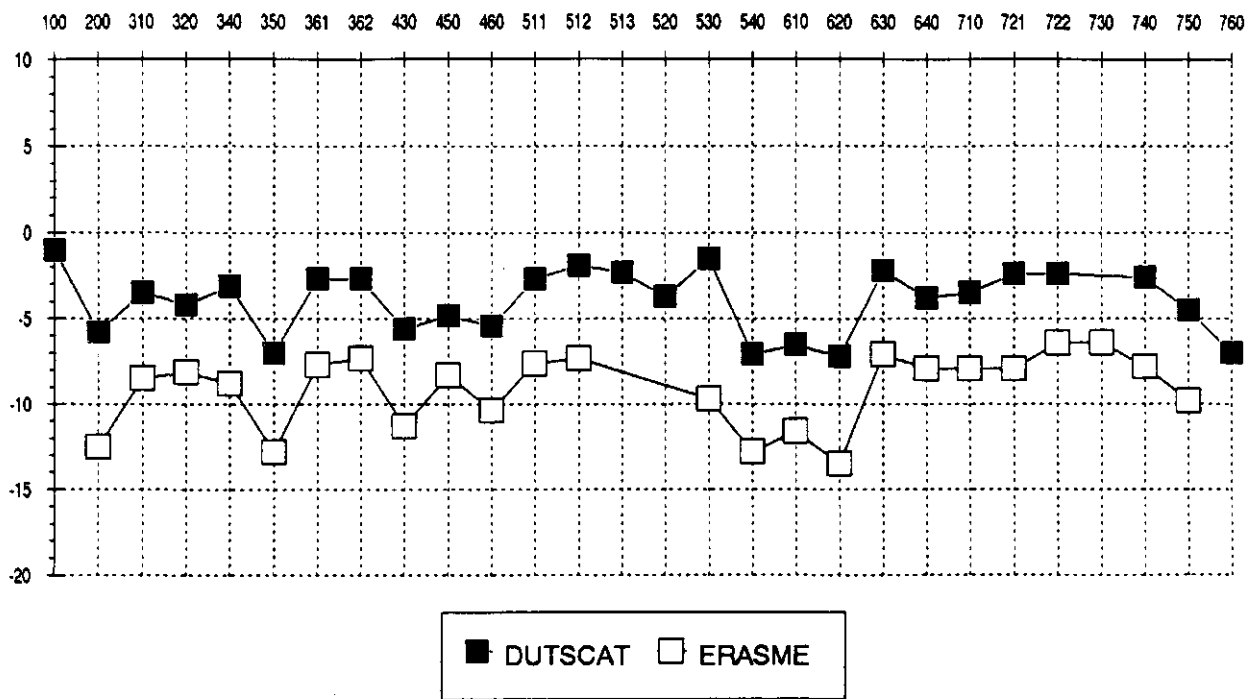


Fig. 80 DUTSCAT and ERASME radar backscatter (sortie 3, C-band, 20° i.a., HH) along the flight track

CABO

Sortie 6; C-band; 40° incidence angle; HH

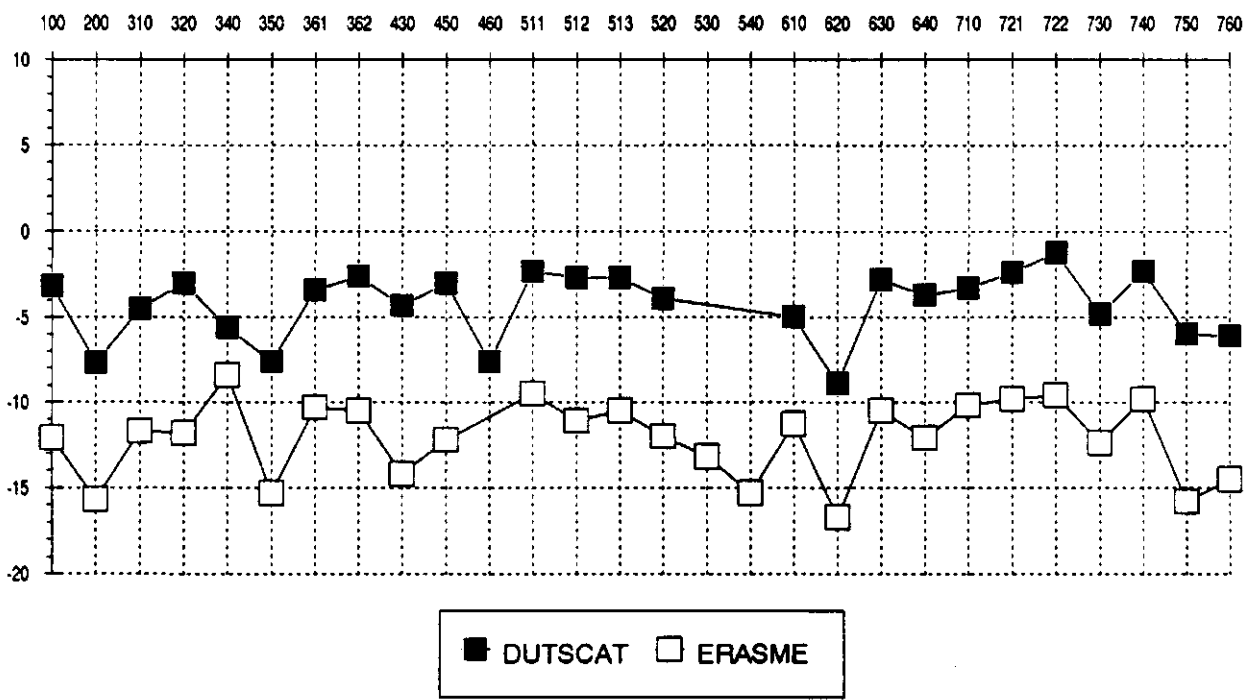


Fig. 81 DUTSCAT and ERASME radar backscatter (sortie 6, C-band, 40° i.a., HH) along the flight track

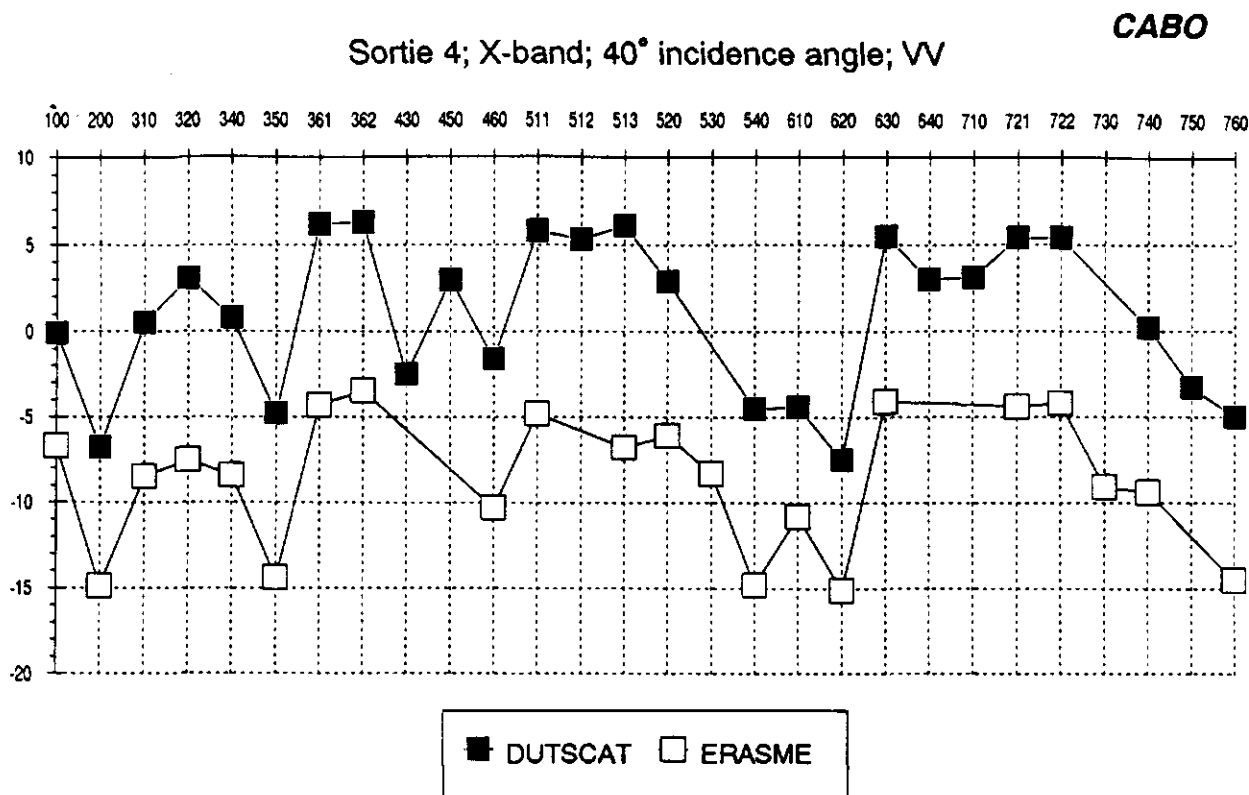


Fig. 82 DUTSCAT and ERASME radar backscatter (sortie 4, X-band, 40° i.a., VV) along the flight track

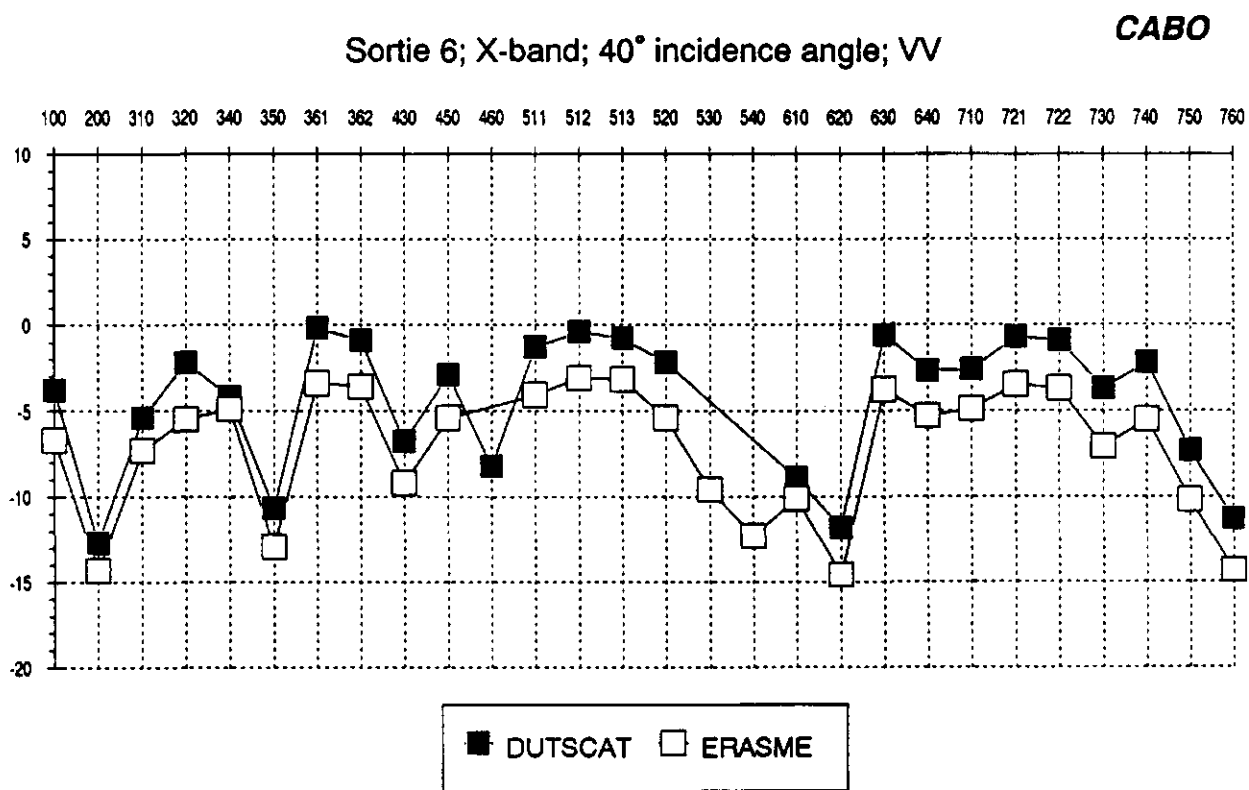


Fig. 83 DUTSCAT and ERASME radar backscatter (sortie 6, X-band, 40° i.a., VV) along the flight track

The figures 80-83 show that the patterns of both systems are very similar. Table 6 gives the coefficient of correlation ( $r^2$ ) between the track data of DUTSCAT and ERASME. Although the offset is significant, the correlation is high to very high. The dynamic range of the sets seems to be equal (Hoekman, 1990).

The fact that the patterns are very similar but that a significant offset is present could indicate that one or both systems were not properly absolutely calibrated.

Table 6 Coefficient of correlation ( $r^2$ ) between track data of DUTSCAT and ERASME

SORTIE	BAND	POL	20°	30°a	30°b	40°
3	C	HH	0.87	*	*	0.74
4	C	HH	0.93	0.92	0.87	0.89
5	C	HH	0.64	0.86	0.46	0.55
6	C	HH	0.59	0.47	0.56	0.48
3	X	HH	0.90	*	*	0.74
4	X	HH	0.85	0.92	0.90	0.90
5	X	HH	0.92	0.88	0.74	0.79
6	X	HH	0.93	0.81	0.88	0.82
3	X	VV	0.97	0.96	0.93	0.97
4	X	VV	0.97	0.95	0.95	0.92
5	X	VV	0.95	0.96	0.94	0.93
6	X	VV	0.96	0.94	0.96	0.93

The time dependency of the ERASME data is presented in figures 84-85 for the X-band VV polarization at 20° and 40° incidence angle for the three main crops. The relative positions of the curves of the crops are in accordance with the DUTSCAT data (§ 3.4). At the steep angle of incidence (20°) the backscatter of potato remains fairly stable while the backscatter of beet decreases in the midst of the growing season. At higher angles of incidence, the backscatter of beet remains higher than that of potato. This was also found in the DUTSCAT data. The relative position of the wheat curve (approximately 8 dB lower than potato) is also in accordance with the DUTSCAT data.

The large (small) dip at 40° incidence angle after sortie 3 for potato and beet (wheat) cannot be explained. This feature was not present in the DUTSCAT data, nor in any of the 'historical' data (§ 4.1-4.3).

Overall, the general trends in the ERASME data compare well with those in the DUTSCAT data. Like in the comparison with X-band SLAR and ground-based data, the DUTSCAT data are again higher than the ERASME data.

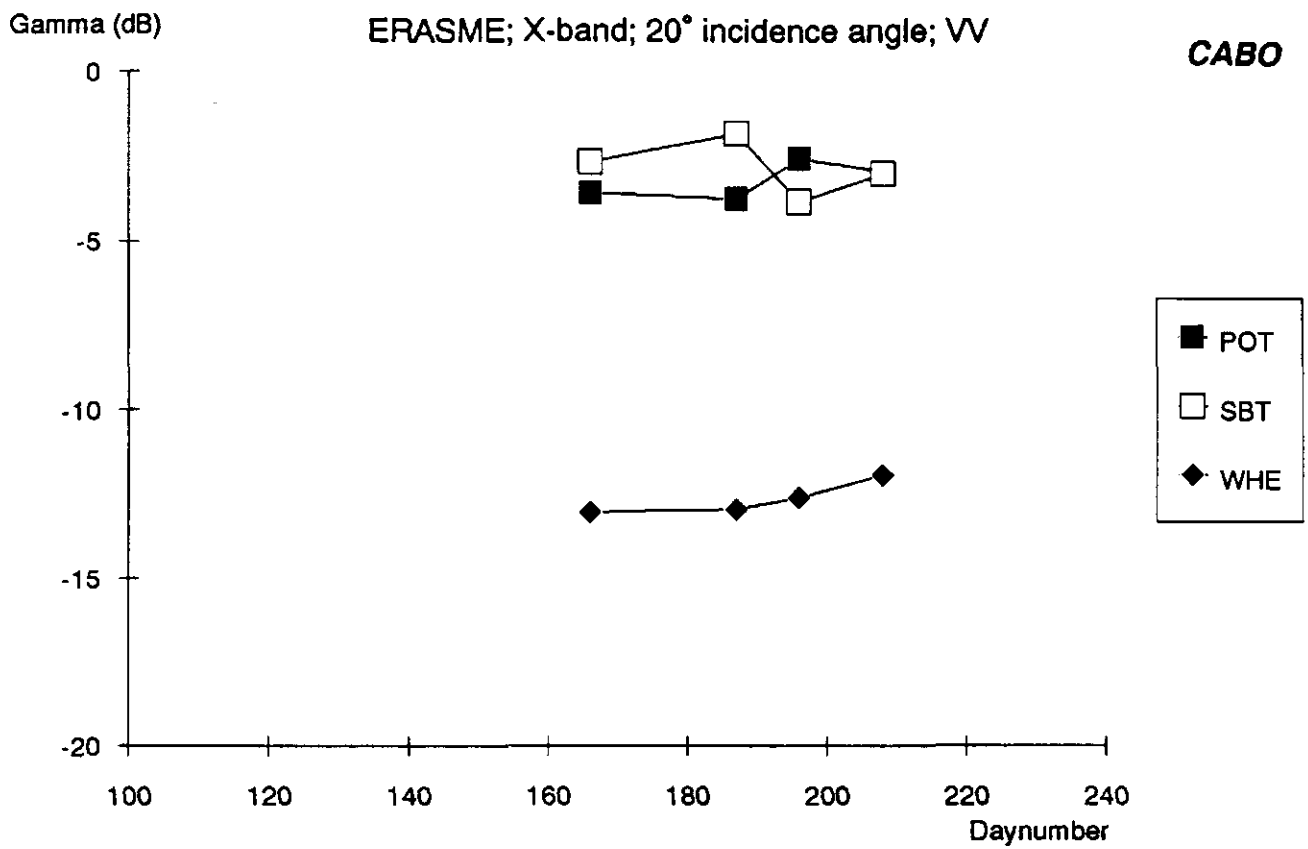


Fig. 84 ERASME X-band radar backscatter (20° i.a., VV) for the main crops in the course of the growing season

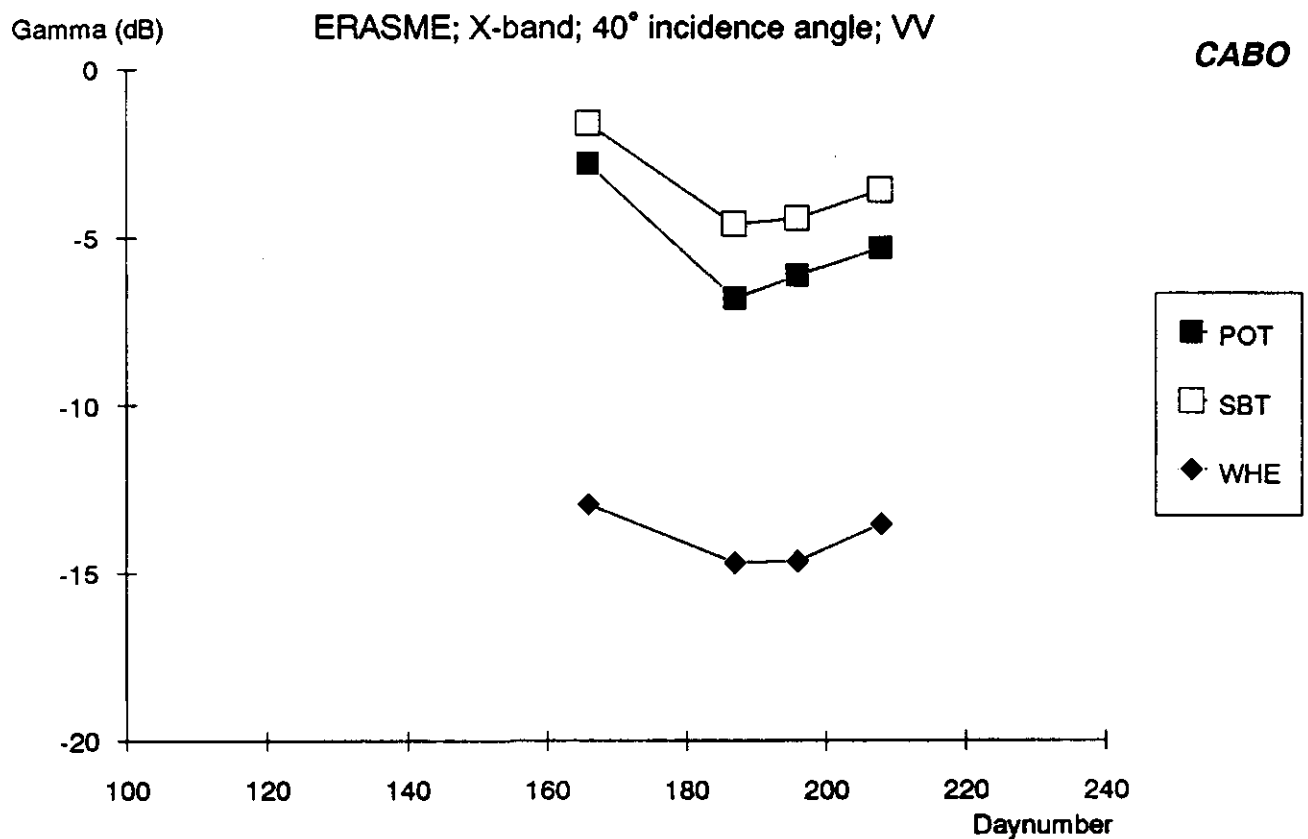


Fig. 85 ERASME X-band radar backscatter (40° i.a., VV) for the main crops in the course of the growing season

## 5 Statistical analysis

So far the radar data have been described qualitatively by means of visual interpretation of graphs and figures. To support these interpretations and to get a quantitative insight in the radar data, a statistical analysis was carried out. First, radar data were analysed in different states of polarization, frequencies and incidence angles (§ 5.1 and 5.2). Next, the correlation between radar backscattering and crop parameters was investigated (§ 5.3).

### 5.1 Correlation analysis of the radar backscatter

A correlation analysis on the radar data was carried out to determine the correlation between the radar backscatter at different states of polarization, frequency bands and incidence angles.

State of polarization. The coefficient of correlation ( $r^2$ ) between the two states of polarization of the radar backscatter was calculated for each frequency, sortie and nominal incidence angle (table 7).

With mainly bare soil (sorties 1 and 2), there is a high variability in  $r^2$  (varies from 0.15 to 0.93) with only 7% of  $r^2$  over 0.90. The L- and the S-band have relatively the highest correlation. With closed crop covers (sorties 4-6/7) there is also a high variability in  $r^2$  (varies from 0.33 to 0.99) but with 47% of  $r^2$  over 0.90. Here the X-, Ku1- and Ku2-band have relatively the highest correlation.

Frequency bands. The coefficient of correlation between the radar backscatter of the six frequency bands was calculated for each sortie, state of polarization and nominal incidence angle.

In tables 8-10,  $r^2$  is presented for 20°, 40° and 60° nominal incidence angle. The following generalizations are derived:

- The correlations are higher with closed crop covers (sorties 4-6/7) than with mainly bare soil (sorties 1 and 2), namely in the high frequencies.
- $r^2$  is high to very high ( $> 0.90$ ) between the X-, Ku1- and Ku2-bands (sortie 3-6/7)
- The C-band correlates well with the X-, Ku1- and Ku2-bands ( $r^2$  generally  $> 0.80$ , except at 60° incidence angle), and sometimes with the S-band.
- The L- and the S-band are generally decorrelated with the higher frequency bands, and with each other ( $r^2 < 0.75$ ).
- The correlation between the different frequency bands decreases with increasing difference in wavelength.

Incidence angle. The coefficient of correlation between radar backscatter at different angles of incidence was calculated for each frequency band, state of polarization and sortie. In tables 11-12,  $r^2$  is presented for mainly bare soil (sortie 2) and for closed crop covers (sortie 6).

The following generalizations are derived:

- With mainly bare soil,  $r^2$  is generally lower than with closed crop cover. The highest coefficients of correlation appear in the L- and the S-band with no more than 10° difference between the incidence angles ( $0.80 < r^2 < 0.90$ ). In the C- to Ku2-bands,  $r^2$  ranges from medium ( $0.70 < r^2 < 0.80$ ) to low ( $r^2 < 0.70$ ).
- With closed crop covers,  $r^2$  is generally higher than with mainly bare soil. The highest correlations are now in the high frequency bands X-, Ku1- and Ku2- with no more than 10° difference between the angles ( $r^2 > 0.90$ ).

The low correlations with mainly bare soil in the high frequencies are caused by the lack of differentiation in the data (compare figure 23). The radar backscatter at the different angles of incidence is nearly the same from all fields (beet, potato and wheat). In the low frequencies, there are differences in the radar backscatter from the various (mainly) bare fields, and these differences appear to be correlated (with no more than 10° difference between the angles; see also figure 22).

Table 7 Coefficient of correlation ( $r^2$ ) between HH and VV polarized radar backscatter, per sortie, frequency and nominal incidence angle; All track data were used and the number of data pairs was = 28 per correlation (average for whole table)

Sortie	Frequency	Nominal incidence angle						
		10°	15°	20°	30°	40°	50°	60°
1	L	0.38	0.66	0.91	0.93	0.93	0.87	0.90
	S	0.55	0.52	0.73	0.79	0.80	0.85	0.72
	C	0.66	*	0.63	0.68	*	0.69	0.85
	X	0.55	0.29	0.57	0.68	0.39	0.15	*
	Ku1	0.91	0.74	0.71	0.68	*	0.52	0.77
	Ku2	0.62	0.47	0.70	0.33	0.43	0.60	0.46
2	L	0.77	0.90	*	0.82	0.86	0.66	*
	S	0.73	0.75	*	0.93	0.78	0.68	0.20
	C	0.18	0.75	*	*	*	0.61	0.55
	X	0.31	0.37	*	0.60	0.53	0.66	0.44
	Ku1	0.54	0.62	*	0.81	0.25	0.66	*
	Ku2	0.45	0.46	*	*	0.35	0.50	0.48
3	L			0.86	*	0.80	0.81	0.69
	S			0.61	*	0.74	0.86	0.74
	C			0.88	*	0.84	*	0.67
	X			0.97	*	0.94	0.91	0.76
	Ku1			0.98	*	0.95	0.82	0.72
	Ku2			0.95	*	0.89	0.91	0.81
4	L			0.79	0.76	0.79	0.89	0.78
	S			*	0.81	0.84	0.62	0.56
	C			*	*	*	*	*
	X			0.97	0.95	0.97	0.93	0.91
	Ku1			0.97	0.97	0.96	0.94	0.91
	Ku2			0.97	0.83	0.97	0.97	0.93
5	L			0.67	0.60	0.82	0.76	0.79
	S			*	0.64	0.76	0.86	0.74
	C			*	0.87	0.80	*	0.71
	X			0.94	0.88	0.94	0.92	0.88
	Ku1			0.98	0.98	0.93	0.93	*
	Ku2			0.98	0.97	*	0.96	0.90
6	L			0.71	0.72	0.69	0.66	0.53
	S			0.33	0.34	0.41	0.69	0.74
	C			0.83	0.76	*	0.80	0.85
	X			0.95	0.94	0.95	0.90	0.89
	Ku1			0.99	0.96	0.96	0.93	*
	Ku2			0.98	*	0.94	0.91	0.95
7	L			0.87	*	0.94	0.91	0.93
	S			0.73	*	0.77	0.82	0.81
	C			*	*	*	*	*
	X			0.91	*	0.95	0.94	0.93
	Ku1			0.98	*	0.97	0.98	0.97
	Ku2			0.97	*	0.98	*	0.96



Table 8 Coefficient of correlation ( $r^2$ ) between the radar backscatter at 20° incidence angle at the 6 DUTSCAT frequencies, per sortie and per state of polarization; The number of data pairs was ~ 25 per coefficient of correlation (average for whole table)

Sortie Band		L	S	C	X	Ku1	L	S	C	X	Ku1
HH polarization						VV polarization					
1	S	0.48					0.46				
	C	0.32	0.67				0.18	0.49			
	X	0.18	0.42	0.34			0.45	0.17	0.53		
	Ku1	0.02	0.16	0.17	0.72		0.41	0.18	0.50	0.78	
	Ku2	0.05	0.17	0.16	0.72	0.87	0.11	0.06	0.29	0.61	0.76
2	S	0.63					*				
	C	0.30	0.53				*	*			
	X	0.02	0.06	0.39			*	*	*		
	Ku1	0.00	0.00	0.25	0.76		*	*	*	*	
	Ku2	0.00	0.06	0.34	0.79	0.77	*	*	*	*	*
3	S	0.46					0.14				
	C	0.09	0.56				0.06	0.82			
	X	0.00	0.26	0.79			0.02	0.74	0.92		
	Ku1	0.00	0.27	0.80	0.98		0.03	0.66	0.89	0.98	
	Ku2	0.03	0.31	0.80	0.93	0.96	0.04	0.69	0.91	0.97	0.99
4	S	*					0.56				
	C	*	*				0.55	0.89			
	X	0.15	*	*			0.55	0.90	0.96		
	Ku1	0.27	*	*	0.98		0.62	0.91	0.94	0.99	
	Ku2	0.27	*	*	0.94	0.97	0.63	0.88	0.89	0.96	0.99
5	S	*					*				
	C	0.03	*				*	*			
	X	0.03	*	0.87			0.40	*	*		
	Ku1	0.03	*	0.81	0.97		0.39	*	*	0.99	
	Ku2	0.05	*	0.73	0.95	0.97	0.43	*	*	0.97	0.99
6	S	0.47					0.54				
	C	0.07	0.02				0.28	0.74			
	X	0.02	0.00	0.87			0.29	0.57	0.92		
	Ku1	0.13	0.01	0.89	0.98		0.48	0.59	0.93	0.99	
	Ku2	0.02	0.01	0.78	0.96	0.97	0.26	0.47	0.89	0.97	0.99
7	S	0.74					0.74				
	C	*	*				*	*			
	X	0.38	0.26	*			0.24	0.54	*		
	Ku1	0.38	0.20	*	0.97		0.04	0.57	*	0.99	
	Ku2	0.33	0.18	*	0.95	0.98	0.23	0.53	*	0.98	0.98

Table 9 Coefficient of correlation ( $r^2$ ) between the radar backscatter at 40° incidence angle at the 6 DUTSCAT frequencies, per sortie and per state of polarization; The number of data pairs was ~ 25 per coefficient of correlation (average for whole table)

Sortie Band		L	S	C	X	Ku1	L	S	C	X	Ku1
		HH polarization					VV polarization				
1	S	0.60					0.55				
	C	*	*				0.67	0.52			
	X	0.24	0.50	*			0.22	0.40	0.30		
	Ku1	*	*	*	*		0.36	0.30	0.55	0.41	
	Ku2	0.02	0.34	*	0.49	*	0.25	0.33	0.34	0.68	0.43
2	S	0.70					0.34				
	C	*	*				*	*			
	X	0.14	0.24	*			0.24	0.47	*		
	Ku1	*	*	*	*		0.09	0.33	*	0.60	
	Ku2	0.26	0.02	*	0.21	*	0.18	0.03	*	0.34	0.62
3	S	0.36					0.14				
	C	0.21	0.75				0.11	0.87			
	X	0.11	0.37	0.75			0.09	0.65	0.81		
	Ku1	0.14	0.38	0.75	0.97		0.12	0.66	0.82	0.99	
	Ku2	0.18	0.43	0.75	0.90	0.91	0.13	0.67	0.83	0.98	0.99
4	S	0.40					0.69				
	C	*	*				0.63	0.77			
	X	0.16	0.65	*			0.62	0.73	0.93		
	Ku1	0.22	0.70	*	0.97		0.66	0.73	0.92	0.99	
	Ku2	0.23	0.75	*	0.95	0.98	0.66	0.78	0.94	0.98	0.98
5	S	0.36					0.41				
	C	0.17	0.38				0.32	0.73			
	X	0.19	0.29	0.91			0.27	0.53	0.88		
	Ku1	0.23	0.24	0.87	0.98		0.27	0.51	0.88	0.99	
	Ku2	*	*	*	*	*	0.24	0.45	0.86	0.98	0.98
6	S	0.20					0.57				
	C	0.09	0.30				*	*			
	X	0.05	0.10	0.85			0.30	0.68	*		
	Ku1	0.06	0.10	0.84	0.99		0.31	0.69	*	0.99	
	Ku2	0.08	0.11	0.82	0.98	0.98	0.31	0.70	*	0.98	0.98
7	S	0.76					0.73				
	C	*	*				*	*			
	X	0.45	0.73	*			0.45	0.83	*		
	Ku1	0.42	0.59	*	0.94		0.36	0.77	*	0.97	
	Ku2	0.40	0.60	*	0.95	0.99	0.43	0.78	*	0.97	0.99

Table 10 Coefficient of correlation ( $r^2$ ) between the radar backscatter at 60° incidence angle at the 6 DUTSCAT frequencies, per sortie and per state of polarization; The number of data pairs was = 25 per coefficient of correlation (average for whole table)

Sortie	Band	L	S	C	X	Ku1	L	S	C	X	Ku1
HH polarization						VV polarization					
1	S	0.30					0.38				
	C	0.48	0.82				0.53	0.52			
	X	*	*	*			*	*	*		
	Ku1	0.45	0.48	0.84	*		0.35	0.50	0.65	*	
	Ku2	0.23	0.23	0.64	*	0.84	0.08	0.13	0.72	*	0.70
2	S	*					0.27				
	C	*	0.86				0.25	0.59			
	X	*	0.36	0.60			0.20	0.50	0.83		
	Ku1	*	*	*	*		0.21	0.35	0.71	0.79	
	Ku2	*	0.35	0.55	0.72	*	0.23	0.33	0.77	0.72	0.78
3	S	0.80					0.41				
	C	0.52	0.71				0.26	0.53			
	X	0.26	0.29	0.70			0.10	0.02	0.47		
	Ku1	0.26	0.27	0.67	0.96		0.11	0.01	0.36	0.89	
	Ku2	0.26	0.30	0.71	0.95	0.98	0.10	0.02	0.46	0.98	0.92
4	S	0.62					0.42				
	C	*	*				*	*			
	X	0.12	0.37	*			0.28	0.10	*		
	Ku1	0.14	0.39	*	0.97		0.22	0.10	*	0.98	
	Ku2	0.17	0.46	*	0.94	0.97	0.21	0.13	*	0.95	0.97
5	S	0.58					0.42				
	C	0.26	0.61				0.22	0.51			
	X	0.18	0.23	0.80			0.15	0.02	0.54		
	Ku1	*	*	*	*		0.16	0.02	0.46	0.98	
	Ku2	0.18	0.20	0.74	0.92	*	0.12	0.01	0.42	0.96	0.98
6	S	0.52					0.44				
	C	0.15	0.51				0.21	0.72			
	X	0.02	0.11	0.73			0.08	0.21	0.69		
	Ku1	0.01	0.10	0.73	0.99		*	*	*	*	
	Ku2	0.02	0.10	0.71	0.98	0.98	0.05	0.17	0.64	0.96	*
7	S	0.81					0.85				
	C	*	*				*	*			
	X	0.35	0.58	*			0.29	0.56	*		
	Ku1	0.25	0.44	*	0.94		0.26	0.49	*	0.96	
	Ku2	0.23	0.43	*	0.94	0.98	0.23	0.45	*	0.95	0.99

Table 11 Coefficient of correlation ( $r^2$ ) between the radar backscatter at five incidence angles, per frequency band and per state of polarization (sortie 2); The number of data pairs was  $\sim 25$  for each coefficient of correlation (average for whole table)

Band	Incidence angle	20	30	40	50	20	30	40	50
		HH polarization				VV polarization			
L	30	0.89				*			
	40	0.83	0.87			*	0.81		
	50	0.64	0.59	0.56		*	0.51	0.34	
	60	*	*	*	*	*	0.45	0.28	0.89
S	30	0.80				*			
	40	0.75	0.89			*	0.77		
	50	0.68	0.86	0.92		*	0.71	0.81	
	60	0.44	0.59	0.70	0.66	*	0.26	0.40	0.37
C	30	*				*			
	40	*	*			*	*		
	50	0.56	*	*		*	0.39	*	
	60	0.39	*	*	0.77	*	0.19	*	0.77
X	30	0.77				*			
	40	0.42	0.52			*	0.54		
	50	0.30	0.31	0.52		*	0.57	0.53	
	60	0.09	0.05	0.55	0.58	*	0.32	0.30	0.61
Ku1	30	0.78				*			
	40	*	*			*	0.65		
	50	0.45	0.57	*		*	0.65	0.58	
	60	*	*	*	*	*	0.15	0.25	0.26
Ku2	30	*				*			
	40	0.72	*			*	0.76		
	50	0.61	*	0.53		*	0.41	0.05	
	60	0.30	*	0.27	0.44	*	0.10	0.07	0.14

Table 12 Coefficient of correlation ( $r^2$ ) between the radar backscatter at five incidence angles, per frequency band and per state of polarization (sortie 6); The number of data pairs was  $\approx 25$  for each coefficient of correlation (average for whole table)

Band	Incidence angle	20	30	40	50	20	30	40	50
		HH polarization				VV polarization			
L	30	0.71				0.83			
	40	0.41	0.77			0.74	0.87		
	50	0.31	0.73	0.87		0.71	0.74	0.90	
	60	0.24	0.53	0.83	0.91	0.70	0.79	0.85	0.88
S	30	0.46				0.86			
	40	0.06	0.53			0.67	0.89		
	50	0.03	0.48	0.81		0.40	0.57	0.77	
	60	0.01	0.32	0.68	0.92	0.17	0.32	0.44	0.83
C	30	0.85				0.91			
	40	0.70	0.88			*	*		
	50	0.36	0.62	0.79		0.62	0.76	*	
	60	0.17	0.40	0.62	0.93	0.30	0.46	*	0.85
X	30	0.96				0.97			
	40	0.90	0.97			0.92	0.96		
	50	0.73	0.86	0.93		0.78	0.86	0.96	
	60	0.51	0.66	0.77	0.94	0.55	0.67	0.80	0.93
Ku1	30	0.98				0.99			
	40	0.94	0.95			0.98	0.97		
	50	0.79	0.86	0.92		0.83	0.88	0.93	
	60	0.63	0.65	0.76	0.93	*	*	*	*
Ku2	30	0.97				*			
	40	0.91	0.96			0.93	*		
	50	0.72	0.83	0.92		0.80	*	0.93	
	60	0.51	0.64	0.75	0.91	0.52	*	0.73	0.89

## 5.2 Principle Component Analysis of the radar backscatter

To investigate the relative amount of variation contained in each frequency, Principal Component Analysis (PCA) is a suitable tool. This well known method in optical remote sensing consists of a transformation of multivariate data to principal axes, based on a linear transformation (Donker and Mulder 1977). It is mostly used as a data reduction technique: the number of wavelength bands in which remote sensing data are collected, is reduced into one or two synthetic bands - principal axes - which contain a large amount (usually > 95%) of the variation present in the original data set. A principal axis is a linear combination of the contributions of each original band. Beers (1975) and Bunnik (1978) used these contributions to determine the relative 'information content' of individual (spectral) bands. They defined the information obtained by measurements of the reflectance (in our case, radar backscatter) at a wavelength value by the measured variance. However, we think that variance is not always synonymous for (useful) information. Therefore, we applied the term 'variation content' instead of 'information content'. Frequency bands with a relatively high content of variation may be relatively suitable for further investigation to information content.

The relative variation content of the six frequency bands was calculated with the aid of the statistical package GENSTAT 5 (GENSTAT Reference manual 1988). The PCA resulted in six synthetic principal axes, with each axis accounting for  $C_i$  percent of the total variation. The matrix of latent vectors gave the contributions  $L_{i,j}$  of each original band  $j$  to each principal axis  $i$ . The total relative variation content  $P_j$  of each original band was calculated as:

$$P_j = \sum [ | C_i * L_{i,j} | ] \quad i = 1, 6$$

Three different PCA's were performed:

- Spatial analysis. For each sortie, the PCA was performed on all (track) data per state of polarization and per incidence angle. This way, the PCA indicated the frequency bands containing most variation in the whole track (useful for applications like crop discrimination).
- Temporal analysis, main crop types. Per crop type, the PCA was performed on the data of all sorties per state of polarization and per incidence angle. This PCA indicated the frequency bands with most variation in time (useful for growth monitoring of specific crop types).
- Temporal analysis, all crops. The PCA was performed on all track data of all sorties, per state of polarization and per incidence angle (useful for growth monitoring of all crops together).

### 5.2.1 Spatial analysis

For this PCA, the C-band was excluded from the data set because of the low amount of data in this band (a low amount of data hinders a meaningful PCA). The results of the PCA are presented in figures 86-95 where the total relative variation content ( $P_j$ ) of each original band is given for each frequency band and nominal incidence angle. All sorties are represented by VV polarization (figures 86-92). The HH polarization is presented only for three sorties for comparison (figures 93-95). Three different situations can be distinguished:

- mainly bare soil (sorties 1 and 2),
- crop cover (sorties 3, 4, 5 and 6),
- end of growing season (sortie 7).

Mainly bare soil (figures 86-87). The content of variation is highest in the L-band, and decreases through the S-band to the X-band. In the Ku1- and Ku2-bands, the variation content increases again. Except for 20° at sortie one, this pattern is the same for all incidence angles. At HH polarization (figure 93), the pattern resembles in general lines those at VV polarization, but it is less pronounced.

Crop cover (figures (88-91). In this situation, the high frequency bands X-, Ku1- and Ku2-, have the highest contents of variation (which are mutually comparable). The difference with the lower frequencies gets more pronounced in the course of the growing season.

In the L-band, the high incidence angles 50° and 60° give relative higher contents of variation than the low incidence angles 20° and 30°. In the other frequency bands, this pattern is the other way around (figures 88-91).

At HH polarization (figure 94), the distribution of the variation content is similar to that at VV polarization. Here, the differences between the low (L- and S-) and the high (X-, Ku1- and Ku2-) frequencies, and the relative distribution over the low (20°, 30°) and the high (50°, 60°) incidence angles are more pronounced than at VV.

End of season (figure 92). At sortie seven, a number of crops was harvested (e.g. wheat, rapeseed, peas), leaving the fields bare or with stubble. This resulted in a mixture of the 'bare soil' situation of figures 86 and 87, and the 'closed cover' situation of figures 88-91. At low incidence angles (20°), the high frequencies (X-Ku2-bands) have the highest contents of variation. With increasing incidence angle, the pattern reverses. At 40°, the low frequencies (L- and S-band) have the highest contents of variation.

At HH polarization (figure 95), the patterns no longer resemble those at VV polarization. At all incidence angles, the differences in variation content between the frequencies are small. The low L-band frequency, and the high Ku1- and Ku2-band frequencies have relatively the highest contents of variation ( $\approx 0.20$ - $0.27$ , versus  $\approx 0.15$ - $0.20$  in the S- and the X-band).

When the C-band is included in the PCA's for selected data sets (e.g. specific sorties or incidence angles with enough C-band data), the relative content of variation of the C-band appears to be somewhat lower than those in the Ku1- and Ku2-bands.

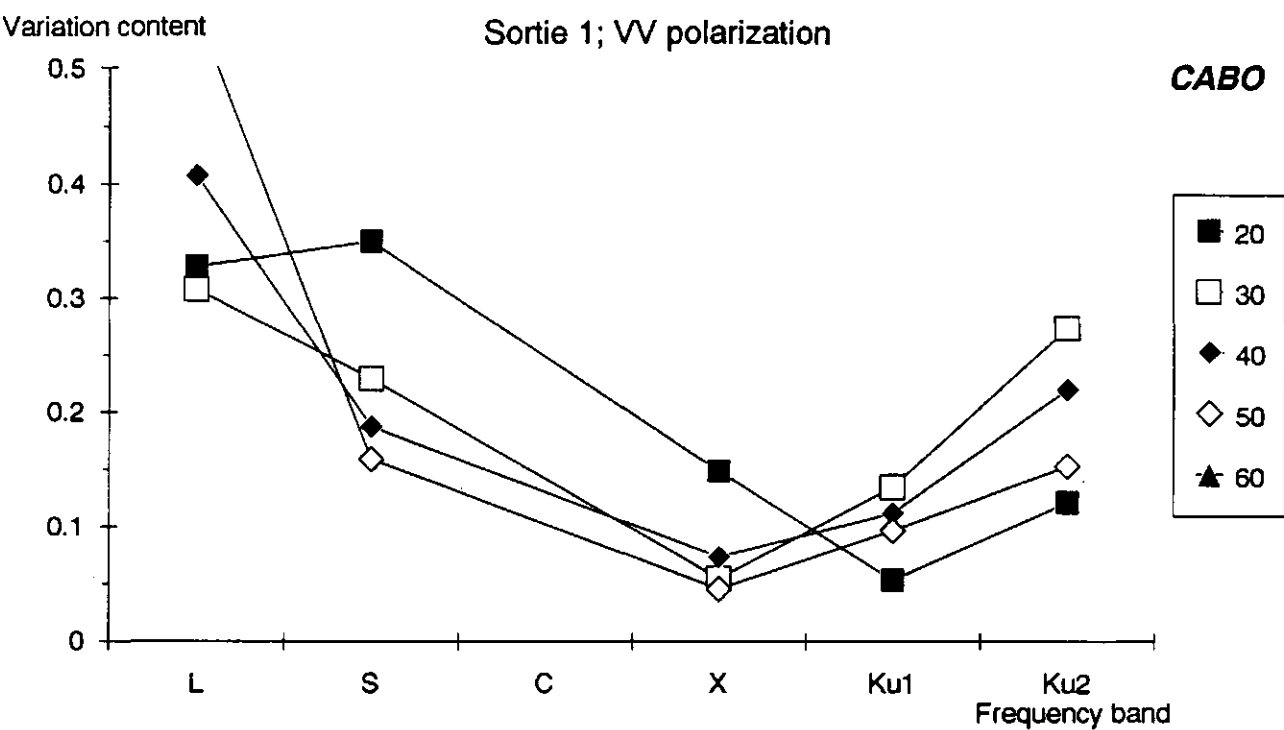


Fig. 86 Relative content of variation in the frequency bands, per incidence angle (all track data of sortie 1, VV polarization)

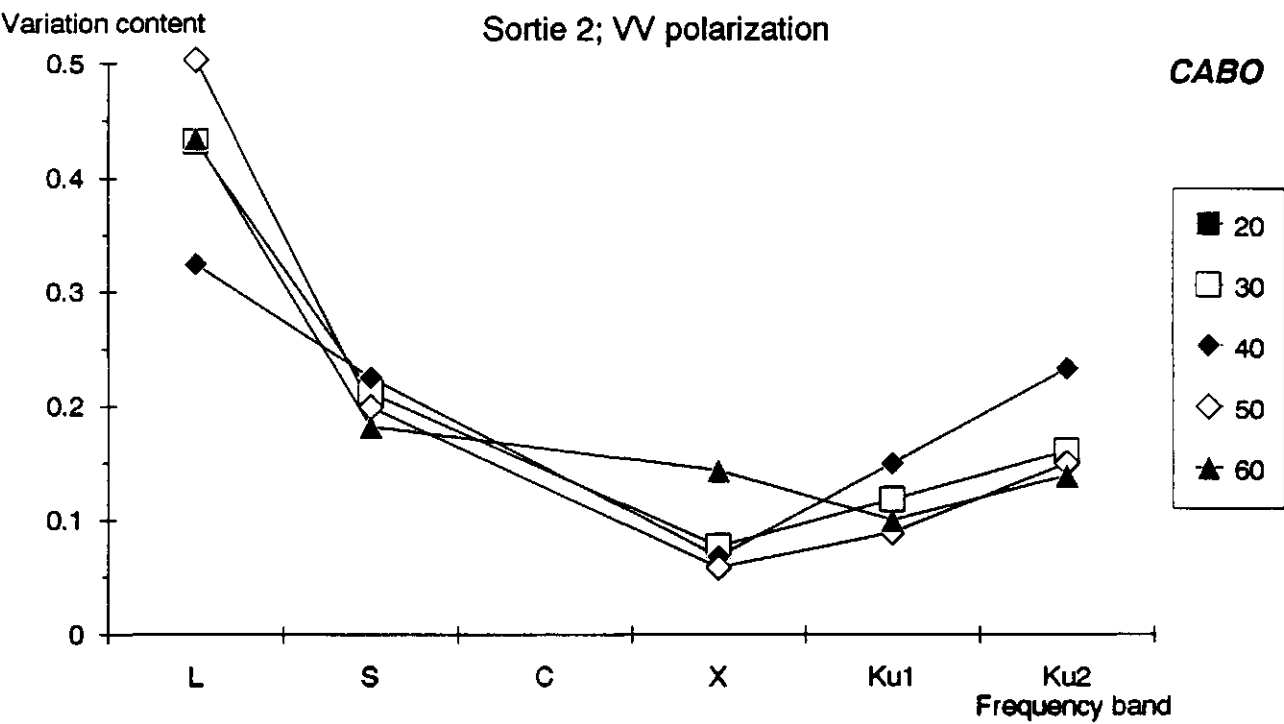


Fig. 87 Relative content of variation in the frequency bands, per incidence angle (all track data of sortie 2, VV polarization)



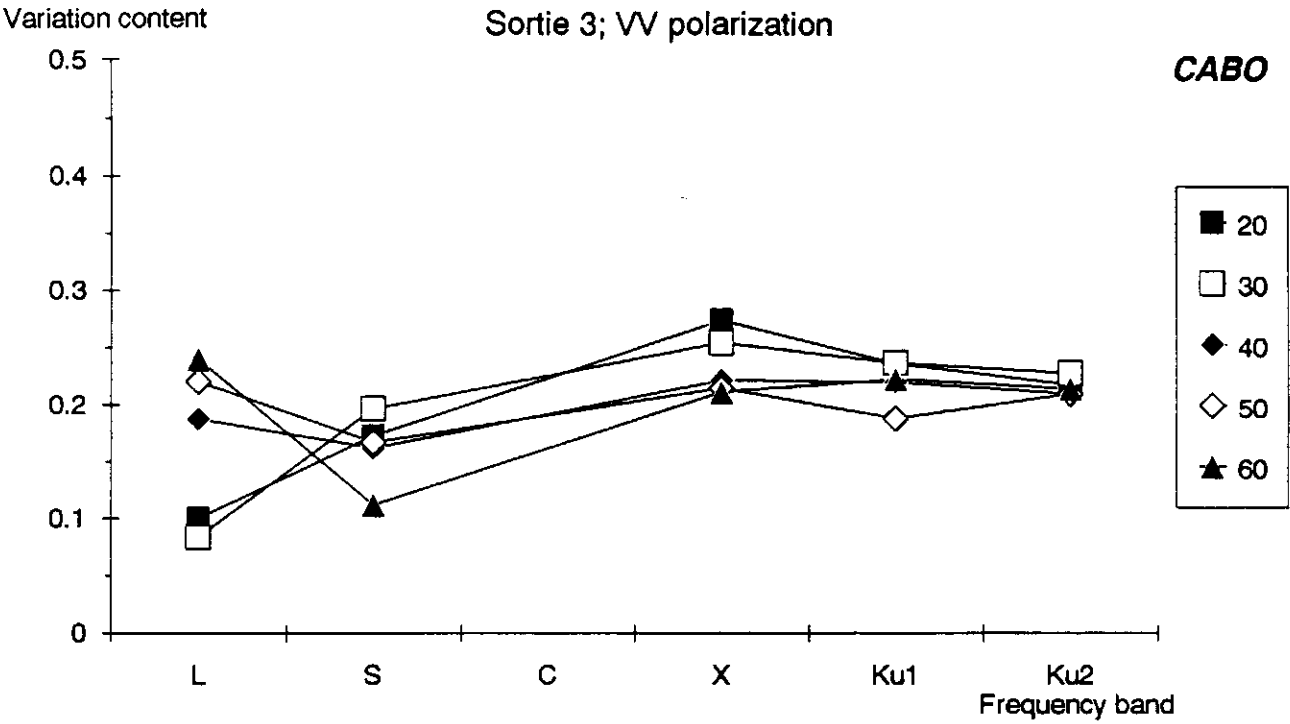


Fig. 88 Relative content of variation in the frequency bands, per incidence angle (all track data of sortie 3, VV polarization)

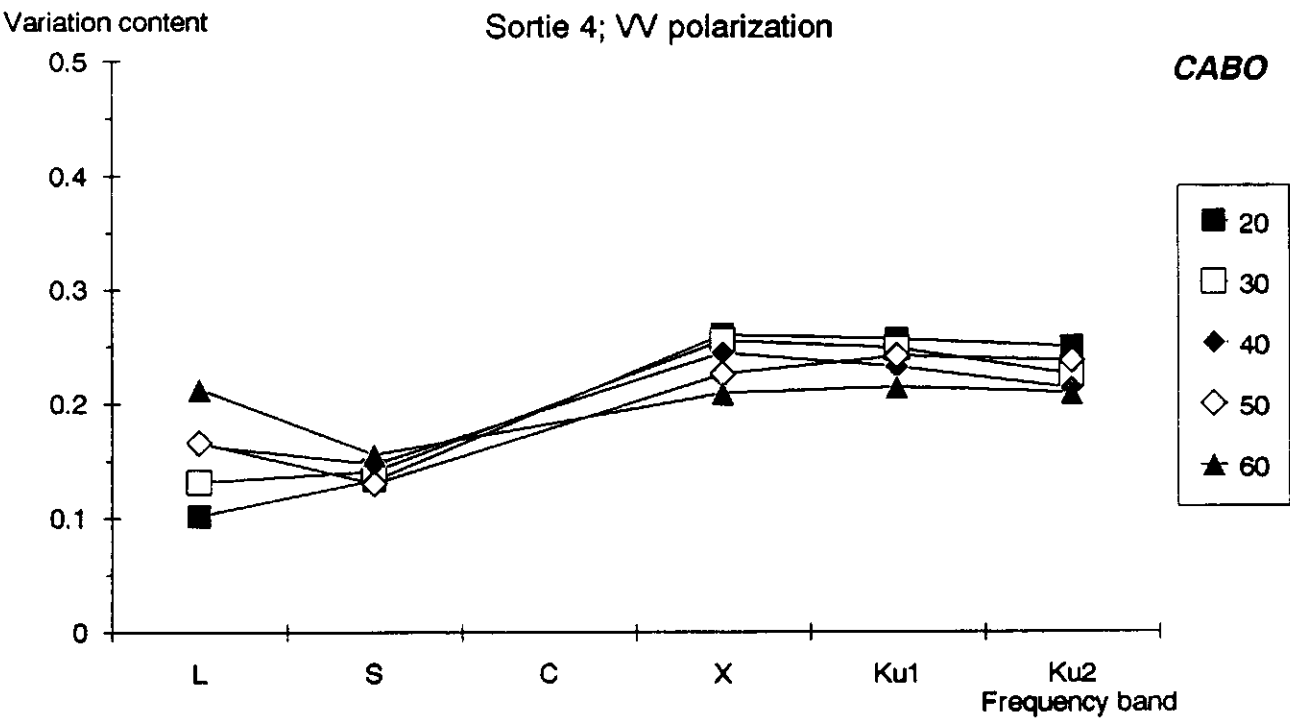


Fig. 89 Relative content of variation in the frequency bands, per incidence angle (all track data of sortie 4, VV polarization)

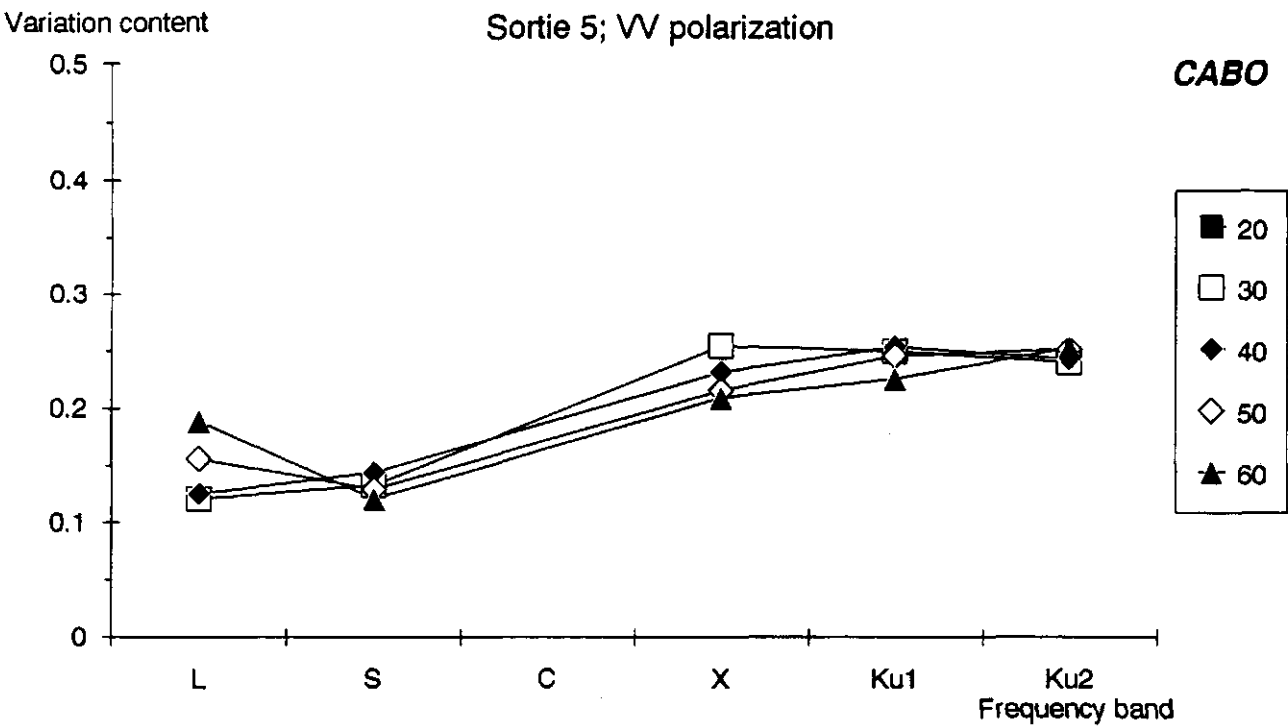


Fig. 90 Relative content of variation in the frequency bands, per incidence angle (all track data of sortie 5, VV polarization)

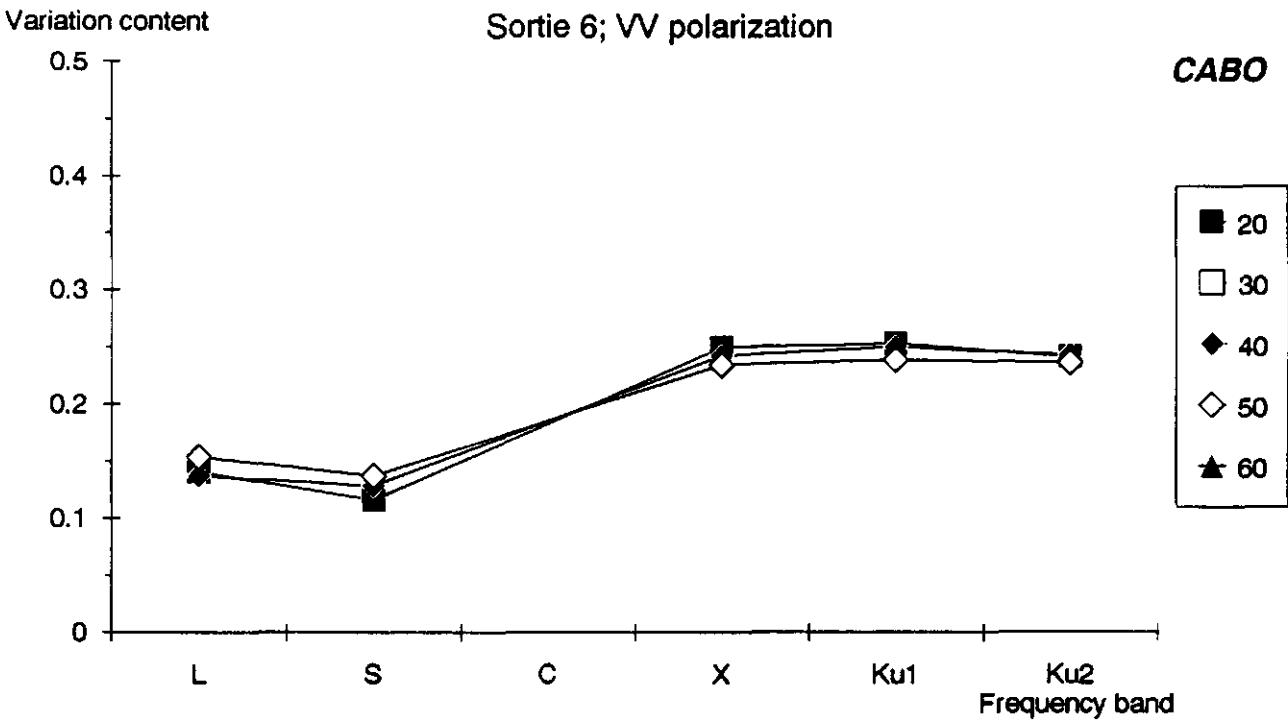


Fig. 91 Relative content of variation in the frequency bands, per incidence angle (all track data of sortie 6, VV polarization)

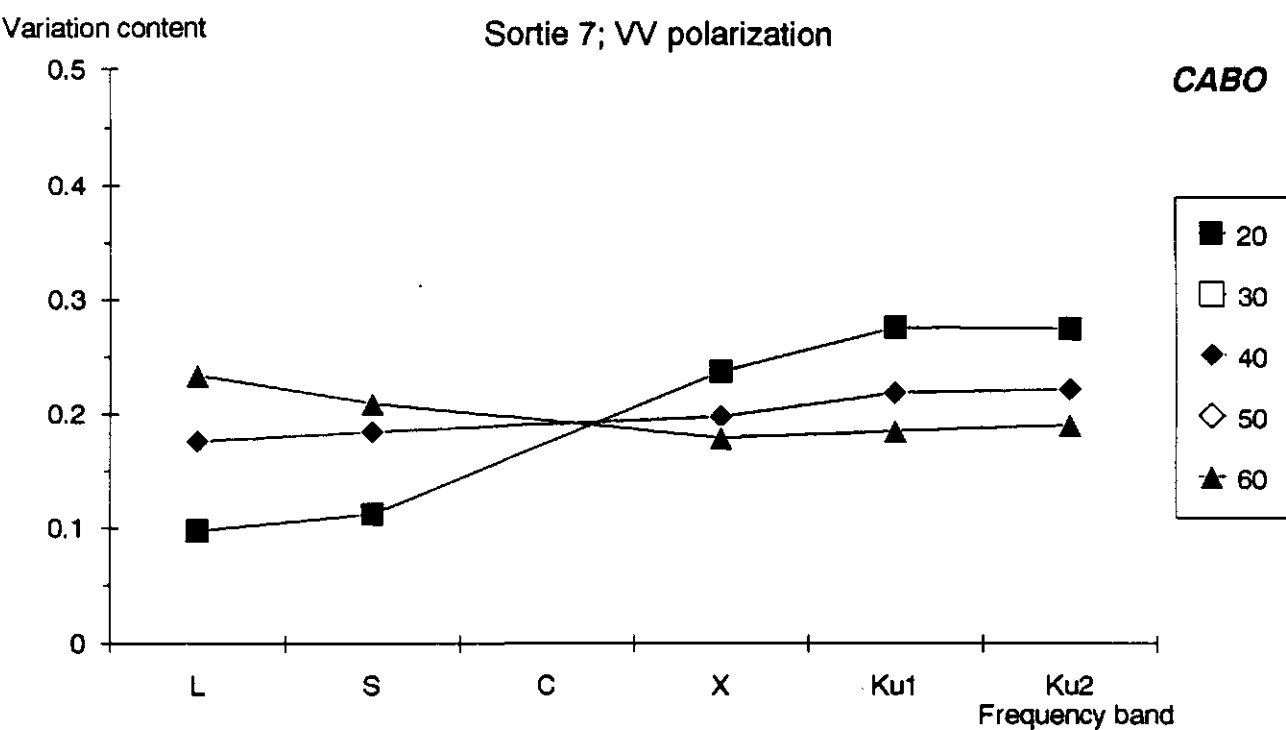


Fig. 92 Relative content of variation in the frequency bands, per incidence angle (all track data of sortie 7, VV polarization)

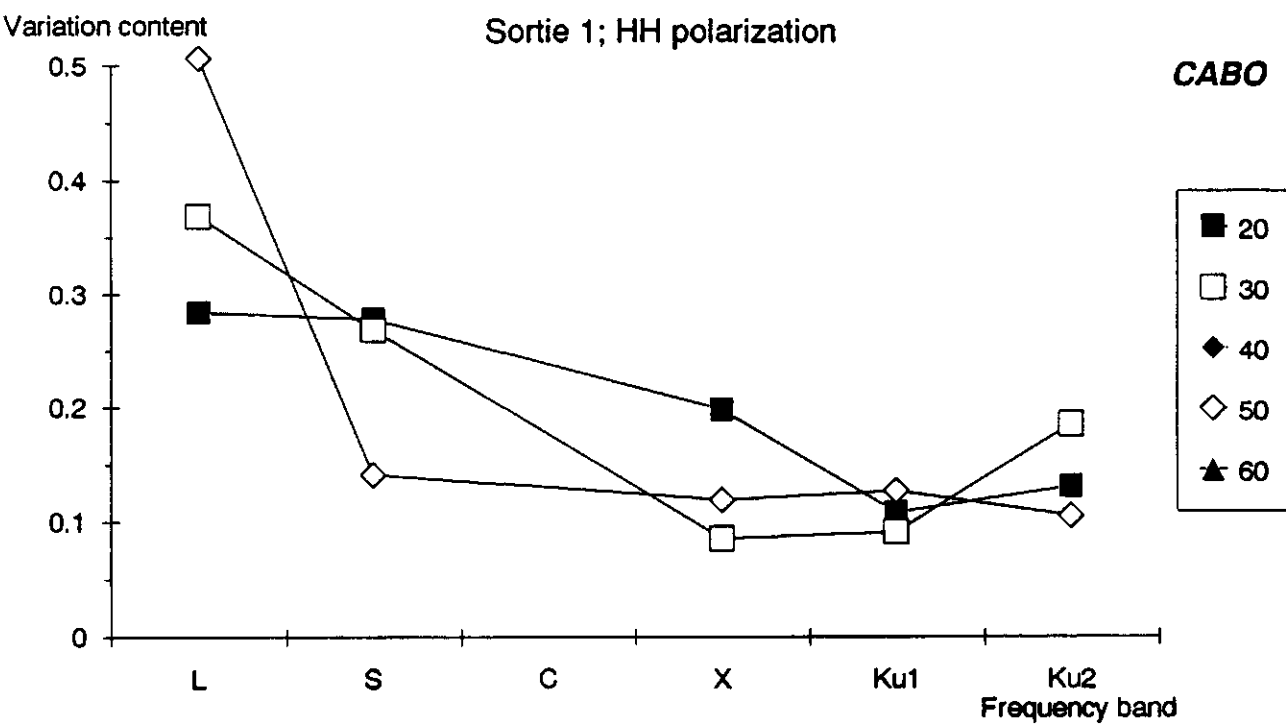


Fig. 93 Relative content of variation in the frequency bands, per incidence angle (all track data of sortie 1, HH polarization)

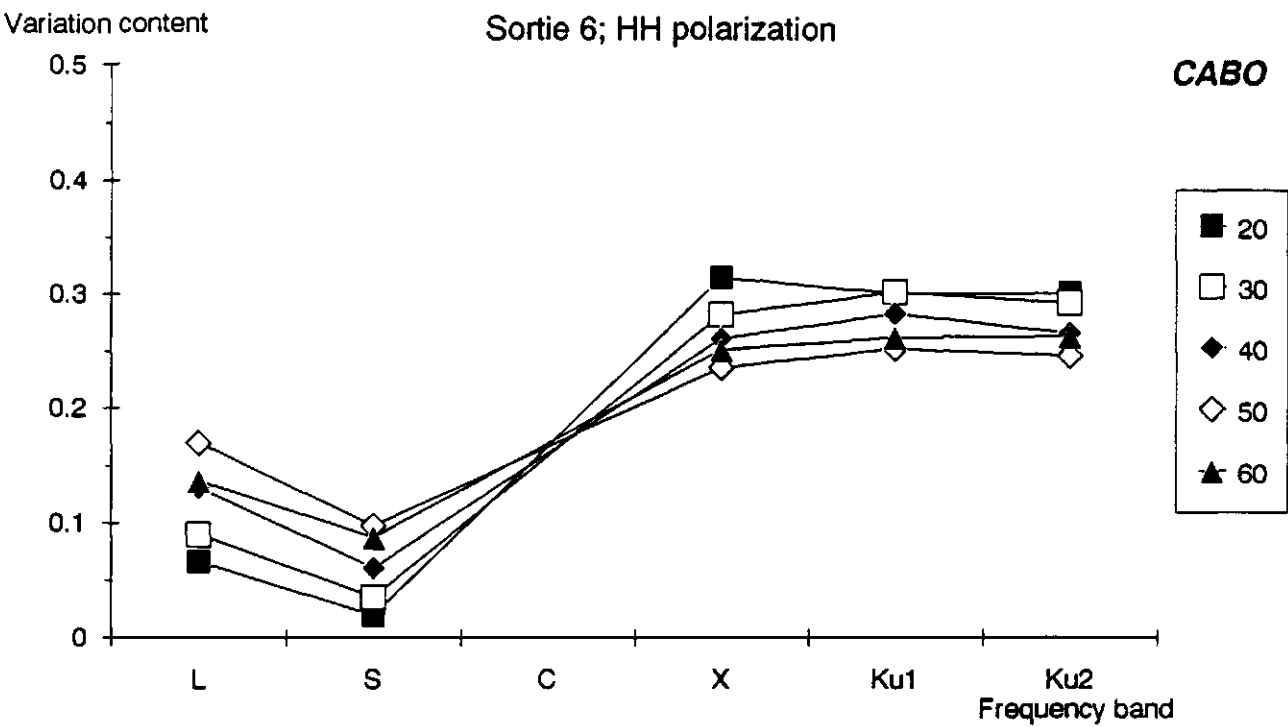


Fig. 94 Relative content of variation in the frequency bands, per incidence angle (all track data of sortie 6, HH polarization)

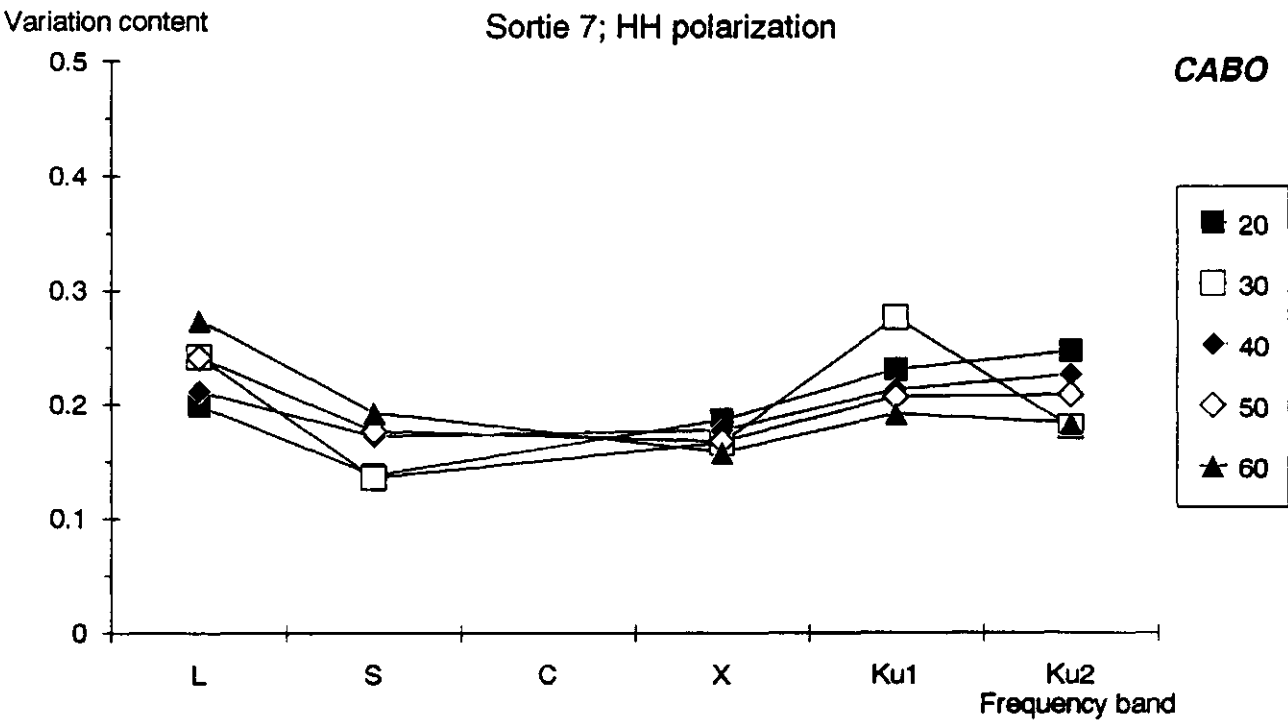


Fig. 95 Relative content of variation in the frequency bands, per incidence angle (all track data of sortie 7, HH polarization)

### 5.2.2 Temporal variation, selected crops

PCA's were carried out to determine the 'temporal' variation content for beet, potato and wheat separately. To obtain a statistically reliable analysis, it is necessary to work with a sufficiently large number of data. Therefore the radar data of two neighbouring incidence angles were taken together. Table 13 gives the coefficients of correlation ( $r^2$ ) for the temporal (all sorties) radar backscatter between 10° neighbouring incidence angles. This table shows that it is justified to lump two neighbouring incidence angles because 92% of  $r^2$  is over 0.90.

Table 13 Coefficient of correlation ( $r^2$ ) between radar backscatter at two 10° neighbouring incidence angles; The data of all seven sorties were lumped for all crop types

Polarization	Frequency band	Neighbouring incidence angles			
		20°-30°	30°-40°	40°-50°	50°-60°
HH	L	0.94	0.95	0.94	0.95
	S	0.92	0.95	0.98	0.98
	C	0.95	0.92	0.82	0.95
	X	0.94	0.92	0.98	0.97
	Ku1	0.96	0.98	0.98	0.98
	Ku2	0.95	0.93	0.96	0.95
VV	L	0.89	0.92	0.89	0.92
	S	0.93	0.92	0.96	0.94
	C	0.96	0.97	0.98	0.96
	X	0.88	0.98	0.98	0.94
	Ku1	0.99	0.98	0.98	0.94
	Ku2	0.97	0.97	0.97	0.92

Again, the C-band was excluded from the analyses. The results of the PCA's are presented per crop type in figures 96-101. It should be noted, that in a temporal analysis, the deviating temporal behaviour of the X-band (§ 3.4, 4) is likely to 'disturb' the results. The relative high radar backscatter at sortie 3 and 4 will cause an overrating of the (relative) content of variation.

**Beet** (figures 96 and 97). At both VV and HH polarization, the high frequencies X-, Ku1- and Ku2-bands contain the largest content of variation. Within these high frequencies, the relative high content of variation in the X-band is probably an artefact (see above). The distribution of the content of variation over the frequencies is comparable at all incidence angles.

**Potato** (figures 98 and 99). Compared to the distribution pattern for beet, the contents of variation in the L- and the S-band have increased. With the hypothesis that the relatively high variation in the X-band is an artefact, the variation contents are equally distributed over all bands. Only at HH polarization does the L-band seem to have a slightly higher content of variation than the other bands.

Like for beet, the distribution of the content of variation over the frequencies is comparable at all incidence angles.

Wheat (figures 100 and 101). The distribution of the content of variation over the frequencies differs from that for beet and potato, and appears to be more polarization and angle-specific. At VV polarization, the highest content of variation is found in the S-band (compare with figures 42 and 44). At HH polarization, the highest contents of variation appear in the L- and the S-bands, and the lowest in the Ku1- and Ku2-bands (with the assumption of an artefact in the X-band).

The differences in the distribution of the contents of variation over the frequencies for beet, potato and wheat indicate that the interaction of microwaves of different wavelengths with crop canopies depends on crop type. However, the differences in the contents of variation in the frequency bands are small for all crops.

Again, when the C-band is included in the PCA's for selected data sets (e.g. specific incidence angles with enough C-band data), the relative content of variation of the C-band appears to be somewhat lower than those in the Ku1- and Ku2-bands.

### 5.2.3 Temporal variation, all crops

Finally a PCA was carried out to determine the contents of variation with temporal variation for all crops together (including peas, corn etc.). Again, the 10° neighbouring incidence angles were taken together. Because all track-data were used now, the C-band contained a sufficiently large number of data and was included in the analysis. The results of the PCA are presented in figures 102-103.

The mixture of different crop types resulted in very small differences in contents of variation between the frequency bands. At both states of polarization, the contents of variation in the high frequencies X-, Ku1- and Ku2-bands, was only a little bit larger (VV ~ 0.17; HH ~ 0.18) than in the low frequencies L- and S-bands (VV ~ 0.14; HH ~ 0.12-0.15).

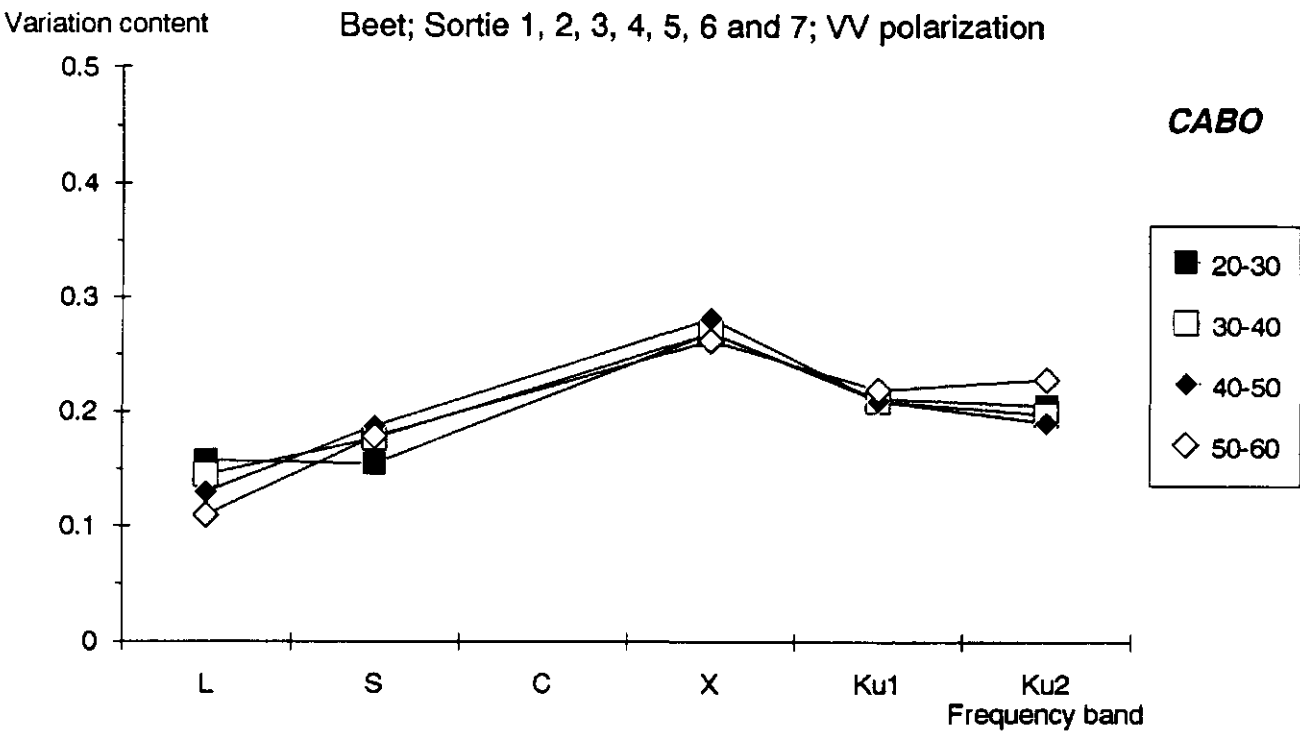


Fig. 96 Relative content of variation in the frequency bands, per incidence angle group (Beet, all sorties, VV polarization)

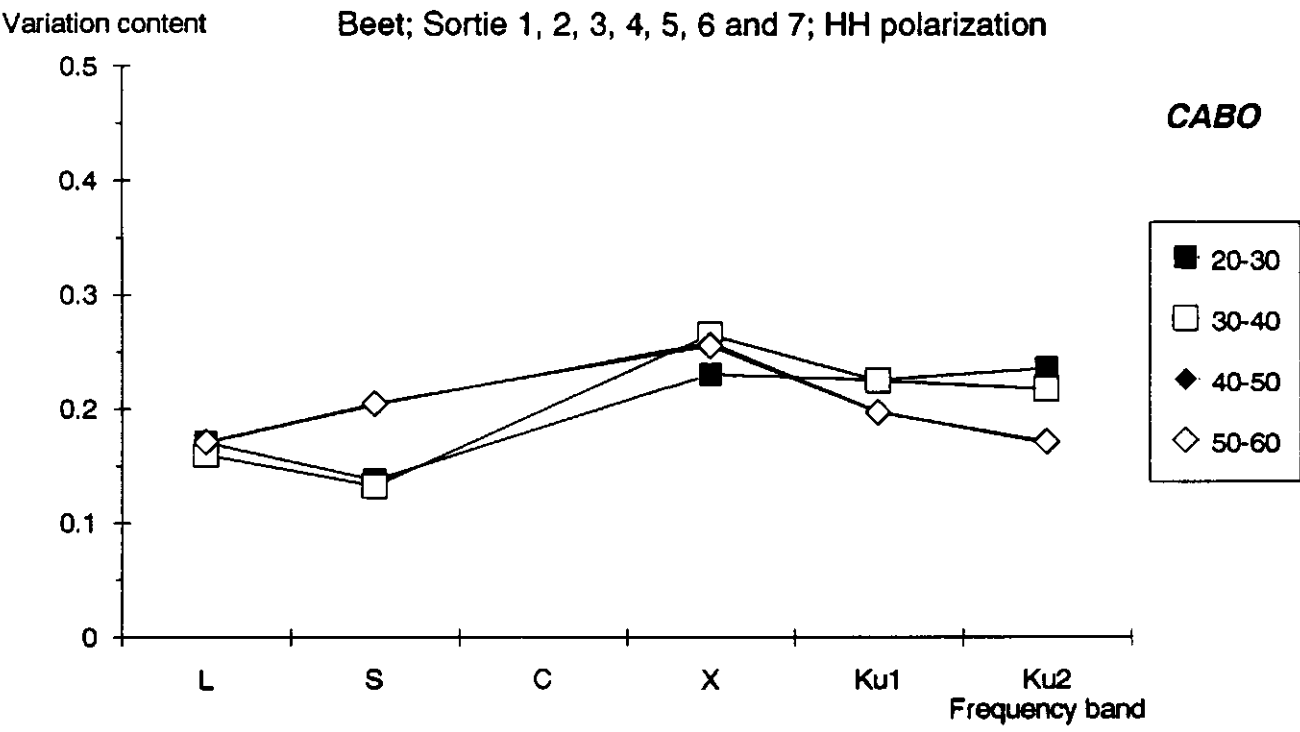


Fig. 97 Relative content of variation in the frequency bands, per incidence angle group (Beet, all sorties, HH polarization)

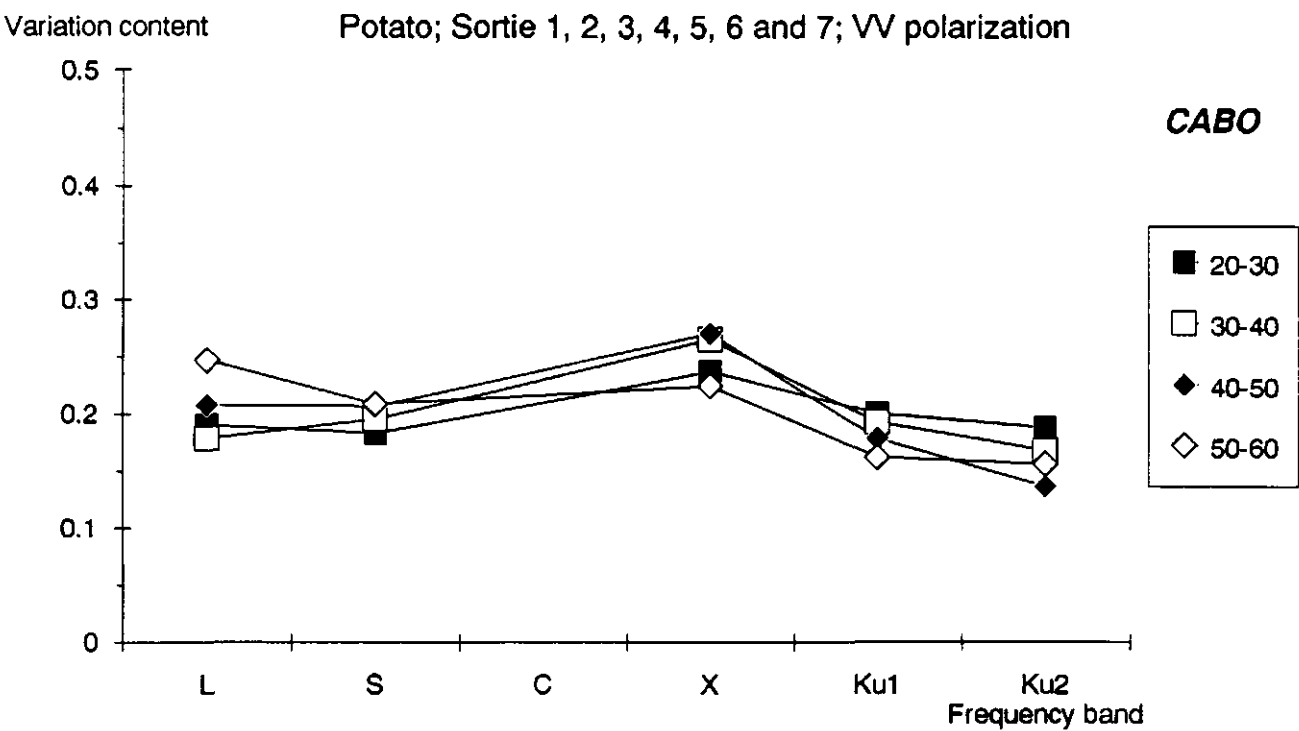


Fig. 98 Relative content of variation in the frequency bands, per incidence angle group (Potato, all sorties, VV polarization)

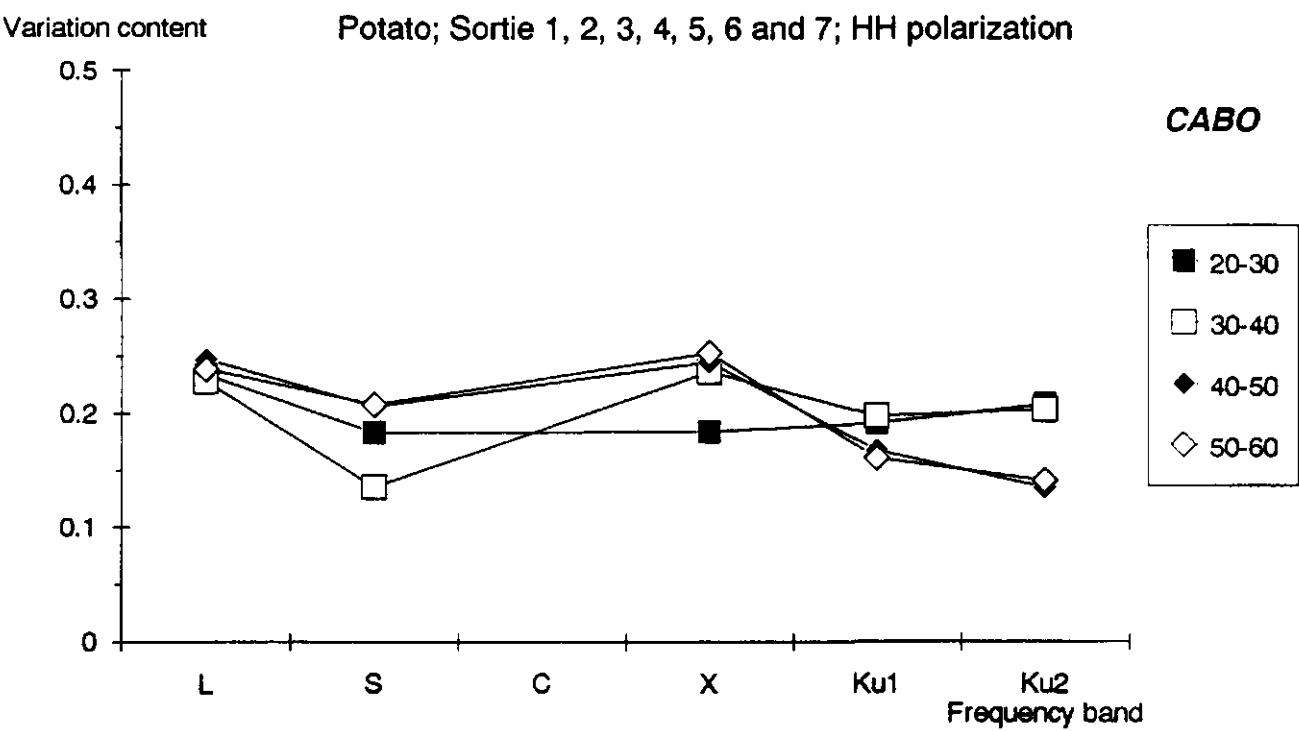


Fig. 99 Relative content of variation in the frequency bands, per incidence angle group (Potato, all sorties, HH polarization)



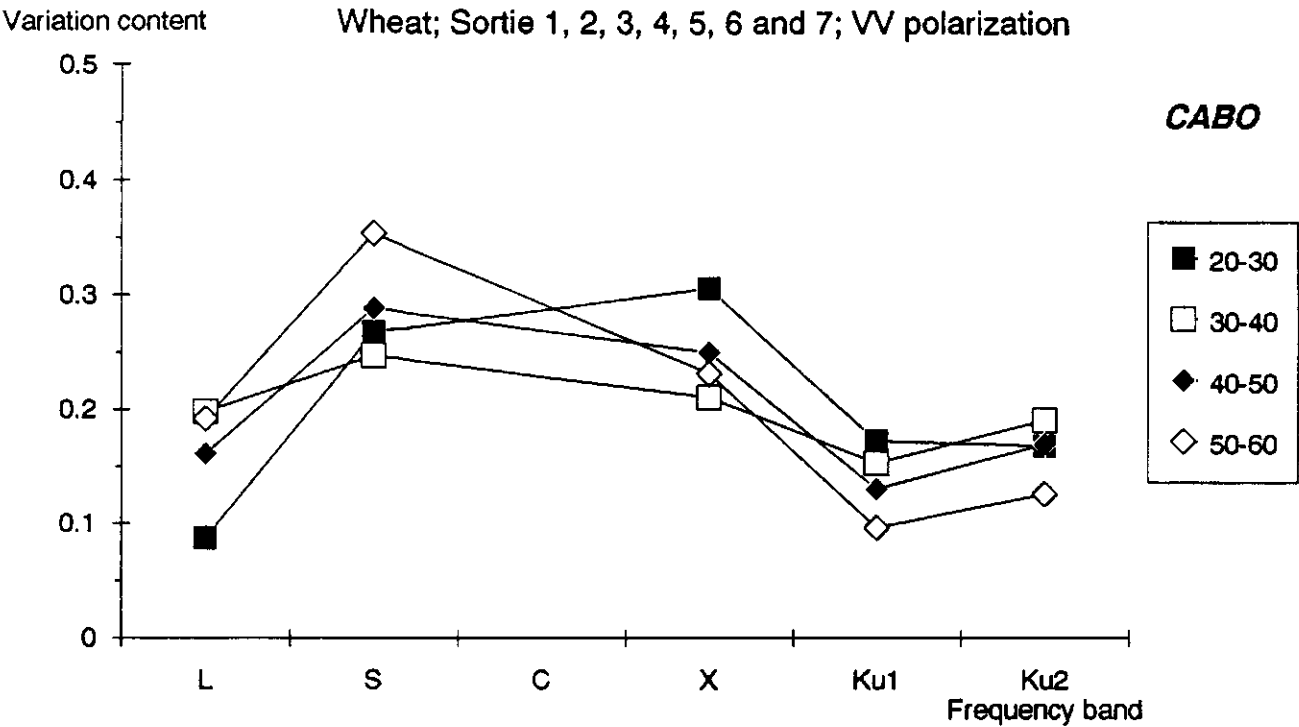


Fig. 100 Relative content of variation in the frequency bands, per incidence angle group (Wheat, all sorties, VV polarization)

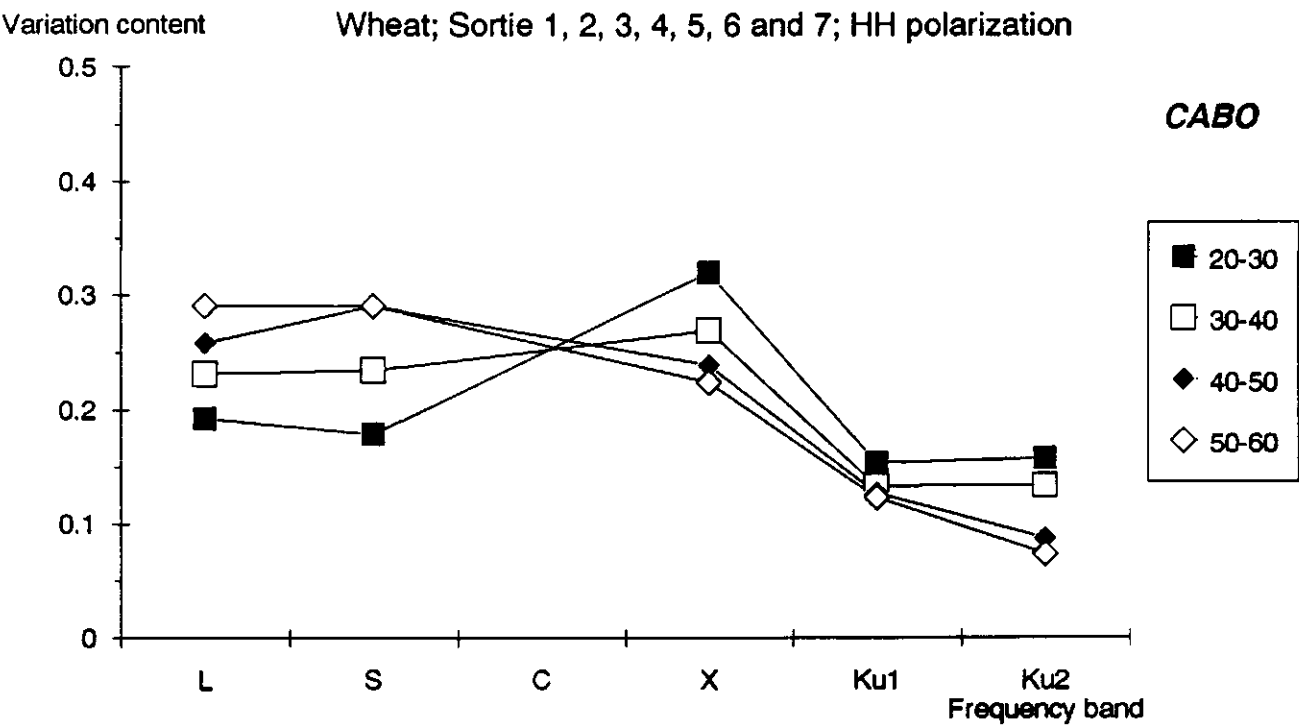


Fig. 101 Relative content of variation in the frequency bands, per incidence angle group (Wheat, all sorties, HH polarization)

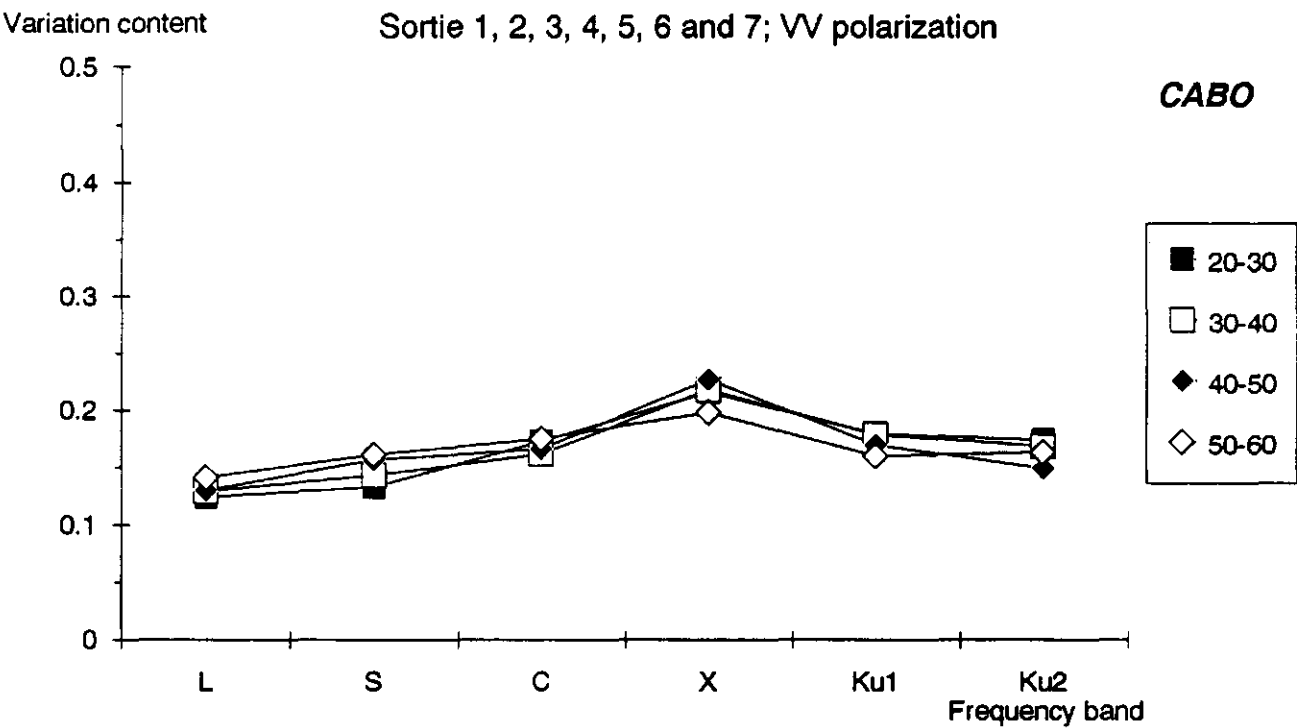


Fig. 102 Relative content of variation in the frequency bands, per incidence angle group (all track data of all sorties, VV polarization)

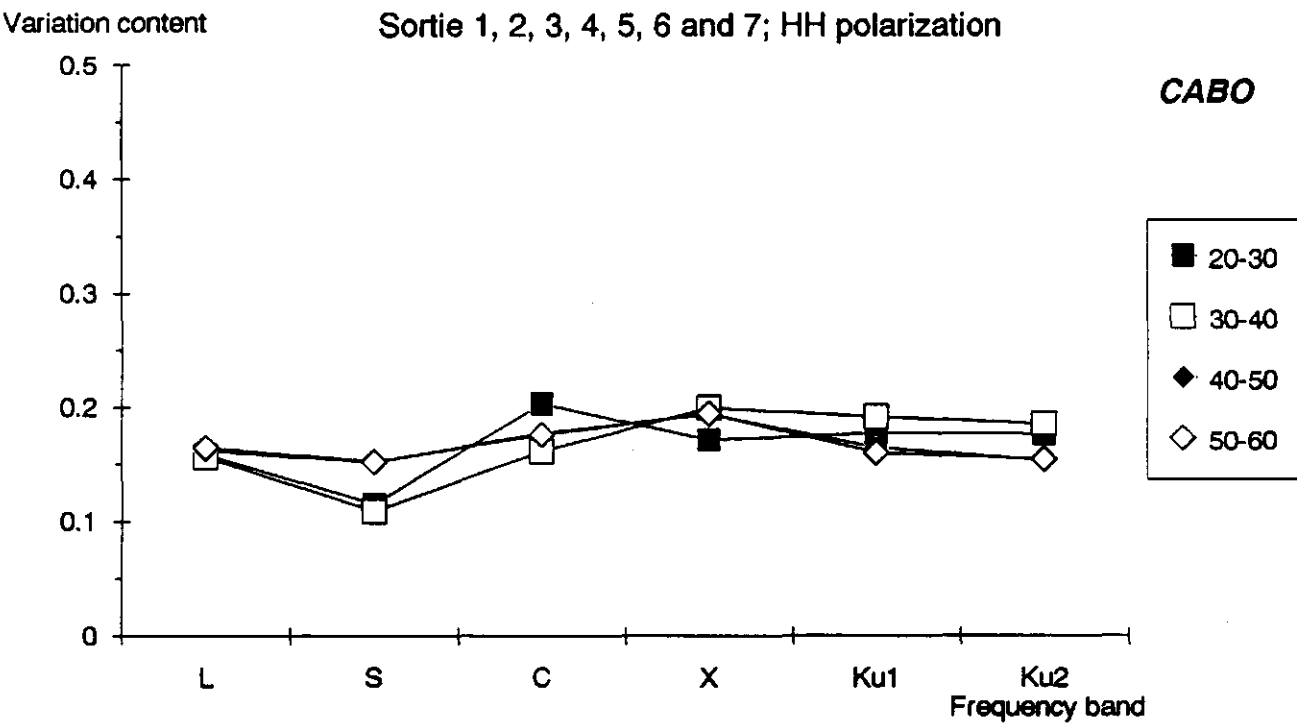


Fig. 103 Relative content of variation in the frequency bands, per incidence angle group (all track data of all sorties, HH polarization)

### 5.3 Correlation analysis between radar backscatter and crop growth parameters and soil moisture

#### 5.3.1 Crop growth parameters

The coefficient of correlation ( $r^2$ ) between radar backscatter in time and the crop growth parameters cover, height, fresh weight, dry weight and LAI was calculated per crop type for each frequency, state of polarization and nominal incidence angle (tables 14-16). Again, the C-band was excluded from the analysis because of the many missing data.

Consistently high coefficients of correlations ( $r^2 > 0.90$ ) are only found for potato with crop cover and height, in the L- and the S-band, at all angles of incidence and at both VV and HH polarization. In these bands, the radar backscatter also correlates well ( $r^2 > 0.80$ ) with fresh and dry biomass, and with LAI, at low to medium angles of incidence. In the Ku1- and Ku2-band, the correlation between backscatter and cover and height is medium to high ( $r^2 > 0.80$ ) mostly at VV polarization. The coefficients of correlation in the X-band were low because of the 'disturbed' temporal backscatter curves.

For beet, the radar backscatter only consistently correlates somewhat ( $r^2 > 0.70$ ) with cover and height in the Ku1- and the Ku2-band at VV polarization. For wheat, the radar backscatter does not consistently correlate with any crop growth parameter at any frequency band, incidence angle or state of polarization.

Compared to the correlations in the X-band ROVE data set (Bouman and van Kasteren, 1989), the coefficients of correlation presented here are very low. This may be caused by the relatively low number of radar observations (only seven, versus 20-35 in the ROVE set), their frequency in time (two measurements on mainly bare soil, four on completely closed crop canopies, and only one in between), or by the relatively lower (absolute) accuracy of the DUTSCAT measurements (thought to be  $\sim 1-2$  dB, versus  $\sim 0.5$  for the ROVE data set). Moreover, the fact that the mainly bare soil measurements (sortie 1 and 2) were originally compressed, and the measurements on the crops were not, may affect temporal analyses.

#### 5.3.2 Soil moisture

The coefficient of correlation ( $r^2$ ) between radar backscatter in time and the volumetric moisture content of the 0-5 cm top soil was calculated per crop for each frequency, state of polarization and nominal incidence angle (table 17).

Only four out of 150 coefficients of correlation were larger than 0.70. It is concluded that, in this data set, the radar backscatter does not correlate with soil moisture. However, data from all seven sorties were used in the correlation analysis, thereby lumping data on bare soil with data on closed crop covers (high frequency microwaves are not expected to penetrate closed crop covers).

The low  $r^2$  between the VV S-band radar backscatter and soil moisture content for wheat does not support the earlier observation of a relatively high transparency of wheat for S-band microwaves (§ 3.4, wheat, and figures 44 and 46).

The observation that L-band microwaves penetrate potato canopies (§ 3.1) would suggest a relatively high correlation with soil moisture content. General radar backscatter theory also indicates relatively high transparencies of crop canopies with longer wavelengths, theoretically leading to high correlations with soil moisture content. However  $r^2$  (table 17) was also low in the low frequencies, the L- and the S-band. This low correlation between the radar backscatter at the low frequencies and the soil moisture content may be explained by the relative uniformity in soil moisture content during the seven sorties (figure 46). The soil moisture content was always high to very high at all sorties.

The low coefficients of correlation in the high frequencies are not surprising, since the high frequency-microwaves are not expected to penetrate the crop canopies (as opposed to lower-frequency microwaves; compare § 3.1).

Table 14 Coefficient of correlation ( $r^2$ ) between the radar backscatter (of all seven sorties) and the crop growth parameters cover, height, fresh canopy biomass, dry canopy biomass and Leaf Area Index (LAI) for potato;  $r^2$  was calculated per frequency band, incidence angle and state of polarization; The number of data pairs was ~ 25 for each coefficient of correlation (average for whole table)

Band	Incidence angle	Cover	Height	Fresh	Dry	LAI	Cover	Height	Fresh	Dry	LAI
HH polarization						VV polarization					
L	20	0.97	0.95	0.86	0.78	0.84	0.93	0.86	0.87	0.76	0.84
	30	0.98	0.94	0.91	0.84	0.90	0.94	0.94	0.88	0.84	0.90
	40	0.93	0.93	0.80	0.71	0.78	0.88	0.90	0.76	0.67	0.74
	50	0.94	0.95	0.82	0.73	0.80	0.87	0.92	0.69	0.60	0.68
	60	0.81	0.89	0.60	0.50	0.57	0.85	0.93	0.65	0.55	0.64
S	20	0.96	0.92	0.91	0.87	0.88	0.96	0.94	0.73	0.64	0.73
	30	0.93	0.94	0.78	0.69	0.78	0.97	0.97	0.83	0.79	0.87
	40	0.90	0.94	0.70	0.61	0.68	0.91	0.95	0.73	0.63	0.71
	50	0.86	0.92	0.67	0.57	0.65	0.88	0.95	0.67	0.58	0.65
	60	0.83	0.92	0.62	0.53	0.59	0.88	0.94	0.69	0.59	0.66
X	20	0.55	0.61	0.32	0.29	0.34	0.35	0.43	0.12	0.10	0.14
	30	0.74	0.77	0.46	0.40	0.52	0.75	0.84	0.48	0.43	0.53
	40	0.61	0.76	0.32	0.24	0.34	0.67	0.77	0.40	0.33	0.41
	50	0.56	0.72	0.29	0.22	0.30	0.71	0.80	0.46	0.39	0.48
	60	0.13	0.32	0.00	0.00	0.00	0.14	0.30	0.00	0.00	0.01
Ku1	20	0.85	0.94	0.70	0.59	0.66	0.87	0.97	0.69	0.53	0.62
	30	0.82	0.87	0.70	0.59	0.64	0.91	0.90	0.84	0.81	0.83
	40	0.02	0.21	0.00	0.02	0.02	0.81	0.88	0.66	0.58	0.61
	50	0.73	0.86	0.57	0.46	0.51	0.84	0.91	0.65	0.55	0.61
	60	0.38	0.65	0.17	0.09	0.12	0.68	0.83	0.48	0.36	0.44
Ku2	20	0.91	0.92	0.82	0.73	0.78	0.80	0.89	0.61	0.47	0.53
	30	0.68	0.72	0.68	0.53	0.57	0.93	0.96	0.91	0.88	0.88
	40	0.78	0.88	0.61	0.51	0.56	0.70	0.85	0.51	0.38	0.43
	50	0.58	0.76	0.42	0.30	0.36	0.82	0.88	0.68	0.64	0.70
	60	0.57	0.76	0.38	0.27	0.34	0.56	0.73	0.38	0.28	0.34

Table 15 Coefficient of correlation ( $r^2$ ) between the radar backscatter (of all seven sorties) and the crop growth parameters cover, height, fresh canopy biomass, dry canopy biomass and Leaf Area Index (LAI) for beet;  $r^2$  was calculated per frequency band, incidence angle and state of polarization; The number of data pairs was  $\approx 25$  for each coefficient of correlation (average for whole table)

Band	Incidence angle	Cover	Height	Fresh	Dry	LAI	Cover	Height	Fresh	Dry	LAI
HH polarization						VV polarization					
L	20	0.46	0.41	0.22	0.14	0.26	0.45	0.44	0.27	0.15	0.28
	30	0.72	0.70	0.48	0.37	0.55	0.88	0.83	0.64	0.64	0.77
	40	0.48	0.43	0.23	0.19	0.28	0.45	0.39	0.19	0.14	0.25
	50	0.35	0.32	0.18	0.14	0.22	0.10	0.06	0.01	0.01	0.03
	60	0.26	0.20	0.06	0.04	0.09	0.29	0.24	0.12	0.10	0.17
S	20	0.22	0.19	0.12	0.10	0.14	0.05	0.02	0.01	0.03	0.00
	30	0.59	0.54	0.33	0.27	0.43	0.74	0.67	0.41	0.42	0.55
	40	0.68	0.62	0.37	0.33	0.46	0.67	0.60	0.34	0.29	0.45
	50	0.74	0.68	0.43	0.39	0.53	0.71	0.64	0.37	0.32	0.48
	60	0.76	0.71	0.46	0.41	0.55	0.72	0.66	0.39	0.34	0.49
X	20	0.08	0.04	0.00	0.00	0.01	0.01	0.00	0.09	0.09	0.02
	30	0.38	0.29	0.09	0.05	0.20	0.61	0.50	0.23	0.24	0.36
	40	0.47	0.39	0.15	0.13	0.23	0.54	0.45	0.20	0.18	0.30
	50	0.59	0.51	0.25	0.21	0.34	0.64	0.55	0.29	0.27	0.39
	60	0.36	0.28	0.07	0.05	0.14	0.45	0.35	0.12	0.10	0.20
Ku1	20	0.57	0.48	0.26	0.19	0.33	0.45	0.35	0.13	0.09	0.20
	30	0.70	0.67	0.46	0.36	0.53	0.86	0.83	0.61	0.64	0.72
	40	0.00	0.00	0.02	0.09	0.03	0.70	0.64	0.39	0.31	0.47
	50	0.73	0.71	0.47	0.41	0.54	0.79	0.76	0.51	0.44	0.58
	60	0.52	0.49	0.25	0.20	0.32	0.74	0.72	0.45	0.38	0.53
Ku2	20	0.58	0.52	0.30	0.25	0.35	0.39	0.36	0.15	0.09	0.17
	30	0.62	0.62	0.44	0.30	0.45	0.81	0.79	0.62	0.66	0.65
	40	0.65	0.62	0.37	0.32	0.45	0.65	0.61	0.37	0.32	0.42
	50	0.67	0.63	0.39	0.33	0.43	0.81	0.78	0.55	0.58	0.60
	60	0.59	0.54	0.30	0.24	0.37	0.66	0.61	0.38	0.32	0.42

Table 16 Coefficient of correlation ( $r^2$ ) between the radar backscatter (of all seven sorties) and the crop growth parameters cover, height, fresh canopy biomass, dry canopy biomass and Leaf Area Index (LAI) for wheat;  $r^2$  was calculated per frequency band, incidence angle and state of polarization; The number of data pairs was ~ 25 for each coefficient of correlation (average for whole table)

Band	Incidence angle	Cover	Height	Fresh	Dry	LAI	Cover	Height	Fresh	Dry	LAI
HH polarization						VV polarization					
L	20	0.29	0.48	0.56	0.51	0.00	0.02	0.03	0.06	0.14	0.21
	30	0.39	0.57	0.61	0.40	0.04	0.01	0.09	0.04	0.03	0.12
	40	0.44	0.63	0.67	0.49	0.09	0.09	0.14	0.16	0.09	0.08
	50	0.46	0.69	0.72	0.57	0.08	0.25	0.55	0.58	0.55	0.00
	60	0.39	0.85	0.83	0.58	0.12	0.01	0.07	0.09	0.18	0.05
S	20	0.07	0.07	0.03	0.16	0.12	0.41	0.20	0.19	0.04	0.42
	30	0.15	0.50	0.48	0.38	0.01	0.07	0.00	0.00	0.05	0.26
	40	0.17	0.63	0.62	0.69	0.00	0.07	0.29	0.36	0.40	0.01
	50	0.25	0.75	0.73	0.76	0.03	0.25	0.56	0.66	0.55	0.02
	60	0.26	0.82	0.77	0.78	0.05	0.39	0.77	0.79	0.88	0.02
X	20	0.03	0.22	0.17	0.27	0.10	0.03	0.27	0.16	0.31	0.04
	30	0.00	0.13	0.06	0.14	0.30	0.18	0.01	0.07	0.00	0.37
	40	0.48	0.16	0.28	0.09	0.62	0.31	0.15	0.26	0.12	0.43
	50	0.66	0.52	0.62	0.38	0.53	0.57	0.57	0.65	0.47	0.45
	60	0.33	0.00	0.04	0.05	0.40	0.10	0.00	0.02	0.00	0.17
Ku1	20	0.12	0.46	0.23	0.37	0.12	0.10	0.52	0.22	0.43	0.16
	30	0.01	0.18	0.05	0.27	0.01	0.11	0.07	0.02	0.01	0.14
	40	0.07	0.05	0.32	0.01	0.01	0.13	0.15	0.06	0.09	0.08
	50	0.05	0.06	0.01	0.07	0.04	0.08	0.03	0.01	0.01	0.12
	60	0.00	0.00	0.02	0.03	0.00	0.05	0.05	0.11	0.15	0.03
Ku2	20	0.00	0.09	0.02	0.08	0.13	0.04	0.39	0.14	0.28	0.19
	30	0.00	0.39	0.18	0.39	0.14	0.26	0.17	0.10	0.07	0.38
	40	0.02	0.26	0.11	0.19	0.24	0.08	0.18	0.05	0.08	0.26
	50	0.01	0.31	0.12	0.30	0.23	0.19	0.27	0.18	0.15	0.41
	60	0.06	0.06	0.10	0.05	0.10	0.01	0.00	0.00	0.00	0.29

Table 17 Coefficient of correlation ( $r^2$ ) between the radar backscatter (of all seven sorties) and volumetric moisture content of 0-5 cm top soil, per crop(-soil) type, state of polarization, incidence angle and frequency band; The number of data pairs was ~ 17 for each coefficient of correlation (average for whole table)

Crop	Polarization	Incidence Angle	Frequency band				
			L	S	X	Ku1	Ku2
Potato	HH	20	0.39	0.27	0.23	0.50	0.41
		30	0.44	0.54	0.43	0.67	0.33
		40	0.31	0.43	0.29	0.66	0.18
		50	0.37	0.40	0.23	0.45	0.32
		60	0.20	0.40	0.10	0.26	0.31
Potato	VV	20	0.29	0.34	0.10	0.43	0.43
		30	0.74	0.73	0.41	0.63	0.57
		40	0.42	0.46	0.25	0.51	0.39
		50	0.43	0.47	0.23	0.49	0.47
		60	0.36	0.39	0.04	0.30	0.29
Beet	HH	20	0.51	0.17	0.23	0.49	0.33
		30	0.44	0.44	0.40	0.61	0.26
		40	0.25	0.36	0.32	0.81	0.31
		50	0.29	0.33	0.32	0.50	0.34
		60	0.14	0.32	0.31	0.34	0.35
Beet	VV	20	0.49	0.79	0.18	0.44	0.35
		30	0.69	0.59	0.42	0.61	0.46
		40	0.37	0.45	0.30	0.49	0.42
		50	0.23	0.43	0.24	0.45	0.42
		60	0.20	0.39	0.26	0.35	0.34
Wheat	HH	20	0.27	0.31	0.25	0.00	0.08
		30	0.45	0.41	0.16	0.01	0.44
		40	0.30	0.35	0.03	0.05	0.03
		50	0.26	0.34	0.00	0.03	0.02
		60	0.07	0.18	0.13	0.05	0.01
Wheat	VV	20	0.05	0.37	0.10	0.00	0.01
		30	0.00	0.64	0.04	0.01	0.02
		40	0.24	0.61	0.00	0.07	0.04
		50	0.26	0.38	0.00	0.11	0.00
		60	0.15	0.28	0.09	0.31	0.03



## 6 Summary and conclusions

Based on a general quality analysis, the data set of DUTSCAT 88 is reduced for so called 'suspicious' data. Especially the C-band was hampered with a lot of instrument failures and unreliable data. All data with a standard deviation larger than 3 dB were removed, in analogy with the DUTSCAT 87 data treatment. Also data were removed which had a large deviating pattern in relation to neighbouring data (in other frequency bands, incidence angles or state of polarization). However, the final DUTSCAT 88 data set was less affected by data removal than the final DUTSCAT 87 data set. It appeared fairly consistent after a first visual interpretation. The only exceptions were the data in the X-band which proved also 'suspicious' after careful analysis of the temporal curves.

### 6.1 Backscatter trends and crops

The following general trends are summarized from the analysis of the final data set:

- The field average  $\gamma$  values of the different crop types are very well clustered in all frequency bands, angles of incidence and at all sorties. The relatively broad clusters of wheat matches the relatively large spread in the ground truth.
- The relative position of the frequency bands L, S, C and X is in accordance with general theory: backscatter L-band < backscatter S-band < backscatter C-band < backscatter X-band. After the X-band, the backscatter either further increases in the Ku1-band (bare soil, beet and potato at the end of the season), remains on the same level in the Ku1-band, or decreases a bit in the Ku1-band (all crops in the middle of the growing season). Since the high levels of X-band radar backscatter at sortie 3 and 4 are suspicious, the last trend (decreasing backscatter in Ku1-band) seems not very likely. After the Ku1-band the radar backscatter generally decreases a little (1-2 dB) in the Ku2-band.  
The shape of the frequency curves is very similar for all crops and (mainly) bare soil. The curves of beet and potato are generally 8-10 dB higher (40° incidence angle) than that of bare soil. The level of the curve of wheat is about the same as that of mainly bare soil.
- The so called angular-dependency curve of the radar backscatter is smooth in all frequency bands. For (mainly) bare soil, the backscatter decreases with increasing incidence angle from 10° to 20°. Hereafter, it only decreases very slowly with further increasing incidence angle. For crops (with closed cover), the curves are more or less horizontal except for those of potato in the C-, X-, Ku1- and Ku2-band. Here, the backscatter steadily decreases with increasing incidence angle. The differences in the angular dependency of beet and potato in these bands reflects the differences in leaf angle distribution: beet has a plagiophile distribution, potato a planophile.
- Crops and fields of (mainly) bare soil are differentiated in the different frequency bands. For mainly bare soil the L-band clearly separates all three 'crop-soils' at low angles of incidence. For crops, the best band for discrimination is one of the high frequency bands X-, Ku1- or Ku2-band at a medium to high angle of incidence: beet has the highest level of radar backscatter, potato a medium level, and wheat the lowest level.

- The temporal curves of the radar backscatter of the crops are comparable in trend in all frequency bands. For beet and potato, the backscatter increases with crop growth until the midst of the growing season (for beet cover: 0.78-0.82, biomass: 2250-3500, LAI: 3-3.5; for potato cover: 0.89-0.93, biomass: 1500-2750, LAI: 2.5-3.5). With one exception (Ku2-band for potato), the range in backscatter (VV, 40° incidence angle) from bare soil to that from a closed crop canopy is some 10-12 dB in all frequencies. For wheat, no 'radar-growth' curves were recognized at all in the temporal radar backscatter curves.

- The data set can tentatively be divided into two general frequency classes: the so-called 'high frequency bands' (C-, X-, Ku1- and Ku2-bands; and the so-called 'low frequency bands' L- and S-band. Especially in the class of high frequency bands the similarity between the radar backscatter of the crops is large. The changes from one frequency class, or band, to another are gradual and not abrupt.

The radar backscatter in the high frequencies generally reacts more on the canopy structure than that in the low frequencies (e.g. the increase in radar backscatter with the lodging of wheat; the possible relationship between leaf angle distribution and angular-dependency for beet and potato). The C-band displays the lowest dynamic range while that of the other three bands is generally comparable. The example of the ridge orientation of potato indicates that the microwaves in the L-band can penetrate the canopy, whereas those in the S-band and the high frequencies can not. Also for potato, the radar backscatter in the L-band increases for a longer period of time with crop growth than for the other crops, and than for that in the other frequency bands.

## 6.2 Comparison with other data sets

Most of the general trends described here were also observed in the 1987 data set. However, there are two major differences between the sets:

- 1) The dynamic range is larger in 1988 than in 1987; the range in backscatter from bare soil to that from a closed crop canopy (beet or potato) is about twice as large in 1988 as in 1987.
- 2) The average radar backscatter (track-averages) is some 1-2 dB higher in 1988 than in 1987.

This implies that the compression of the 1987 recordings still is notable in the decompressed data set. Therefore, attention of further analyses are best to be focussed on the 1988 data set with back-up, or support from the 1987 data.

The backscatter trends (temporal and angular dependency) in the Ku1-band agree with those observed in historical X-band ground-based and airborne SLAR (1984 campaign) data for beet and potato. The backscatter of wheat in the Ku1-band resembles that of the SLAR, but not that of the ground-based observations. However, in the latter data set, there is a lot of variability in the backscatter of wheat. The SLAR data of beet and potato (temporal backscatter curves) are both in agreement with the ground-based data, but here too, the data of wheat are not.

The absolute level of the backscatter in the Ku1-band, and of the part of the X-band data that is considered reliable, is on the average 3-5 dB higher than that of both historical data sets. In the ground-based data set of 1980, both X- and Q-band (35 GHz) measurements were made. For all crops and mainly bare soil the backscatter in the Q-band was about 3-5 dB (on the average) higher than in the X-band. This pattern was not observed in the frequency dependence of the DUTSCAT data between the X- and the Ku2-band. The general trends found in the ERASME data set (C-band HH and X-band VV/HH) compare well with those in the DUTSCAT data set. Again the DUTSCAT data were (consequently) higher.

### 6.3 Statistical analysis

- With mainly bare soil (sorties 1 and 2), the coefficients of correlation  $r^2$  between VV and HH polarization, frequency bands, and incidence angles were lower than with full crop covers.  $R^2$  between VV and HH polarization, and  $10^\circ$ -neighbouring incidence angles was relatively highest in the L- and in the S-band. Secondly, the relative content of variation was larger in the lower frequencies (especially the L-band) than in the higher frequencies.

- With closed crop covers (sorties 4-6/7), the coefficients of correlation between VV and HH polarization, frequency bands, and incidence angles were higher than with mainly bare soil. Here,  $r^2$  between VV and HH polarization, and  $10^\circ$ -neighbouring incidence angles was relatively highest in the high frequencies, X-, Ku1- and Ku2-bands. Also, the relative content of variation was larger in the high frequencies than in the low frequencies, L- and S-band.

$R^2$  was high between the high frequencies (X-, Ku1- and Ku2-), while the L- and the S-band were mostly decorrelated with the high frequencies, and with each other.

- In time (from bare soil through closed crop cover to harvesting) the highest relative content of variation was found in the high frequencies for beet and in the low frequencies (especially the S-band) for wheat. For potato, the relative content of variation was about equally distributed over all frequencies.

- For potato, high correlations were found between  $\gamma$  (especially in the L- and the S-band) and crop cover and height. For beet and wheat, the correlations between  $\gamma$  and crop growth parameters were low to medium (at all frequencies). The coefficients of correlation between  $\gamma$  and soil moisture content (in the 0-5 cm top soil) were low for all crops and at all frequencies (correlation of all data throughout the growing season).

### 6.4 Conclusions and preliminary prospects for agricultural applications

The data description and the statistical analyses indicated that the backscatter behaviour of beet, potato and wheat was very much the same in the high frequencies, the X-, Ku1- and Ku2-band. The backscatter behaviour in the C-band also resembled strongly that in the other high frequency bands, but the dynamic range was lower. The backscatter behaviour in the low frequencies, L- and S-band, also resembled that in the high frequencies in general lines. Only some differences in angular behaviour of crops and soil, the low correlations between the low and the high frequencies, and specific examples like ridge orientation in potato and lodging in wheat (namely the L-band versus the high frequencies), indicated that low frequency microwaves interacted differently with crop canopies than high frequency microwaves. Preliminary prospects for agricultural application of multi-frequency radar observations can be derived for crop classification and growth monitoring (of sugar beet, potato and winter wheat).

Crop classification. Bare soil types ('beet-soil', 'potato-soil', 'wheat-soil' (40-50% cover)) could already be discriminated in the low frequencies, especially in the L-band. Crop types with half to full crop cover were (equally) well discriminated in the high frequencies, X-, Ku1-, Ku2-bands. The combined use of a low and a high frequency probably will increase the (classification) sensitivity, but does not seem imperative.

Growth monitoring. The temporal curves of  $\gamma$  of the crop types were comparable in trend in all frequency bands (except the S-band for wheat). For beet and potato,  $\gamma$  increased with crop growth until the midst of the growing season (beginning of July). The range in  $\gamma$  with the growth of beet and potato was in the order of 10-12 dB (at 40° incidence angle). There was no unique frequency band that had the highest (temporal) relative content of variation for both crops. For wheat, no 'radar-growth' curves were recognized at any frequency.

Possibilities for growth monitoring seem limited to potato and beet, with a slight preference for the low frequency bands for potato (high coefficients of correlation between crop cover and  $\gamma$  in the L- and S-band).

For classification and (possible) growth monitoring in agriculture, radar observations in one low frequency (namely the L-band) and in one high frequency (either one of the X-, Ku1- or Ku2-bands) seem to suffice (for beet, potato and wheat).

Finally, two notes on the formulated conclusions are in place here:

- The conclusions are derived from phenomenological data description and statistical analyses only, hence 'preliminary' conclusions. They have to be validated (and extended) through knowledge (modelling) of the physical interaction processes of multi-frequency microwaves with vegetation canopies [research is currently being carried out by ROVE-partners at the Agricultural University of Wageningen; BCRS-project AO-2.15].
- The quality of the DUTSCAT data set from the Agriscatt campaign is not sufficient to draw firm conclusions on the suitability of radar observations for precise growth monitoring [e.g. compression/decompression problems, absolute calibration problems, the lack of any radar observations in the important phase of growth between early May and mid June, 'suspicious' X-band, much loss of C-band data].

## References

- Attema, E., 1989, Radar signature measurements during the Agriscatt campaign, Proceedings of IGARSS'88 Symposium, Edinburgh, Scotland, 13-16 September, ESA SP-284: 1141-1144.
- Beers, J.N.P., 1975. Analysis of significance within crop-spectra. A comparison study of different multispectral scanners. Netherlands Interdepartmental Working Community for the Application of Remote Sensing Techniques (NIWARS). NIWARS publication no. 30.
- Bernard, R. et al., 1986. Data processing and calibration for an airborne scatterometer. IEEE Transactions on Geoscience and Remote Sensing. Vol. GE-24, no. 5.
- Bouman, B.A.M. and H.W.J. van Kasteren, 1989. Ground based X-band radar backscatter measurements of wheat, barley and oats, 1975-1981. CABO report 119.
- Bouman, B.A.M. et al., 1990. Agriscatt, quality analysis and data description of the DUTSCAT 1987 data. CABO report 135.
- Bouman, B.A.M. and H.W.J. van Kasteren, 1991. The X-band (3-cm wave) radar backscattering of agricultural crops. I: Beet and potato; radar backscattering and crop growth. Remote Sensing of Environment, in press.
- Bunnik, N. J., 1978, The multispectral reflectance of shortwave radiation by agricultural crops in relation with their morphological and optical properties, Communications Agricultural University Wageningen, The Netherlands 78-1.
- Burg, G. van der, and D. Uenk, 1989. Comparison of calibrated (X-band) SLAR data measured in three different test sites in The Netherlands. BCRS report 89-08, Delft.
- Genstat 5, Reference Manual (1988), Oxford science publishers, Oxford.
- Hoekman, D.H., 1990. The AGRISCATT campaign. Radar data acquisition at agricultural sites in five West-European countries during the 1987 and 1988 growing seasons. Department of Landsurveying and Remote Sensing, Wageningen Agricultural University.
- James, G., 1989a, Agriscatt 1988, Quality assessment of DUTSCAT data, ESA/EARTHNET, November 1989, Frascati.
- James, G., 1989b, Agriscatt 1988, Quality assessment of ERASME data, ESA/EARTHNET, November 1989, Frascati.
- Luik, P.C., 1990, Werkwijze voor het corrigeren van fouten in de DUTSCAT data 1987/1988, BCRS report 90-14, Delft, The Netherlands (In Dutch).
- Morin, J.C., 1988. Agriscatt 1988: operational campaign report. n° 640/15/11/88. GDТА.

Snoeij, P., and P.J.F. Swart, 1987. The DUT airborne scatterometer. *International journal of Remote Sensing*. Vol. 8, no. 11, pp. 1709-1716.

Snoeij, P. et al., 1989. ESA Agriscatt-88 campaign. Processing of the DUTSCAT data, Final report. Telecommunication and Remote Sensing technology, Technical University Delft.

Vissers, M.A.M. et al., 1989. Agriscatt 88 Ground data collection Flevoland (NL). CABO report 108.

Wit, C.T. de, 1965. Photosynthesis of leaf canopies. Centre for Agricultural Publications and Documentations PUDOC, Wageningen.